Escuela Superior de Tecnología y Ciencias Experimentales

Departamento de Química Inorgánica y Orgánica

PhD Thesis

New Pseudopeptidic Bis(Amino Amides): Supramolecular Behaviour in the Presence of Transition Metals

Lingaraju Gorla

Directors:

Dr. Santiago V. Luis Lafuente

Dra. Belén Altava Benito

Castellón de la Plana, June 2016

D. **Santiago Vicente Luis Lafuente**, Catedrático Universitario y Doctor del área de Química Orgánica en el Departamento de Química Inorgánica y Orgánica de la Universitat Jaume I de Castellón y Dña. **Belén Altava Benito**, Doctora y Profesora Titular Universitaria del área de Química Orgánica en el Departamento de Química Inorgánica y Orgánica de la Universitat Jaume I de Castellón,

CERTIFICAN: Que D. **Lingaraju Gorla**, Máster en Química Sostenible por la Universitat Jaume I, Castellón, ha realizado bajo su dirección, en el programa de doctorado interuniversitario de Química Sostenible coordinado por la Universitat Jaume I, el trabajo titulado "***New Pseudopeptidic Bis(Amino Amides): Supramolecular Behaviour in the Presence of Transition Metals***" y que ésta constituye su memoria de tesis doctoral para optar al grado de Doctor en Química Sostenible.

Y para que así conste y en cumplimiento de la legislación vigente, firman el presente certificado en Castellón de la Plana, Junio de 2016.

Dr. Santiago V. Luis Lafuente
Catedrático de Química Orgánica
Dpto. de Química Inorgánica y Orgánica
Universitat Jaume I

Dra. Belén Altava Benito
Dpto. de Química Inorgánica y Orgánica
Universitat Jaume I

La realización de esta Tesis Doctoral ha sido posible gracias a la Generalitat Valencia por la concesión de una beca predoctoral "Santiago Grisolía" (GRISOLIA 2012/015). La financiación de la actividad investigadora ha sido posible gracias al proyecto concedido por el Ministerio de Ciencia y Tecnología (CTQ2015-68429-R), Generalitat Valenciana (PROMETEO/2012/020), ACOMP/2015/111 y al PPI-UJI (P1-1B-2013-38).

To my parents and lovely family members

Sahasra and Sweety

karmany evadhikaras te

ma phalesu kadachana

ma karma-phala-hetur bhur

ma te sango ’stv akarmani

- Bhagwat Gita -

ACKNOWLEDGEMENTS

At first, I would like to thank Prof. Santiago and Prof. Maribel, for providing me this great opportunity to work in this potential research group, and for their guidance throughout the period of this thesis. The profundity and range of ideas of Prof. Santiago mesmerized me. I am also thankful for the co-director of this PhD thesis Dra. Belén, who was very generous in sharing the time and knowledge with me, and also for her guidance, good advice, unconditional support, and all the valuable discussions during the period of these four years.

I am also thankful to Prof. Eduardo for his kind support, helpful discussions, and being so nice to me always.

I would like to express my deepest gratitude towards all the fellow labmates, *i.e.*Victor, Noelia, Diana, Cristina, Josefa, Alicia, Laura, Vanessa, Chen, Bogdan, Lars, Lucia, Edgar, Pascual, Daniel, Sergio, Luis, María Macia, María Catala, Silvia, Adriana, María Tejeda, Lucas for their friendship, support, and the nice time we spent together inside and outside the laboratory. I am thankful to Prof. Armando and Dra. Inés for teaching potentiometric measurements. I would like to thank Dra. Jenifer for her CD course with my compounds. I would like to thank Dr. Raul and Silvana for their so kind words and nice friendship with me always. I am greatly thankful to Dr. Vicente for his valuable help in my whole work, especially with X-ray crystallographic part and preparing the cover of the thesis.

I would like to thank Dr. Prashant for his helpful suggestions before I come to Spain and Prof. Pandey and Dr. Ahmed for their support, encouragement and healthy discussions and solving early stage problems in Castellón.

I would like to thank all my flatmates during this four years of journey *i.e.* Hono, Dany, Carmen, Majo, Idham, Marcela, Adrian, Nadhir, Oswald, Nayeli, Ramon, Jaya, Harsha, Carla and knowing about different cultures with them. I would like to thank Nacho, who is also becoming a doctor soon and the good time we spent on the weekends.

I would like to thank Maria José for administrative things and Maribel Gil for Santiago Grisolía scholarship papers.

I would like to thank friends from Tarragona like Balakrishna, Prasad, Vijay, Sandeep, and Purushothham for their kind support and taking care much when I travel over there.

I am also thankful to the technicians from SCIC, Dr. Cristian for help in NMR spectroscopy, Dr. Jose Miguel for IR and mass spectrometry, Dr. Gabriel for single crystal X- ray diffraction studies.

Lastly, I would like to thank my whole family for always stood behind me in every situation, and their invaluable guidance, and support throughout the time. I am grateful to inspire speeches from Swami Vivekananda and APJ Abdul Kalam for providing me motivation and energy in every difficult situation.

I am grateful to Lord Sai and Ayyappa, for showering me with the blessings and all the energy he provided me to fulfill all the tasks in my life.

Lingaraju Gorla

ABOUT THE THESIS

This thesis has been divided into 8 chapters and has been formatted following the scientific articles with the research work carried out. The results obtained have allowed the publication of one manuscript and the preparation of 3 manuscripts in international journals with high-level impact.

First of all, chapter 1 is based general introduction to Supramolecular Chemistry, specifically emphasizing those aspects most relevant to the work developed in this PhD.

In the second chapter, the general objectives of the thesis are described.

Then, in the third chapter general discussion of the results has been highlighted. So, this chapter has been divided into 4 parts corresponding to each one of the articles. In the following chapters 4, 5, 6 and 7 the articles have been included.

Finally, in chapter 8, the main results have been summarized and the conclusions are presented.

According to the regulations of the Universitat Jaume I, a resume of the thesis work having been carried out is presented in the Spanish language at the beginning of the thesis.

RESULTS OF THE WORK

The results obtained during the development of the current PhD Thesis have led to the publication in scientific journals:

- Wadhavane, P. D.; Gorla, L.; Ferrer, A.; Altava, B.; Burguete, M. I.; Izquierdo, M. A.; Luis, S. V., Coordination behaviour of new open chain and macrocyclic peptidomimetic compounds with copper(II). *RSC Adv.* **2015**, *5*, 72579-72589.

The article manuscripts are being prepared in progress to be published in scientific journals are:

- Cu^{2+}, Zn^{2+} and Ni^{2+} Complexes of C_2-symmetric pseudopeptides with an aromatic central spacer. Lingaraju Gorla, Vicente Martí-Centelles, Lena Freimuth, Belén Altava, M. Isabel Burguete and Santiago V. Luis (The manuscript has submitted in Inorganic Chemistry).
- Selective Cu^{2+} recognition by *N*,*N'*-benzylated bis(amino amides). Lingaraju Gorla, Vicente Martí-Centelles, Belén Altava, M. Isabel Burguete and Santiago V. Luis (Manuscript to be submitted in Dalton Transactions).
- Self-assembled structures of pseudopetidic compounds. Lingaraju Gorla, Vicente Martí-Centelles, Belén Altava, M. Isabel Burguete and Santiago V. Luis (Manuscript to be submitted in CrystEngComm).

Some of the results obtained have also been presented in various scientific congresses and conferences, from both national and international relevance are:

- New pseudopeptidic ligands: synthesis and metal recognition behaviour. Lingaraju Gorla, Vicente Martí, Belén Altava, M. Isabel Burguete and Santiago V. Luis, presented in XII Simposio de Investigadores Jóvenes RSEQ - Sigma-Aldrich. Barcelona (3-6 November 2015).
- New pseudopeptidic ligands: synthesis and metal recognition behaviour. Lingaraju Gorla, Belén Altava, M. Isabel Burguete and Santiago V. Luis, presented in IX International Workshop on Sensors and Molecular Recognition. Valencia (6-7 July 2015).
- Novel metal complexes derived from pseudopeptidic ligands. Lingaraju Gorla, Vicente Martí, Belén Altava, M. Isabel Burguete and Santiago V. Luis, presented in XI Simposio de Investigadores Jóvenes RSEQ - Sigma Aldrich. Bilbao (4-7 November 2014).

STRUCTURE OF THE COMPOUNDS CONSIDERED IN THIS WORK

Chapter 4: *Cu^{2+}, Zn^{2+} and Ni^{2+} Complexes of C_2-symmetric pseudopeptides with an aromatic central spacer.*

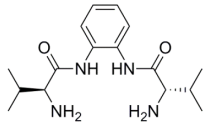

1a

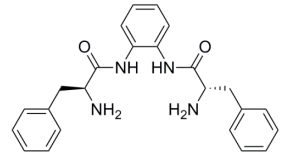

1b

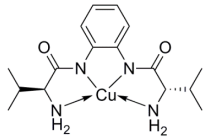

2a

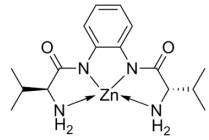

3a

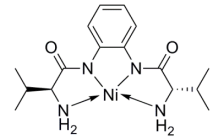

4a

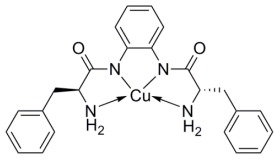

2b

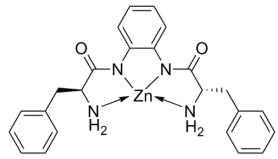

3b

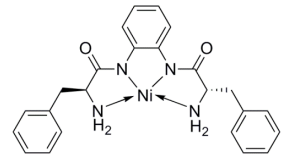

4b

Chapter 5: *Selective Cu^{2+} recognition by N,N'-benzylated bis(amino amides).*

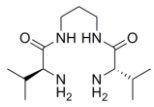

5a

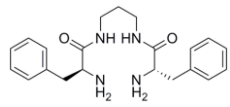

5b

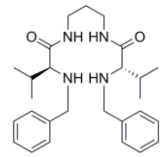

6a

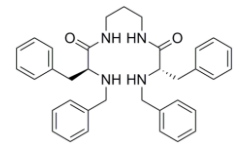

6b

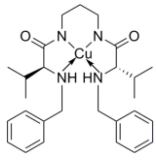

7a

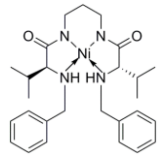

8a

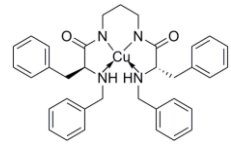

7b

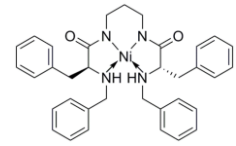

8b

Chapter 6: *Coordination behaviour of new open chain and macrocyclic peptidomimetic compounds with* Cu^{2+}.

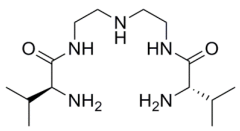

9a

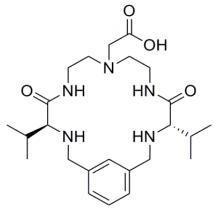

10

Chapter 7. *Self-Assembly of pseudopeptidic systems.*

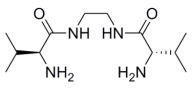

11a

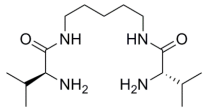

12a

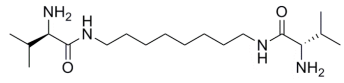

13a

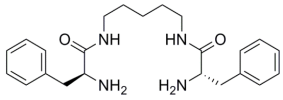

12b

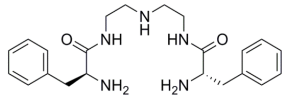

9b

ABBREVIATION LIST

Val	Valine
Phe	Phenylalanine
ATR	Attenuated total reflection
Bn	Benzyl
Cbz	Carboxybenzyl
CDC	Constitutional dynamic chemistry
CD	Circular dichroism
DMSO	Dimethyl sulfoxide
DNA	Deoxyribonucleic acid
ESI-MS	Electrospray ionization mass spectrometry
Ph	Phenyl
FT-IR	Fourier transform infrared spectroscopy
HPLC	High-performance liquid chromatography
*i*Pr	Isopropyl
IR	Infrared
Me	Methyl
mp	Melting point
NaCl	Sodium chloride
ACN	Acetonitrile
NMR	Nuclear magnetic resonance spectroscopy
rt	room temperature
i-PrOH	Isopropanol
UV-Vis	Ultraviolet-Visible spectroscopy

DCM	Dichloromethane

RESUMEN DE LA TESIS

La presente tesis doctoral se ubica dentro del área de la Química Supramolecular y más concretamente en el campo del reconocimiento molecular de cationes metálicos. Los capítulos siguientes describen la síntesis y el estudio de nuevos sistemas supramoleculares pseudopeptídicos, así como su aplicación en el reconocimiento molecular de cationes.

Como se mencionó anteriormente, esta tesis se ha dividido en 8 capítulos y se ha redactado siguiendo el formato de los artículos científicos derivados del trabajo de investigación desarrollado. Los resultados obtenidos a lo largo del desarrollo de la tesis han permitido la publicación de 1 artículo que se ha la publicado en una revista de alto índice de impacto, así como la preparación de 3 artículos que serán publicados también en revistas internacionales de alto índice de impacto.

Este trabajo se divide, en primer lugar, en una introducción general de la Química Supramolecular, haciendo hincapié específicamente en aquellos aspectos más relevantes para el desarrollo de esta Tesis doctoral (Capitulo 1). A continuación, se describen los objetivos generales de la tesis (Capítulo 2). Posteriormente en el capítulo 3, se resumen y analizan los resultados más importantes que se han obtenido. Estos resultados se recogen en los artículos que han sido obtenidos a partir de este trabajo científico (las publicaciones se presentan en los capítulos: 4, 5, 6 y 7). Finalmente, en el último capítulo (Capítulo 8) se hace un resumen de los principales resultados y se presentan las conclusiones.

En la primera parte de este trabajo, se ha llevado a cabo el diseño y la síntesis de estructuras pseudopeptídicas con espaciadores aromáticos así como sus complejos derivados de Cu^{2+}, Zn^{2+} y Ni^{2+}. Los resultados de este trabajo han permitido la preparación de la publicación titulada " *Complejos de Cu^{2+}, Zn^{2+} y Ni^{2+} derivados de pseudopéptidos con simetría C_2 con un separador central aromático* " que se incluye en el Capítulo 4.

Se ha estudiado el comportamiento ácido-base de los nuevos ligandos sintetizados y su capacidad de interacción con metales como Cu^{2+}, Zn^{2+} y

Ni^{2+}, con el fin de analizar los principales factores críticos que determinan la estructura final de los complejos formados. Para este propósito, se han utilizado diferentes técnicas experimentales, tales como valoraciones potenciométricas, espectroscopia de UV-Vis, espectroscopia de FT-IR, espectrometría de masas y difracción de rayos X.

Una vez estudiado el comportamiento de los ligandos de estructuras pseudopetídicas con espaciador aromático, se ha llevado a cabo la síntesis de una nueva familia de bis(amino amidas) *N,N´*-benciladas con simetría C_2 para su estudio como sensores selectivos de Cu^{2+}. A partir de los resultados de esta parte de la Tesis, se ha elaborado el manuscrito titulado ‘‘*Bis (amino amida) pseudopeptídicas N,N´-bencilados para el reconocimiento de* Cu^{2+} *selectiva’’* incluidos en el Capítulo 5.

La síntesis de estos compuesto *N,N´*-bencilados se llevó a cabo mediante una reacción de aminación reductiva a partir de las bis(amino amidas) derivadas de *L*-Val y *L*-Phe correspondientes. Estos compuestos se han estudiado como sensores para la detección selectiva de Cu^{2+} utilizando técnicas de absorción UV-Vis, dicroísmo circular, y espectrometría de ESI-MS.

En la parte final de la Tesis, se ha llevado a cabo el diseño y la síntesis de estructuras pseudopetídicas de cadena abierta y cerrada conteniendo un grupo amino en el espaciador alifático. Los resultados de este trabajo han permitido la publicación que lleva por título " *Estudio de coordinación con cobre (II) de nuevos compuestos peptidomiméticos de cadena abierta y macrocíclicos*" que se incluye en el Capítulo 6.

Se ha estudiado el comportamiento ácido-base de estos ligandos abierto y macrocíclico y su capacidad de interacción con Cu^{2+}. Para este propósito, se han utilizado diferentes técnicas experimentales, tales como valoraciones potenciométricas, espectroscopía de UV-Vis, y espectrometría de masas.

Finalmente, se han estudiado las propiedades de autoasociación en estado sólido de diferentes bis(amino amidas) con simetría C_2 derivadas de *L*-Val y *L*-Phe. Para dicho estudio se han podido obtener cristales óptimos para

difracción de de rayos X de la mayoría de los compuestos pseudopeptídicos con simetría C_2. También se ha estudiado el papel que juega la naturaleza del aminoácido, la longitud de la cadena espaciadora y la *N*-sustitución en las propiedades de autoensamblaje de estos compuestos pseudopeptídicos. Los resultados de esta parte del trabajo se presentan en el artículo titulado ‘‘*Propiedades de autoensamblado de diferentes bis(amino amidas) con simetría* C_2’’ y se incluye en el Capítulo 7.

SUMMARY OF THE THESIS

The present thesis is outlined within supramolecular chemistry and more specifically in the field of molecular recognition of metal cations. The following chapters describe the synthesis and study of new pseudopeptidic supramolecular systems as well as their application in molecular recognition of cations.

As previously mentioned, this thesis has been divided into 8 chapters and has been formatted following the scientific articles with the research work carried out. The results obtained have allowed the publication of one manuscript and the preparation of 3 manuscripts in international journals with high-level impact.

The structure of this work consists firstly of a general introduction to Supramolecular Chemistry, specifically emphasizing those aspects most relevant to the work developed in this PhD (Chapter 1). Then, the general objectives of the thesis are described (Chapter 2). Subsequently, the most important results that have been obtained are summarized and analyzed in Chapter 3. These results are collected in the articles that have been obtained from this scientific work (the publications are presented in the next Chapters 4, 5, 6 and 7). Finally, in the last chapter (Chapter 8) the main results are summarized and conclusions are presented.

In the first part of this work, the design and synthesis of new pseudopetidic ligands with C_2-symmetry containing aromatic spacer and their metal complexes have been studied. The results of this work have allowed the preparation of manuscript entitled ‘‘*Cu^{2+}, Zn^{2+} and Ni^{2+} Complexes of C_2-symmetric pseudopeptides with an aromatic central spacer*’’ and included in Chapter 4.

The acid-base behaviour of the synthesized ligands and their analysis of binding ability towards Cu^{2+}, Zn^{2+}, and Ni^{2+} metal cations have been studied in order to analyze the main critical factors determining the final structure of the complexes formed. For this purpose, different experimental

techniques such as potentiometric titrations, UV-Vis spectroscopy, IR spectroscopy, mass spectrometry and X-ray diffraction have been used.

Once studied the complexation behaviour of the pseudopetidic compounds containing aromatic spacers, a novel family of *N,N'*-benzylated bis(amino amides) with interesting properties as sensors for metal cations has been synthesized. Thus, the synthesis, design, and study of the properties of *N,N´*-benzylated bis(amino amides) with C_2-symmetry are presented. From the results of this part of the thesis, the manuscript entitled ‘‘Selective Cu^{2+} *recognition by N,N´-benzylated bis(amino amides)*’’ has been prepared and included in Chapter 5.

For the synthesis of the *N,N´*-benzylated pseudopeptidic compounds derived from *L*-Val and *L*-Phe reductive amination processes were carried. These compounds have been studied as selective sensors for metals using UV-Vis absorption, circular dichroism, and ESI-MS techniques.

In the final part of the thesis work, new open chain and macrocyclic peptidomimetic compounds with central amino spacer has been synthesized and studied their coordination ability with Cu(II). The results obtained entitled as ‘‘*Coordination behaviour of new open chain and macrocyclic peptidomimetic compounds with copper(II)*’’ has been published and included in Chapter 6.

The acid-base behaviour of the new ligands and their analysis of binding ability towards Cu^{2+} have been studied. For this purpose, different experimental techniques such as potentiometric titrations, UV-Vis spectroscopy, and mass spectrometry have been used.

Finally, the self-assembly properties in the solid state of open chain bis(amino amides) with C_2-symmetry has been studied. Suitable crystals for X-ray diffraction of the different compounds have been obtained. Thus, the role of the different structural parameters as the amino acid residue, the length, and nature of the spacer and the *N*-substitution in the self-assembly of this compounds has been studied. The results of this part of work are

presented in the article entitled "*self-assembling properties of different C_2-symmetric bis(amino amides)*'' and included in chapter 7.

TABLE OF CONTENTS

ANNEXES: Annexes are presented as Electronic Supplementary Information on the enclosed CD.

Annex I. Supporting Information Chapter 4

Annex II. Supporting Information Chapter 5

Annex III. Supporting Information Chapter 6

Annex IV. Supporting Information Chapter 7

Chapter I

General Introduction

1 General Introduction

1.1 Supramolecular Chemistry

Supramolecular Chemistry is a young discipline and is often defined as the "*chemistry beyond the molecule''* or the "*chemistry of the noncovalent bond''*.[1] Beyond the molecule, supramolecular chemistry aims at constructing highly complex functional chemical systems from molecular components interacting through non-covalent intermolecular interactions.[2] The non-covalent interactions like electrostatic interactions, hydrogen bonding, π-interactions, van der Waals forces, metal-ligand coordination or hydrophobic effects[3] assist the molecules to organize themselves in well-defined structures and increases complexity beyond molecule towards *supermolecules*.[4]

The concept and term of supramolecular chemistry were first coined by J.M. Lehn and led him to obtain the Nobel Prize in 1987 together with Donald J. Cram and Charles J. Pedersen for their *development and use of molecules with structure-specific interactions of high selectivity*[5] called as *molecular recognition* or *host-guest chemistry* involving a 'host' and a 'guest' molecule as highlighted in Figure 1, which illustrates the relationship between molecular and supramolecular chemistry in terms of structures.[6]

[1] a) Lehn, J. M., Supramolecular Chemistry-Scope and Perspectives Molecules, Supermolecules, and Molecular Devices (Nobel Lecture). *Angew. Chem., Int. Ed. Engl.* **1988**, *27*, 89-112; b) Lehn, J. M., Toward Self-Organization and Complex Matter. *Science* **2002**, *295*, 2400-2403.
[2] Lehn, J. M., Toward complex matter: Supramolecular chemistry and self-organization. *Proc. Natl. Acad. Sci.* **2002**, *99*, 4763-4768.
[3] Nguyen, S. T.; Gin, D. L.; Hupp, J. T.; Zhang, X., Supramolecular chemistry: Functional structures on the mesoscale. *Proc. Natl. Acad. Sci.* **2001**, *98*, 11849-11850.
[4] Lehn, J. M. *Supramolecular Chemistry: Concepts and Perspectives.* Wiley: 1995.
[5] http://www.nobelprize.org/nobel_prizes/chemistry/laureates/1987/press.html
[6] Steed, J. W.; Atwood, J. L. *Supramolecular Chemistry*. Wiley: 2013.

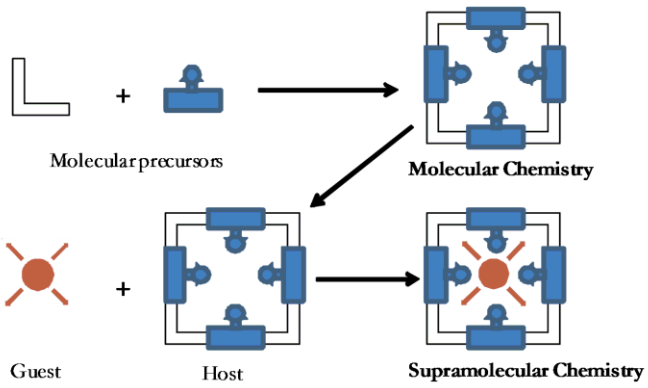

Figure 1. Comparison between the scope of molecular and supramolecular chemistry according to Lehn.[7]

The non-covalent bonding interactions are the principal element of supramolecular chemistry and are essential in biological systems and vital for biological metabolism, with many essential functions like transduction of signals, selective transport of ions and small molecules across membranes, enzymatic reactions, and the formation of larger aggregates.[8]

In abiotic chemistry, the design of artificial receptor molecules capable of displaying processes of highest efficiency and selectivity requires the correct manipulation of the energetic and stereochemical features of the non-covalent intermolecular forces within a defined molecular architecture. Inspired from nature, chemists have developed highly complex chemical systems from components that interact via non-covalent intermolecular forces.[9] The newly prepared artificial receptors not only recognize the molecules selectively but also achieve applications in different fields including catalysis and transport processes. Thus, supramolecular chemistry is a highly interdisciplinary field of science covering the chemical, physical, and biological features of chemical species of higher complexity, which are held together and organized by means of intermolecular (non-

[7] Kumar, D.; Sharma, D.; Singh, G.; Singh, M.; Rathore, M. S., Lipoidal Soft Hybrid Biocarriers of Supramolecular Construction for Drug Delivery. *ISRN Pharm.* **2012**, *2012*, 14.
[8] Campbell, N. A.; Reece, J. B.; Urry, L. A.; Cain, M. L.; Wasserman, S. A.; Minorsky, P. V.; Jackson, R. B. *Biology*, 8th ed.; Pearson Benjamin Cummings: San Francisco, 2008.
[9] Leslie, M., Strength in Numbers. *Science* **2014**, *343*, 725-727.

covalent) bonding and has also been rapidly expanding at the frontiers of chemical science with physical and biological phenomena.[4]

In the beginning, the fundaments of supramolecular chemistry have sprung from developments in macrocyclic chemistry dating back to the late 1960s which are particularly related to the development of macrocyclic ligands for metal cations (Figure 2).[6]

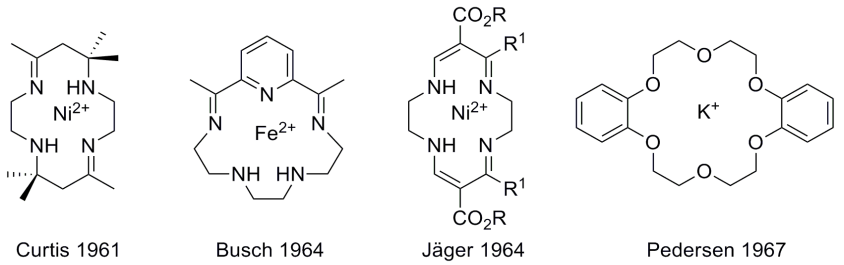

Figure 2. Four macrocyclic systems of fundamental importance in the evolution of supramolecular chemistry.

These initial macrocyclic systems provided an important impact on supramolecular chemistry and in the understanding of naturally occurring macrocycles such as ionophores, hemes, and porphyrins. Later on, the research work pioneered by Donald Cram on macrocyclic cyclophanes, spherands, and carcerands,[10] and the great contribution from Jean-Marie Lehn, who prepared and studied cryptands,[11] conceptualized supramolecular chemistry as an emerging field.

Supramolecular chemistry is dynamic by nature and allows the access to a wide range of substances assembled from relatively small libraries of components by virtue of their reversible non-covalent interactions. This gives place to the so-called *dynamic combinatorial chemistry (DCC)*. A DCC process allows for the generation of diversity and is a major factor in the emergence of complexity,[12] which opens a wide perspective in a variety

[10] Cram, D. J., The design of molecular hosts, guests, and their complexes. *Science* **1988**, *240*, 760-767.
[11] Dietrich, B.; Lehn, J. M.; Sauvage, J. P., Les Cryptates. *Tetrahedron Lett.* **1969**, *10*, 2889-2892.
[12] a) Lehn, J. M.; Eliseev, A. V., Dynamic Combinatorial Chemistry. *Science* **2001**, *291*, 2331-2332; b) Lehn, J. M., From supramolecular chemistry towards constitutional dynamic chemistry and adaptive chemistry. *Chem. Soc. Rev.* **2007**, *36*, 151-160; c) Lehn, J. M. Constitutional Dynamic Chemistry:

of areas of science and technology, such as the discovery of biologically active substances and that of new materials.[13]

Nowadays, supramolecular chemistry even became more sophisticated, playing a crucial role in the development of molecular machines,[14] sensors,[15] nanotechnology,[16] drug delivery,[17] synthetic molecular logic gates,[18] and semi-synthetic DNA computers.[19] There has been considerable interest arisen over the past 20 years in supramolecular chemistry, which resulted in a vast number of publications (Figure 3) and an enormous range of diversity in chemical systems.

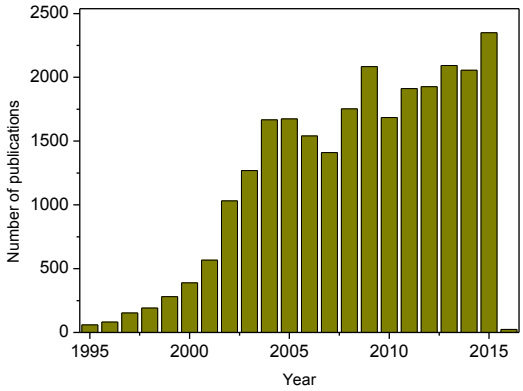

Figure 3. Evolution of the number of publications from the last 20 years in the field of Supramolecular chemistry (Search "Supramolecular chemistry'' as a keyword in Scopus database).

Bridge from Supramolecular Chemistry to Adaptive Chemistry. In *Constitutional Dynamic Chemistry*; Barboiu, M., Ed.; Springer Berlin: Heidelberg, 2012; Vol. 322, pp 1-32.

[13] H.-J. Schneider, *Applications of Supramolecular Chemistry*, CRC Press, 2012.

[14] Erbas-Cakmak, S.; Leigh, D. A.; McTernan, C. T.; Nussbaumer, A. L., Artificial Molecular Machines. *Chem. Rev.* **2015**, *115*, 10081-10206.

[15] a) Fabbrizzi, L.; Poggi, A., Sensors and switches from supramolecular chemistry. *Chem. Soc. Rev.* **1995**, *24*, 197-202; b) Anslyn, E. V., Supramolecular Analytical Chemistry. *J. Org. Chem.* **2007**, *72*, 687-699.

[16] Ling. X. Y.; Reinhoudt, D. N.; Huskens. J., From supramolecular chemistry to nanotechnology: Assembly of 3D nanostructures. *Pure Appl. Chem.* **2009**, *81*, 2225–2233.

[17] Kawakami, K.; Ebara, M.; Izawa, H.; Sanchez-Ballester, N. M.; Hill, J. P.; Ariga, K., Supramolecular Approaches for Drug Development. *Curr. Med. Chem.* **2012**, *19*, 2388-2398.

[18] Semeraro, M.; Baroncini, M.; Credi, A., Binary Logic with Synthetic Molecular and Supramolecular Species. In *Molecular and Supramolecular Information Processing*, Wiley-VCH Verlag GmbH & Co. KGaA: 2012; pp 25-52.

[19] Ling, J.; Daly, B.; Silverson, V. A. D.; de Silva, A. P., Taking baby steps in molecular logic-based computation. *Chem. Commun.* **2015**, *51*, 8403-8409.

The present thesis is outlined within supramolecular chemistry and more specifically in the field of molecular recognition of metal cations. The following chapters describe the synthesis and study of new pseudopeptidic supramolecular systems as well as their application in molecular recognition.

1.2 Pseudopeptidic compounds in Supramolecular Chemistry

Amino acids are the basic elements used by nature to construct complex systems. Although a limited number of amino acids are used, their combination forming long peptidic chains allows the building of an infinite number of structures. The generation of a precise functional structure usually requires large individual macromolecules, for which, however, the activity can be associated with a small specific peptidic fragment. Thus, the building of small model compounds has been used for the understanding of the structural parameters and factors determining the properties of interest in proteins and peptides.[20]

Ideally, however, the combination of natural and non-natural components, properly designed using the knowledge gathered from natural systems, could achieve the desired functionality with low molecular weight molecules. Thus, development of new ligands based on the presence of amino acid subunits is a fundamental approach to mimic proteins and peptides.[21] In this regard, the first examples of simple pseudopeptidic systems with C_2 symmetry as metal ligands in the field of supramolecular chemistry appeared in the 1990s and were reported by Burrows,[22] Kilburn,[23] Hamilton[24] and others.[25] Such studies revealed the potential of metal complexes of pseudopeptides as biomimetic metalloenzymes. Some

[20] Wu, Y.-D.; Gellman, S., Peptidomimetics. *Acc. Chem. Res.* **2008**, *41*, 1231-1232.
[21] a) Luis, S. V.; Alfonso, I., Bioinspired Chemistry Based on Minimalistic Pseudopeptides. *Acc. Chem. Res.* **2014**, *47*, 112-124; b) Alfonso, I., From simplicity to complex systems with bioinspired pseudopeptides. *Chem. Commun.* **2016**, *52*, 239-250.
[22] Wagler, T. R.; Fang, Y.; Burrows, C. J., Optically active difunctionalized dioxocyclam macrocycles: ligands for nickel-catalyzed oxidation of alkenes. *J. Org. Chem.* **1989**, *54*, 1584-1589.
[23] Fessmann, T.; Kilburn, J. D., Identification of Sequence-Selective Receptors for Peptides with a Carboxylic Acid Terminus. *Angew. Chem., Int. Ed.* **1999**, *38*, 1993-1996.
[24] Hopkins, R. B.; Albert, J. S.; Van Engen, D.; Hamilton, A. D., Synthesis and structure of chiral macrocycles containing 2,2′-bipyridine subunits. *Bioorg. Med. Chem.* **1996**, *4*, 1121-1128.
[25] Still, W. C., Discovery of Sequence-Selective Peptide Binding by Synthetic Receptors Using Encoded Combinatorial Libraries. *Acc. Chem. Res.* **1996**, *29*, 155-163.

years later, for instance, Polt *et al* studied the applications of compounds derived from bis(imino amides) containing an aromatic spacer derived from 1,2-diaminobenzene in diethylzinc addition reactions to benzaldehyde (Figure 4).[26]

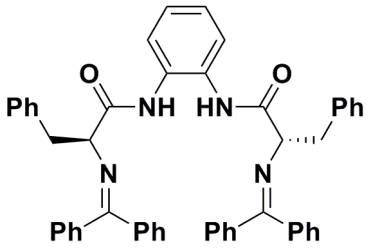

Figure 4. The structure of the ligand studied by Polt *et al*.

Within this context, our group has been working with different families of pseudopeptidic systems, most of them with C_2 symmetry, prepared by a combination of structural subunits derived from amino acids with abiotic units not present in natural peptides and proteins. These systems can have both open-chain structures of type I and macrocyclic structures of type II and III (Figure 5). For the synthesis of the macrocyclic pesudopeptides II and III, the corresponding macrocyclization processes have been based on the preorganization induced by conformational elements,[27] configurational factors,[28] or through the use of anionic templates.[29]

[26] a) Dangel, B.; Clarke, M.; Haley, J.; Sames, D.; Polt, R., Amino Acid-Derived Ligands for Transition Metals: Catalysis via a Minimalist Interpretation of a Metalloprotein. *J. Am. Chem. Soc.* **1997**, *119*, 10865-10866; b) Polt, R.; Kelly, B. D.; Dangel, B. D.; Tadikonda, U. B.; Ross, R. E.; Raitsimring, A. M.; Astashkin, A. V., Optically Active 4- and 5-Coordinate Transition Metal Complexes of Bifurcated Dipeptide Schiff Bases. *Inorg. Chem.* **2003**, *42*, 566-574; c) Dangel, B. D.; Polt, R., Catalysis by Amino Acid-Derived Tetra coordinate Complexes: Enantioselective Addition of Dialkylzincs to Aliphatic and Aromatic Aldehydes. *Org. Lett.* **2000**, *2*, 3003-3006.

[27] a) Adrián, F.; Burguete, M. I.; Luis, S. V.; Miravet, J. F.; Querol, M.; García-España, E., An efficient β-turn directed cyclization of simple peptidomimetics. *Tetrahedron Lett.* **1999**, *40*, 1039-1040; b) Becerril, J.; Bolte, M.; Burguete, M. I.; Galindo, F.; García-España, E.; Luis, S. V.; Miravet, J. F., Efficient Macrocyclization of U-Turn Preorganized Peptidomimetics: The Role of Intramolecular H-Bond and Solvophobic Effects. *J. Am. Chem. Soc.* **2003**, *125*, 6677-6686.

[28] a) Bru, M.; Alfonso, I.; Burguete, M. I.; Luis, S. V., Efficient syntheses of new chiral peptidomimetic macrocycles through a configurationally driven preorganization. *Tetrahedron Lett.* **2005**, *46*, 7781-7785; b) Alfonso, I.; Bolte, M.; Bru, M.; Burguete, M. I.; Luis, S. V., Designed Folding of Pseudopeptides: The Transformation of a Configurationally Driven Preorganization into a Stereoselective Multicomponent Macrocyclization Reaction. *Chem. - Eur. J.* **2008**, *14*, 8879-8891.

[29] a) Martí-Centelles, V.; Pandey, M. D.; Burguete, M. I.; Luis, S. V., Macrocyclization Reactions: The Importance of Conformational, Configurational, and Template-Induced Preorganization. *Chem. Rev.*

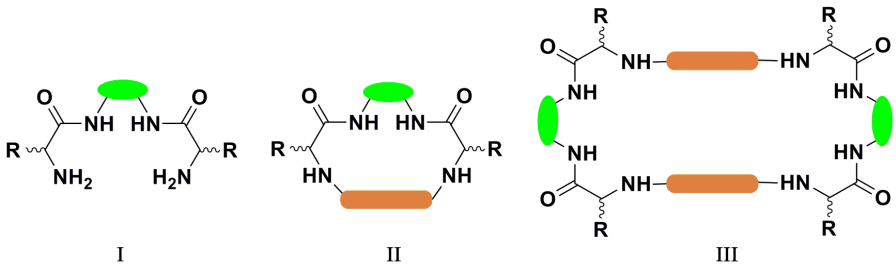

Figure 5. Structural variables in bis(amino amide) receptors.

These compounds represent an attractive family of tetradentate ligands with C_2 symmetry that can be easily prepared by standard and simple synthetic protocols. They contain two kinds of nitrogen atoms, with different coordination capabilities, connected through a chiral backbone. Amine and amide functionalities can be involved in electrostatic and H-bonding interactions (Figure 6).

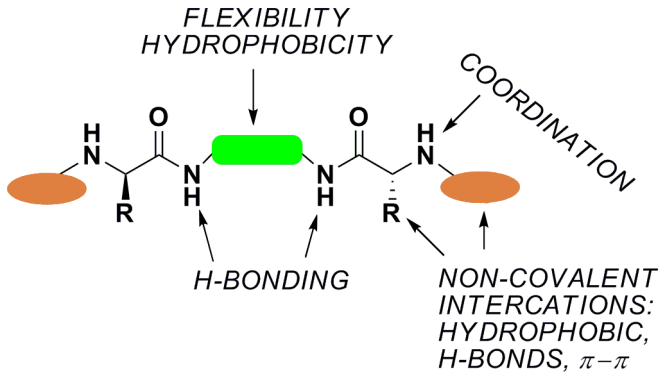

Figure 6. The general structure of C_2-symmetric bis(amino amides).[21]

The possibility of carrying out in a simple manner a structural modification on the basic structure of the pseudopeptide through various alternative

2015, *115*, 8736-8834; b) Bru, M.; Alfonso, I.; Burguete, M. I.; Luis, S. V., Anion-Templated Syntheses of Pseudopeptidic Macrocycles. *Angew. Chem., Int. Ed.* **2006**, *45*, 6155-6159; c) Alfonso, I.; Bolte, M.; Bru, M.; Burguete, M. I.; Luis, S. V.; Rubio, J., Supramolecular Control for the Modular Synthesis of Pseudopeptidic Macrocycles through an Anion-Templated Reaction. *J. Am. Chem. Soc.* **2008**, *130*, 6137-6144; d) Martí-Centelles, V.; Burguete, M. I.; Luis, S. V., Macrocycle Synthesis by Chloride Templated Amide Bond Formation. *J. Org. Chem.* **2016**, *81*, 2143–2147.

approaches represents one of the major potentials of these compounds. Thus, their properties can be easily tuned by the selection of the appropriate amino acid residue, the N-substitution and the nature and flexibility of the spacer.

Some of those systems have been able to display interesting features, behaving as organogelators[30] or acting as '*in vivo*' fluorescent pH probes.[31] They are also capable of acting as selective receptors for substrates of biological relevance,[32] as minimalistic molecular machines,[33] as ligands for

[30] a) Becerril, J.; Escuder, B.; Miravet, J. F.; Gavara, R.; Luis, S. V., Understanding the Expression of Molecular Chirality in the Self-Assembly of a Peptidomimetic Organogelator. *Eur. J. Org. Chem.* **2005**, *2005*, 481-485; b) Becerril, J.; Burguete, M. I.; Escuder, B.; Luis, S. V.; Miravet, J. F.; Querol, M., Minimalist peptidomimetic cyclophanes as strong organogelators. *Chem. Commun.* **2002**, 738-739; c) Becerril, J.; Burguete, M. I.; Escuder, B.; Galindo, F.; Gavara, R.; Miravet, J. F.; Luis, S. V.; Peris, G., Self-Assembly of Small Peptidomimetic Cyclophanes. *Chem. - Eur. J.* **2004**, *10*, 3879-3890; d) Burguete, M. I.; Galindo, F.; Gavara, R.; Izquierdo, M. A.; Lima, J. C.; Luis, S. V.; Parola, A. J.; Pina, F., Use of Fluorescence Spectroscopy To Study Polymeric Materials with Porous Structure Based on Imprinting by Self-Assembled Fibrillar Networks. *Langmuir* **2008**, *24*, 9795-9803; e) Burguete, M. I.; Izquierdo, M. A.; Galindo, F.; Luis, S. V., Time resolved fluorescence of naproxen in organogel medium. *Chem. Phys. Lett.* **2008**, *460*, 503-506.

[31] a) Saura, A. V.; Marin, M. J.; Burguete, M. I.; Russell, D. A.; Galindo, F.; Luis, S. V., The synthesis of new fluorescent bichromophoric compounds as ratiometric pH probes for intracellular measurements. *Org. Biomol. Chem.* **2015**, *13*, 7736-7749; b) Wadhavane, P. D.; Izquierdo, M. A.; Lutters, D.; Burguete, M. I.; Marin, M. J.; Russell, D. A.; Galindo, F.; Luis, S. V., Fluorescent macrocyclic probes with pendant functional groups as markers of acidic organelles within live cells. *Org. Biomol. Chem.* **2014**, *12*, 823-831; c) Galindo, F.; Burguete, M. I.; Vigara, L.; Luis, S. V.; Kabir, N.; Gavrilovic, J.; Russell, D. A., Synthetic Macrocyclic Peptidomimetics as Tunable pH Probes for the Fluorescence Imaging of Acidic Organelles in Live Cells. *Angew. Chem., Int. Ed.* **2005**, *44*, 6504-6508.

[32] a) Burguete, M. I.; Galindo, F.; Izquierdo, M. A.; Luis, S. V.; Vigara, L., Novel peptidomimetic macrocycles showing exciplex fluorescence. *Tetrahedron* **2007**, *63*, 9493-9501; b) Alfonso, I.; Burguete, M. I.; Galindo, F.; Luis, S. V.; Vigara, L., Unraveling the Molecular Recognition of Amino Acid Derivatives by a Pseudopeptidic Macrocycle: ESI-MS, NMR, Fluorescence, and Modeling Studies. *J. Org. Chem.* **2009**, *74*, 6130-6142; c) Burguete, M. I.; Galindo, F.; Luis, S. V.; Vigara, L., Ratiometric fluorescence sensing of phenylalanine derivatives by synthetic macrocyclic receptors. *J. Photochem. Photobiol., A* **2010**, *209*, 61-67; d) Martí-Centelles, V.; Izquierdo, M. A.; Burguete, M. I.; Galindo, F.; Luis, S. V., Recognition of Free Tryptophan in Water by Synthetic Pseudopeptides: Fluorescence and Thermodynamic Studies. *Chem. - Eur. J.* **2014**, *20*, 7465-7478.

[33] a) Alfonso, I.; Burguete, M. I.; Luis, S. V., A Hydrogen-Bonding-Modulated Molecular Rotor: Environmental Effect in the Conformational Stability of Peptidomimetic Macrocyclic Cyclophanes. *J. Org. Chem.* **2006**, *71*, 2242-2250; b) Alfonso, I.; Burguete, M. I.; Galindo, F.; Luis, S. V.; Vigara, L., Molecular Rotors as Simple Models to Study Amide NH−Aromatic Interactions and Their Role in the Folding of Peptide-like Structures. *J. Org. Chem.* **2007**, *72*, 7947-7956.

the preparation of enantioselective catalysts[34] or as chiral solvating agents.[35]

More recently complex structures of pseudopeptidic cages derived from tris(amido amines) ligands have been synthesized for the selective encapsulation of chloride ions. The chloride anion perfectly fits within the cage cavity and could transport chloride through lipid bilayers as models of cell membranes (Figure 7).[36]

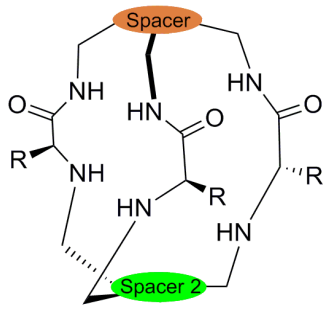

Figure 7. The general structure of tripodal pseudopeptidic cages.[36]

In the same way, pseudopeptidic cage receptors of larger size have shown to be able to act as receptors for *N*-protected dipeptides (Figure 8).[37]

[34] Adrián, F.; Burguete, M. I.; Fraile, J. M.; García, J. I.; García, J.; García-España, E.; Luis, S. V.; Mayoral, J. A.; Royo, A. J.; Sánchez, M. C., Homogeneous and Supported Copper Complexes of Cyclic and Open-Chain Polynitrogenated Ligands as Catalysts of Cyclopropanation Reactions. *Eur. J. Inorg. Chem.* **1999**, *1999*, 2347-2354.

[35] Altava, B.; Burguete, M. I.; Carbó, N.; Escorihuela, J.; Luis, S. V., Chiral bis(amino amides) as chiral solvating agents for enantiomeric excess determination of α-hydroxy and arylpropionic acids. *Tetrahedron: Asymmetry* **2010**, *21*, 982-989.

[36] a) Martí, I.; Rubio, J.; Bolte, M.; Burguete, M. I.; Vicent, C.; Quesada, R.; Alfonso, I.; Luis, S. V., Tuning Chloride Binding, Encapsulation, and Transport by Peripheral Substitution of Pseudopeptidic Tripodal Small Cages. *Chem. - Eur. J.* **2012**, *18*, 16728-16741; b) Martí, I.; Bolte, M.; Burguete, M. I.; Vicent, C.; Alfonso, I.; Luis, S. V., Tight and Selective Caging of Chloride Ions by a Pseudopeptidic Host. *Chem. - Eur. J.* **2014**, *20*, 7458-7464.

[37] a) Faggi, E.; Moure, A.; Bolte, M.; Vicent, C.; Luis, S. V.; Alfonso, I., Pseudopeptidic Cages as Receptors for N-Protected Dipeptides. *J. Org. Chem.* **2014**, *79*, 4590-4601; b) Faggi, E.; Vicent, C.; Luis, S. V.; Alfonso, I., Stereoselective recognition of the Ac-Glu-Tyr-OH dipeptide by pseudopeptidic cages. *Org. Biomol. Chem.* **2015**, *13*, 11721-11731.

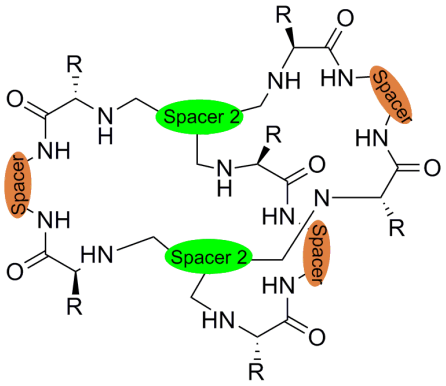

Figure 8. The general structure of large pseudopeptidic cages.[37]

1.2.1 Metal Complexes of Pseudopeptidic Compounds

The design and synthesis of ligands functionalized to achieve metal complexation in a biomimetic approach is a challenge of current interest.[38] The inclusion of amino acid residues in the structure is one of the clearest strategies to provide coordination environments of the metal ions similar to those found in metalloproteins.[39] On the other hand, the presence of chirality derived from the amino acid subunits allows the potential application of those derivatives in enantioselective catalysis to be considered.[40]

[38] a) Miyake, H.; Kojima, Y., Macrocyclic pseudopeptides containing N,N′-ethylene-bridged-dipeptide units: synthesis, binding properties toward metal and organic ammonium cations, and conformations. The first step in designing artificial metalloproteins. *Coord. Chem. Rev.* **1996**, *148*, 301-314; b) Bazzicalupi, C.; Bianchi, A.; García-España, E.; Delgado-Pinar, E., Metals in supramolecular chemistry. *Inorg. Chim. Acta* **2014**, *417*, 3-26.

[39] a) Burke, S. K.; Xu, Y.; Margerum, D. W., Cu(II)Gly2HisGly Oxidation by H_2O_2/Ascorbic Acid to the Cu(III) Complex and Its Subsequent Decay to Alkene Peptides. *Inorg. Chem.* **2003**, *42*, 5807-5817; b) Green, B. J.; Tesfai, T. M.; Xie, Y.; Margerum, D. W., Oxidative Self-Decomposition of the Nickel(III) Complex of Glycylglycyl-l-histidylglycine. *Inorg. Chem.* **2004**, *43*, 1463-1471; c) Green, B. J.; Tesfai, T. M.; Margerum, D. W., Nickel(III) oxidation of its glycylglycylhistamine complex. *Dalton Trans.* **2004**, 3508-3514; d) Tesfai, T. M.; Green, B. J.; Margerum, D. W., Decomposition Kinetics of Ni(III)−Peptide Complexes with Histidine and Histamine as the Third Residue. *Inorg. Chem.* **2004**, *43*, 6726-6733; e) Kizirian, J.-C., Chiral Tertiary Diamines in Asymmetric Synthesis. *Chem. Rev.* **2008**, *108*, 140-205; f) Prell, J. S.; Flick, T. G.; Oomens, J.; Berden, G.; Williams, E. R., Coordination of Trivalent Metal Cations to Peptides: Results from IRMPD Spectroscopy and Theory. *J. Phys. Chem. A* **2010**, *114*, 854-860; g) Sharma, S. K.; Hundal, G.; Gupta, R., The Effect of Ligand Architecture on the Structure and Properties of Nickel and Copper Complexes of Amide-Based Macrocycles. *Eur. J. Inorg. Chem.* **2010**, *2010*, 621-636

[40] a) Burguete, M. I.; Collado, M.; Escorihuela, J.; Luis, S. V., Efficient Chirality Switching in the Addition of Diethylzinc to Aldehydes in the Presence of Simple Chiral α-Amino Amides. *Angew. Chem., Int. Ed.* **2007**, *46*, 9002-9005; b) Burguete, M. I.; Escorihuela, J.; Luis, S. V.; Lledós, A.;

In this regard, pseudopeptidic compounds are excellent candidates for forming metal complexes with transition metals. The ability of pseudopeptidic bis(amino amide) compounds and other related systems to form metal complexes through the involvement of the amino and amide groups has been demonstrated in recent years.[41] Depending on the nature of the central spacer, different metal coordination modes can be obtained as illustrated in Figure 9.

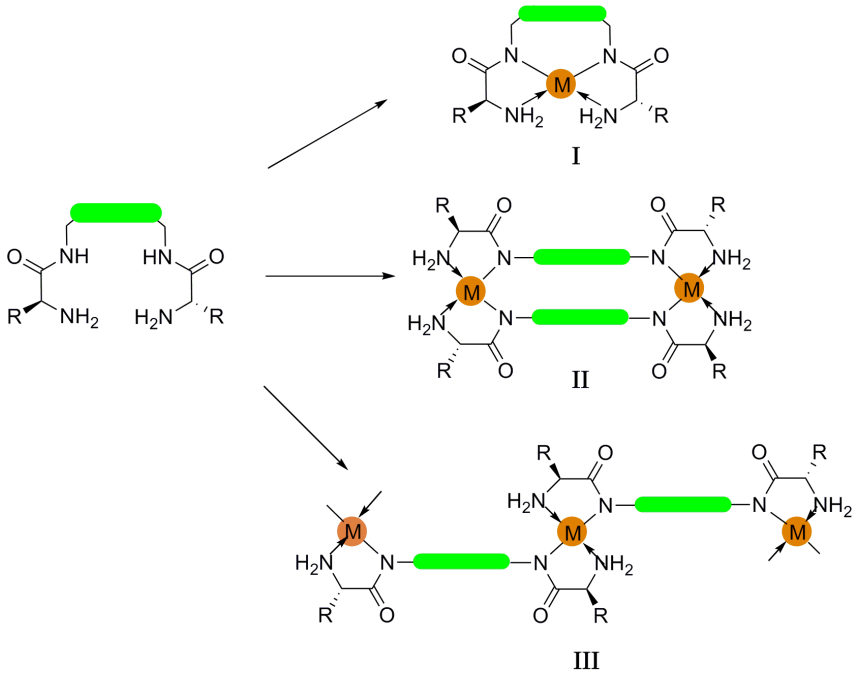

Figure 9. Possible coordination of metals with pseudopeptidic ligands.[42]

Ujaque, G., New chiral tetraaza ligands for the efficient enantioselective addition of dialkylzinc to aromatic aldehydes. *Tetrahedron* **2008**, *64*, 9717-9724.

[41] a) Blasco, S.; Burguete, M. I.; Clares, M. P.; García-España, E.; Escorihuela, J.; Luis, S. V., Coordination of Cu^{2+} Ions to C_2 Symmetric Pseudopeptides Derived from Valine. *Inorg. Chem.* **2010**, *49*, 7841-7852; b) Marti, I.; Ferrer, A.; Escorihuela, J.; Burguete, M. I.; Luis, S. V., Copper(II) complexes of bis(amino amide) ligands: effect of changes in the amino acid residue. *Dalton Trans.* **2012**, *41*, 6764-6776.

[42] Marti-Centelles, V.; Kumar, D. K.; White, A. J. P.; Luis, S. V.; Vilar, R., Zinc(II) coordination polymers with pseudopeptidic ligands. *CrystEngComm* **2011**, *13*, 6997-7008.

1.3 Supramolecular Interactions

The non-covalent bonding interactions are relatively weaker than covalent bonds and play an important role in supramolecular chemistry by creating huge attractive and repulsive effects, in particular when large surfaces and multiple interactions are involved. These interactions are very important not only considering host-guest systems, but also their surroundings.[43] Many research groups have focused on such reversible multi-bond interactions to acquire a better understanding of the complex systems in biology. Such interactions include electrostatic, H-bonding, π-interactions and are detailed in Table 1 below.

Table 1. Main types of supramolecular interactions.

Interaction	**Direction**	**Bond energy** (kJ mol^{-1})	**Examples**
Ion-Ion	Non-directional	100-350	NaCl
Ion-Dipole	Partially directional	50-200	K^+ - Crown ether
Dipole-Dipole	Partially directional	5-50	Groups –C≡N–
Hydrogen Bonding	Directional	4-120	Carboxylic acid dimers
Cation-π	Directional	5-80	Lariat crown ethers[44]
Anion-π	Directional	2-40	Hexafluoro benzene[45]

[43] Schneider, H.-J., Binding Mechanisms in Supramolecular Complexes. *Angew. Chem., Int. Ed.* **2009**, *48*, 3924-3977.

[44] a) Gokel, G. W.; Barbour, L. J.; Ferdani, R.; Hu, J., Lariat Ether Receptor Systems Show Experimental Evidence for Alkali Metal Cation-π Interactions. *Acc. Chem. Res.* **2002**, *35*, 878-886; b) De Wall, S. L.; Meadows, E. S.; Barbour, L. J.; Gokel, G. W., Synthetic receptors as models for alkali metal cation-π binding sites in proteins. *Proc. Natl. Acad. Sci.* **2000**, *97*, 6271-6276.

[45] Quiñonero, D.; Garau, C.; Rotger, C.; Frontera, A.; Ballester, P.; Costa, A.; Deyà, P. M., Anion–π Interactions: Do They Exist? *Angew. Chem., Int. Ed.* **2002**, *41*, 3389-3392.

π-π	Directional	2-50	Benzene and DNA
Metal coordination	Directional	100-300	Pyridine-Metal
Van der Waals	Non-directional	<5	Inclusion compounds
Halogen bonds	Directional	~200	Pseudorotaxanes, Catenanes[46]

1.3.1 Electrostatic interactions

Electrostatic interactions such as ion-ion, ion-dipole, and dipole-dipole interactions are based on the Coulomb attraction between opposite charges. Among these interactions ion-ion are non-directional interactions. The high strength of electrostatic interactions has made them an optimized tool for achieving strong binding.[47] Solvation of a metal cation and complexes of alkali metal cations with macrocyclic ethers termed as crown ethers are classical examples of electrostatic interactions normally found in supramolecular chemistry (Figure 10).

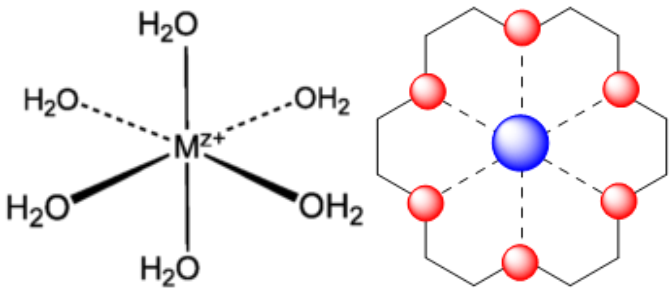

Figure 10. Electrostatic interactions in an aqua metallic complex (left) and a crown ether structure interacting with a metal (right).

[46] Gilday, L. C.; Robinson, S. W.; Barendt, T. A.; Langton, M. J.; Mullaney, B. R.; Beer, P. D., Halogen Bonding in Supramolecular Chemistry. *Chem. Rev.* **2015**, *115*, 7118-7195.
[47] Adamczyk, Z., Electrostatic Interactions. *Encyclopedia of Colloid and Interface Science*, Springer: Berlin, Heidelberg, 2013.

1.3.2 Hydrogen bonding

The hydrogen bonding can be considered as a special case of dipole-dipole interaction, where a hydrogen atom attached to an electronegative atom (or electron attractive group) is attracted to a neighboring dipole on an adjacent molecule or functional group.[48] It has been termed as ‘‘the key interaction in supramolecular chemistry’’ because of its relatively strong and highly directional nature.

Hydrogen bonding plays an important role in both stabilizing the final structure of the proteins or DNA double helices and in the case of interaction of anions or neutral species with synthetic ligand systems (Figure 11).

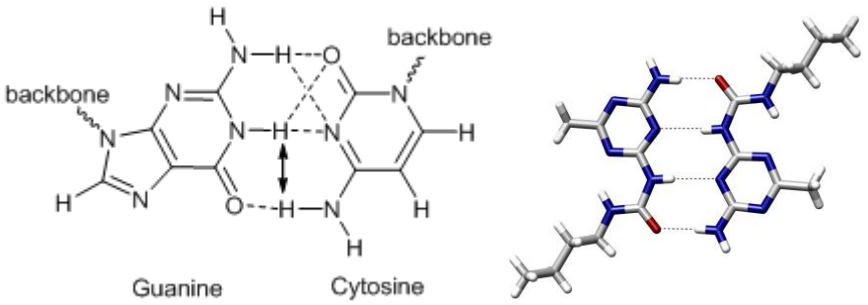

Figure 11. Hydrogen bond interactions between guanine and cytosine base pairs in DNA (left) and a self-assembled dimeric complex stabilized by hydrogen bonds (right).[49] The hydrogen bonds are represented by dotted lines.

1.3.3 π-system interactions

Interactions based on π-system (π-effects) refer to the set of non-covalent interactions that involve π-systems, often in situations where the π system is relatively electron rich or electron poor. These interactions just resemble an electrostatic interaction in which the electron-rich or electron-poor π system interacts with a metal (cationic or neutral), an anion, another molecule and even another π system, and are known to be pivotal for biological events such as protein-ligand recognition and for effective drug

[48] Jeffrey, G. A. *An Introduction to Hydrogen Bonding*; Oxford University Press: Oxford, 1997.
[49] Beijer, F. H.; Kooijman, H.; Spek, A. L.; Sijbesma, R. P.; Meijer, E. W., Self-Complementarity Achieved through Quadruple Hydrogen Bonding. *Angew. Chem., Int. Ed.* **1998**, *37*, 75-78.

design. The complex of the enzyme acetylcholinesterase (AChE) with the drug E2020 (Aricept), which was developed to treat symptoms of Alzheimer's disease, is one example of the diversity of this type of interactions (Figure 12).[50]

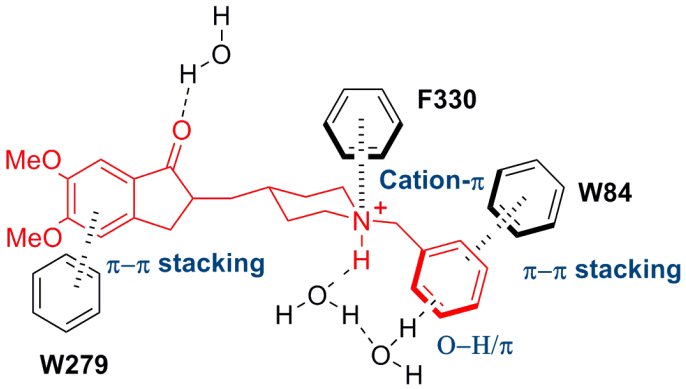

Figure 12. π-system interactions in the acetylcholinesterase (AChE) enzyme complex with the drug E2020.[50]

1.3.4 Metal coordination

In coordination complexes, the metal ions are coordinated with a regular polyhedron of ligands by its dative bonds. The lone pair of ligand electrons forms a dative bond to a metal cation, having this interaction a non-covalent nature. The coordination bond, in the field of inorganic chemistry, provides a variety of elements for defining the functionality in the generation of supramolecular structures as are the coordination number, the presence of different donor atoms or the use of polydentate chelating ligands. The geometric requirements of metal ions, combined with the design of specific ligands have permitted the construction of functional complex supramolecular assemblies.[51]

1.3.5 Van der Waals forces

Van der Waals forces are defined as interactions arising from the polarization of an electron cloud by the proximity of an adjacent nucleus,

[50] Meyer, E. A.; Castellano, R. K.; Diederich, F., Interactions with Aromatic Rings in Chemical and Biological Recognition. *Angew. Chem., Int. Ed.* **2003**, *42*, 1210-1250.
[51] Chakrabarty, R.; Mukherjee, P. S.; Stang, P. J., Supramolecular Coordination: Self-Assembly of Finite Two- and Three-Dimensional Ensembles. *Chem. Rev.* **2011**, *111*, 6810-6918.

resulting in a weak electrostatic attraction.[52] These forces are nondirectional, weaker than electrostatic interactions which provide additional enthalpy stabilization to the coordination of a guest into a host molecule. Inclusion compounds are one of the suitable examples for such type of forces in supramolecular chemistry.[53]

1.3.6 Crystal close packing

The solid state crystal structures of compounds can be described geometrically in terms of a close-packing arrangement, which are held together by non-covalent interactions. In the final structure, a maximum number of contacts will be achieved with other adjacent molecules leading to stabilizing the final structure. In supramolecular chemistry many crystal structures which have large ions are closely packed with the smaller ions filling the spaces in between them have shown very useful properties in molecular recognition and catalysis. In crystallography, the volumes of filled space are known as the packing coefficient (PC). The PC of a compound is defined as the ratio between the sum (V_W) of the van der Waals volumes (v_W) of the *n* molecules in a given volume (V) and the volume (V) (Equation 1).

$$PC = \frac{V\mathrm{w}}{V} \qquad \text{(Equation 1)}$$

Thus, PC of a supramolecular complex can predict the formation of an ideal host-guest complex which is reported by Rebek *et al* in molecular capsules and in the container molecules.[54]

1.3.7 Hydrophobic and solvent effect

The hydrophobic effect is an important specific driving force for the association of apolar substances that tend to aggregate in an aqueous solution excluding concomitantly water molecules from their solvation sphere. Water molecules around the apolar substances of a hydrophobic cavity arrange themselves to form a structured system. Upon guest complexation, the water molecules are released and become disordered

[52] Parsegian, V. A., *Van der Waals Forces: A Handbook for Biologists, Chemists, Engineers and Physicists*, Cambridge University Press, New York, 2006.
[53] Frank, S. G., Inclusion compounds. *J. Pharm. Sci.* **1975**, *64*, 1585-1604.
[54] Mecozzi, S.; Rebek, J. J., The 55 % Solution: A Formula for Molecular Recognition in the Liquid State. *Chem. - Eur. J.* **1998**, *4*, 1016-1022.

which results in a favorable increase of the entropy (Figure 13).[55] Thus, receptors containing hydrophobic interior cavities are designed to encapsulate organic guest molecules in aqueous solution. The hydrophobic effect is seen as the driving force for a variety of phenomena, such as the formation of micelles, protein folding and poor solubility of non-polar solvent in aqueous media.[56] Ideally, the reverse situation is also possible for polar entities in apolar solvents.

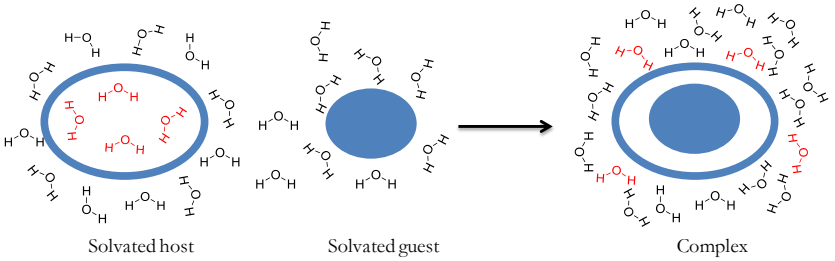

Figure 13. Hydrophobic binding of organic guests by a hydrophobic host in aqueous solution.

The proper selection of solvent is also playing an important role in the recognition processes, and solvent effects can be very important when the solvent molecules strongly solvate either the host, the guest or the complex, this can have a significant effect on the final host-guest equilibrium.[57]

1.4 Self-Assembly

Self-assembly is a key concept in supramolecular chemistry and can be defined as the spontaneous and reversible non-covalent association of molecules or ions to form larger, more complex supramolecular entities according to the intrinsic information contained in the molecules themselves.[2] Self-assembly process can occur with the components having sizes from molecular to macroscopic, using reversible, non-covalent

[55] Southall, N. T.; Dill, K. A.; Haymet, A. D. J., A View of the Hydrophobic Effect. *J. Phys. Chem. B* **2002**, *106*, 521-533.
[56] a) Thangavel, A.; Rawashdeh, A. M. M.; Sotiriou-Leventis, C.; Leventis, N., Simultaneous Electron Transfer from Free and Intercalated 4-Benzoylpyridinium Cations in Cucurbit[7]uril. *Org. Lett.* **2009**, *11*, 1595-1598; b) Anslyn, E. V.; Dougherty, D. A. *Modern Physical Organic Chemistry*; University Science Books: Sausalito, 2006, pp 189-194, 207-241.
[57] Sommer, F.; Kubik, S., Anion binding of a neutral bis(cyclopeptide) in water-methanol mixtures containing up to 95% water. *Org. Biomol. Chem.* **2014**, *12*, 8851-8860.

interactions, and the process is always in dynamic equilibrium. Much of the work in self-assembly has focused on molecular components, and many of the most interesting applications of self-assembling processes can be found in the larger sizes (from nanometers to micrometers) as they represent the most promising and efficient, even from a sustainability perspective, bottom-up approach to constructing nanotechnology systems.[58]

Self-assembly processes exist widely in nature that uses them to generate functional systems. Probably, the most significant example in nature is the formation of the DNA double helix from two complementary strands of oligonucleostrands. The two chains are held together to maintain the double helical structure by hydrogen bonds between purine and pyrimidine bases and other intermolecular forces (Figure 14).[59]

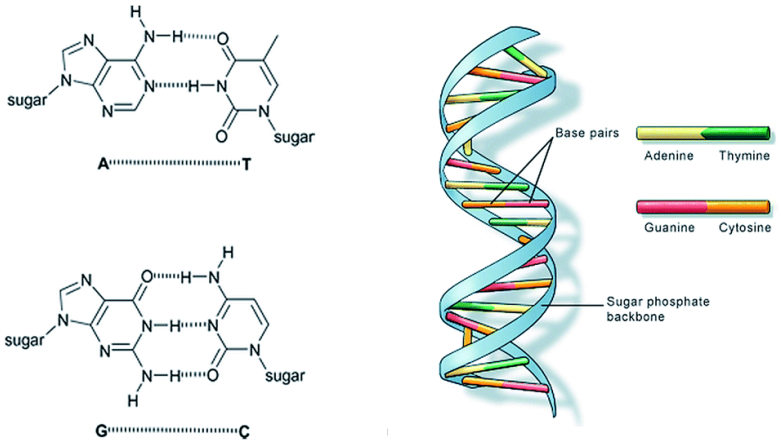

(a) (b)

Figure 14. The DNA-double helix chemical composition and structure. (a) Complementary nucleotide bases: adenine (A) and thymine (T), and guanine (G) and cytosine (C); (b) The double-stranded DNA-helix.[60]

[58] Whitesides, G. M.; Grzybowski, B., Self-Assembly at All Scales. *Science* **2002**, *295*, 2418-2421.
[59] Watson, J. D.; Crick, F. H. C., Molecular structure of nucleic acids: a structure for deoxyribose nucleic acid. *Am. J. Psychiatry* **2003**, *160*, 623-624.
[60] Catherall, T.; Huskisson, D.; McAdams, S.; Vijayaraghavan, A., Self-assembly of one dimensional DNA-templated structures. *J. Mater. Chem. C* **2014**, *2*, 6895-6920.

In proteins as well, the linear polypeptide chain sequences fold into significant secondary structures such as α-helices and β-sheets, held together by amide NH---O=C hydrogen bonding interactions and hydrophobic effects in aqueous solution, and these components can further self-assembly to generate well-defined nanostructures in biological systems (Figure 15).[61]

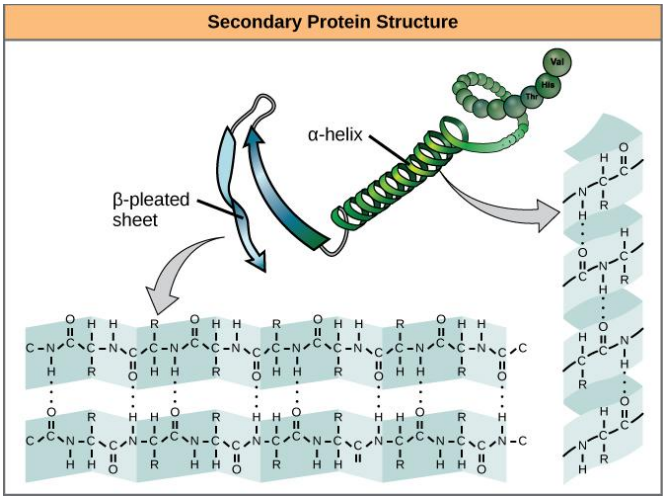

Figure 15. The α-helix and β-pleated sheet are secondary structures of proteins that form because of hydrogen bonding between carbonyl and amino groups in the peptide backbone. Certain amino acids have the propensity to form a α-helix while others have the propensity to form a β-pleated sheet.[61] These structural arrangements further favor the corresponding intermolecular self-assembly.

In abiotic supramolecular chemistry, self-assembly processes mainly relied, in initial studies, on taking advantage of interactions like metal-ligand coordination and hydrogen bonding. One of the earliest examples of molecular self-assembly was provided in the field of metal coordination chemistry and was reported by Curtis showing how Schiff base macrocycles complexed to Ni^{2+} were self-assembled, presumably with the Ni^{2+} cation acting as the template around which the macrocycle is assembled (Scheme 1).[62]

[61] Voet, D.; Voet, J. G. *Biochemistry*; Second Edition ed.; John Wiley & Sons, Inc.: New York, 1994.
[62] Curtis, N. F., The advent of macrocyclic chemistry. *Supramol. Chem.* **2012**, *24*, 439-447.

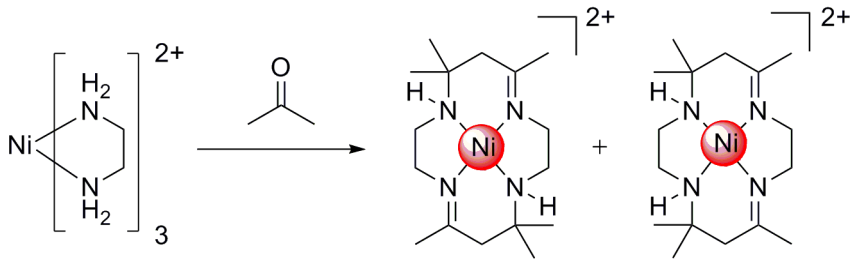

Scheme 1. Schiff's base macrocycle by reaction of acetone with tris(ethylenediamine) Ni^{2+}.[62]

Synthetic receptors containing amine and amide functionalities, by virtue of their H-bonding ability, are also able to self-assemble into more complex structures. Thus, for example, Figure 16 illustrates the H-bonding mediated self-assembly of triamide based receptor molecules, which assemble into large rod-shaped stacks stabilized by hydrogen bonds between the three amide NH groups of one molecule and the amide CO groups of the next molecule in the stack.[63]

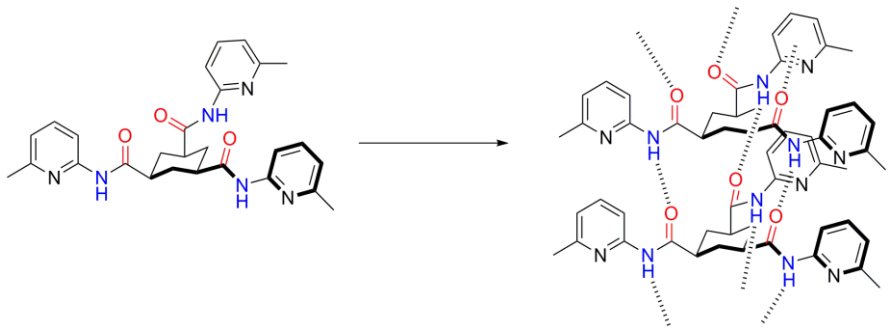

Figure 16. The hydrogen bond directed self-assembly of molecular rods through hydrogen bonding between amide groups.[63]

The use of hydrogen bonds as non-covalent interactions in supramolecular self-assembly was further extended by Rebek *et al*, with the construction of a ''*molecular tennis ball*'' (and related systems) in which a diphenyl

[63] Fan, E.; Yang, J.; Geib, S. J.; Stoner, T. C.; Hopkins, M. D.; Hamilton, A. D., Hydrogen-bonding control of molecular aggregation: self-complementary subunits lead to rod-shaped structures in the solid state. *J. Chem. Soc., Chem. Commun.* **1995**, 1251-1252.

glycoluril subunit is self-complementary and self-associates in solution through the formation of hydrogen bonds to form a dimer having an internal cavity. This dimeric structure is remarkably stable and encapsulates small molecules within these self-assembled cavities (Figure 17). Even catalytic reactions could also be carried out inside the cavity.[64]

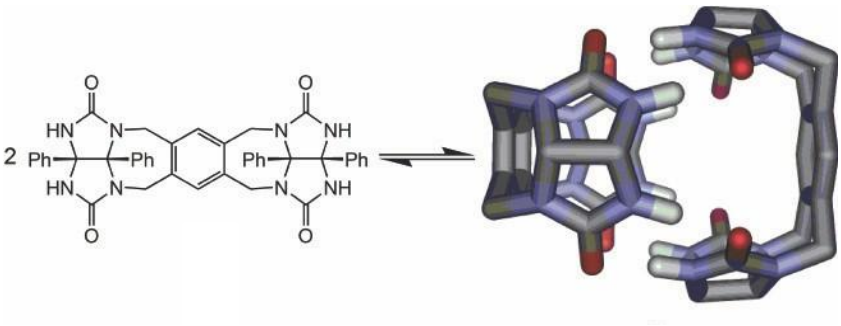

Figure 17. Self-association of a cyclic bis(urea) derivative through hydrogen bonds gives a structure that resembles a tennis ball. The phenyl rings have been omitted for clarity.[65]

In this context, self-assembly has been applied to a large number of different systems in supramolecular chemistry. However, still much research work needs to be focused on such processes to generate well-defined structures and materials with new properties and functionalities.

1.4.1 Metal directed self-assembly

During the last years, coordination chemistry has rapidly developed towards the generation of multicomponent architectures involving several ligands and metal ions, which are connected via intra and intermolecular interaction.[66] Transition metal ions, in particular, have proven to be effective synthetic tools for such processes due to their control over

[64] a) Rebek, J., Reversible Encapsulation and Its Consequences in Solution. *Acc. Chem. Res.* **1999**, *32*, 278-286; b) Hof, F.; Rebek, J., Molecules within molecules: Recognition through self-assembly. *Proc. Natl. Acad. Sci.* **2002**, *99*, 4775-4777.

[65] Palmer, L. C.; Rebek, J. J., The ins and outs of molecular encapsulation. *Org. Biomol. Chem.* **2004**, *2*, 3051-3059.

[66] Hamacek, J.; Borkovec, M.; Piguet, C., Simple thermodynamics for unravelling sophisticated self-assembly processes. *Dalton Trans.* **2006**, 1473-1490.

different geometries and bond strengths depending on the metal ions or ligands utilized in the assembly.[67]

The first example of such metal mediated multicomponent self-assembly was the binuclear Cu^{2+} complex synthesized by Maverick,[68] in which Cu^{2+} ions are assembled with bis (β-diketone) ligands in a cofacial manner. Since then a variety of structures evolved including the generation of helices, grids, and metallomacrocycles with various polygonal structures using a wide variety of metals, which include Pd^{2+}, Pt^{2+} (Fujita and Stang)[69], Os^{2+} (Jeong)[70], Cu^{2+} (Hupp)[71] and Re^{+}, Cu^{+} (Puddephat and Huc).[72]

[67] Bilbeisi, R. A.; Olsen, J.-C.; Charbonnière, L. J.; Trabolsi, A., Self-assembled discrete metal-organic complexes: Recent advances. *Inorg. Chim. Acta* **2014**, *417*, 79-108.

[68] a) Maverick, A. W.; Klavetter, F. E., Cofacial binuclear copper complexes of a bis(beta-diketone) ligand. *Inorg. Chem.* **1984**, *23*, 4129-4130; b) Maverick, A. W.; Buckingham, S. C.; Yao, Q.; Bradbury, J. R.; Stanley, G. G., Intramolecular coordination of bidentate Lewis bases to a cofacial binuclear copper (II) complex. *J. Am. Chem. Soc.* **1986**, *108*, 7430-743; c) Bradbury, J. R.; Hampton, J. L.; Martone, D. P.; Maverick, A. W., Preparation, structure and redox activity of nickel (II), palladium (II), and copper (II) cofacial binuclear bis(beta-keto-enamine) complexes. *Inorg. Chem.* **1989**, *28*, 2392-2399.

[69] a) Fujita, M.; Tominaga, M.; Hori, A.; Therrien, B., Coordination Assemblies from a Pd (II)-Cornered Square Complex. *Acc. Chem. Res.* **2005**, *38*, 369-378; b) Sun, W.-Y.; Yoshizawa, M.; Kusukawa, T.; Fujita, M., Multicomponent metal–ligand self-assembly. *Curr. Opin. Chem. Biol.* **2002**, *6*, 757-764; c) Cao, D. H.; Chen, K.; Fan, J.; Manna, J.; Olenyuk, B.; Whiteford, J. A.; Stang, P. J.; Supramolecular chemistry and molecular design: Self assembly of molecular squares. *Pure Appl. Chem.* **1997**, 69, 1979-1986; d) Leininger, S.; Olenyuk, B.; Stang, P. J., Self-Assembly of Discrete Cyclic Nanostructures Mediated by Transition Metals. *Chem. Rev.* **2000**, *100*, 853-908.

[70] a) Jeong, K.-S.; Cho, Y. L.; Song, J. U.; Chang, H.-Y.; Choi, M.-G., Neutral Macrocyclic Boxes Spontaneously Assembled from Osmium Tetraoxide, Olefin, and Pyridyl Ligand. *J. Am. Chem. Soc.* **1998**, *120*, 10982-10983; b) Jeong, K.-S.; Cho, Y. L.; Chang, S.-Y.; Park, T.-Y.; Song, J. U., Assembly and Binding Properties of Osmate Ester-Bridged Binuclear Macrocycles. *J. Org. Chem.* **1999**, *64*, 9459-9466; c) Jeong, K.-S.; Park, E.-J., Self-Assembly of Interlocked Supramolecular Dendrimers. *J. Org. Chem.* **2004**, *69*, 2618-2621.

[71] a) O'Donnell, J. L.; Zuo, X.; Goshe, A. J.; Sarkisov, L.; Snurr, R. Q.; Hupp, J. T.; Tiede, D. M., Solution-Phase Structural Characterization of Supramolecular Assemblies by Molecular Diffraction. *J. Am. Chem. Soc.* **2007**, *129*, 1578-1585; b) Dinolfo, P. H.; Hupp, J. T., Tetra-Rhenium Molecular Rectangles as Organizational Motifs for the Investigation of Ligand-Centered Mixed Valency: Three Examples of Full Delocalization. *J. Am. Chem. Soc.* **2004**, *126*, 16814-16819; c) Dinolfo, P. H.; Williams, M. E.; Stern, C. L.; Hupp, J. T., Rhenium-Based Molecular Rectangles as Frameworks for Ligand-Centered Mixed Valency and Optical Electron Transfer. *J. Am. Chem. Soc.* **2004**, *126*, 12989-13001; d) Dinolfo, P. H.; Coropceanu, V.; Brédas, J.-L.; Hupp, J. T., A New Class of Mixed-Valence Systems with Orbitally Degenerate Organic Redox Centers. Examples Based on Hexa-Rhenium Molecular Prisms. *J. Am. Chem. Soc.* **2006**, *128*, 12592-12593.

[72] a) Irwin, M. J.; Rendina, L. M.; Vittal, J. J.; Puddephatt, R. J., A strategy for synthesis of large gold rings. *Chem. Commun.* **1996**, 1281-1282; b) Hunks, W. J.; MacDonald, M.-A.; Jennings, M. C.; Puddephatt, R. J., Luminescent Binuclear Gold(I) Ring Complexes. *Organometallics* **2000**, *19*, 5063-5070; c) Hunks, W. J.; Lapierre, J.; Jenkins, H. A.; Puddephatt, R. J., Interpenetrating digold(I) diacetylide macrocycles. *J. Chem. Soc., Dalton Trans.* **2002**, 2885-2889; d) Delsuc, N.; Hutin, M.; Campbell, V. E.; Kauffmann, B.; Nitschke, J. R.; Huc, I., Metal-Directed Dynamic Formation of Tertiary Structure in Foldamer Assemblies: Orienting Helices at an Angle. *Chem. - Eur. J.* **2008**, *14*,

The combination of pyridine ligands with Pt^{2+} and Pd^{2+} complexes to form supramolecular self-assembled structures is one of the more studied systems in recent years. The first preparation of these compounds was exploited by Fujita *et al*, who published the formation of cyclic tetramers known as "*molecular squares*" quantitatively prepared by the simple mixing of 4,4'-bipyridine with *cis*-protected Pd^{2+} [enPd$(NO_3)_2$] in aqueous methanolic solution. In water, the cavity of the complex was a hydrophobic space in which aromatic organic compounds could be embedded, such as 1,3,5-tri methoxybenzene (Figure 18).[73]

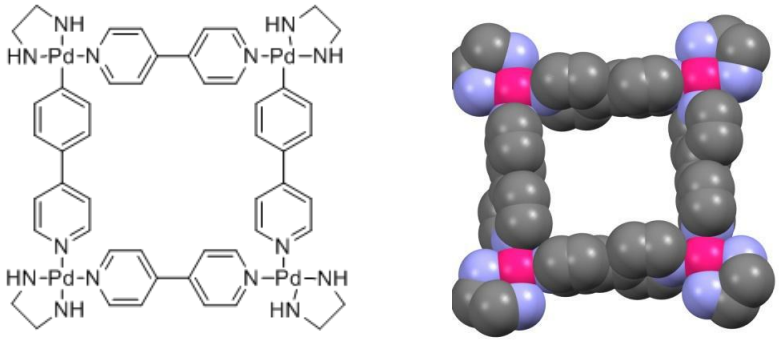

Figure 18. The first metallomacrocyclic structure obtained by Fujita *et al* (left) and the crystal structure showing the central hydrophobic cavity (right).[73]

Lehn *et al* have studied self-selection in a self-recognition oriented metal self-assembly to yield cyclic helicates from different ligand strands and metal ions. The structures containing oligobipyridine [oligo(2,2'-bipyridine] strands in the presence of metal ions spontaneously assemble giving double helical and triple helical structures (Figure 19).[74]

7140-7143; e) Campbell, V. E.; de Hatten, X.; Delsuc, N.; Kauffmann, B.; Huc, I.; Nitschke, J. R., Cascading transformations within a dynamic self-assembled system. *Nat Chem* **2010**, *2*, 684-687.

[73] a) Fujita, M.; Yazaki, J.; Ogura, K., Preparation of a macrocyclic polynuclear complex, [(en)Pd(4,4'-bpy)]$_4$$(NO_3)_8$ (en = ethylenediamine, bpy = bipyridine), which recognizes an organic molecule in aqueous media. *J. Am. Chem. Soc.* **1990**, *112*, 5645-5647; b) Fujita, M.; Yazaki, J.; Ogura, K., Macrocylic polynuclear complexes [(en) M(4,4′-bpy)]$_4$$(NO_3)_8$ (M = Pd or Pt) as "Inorganic Cyclophane." Their Ability for Molecular Recognition. *Tetrahedron Lett.* **1991**, *32*, 5589-5592.

[74] Kramer, R.; Lehn, J. M.; Marquis-Rigault, A., Self-recognition in helicate self-assembly: spontaneous formation of helical metal complexes from mixtures of ligands and metal ions. *Proc. Natl. Acad. Sci.* **1993**, *90*, 5394-5398.

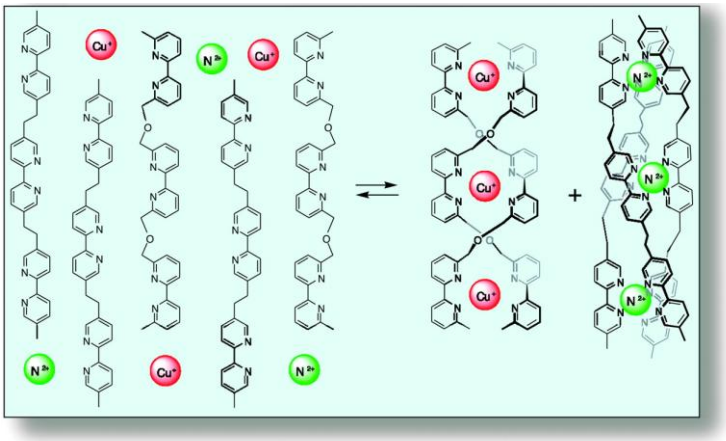

Figure 19. Parallel formation of a double helicate and a triple helicate by oligo(2,2'-bipyridine) strands in the presence of Cu^{+} (red) and Ni^{2+} (green) metal ions.[74]

After the first supramolecular structures published, the studies have been focused on the synthesis of n-dimensional structures with different shapes: triangles, squares, pentagons, hexagons[75] by a suitable selection of ligands and metal centers with appropriate geometric characteristics. However, soon interest arose increasing the complexity of the systems with the goal of obtaining three-dimensional structures such as boxes,[76] cubes,[77] and octahedral cubes.[78] The importance of these three-dimensional structures lies not only in obtaining the structures, representing by themselves a major challenge but also in the great capacity they have shown to act as receptors for different substrates.

[75] a) Stang, P. J.; Persky, N. E.; Manna, J., Molecular Architecture via Coordination: Self-Assembly of Nanoscale Platinum Containing Molecular Hexagons. *J. Am. Chem. Soc.* **1997**, *119*, 4777-4778; b) Yang, H. B.; Das, N.; Huang, F.; Hawkridge, A. M.; Díaz, D. D.; Arif, A. M.; Finn, M. G.; Muddiman, D. C.; Stang, P. J., Incorporation of 2,6-Di(4,4'-dipyridyl)-9-thiabicyclo[3.3.1]nonane into Discrete 2D Supramolecules via Coordination-Driven Self-Assembly. *J. Org. Chem.* **2006**, *71*, 6644-6647.

[76] a) Seidel, S. R.; Stang, P. J., High-Symmetry Coordination Cages via Self-Assembly. *Acc. Chem. Res.* **2002**, *35*, 972-983; b) Takeda, N.; Umemoto, K.; Yamaguchi, K.; Fujita, M., A nanometre-sized hexahedral coordination capsule assembled from 24 components. *Nature* **1999**, *398*, 794-796; c) Nakabayashi, K.; Ozaki, Y.; Kawano, M.; Fujita, M., A Self-Assembled Spin Cage. *Angew. Chem., Int. Ed.* **2008**, *47*, 2046-2048.

[77] Suzuki, K.; Tominaga, M.; Kawano, M.; Fujita, M., Self-assembly of an M_6L_{12} coordination cube. *Chem. Commun.* **2009**, 1638-1640.

[78] a) Olenyuk, B.; Whiteford, J. A.; Fechtenkotter, A.; Stang, P. J., Self-assembly of nanoscale cuboctahedra by coordination chemistry. *Nature* **1999**, *398*, 796-799; b) Ghosh, K.; Hu, J.; White, H. S.; Stang, P. J., Construction of Multifunctional Cuboctahedra via Coordination-Driven Self-Assembly. *J. Am. Chem. Soc.* **2009**, *131*, 6695-6697.

1.5 Molecular recognition: Host-Guest Chemistry

Molecular recognition refers to the selective binding of a substrate molecule (Guest) with the receptor (Host) to produce a host-guest complex or supermolecule through reversible non-covalent interactions. Supermolecules generally comprise a host component (larger in size) with convergent binding sites and a guest component (smaller in size) with divergent binding sites. This phenomenon is also called as *Host-guest chemistry* or *Inclusion phenomenon*, and the intermolecular interactions present between the two species must follow a strong complimentary pattern in good agreement with the lock and key model of enzymatic sites proposed by Emil Fischer which is illustrated in Figure 20.

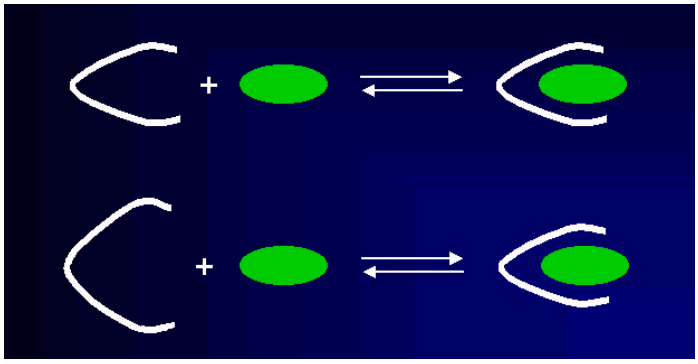

Figure 20. Interaction of an enzyme with a substrate by a lock and key mechanism to give an enzyme-substrate complex (top); Interaction of the enzyme with the substrate by an induced fit mechanism[79] to give the enzyme-substrate complex (bottom).

Host-guest (or receptor-substrate) chemistry is mainly based upon three historical concepts. Firstly, the concept of the *biological receptor*, that was introduced by Paul Ehrlich.[80] Later, Emil Fischer postulated that the binding must be selective, as a part of the study of substrate binding by enzymes, and also suggested that the enzyme-substrate interactions adapt to

[79] Koshland, D. E., The Key-Lock Theory and the Induced Fit Theory. *Angew. Chem., Int. Ed. Engl.* **1995**, *33*, 2375-2378.
[80] Ehrlich, P. *Studies on immunity*, Wiley: New York, 1906.

the *lock and key*[81] principle (Figure 20). This laid the basis for molecular recognition, the discrimination by a host between a number of different guests. Finally, Alfred Werner's theory of *coordination chemistry*, which explains mutual affinity between a substrate and a receptor, was developed.[82] Following Werner's discovery, the field of transition metal coordination chemistry was created and it has had a significant impact on many daily aspects of modern society and on supramolecular chemistry.

The host-guest relationship has also been defined by another supramolecular chemistry scientist, Donald Cram,[83] as follows:

A host-guest relationship involves a complementary stereoelectronic arrangement of binding sites in host and guest… The host component is defined as an organic molecule or ion whose binding sites converge in the complex… The guest component as any molecule or ion whose binding sites diverge in the complex…

1.5.1 Hosts for metal cations

Metal ions play a vital role in nature and also in biological systems. In biology, many naturally occurring small molecules are well defined for their ability to bind metals with high selectivity and affinity. For example, Valinomycin, which is a natural ionophore, gives a strong and selective complex in which a K^+ ion is included in the macrocyclic cavity (Figure 21).[84]

[81] Fischer, E., Einfluss der Configuration auf die Wirkung der Enzyme. *Ber. Dtsch. Chem. Ges.* **1894**, *27*, 2985-2993.
[82] Werner, A., Beitrag zur Konstitution anorganischer Verbindungen. *Zeit. anorg. Chem.* **1893**, *3*, 267-330.
[83] Kyba, E. P.; Helgeson, R. C.; Madan, K.; Gokel, G. W.; Tarnowski, T. L.; Moore, S. S.; Cram, D. J., Host-guest complexation. 1. Concept and illustration. *J. Am. Chem. Soc.* **1977**, *99*, 2564-2571.
[84] Page, M. J.; Di Cera, E., Role of Na^+ and K^+ in Enzyme Function. *Physiol. Rev.* **2006**, *86*, 1049-1092.

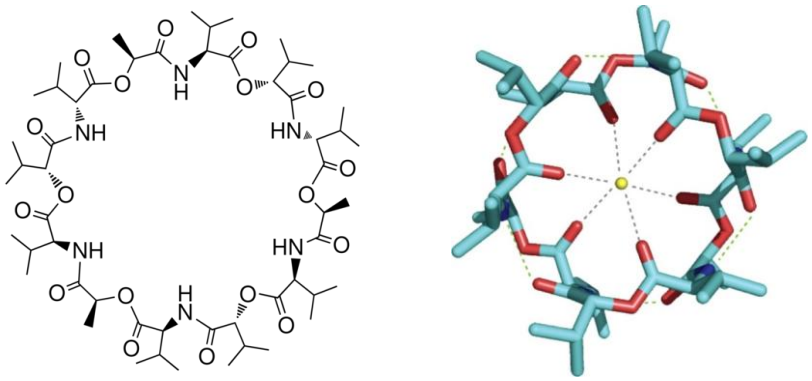

a) b)

Figure 21. a) The structure of Valinomycin; b) Crystal structure of the K^+ complex of Valinomycin.[85]

Apart from natural ionophores, also, many other have played important roles in terms of their ability for recognition of metal ions. These include macro polycyclic (larger rings) structures being able to complex different metal cations by virtue of their chelate and macrocyclic effects. Some characteristic examples are the tetrapyrrole systems like chlorophylls, heme complexes, porphyrinoid nickel (II) complexes or coenzyme F450 (Figure 22).

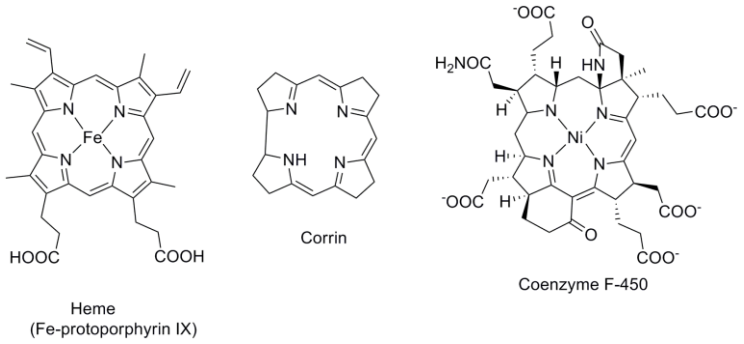

Figure 22. Biological tetrapyrrole macrocyclic compounds.[86]

[85] Kubik, S., Synthetic Peptide-Based Receptors. In *Supramolecular Chemistry*, John Wiley & Sons, Ltd: 2012.
[86] Senge, M. O., Exercises in molecular gymnastics-bending, stretching and twisting porphyrins. *Chem. Commun.* **2006**, 243-256.

In the early 90's, the discovery of crown ethers by Charles Pedersen,[87] cryptands by J. M Lehn,[88] and spherands by Donald J. Cram[89] led to a fast growth in the development of new synthetic receptor molecules and host-guest systems. The newly prepared receptors were selective to cationic, anionic or neutrals substrates and could be from organic, inorganic and biological nature through the use of non-covalent intermolecular interactions.

1.5.2 Host design and preorganization

In order to achieve selective binding between the host and guest molecules, several aspects must be taken into account like the concepts of cooperativity,[90] preorganisation,[91] and complementarity (matching of host-guest steric and electronic requirements), solvation and the shape of molecules.[92] Chelate and macrocyclic effects have contributed their role as well in this regard.

The chelate effect, which is well known in coordination chemistry, relates to the observation that metal complexes of bidentate ligands (such as 1,2-diaminoethane) are significantly more stable than those of closely related materials that contain monodentate ligands (such as ammonia). For example, in the reaction shown in Scheme 2, the value of the equilibrium constant for the replacement of ammonia with 1,2-diaminoethane indicates that the 1,2-diaminoethane chelate complex is significantly more stable (eight orders of magnitude) than the former one.[93]

[87] a) Pedersen, C. J., Cyclic polyethers and their complexes with metal salts. *J. Am. Chem. Soc.* **1967**, *89*, 2495-2496; b) Pedersen, C. J., Cyclic polyethers and their complexes with metal salts. *J. Am. Chem. Soc.* **1967**, *89*, 7017-7036; c) Pedersen, C. J., The Discovery of Crown Ethers (Noble Lecture). *Angew. Chem., Int. Ed. Engl.* **1988**, *27*, 1021-1027.

[88] Lehn, J. M., Cryptates: inclusion complexes of macropolycyclic receptor molecules. *Pure Appl. Chem.* **1978**, *50*, 871-892.

[89] Helgeson, R. C.; Timko, J. M.; Cram, D. J., Structural requirements for cyclic ethers to complex and lipophilize metal cations or alpha-amino acids. *J. Am. Chem. Soc.* **1973**, *95*, 3023-3025.

[90] Werner, A., Beitrag zur Konstitution anorganischer Verbindungen. *Zeit. Anorg. Chem.* **1893**, *3*, 267-330.

[91] Ercolani, G., Assessment of Cooperativity in Self-Assembly. *J. Am. Chem. Soc.* **2003**, *125*, 16097-16103.

[92] Cram, D. J., The Design of Molecular Hosts, Guests, and Their Complexes (Nobel Lecture). *Angew. Chem., Int. Ed. Engl.* **1988**, *27*, 1009-1020.

[93] Hancock, R. D., Chelate ring size and metal ion selection. The basis of selectivity for metal ions in open-chain ligands and macrocycles. *J. Chem. Educ.* **1992**, *69*, 615.

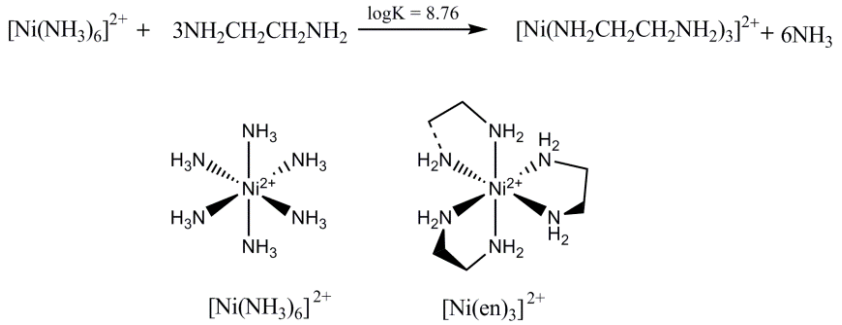

Scheme 2. The chelate effect in metal complexes.

In this regard, EDTA (Ethylenediaminetetraacetic acid) is a classical supramolecular host that in its deprotonated form of $EDTA^{4-}$ is an extremely common chelating ligand able to bind to most metal centers through its two amines and four carboxylates. It represents an excellent illustration for supramolecular host systems with its polydentate nature (Figure 23).[94]

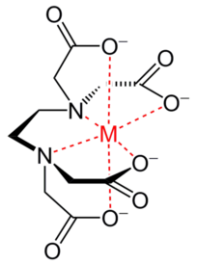

Figure 23. Chelation of EDTA (black) with coordinate bonds to a metal ion (red).

The *macrocyclic effect* follows the same principle as the *chelate effect*, but the effect is further enhanced by the cyclic structure of the ligand. Macrocyclic ligands are not only multi-dentate but also, because of being covalently constrained to their cyclic form, they possess less conformational freedom. Thus, the ligand is said to be "*pre-organized*" for

[94] Holleman, A. F.; Wiberg, E., *Inorganic Chemistry*. San Diego: 2001.

binding, and there is little entropy penalty for wrapping it around the metal ion. For example, Figure 24 shows a specific illustration of acyclic and macrocyclic polyamines where both compounds are able to bind metal cations as Zn^{2+} and Cu^{2+} but, however, the macrocyclic complex is much stronger than its open-chain analogs displayed.[95]

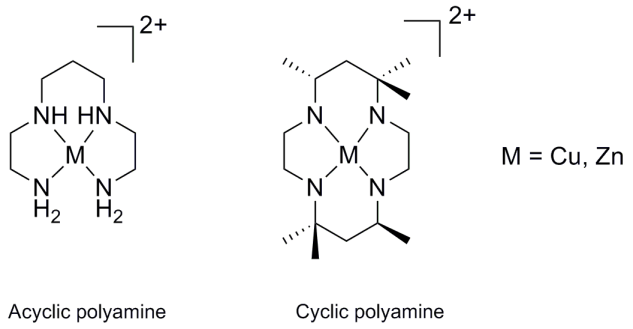

Figure 24. The macrocyclic effect in metal complexes.

Even this effect is much enhanced in the case of bicyclic hosts such as cryptands due to the additional stability achieved through the so-called *macrobicyclic effect*, which simply represents the more rigid, preorganized nature of the macrobicycle with and additional restriction on conformational freedom. For example, Figure 25 compares the stability of the K^+ complexes of acyclic, macrocyclic and macrobicicyclic systems and as a consequence of suitable preorganisation. The stability of the K^+-complex is higher for the macrobicyle than for macrocyclic and open-chain analogs. Thus macrocyclic and macrobicyclic host effects have a significant contribution in alkali metal molecular recognition.

[95] Cabbiness, D. K.; Margerum, D. W., Macrocyclic effect on the stability of copper(II) tetramine complexes. *J. Am. Chem. Soc.* **1969**, *91*, 6540-6541.

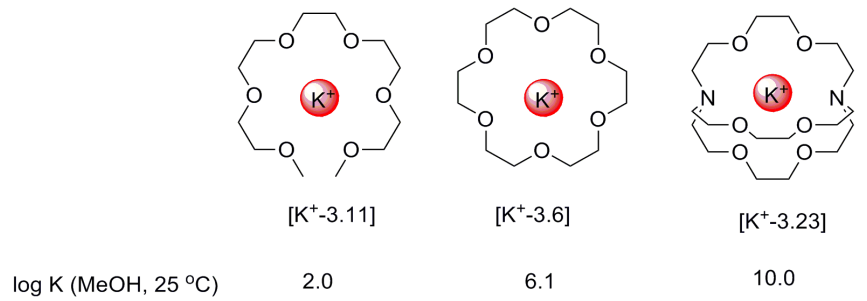

Figure 25. Stabilities of acyclic, macrocyclic and macrobicyclic complexes of K^+.

1.5.3 Binding constants

The binding constant is used as a criterion for the evaluation of the strength of the host-guest complexation process. The binding constant is merely the equilibrium constant for the reaction between host and guest (*i.e.* 1:1 metal (M) and host ligand (L) complex in water, Scheme 3). Strictly, the binding constant is dimensionless, but it is often calculated approximately using concentrations and thus has units of L mol^{-1} or M^{-1}. The binding constant is also known by the terms formation constant (K_f), association constant (K_a) or stability constant (K_s).

$$M(H_2O)_n^{m+} + L \rightleftharpoons ML^{m+} + nH_2O$$

$$K = \frac{[ML^{m+}]}{[M(H_2O)_n^{m+} + L]}$$

Scheme 3. Binding constant between a 1:1 metal (M) and host ligand (L) in water.

The binding constant is the main method by which host-guest affinity in solution is assessed and has fundamental importance in supramolecular chemistry. Binding constants are calculated from experimental data obtained by any method that measures a physical property whose

magnitude significantly changes in the association event (for instance, by potentiometry, NMR, UV-Vis or fluorescence methods).[96]

1.5.3.1 Potentiometric titrations

Potentiometry is one of the most useful techniques for solution equilibrium studies. Thus, for the compounds that are able to suffer protonation, as pseudopeptidic compounds, their protonation constants can be readily determined by potentiometric titrations using pH electrodes to monitor a simple acid-base titration. Potentiometric titrations require the selection of an ionic medium with constant strength in order to ensure that the activity coefficients remain constant for all the species within the experiment. The same technique is used for the study of metal complex stability at different pH values. Figure 26 illustrates a typical setup for the potentiometric experiments performed in our laboratory.

Figure 26. A typical set up for potentiometric or acid-base titration.[97]

The analysis of different acyclic diamines provides an illustration of the influence of electrostatics effects on polyamine protonation and for related

[96] Schalley, C. A.; *Analytical Methods in Supramolecular Chemistry*, Wiley: VCH Verlag, Weinheim, 2007.
[97] Martell, A. E.; Motekaitis, R. J., *The determination and use of stability constants*, Wiley-VCH, 1992.

systems (Table 2).[98] During the titration experiment, a large number of data are obtained regarding the corresponding protonation processes and this has allowed to obtain an extensive set of protonation and complex formation stability constants for many different families of compounds many of them of biological relevance.[41] Once processed, the corresponding raw data can be presented in terms of the overall cumulative stability constants (β) or in terms of the corresponding stepwise stability constants (*K*) (see Table 2). Stepwise stability constants provide more specific information from a chemical perspective. However, in order to be able to obtain such data, the researcher need to be able to properly identify the corresponding individual steps (equilibria) involved and to determine the specific thermodynamic cycle for carrying out the respective calculations. It is very important to take into account that this process does not merely involve a mathematical processing but the researcher needs to be able to properly determine the viability of the corresponding equilibria and their significance under the conditions explored considering also the chemical nature of the species involved.

Table 2. Logarithms of the stepwise protonation constants for the protonation of acyclic diamines.

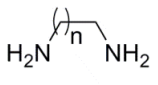

n = 1 (**1**)
n = 2 (**2**)
n = 3 (**3**)
n = 4 (**4**)
n = 5 (**5**)

	1 (n=1)	**2** (n=2)	**3** (n=3)	**4** (n=4)	**5** (n=5)
Log K_1	9.89	10.56	10.72	10.78	10.97
Log K_2	7.08	8.76	9.44	9.85	10.09
Log β [a]	16.97	19.32	20.16	20.63	21.04

[a] Log $\beta = \sum \log K_i$.

[98] Bencini, A.; Bianchi, A.; Garcia-España, E.; Micheloni, M.; Ramirez, J. A., Proton coordination by polyamine compounds in aqueous solution. *Coord. Chem. Rev.* **1999**, *188*, 97-156.

1.6 Biomimetic and Supramolecular Catalysis

Catalysis is one of the main goals of supramolecular chemistry from a biomimetic perspective. This seems reasonable if we consider the historical perspective, with the essential contributions of Fisher for example. Supramolecular catalysis takes place when the host facilitates not only the binding of one or several guests but also their transformation, ideally (again from a biomimetic –enzymatic- perspective) through the additional stabilization of the corresponding transition state via the adequate non-covalent interactions. Different approaches can be considered for these catalytic systems in terms of supramolecular reactivity as is schematically illustrated in Figure 27.

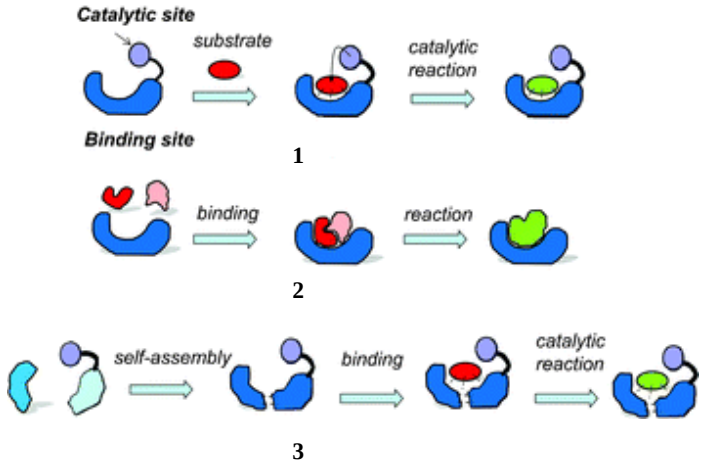

Figure 27. Schematic representation of the supramolecular approaches to catalysis.[99]

Supramolecular approaches to catalysis have been classified into three categories: (1) molecular receptors that place a binding site close to a catalytic centre, (2) molecular receptors that simultaneously bind two reactants and promote their reaction, and (3) systems in which

[99] Escuder, B.; Rodriguez-Llansola, F.; Miravet, J. F., Supramolecular gels as active media for organic reactions and catalysis. *New J. Chem.* **2010**, *34*, 1044-1054.

supramolecular interactions are used to construct a catalytic centre (Figure 27).[100]

Many synthetic supramolecular systems have been designed to mimic the structure or function of more complex biological processes. Such artificial, abiotic (non-biological) molecules or reaction mimics are termed as *enzyme mimic models*. Using this strategy, the artificial synthetic models resemble and help chemists to understand the real world of biological chemistry. Examples of supramolecular structures that mimic the enzyme models are metal complexes of Zn^{2+} and Cu^{2+} (Figure 28) able to display a catalytic activity related to that of carbonic anhydrase. These enzyme models are capable of catalyzing the reversible hydration of CO_2 to bicarbonate.[101]

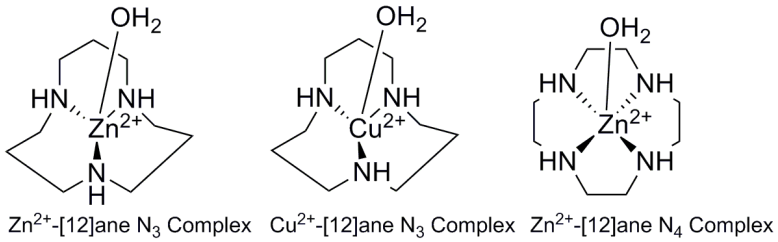

Figure 28. The active site of carbonic anhydrase structural models based on polyamine metal complexes.[101]

In addition to the traditional mimicking of natural enzymes, new important developments in the area of supramolecular catalysis include those based on the encapsulation or inclusion of substrates into cavity-like structures,[102] as is the case of Rebek's supramolecular softball capsules,[103] the octahedral

[100] Ballester, P.; Vidal-Ferran, A., Introduction to Supramolecular Catalysis. In *Supramolecular Catalysis*, Wiley-VCH Verlag GmbH & Co. KGaA: 2008; pp 1-27.
[101] Kimura, E.; Shiota, T.; Koike, T.; Shiro, M.; Kodama, M., A zinc(II) complex of 1,5,9-triazacyclododecane ([12]aneN$_3$) as a model for carbonic anhydrase. *J. Am. Chem. Soc.* **1990**, *112*, 5805-5811.
[102] a) Brown, C. J.; Toste, F. D.; Bergman, R. G.; Raymond, K. N., Supramolecular Catalysis in Metal-Ligand Cluster Hosts. *Chem. Rev.* **2015**, *115*, 3012-3035; b) Yoshizawa, M.; Klosterman, J. K.; Fujita, M., Functional Molecular Flasks: New Properties and Reactions within Discrete, Self-Assembled Hosts. *Angew. Chem., Int. Ed.* **2009**, *48*, 3418-3438.
[103] Kang, J.; Rebek, J., Acceleration of a Diels-Alder reaction by a self-assembled molecular capsule. *Nature* **1997**, *385*, 50-52.

metallocapsule of M. Fujita,[104] and Raymond's tetrahedral metallocapsule that have been reported as catalysts for Diels-Alder reactions (Figure 29).[105]

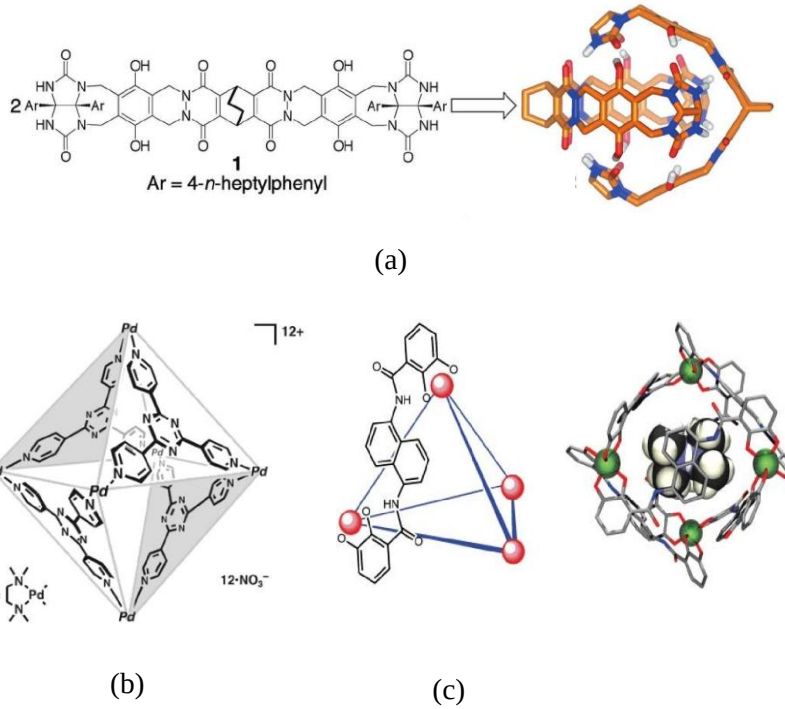

Figure 29. Examples of some capsules used as catalysts (a) softball capsule (Rebek, Jr.); (b) octahedral capsule (Fujita); (c) Tetrahedral capsule (Raymond).

More recently Nitschke *et al* have reported the whole-molecule protecting group approach of capsule-mediated Diels-Alder reaction between furan and maleimide by selectively encapsulating furan by the supramolecular cage receptor.[106]

[104] Kusukawa, T.; Nakai, T.; Okano, T.; Fujita, M., Remarkable Acceleration of Diels-Alder Reactions in a Self-Assembled Coordination Cage. *Chem. Lett.* **2003**, *32*, 284-285.
[105] L. Caulder, D.; N. Raymond, K., The rational design of high symmetry coordination clusters. *J. Chem. Soc., Dalton Trans.* **1999**, 1185-1200.
[106] Smulders, M. M. J.; Nitschke, J. R., Supramolecular control over Diels-Alder reactivity by encapsulation and competitive displacement. *Chem. Sci.* **2012**, *3*, 785-788.

Chapter II

General Objectives

2.1 Objectives

As has been commented previously, this PhD is framed within the area of supramolecular chemistry and more specifically in the field of coordination chemistry of pseudopeptidic compounds with transition metals. The overall goals of this PhD have been:

- To synthesize, characterize and study new open chain and cyclic pseudopeptidic supramolecular systems derived from *L*-valine and *L*-phenylalanine with C_2 symmetry.

- To synthesize, characterize and study the metal complexes derived from these pseudopeptidic compounds.

- To study in detail the binding with different cations using complementary techniques such as potentiometric titrations, NMR, UV-Vis spectroscopy, Circular dichroism, MS, and X-ray diffraction.

- To study the potential of these systems for the selective molecular recognition of cations.

Starting from these overall goals of the PhD, the specific goals and objectives that were defined for each of the chapters contributing to this thesis are presented below.

The specific goals for chapter 4 (*Cu^{2+}, Zn^{2+} and Ni^{2+} Complexes of C_2-symmetric pseudopeptides with an aromatic central spacer*), which is framed in the field of cation molecular recognition and catalysis, were the following ones:

- To synthesize and characterize a family of bis(amino amides) with C_2 symmetry containing aromatic central spacers and amino acid residues derived from *L*-valine and *L*-phenylalanine.

- To study the acid-base behavior of synthesized ligands using potentiometric titrations and ^{1}H NMR experiments.

- To study the coordination of these ligands to transition metal cations such as Cu^{2+}, Zn^{2+}, and Ni^{2+}, using different techniques like potentiometric titrations, UV-Vis spectroscopy, Mass spectrometry, and X-ray diffraction.

- To determine the stability constants associated to the formation of Cu^{2+} and Zn^{2+} complexes.

- To study the potential catalytic activity of some of these metal complexes for the ring-opening of epoxides with amines.

In the case of chapter 5 (*Selective Cu^{2+} recognition by N,N'-benzylated bis(amino amides*), which involve the selective recognition of cations, the specific goals were:

- To synthesize and characterize new *N,N'*-benzylated bis(amino amides) with C_2 symmetry containing an aliphatic central spacer and amino acid residues derived from *L*-valine and *L*-phenylalanine.

- To study the acid-base behavior of the synthesized ligands using potentiometric titrations.

- To study the coordination of these ligands to transition metal cations using different techniques such as UV-Vis spectroscopy, Circular dichroism, mass spectrometry, and X-ray diffraction.

- To determine the stability constants associated to the formation of their Cu^{2+} complexes by potentiometric titrations.

For chapter 6 (*Coordination behavior of new open chain and macrocyclic peptidomimetic compounds with copper(II)*), which is also framed in the field of cation molecular recognition, the specific goals were:

- To synthesize open-chain pseudopeptides containing a diethylene triamine spacer and derived from *L*-valine.

- To synthesize macrocyclic pseudopeptides containing a diethylene triamine spacer and derived from *L*-valine.

- To study the acid-base behavior of the synthesized ligands using potentiometric titrations and ^{1}H NMR experiments.

- To study the coordination of these ligands with Cu^{2+}, using different techniques such as potentiometric titrations, UV-Vis spectroscopy, and mass spectrometry.

- To determine the stability constants for the formation of Cu^{2+} complexes.

Finally, chapter 7 (*Self-Assembly of pseudopeptidic systems*), is framed in the field of the self -assembling of C_2 symmetric open chain bis (amino amides) in solid state and the specific goals were:

- To develop different strategies to obtain suitable crystals for X-ray diffraction of the different C_2 symmetric open chain pseudopeptidic compounds containing aliphatic and aromatic spacers and *N*,*N*′-substitution.

- To study the self-assembly of these pseudopeptidic compounds in the solid state by X-ray diffraction.

- To study the role of the different structural parameters in these systems: amino acid residue, the length, and nature of the spacer and the *N*-substitution, in their self-assembly.

3.1 Cu^{2+}, Zn^{2+} and Ni^{2+} Complexes of C_2-symmetric pseudopeptides with an aromatic central spacer

3.2 Selective Cu^{2+} recognition by N,N'-benzylated bis(amino amides)

3.3 Coordination behaviour of new open chain and macrocyclic peptidomimetic compounds with Cu^{2+}

3.4 Self-assembly of pseudopeptidic systems

3.1 Cu^{2+}, Zn^{2+} and Ni^{2+} Complexes of C_2-symmetric pseudopeptides with an aromatic central spacer

As was mention in the introduction, the design and synthesis of ligands functionalized to achieve metal complexation in a biomimetic approach is a challenge of current interest.[1] Among the various ligands explored in coordination chemistry,[2] the inclusion of amino acid residues in the structure of the ligands is an important strategy, not only due to their strong coordinating ability for a variety of metal ions but also because they provide coordination environments similar to those found in metalloproteins with multiple binding sites.[3] In this context, amino acid derived open-chain and macrocyclic compounds have drawn much attention in different fields like synthetic,[4] bioorganic,[5] medicinal,[6] supramolecular chemistry,[7] and catalysis[8] (See Chapter 1.2).

[1] a) Miyake, H.; Kojima, Y., Macrocyclic pseudopeptides containing N,N′-ethylene-bridged-dipeptide units: synthesis, binding properties toward metal and organic ammonium cations, and conformations. The first step in designing artificial metalloproteins. *Coord. Chem. Rev.* **1996**, *148*, 301-314; b) Bazzicalupi, C.; Bianchi, A.; García-España, E.; Delgado-Pinar, E., Metals in supramolecular chemistry. *Inorg. Chim. Acta* **2014**, *417*, 3-26.

[2] a) Karlin, K. D., Metalloenzymes, structural motifs, and inorganic models. *Science* **1993**, *261*, 701-708; b) Sönmez, M.; Levent, A.; Şekerci, M., Synthesis, Characterization, and Thermal Investigation of Some Metal Complexes Containing Polydentate ONO-Donor Heterocyclic Schiff Base Ligand. *Russ. J. Coord. Chem.* **2004**, *30*, 655-660; c) Gramage-Doria, R.; Armspach, D.; Matt, D., Metallated cavitands (calixarenes, resorcinarenes, cyclodextrins) with internal coordination sites. *Coord. Chem. Rev.* **2013**, *257*, 776-816; d) Wende, C.; Lüdtke, C.; Kulak, N., Copper Complexes of N-Donor Ligands as Artificial Nucleases. *Eur. J. Inorg. Chem.* **2014**, *2014*, 2597-2612; e) Bistri, O.; Reinaud, O., Supramolecular control of transition metal complexes in water by a hydrophobic cavity: a bio-inspired strategy. *Org. Biol. Chem.* **2015**, *13*, 2849-2865.

[3] a) Hechavarría Fonseca, M.; König, B., Chiral Tetraaza Ligands in Asymmetric Catalysis: Recent Progress. *Adv. Synth. Catal.* **2003**, *345*, 1173-1185; b) Green, B. J.; Tesfai, T. M.; Xie, Y.; Margerum, D. W., Oxidative Self-Decomposition of the Nickel(III) Complex of Glycylglycyl-l-histidylglycine. *Inorg. Chem.* **2004**, *43*, 1463-1471; c) Tesfai, T. M.; Green, B. J.; Margerum, D. W., Decomposition Kinetics of Ni(III)−Peptide Complexes with Histidine and Histamine as the Third Residue. *Inorg. Chem.* **2004**, *43*, 6726-6733; d) Prell, J. S.; Flick, T. G.; Oomens, J.; Berden, G.; Williams, E. R., Coordination of Trivalent Metal Cations to Peptides: Results from IRMPD Spectroscopy and Theory. *J. Phys. Chem. A* **2010**, *114*, 854-860; e) Dokorou, V. N.; Milios, C. J.; Tsipis, A. C.; Haukka, M.; Weidler, P. G.; Powell, A. K.; Kostakis, G. E., Pseudopeptidic ligands: exploring the self-assembly of isophthaloylbisglycine (H_2IBG) and divalent metal ions. *Dalton Trans.* **2012**, *41*, 12501-12513; f) Dennis, C. R.; Swarts, J. C.; Margerum, D. W., Proton-transfer reactions of copper(II)- and nickel(II) tetrapeptide complexes with bulky α-carbon substituents. *React. Kinet., Mech. Catal.* **2012**, *107*, 27-38; g) Dong, J.; Wang, Y.; Xiang, Q.; Lv, X.; Weng, W.; Zeng, Q., Synthesis of Chiral Amino Acid Anilides by Ligand-Free Copper-Catalyzed Selective N-Arylation of Amino Acid Amides. *Adv. Synth. Catal.* **2013**, *355*, 692-696.

[4] a) Locardi, E.; Stöckle, M.; Gruner, S.; Kessler, H., Cyclic Homooligomers from Sugar Amino Acids: Synthesis, Conformational Analysis, and Significance. *J. Am. Chem. Soc.* **2001**, *123*, 8189-8196; b)

Furthermore, regarding catalysis, the presence of chirality derived from the amino acid subunits allowed also the potential application of the metal complexes as enantioselective catalysis for different organic transformations.[9]

Recent contributions from our group shown how C_2-symmetrical bis(amino amides) derived from amino acids can form stable complexes with Cu^{2+},

Gibson, S. E.; Lecci, C., Amino Acid Derived Macrocycles-An Area Driven by Synthesis or Application? *Angew. Chem., Int. Ed*. **2006**, *45*, 1364-1377; c) White, C. J.; Yudin, A. K., Contemporary strategies for peptide macrocyclization. *Nat. Chem.* **2011**, *3*, 509-524; d) Lewandowski, B.; De Bo, G.; Ward, J. W.; Papmeyer, M.; Kuschel, S.; Aldegunde, M. J.; Gramlich, P. M. E.; Heckmann, D.; Goldup, S. M.; D'Souza, D. M.; Fernandes, A. E.; Leigh, D. A., Sequence-Specific Peptide Synthesis by an Artificial Small-Molecule Machine. *Science* **2013**, *339*, 189-193.

[5] a) Fernandez-Lopez, S.; Kim, H.-S.; Choi, E. C.; Delgado, M.; Granja, J. R.; Khasanov, A.; Kraehenbuehl, K.; Long, G.; Weinberger, D. A.; Wilcoxen, K. M.; Ghadiri, M. R., Antibacterial agents based on the cyclic d,l-[alpha]-peptide architecture. *Nature* **2001**, *412*, 452-455; b) Kubik, S., Amino acid containing anion receptors. *Chem. Soc. Rev*. **2009**, *38*, 585-605; c) Klemm, K.; Radić Stojković, M.; Horvat, G.; Tomišić, V.; Piantanida, I.; Schmuck, C., Interactions of Multicationic Bis(guanidiniocarbonylpyrrole) Receptors with Double-Stranded Nucleic Acids: Syntheses, Binding Studies, and Atomic Force Microscopy Imaging. *Chem. - Eur. J*. **2012**, *18*, 1352-1363.

[6] a) Hu, X.; Nguyen, K. T.; Verlinde, C. L. M. J.; Hol, W. G. J.; Pei, D., Structure-Based Design of a Macrocyclic Inhibitor for Peptide Deformylase. *J. Med. Chem*. **2003**, *46*, 3771-3774; b) Loughlin, W. A.; Tyndall, J. D. A.; Glenn, M. P.; Fairlie, D. P., Beta-Strand Mimetics. *Chem. Rev*. **2004**, *104*, 6085-6118; c) Silva, G. A.; Czeisler, C.; Niece, K. L.; Beniash, E.; Harrington, D. A.; Kessler, J. A.; Stupp, S. I., Selective Differentiation of Neural Progenitor Cells by High-Epitope Density Nanofibers. *Science* **2004**, *303*, 1352-1355.

[7] a) Choi, K.; Hamilton, A. D., Macrocyclic anion receptors based on directed hydrogen bonding interactions. *Coord. Chem. Rev*. **2003**, *240*, 101-110; b) Wu, Y.-D.; Gellman, S., Peptidomimetics. *Acc. Chem. Res.* **2008**, *41*, 1231-1232; c) Nowick, J. S., Exploring β-Sheet Structure and Interactions with Chemical Model Systems. *Acc. Chem. Res.* **2008**, *41*, 1319-1330; d) Suzuki, M.; Hanabusa, K., l-Lysine-based low-molecular-weight gelators. *Chem. Soc. Rev*. **2009**, *38*, 967-975; e) Brea, R. J.; Reiriz, C.; Granja, J. R., Towards functional bionanomaterials based on self-assembling cyclic peptide nanotubes. *Chem. Soc. Rev*. **2010**, *39*, 1448-1456; f) Ke, D.; Zhan, C.; Li, A. D. Q.; Yao, J., Morphological Transformation between Nanofibers and Vesicles in a Controllable Bipyridine–Tripeptide Self-Assembly. *Angew. Chem., Int. Ed*. **2011**, *50*, 3715-3719; g) Das, D.; Maiti, S.; Brahmachari, S.; Das, P. K., Refining hydrogelator design: soft materials with improved gelation ability, biocompatibility and matrix for in situ synthesis of specific shaped GNP. *Soft Matter* **2011**, *7*, 7291-7303.

[8] a) Merschky, M.; Schmuck, C., Synthesis and kinetic studies of a low-molecular weight organocatalyst for phosphate hydrolysis in water. *Org. Biomol. Chem.* **2009**, *7*, 4895-4903; b) Weseliński, Ł.; Słyk, E.; Jurczak, J., The highly enantioselective 1,3-dipolar cycloaddition of alkyl glyoxylate-derived nitrones to E-crotonaldehyde catalyzed by hybrid diamines. *Tetrahedron Lett.* **2011**, *52*, 381-384; c) Paradowska, J.; Pasternak, M.; Gut, B.; Gryzło, B.; Mlynarski, J., Direct Asymmetric Aldol Reactions Inspired by Two Types of Natural Aldolases: Water-Compatible Organocatalysts and Zn(II) Complexes. *J. Org. Chem.* **2012**, *77*, 173-187.

[9] a) Burguete, M. I.; Collado, M.; Escorihuela, J.; Luis, S. V., Efficient Chirality Switching in the Addition of Diethylzinc to Aldehydes in the Presence of Simple Chiral α-Amino Amides. *Angew. Chem. Int. Ed.* **2007**, *46*, 9002-9005; b) Burguete, M. I.; Escorihuela, J.; Luis, S. V.; Lledós, A.; Ujaque, G., New chiral tetraaza ligands for the efficient enantioselective addition of dialkylzinc to aromatic aldehydes. *Tetrahedron* **2008**, *64*, 9717-9724.

and Zn^{2+} ions.[10,11] These previous results have shown the importance of the different structural factors (nature of the central spacer and constituent amino acid providing the corresponding side chain) in the resulting capacity of these bis(amino amides) to interact with cations and have suggested that the presence of aromatic rings at different positions can be a key structural factor. In particular, the inclusion of benzyl and related groups can be very relevant for the properties of the resulting ligands as has been highlighted by the contributions of Dangel *et al* and Polt *et al* in catalytic applications,[12] and more recently by *Alfonso et al* in cascade-systems for the recognition of dicarboxylates.[13] Herein, we present the synthesis of new C_2-symmetric pseudopeptidic ligands derived from *L*-valine and *L*-phenylalanine containing a central *o*-substituted aromatic spacer (Figure 1) and studied their binding ability towards Cu^{2+}, Zn^{2+}, and Ni^{2+}.

The experimental procedures for carrying out each of these studies are detailed in the article that is presented in Chapter 4 entitled as *''Cu^{2+}, Zn^{2+}*

[10] a) Blasco, S.; Burguete, M. I.; Clares, M. P.; García-España, E.; Escorihuela, J.; Luis, S. V., Coordination of Cu^{2+} Ions to C_2 Symmetric Pseudopeptides Derived from Valine. *Inorg. Chem.* **2010**, *49*, 7841-7852; b) Marti, I.; Ferrer, A.; Escorihuela, J.; Burguete, M. I.; Luis, S. V., Copper(ii) complexes of bis(amino amide) ligands: effect of changes in the amino acid residue. *Dalton Trans.* **2012**, *41*, 6764-6776.

[11] a) Marti-Centelles, V.; Kumar, D. K.; White, A. J. P.; Luis, S. V.; Vilar, R., Zinc(ii) coordination polymers with pseudopeptidic ligands. *CrystEngComm* **2011**, *13*, 6997-7008.

[12] a) Dangel, B.; Clarke, M.; Haley, J.; Sames, D.; Polt, R., Amino Acid-Derived Ligands for Transition Metals: Catalysis via a Minimalist Interpretation of a Metalloprotein. *J. Am. Chem. Soc.* **1997**, *119*, 10865-10866; b) Dangel, B. D.; Polt, R., Catalysis by Amino Acid-Derived Tetracoordinate Complexes: Enantioselective Addition of Dialkylzincs to Aliphatic and Aromatic Aldehydes. *Org. Lett.* **2000**, *2*, 3003-3006; c) Polt, R.; Kelly, B. D.; Dangel, B. D.; Tadikonda, U. B.; Ross, R. E.; Raitsimring, A. M.; Astashkin, A. V., Optically Active 4- and 5-Coordinate Transition Metal Complexes of Bifurcated Dipeptide Schiff Bases. *Inorg. Chem.* **2003**, *42*, 566-574; d) Merschky, M.; Schmuck, C., Synthesis and kinetic studies of a low-molecular weight organocatalyst for phosphate hydrolysis in water. *Org. Biomol. Chem.* **2009**, *7*, 4895-4903; e) Weseliński, Ł.; Słyk, E.; Jurczak, J., The highly enantioselective 1,3-dipolar cycloaddition of alkyl glyoxylate-derived nitrones to E-crotonaldehyde catalyzed by hybrid diamines. *Tetrahedron Lett.* **2011**, *52*, 381-384; f) Paradowska, J.; Pasternak, M.; Gut, B.; Gryzło, B.; Mlynarski, J., Direct Asymmetric Aldol Reactions Inspired by Two Types of Natural Aldolases: Water-Compatible Organocatalysts and Zn(II) Complexes. *J. Org. Chem.* **2012**, *77*, 173-187; g) Adrián, F.; Burguete, M. I.; Fraile, J. M.; García, J. I.; García, J.; García-España, E.; Luis, S. V.; Mayoral, J. A.; Royo, A. J.; Sánchez, M. C., Homogeneous and Supported Copper Complexes of Cyclic and Open-Chain Polynitrogenated Ligands as Catalysts of Cyclopropanation Reactions. *Eur. J. Inorg. Chem.* **1999,** *1999*, 2347-2354.

[13] Faggi, E.; Gavara, R.; Bolte, M.; Fajari, L.; Julia, L.; Rodriguez, L.; Alfonso, I., Copper(ii) complexes of macrocyclic and open-chain pseudopeptidic ligands: synthesis, characterization and interaction with dicarboxylates. *Dalton Trans.* **2015**, *44*, 12700-12710.

and Ni^{2+} Complexes of C_2-symmetric pseudopeptides with an aromatic central spacer''.

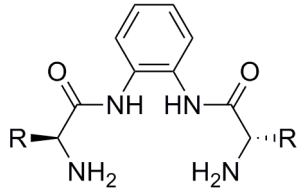

1a R = $CH(CH_3)_2$
1b R = CH_2Ph

Figure 1. General structure of the bis(amino amide) ligands with an aromatic central spacer.

Open-chain pseudopeptides **1a** and **1b** derived from *L*-valine and *L*-phenylalanine, respectively, could be easily prepared starting from the corresponding *N*-Cbz protected amino acid through the initial formation of the corresponding *N*-protected bis(amino amide) by reaction with *o*-phenylene diamine and followed by *N*-deprotection by hydrogenolysis, following the procedures previously reported for similar compounds from our group in good yields.[14] The new compounds were fully characterized by ^{1}H NMR, ^{13}C NMR, FT-IR, and ESI-MS techniques (Annex I).

The study of acid-base properties of the new ligands is essential for correctly understand the properties of nitrogen coordinated compounds.[15] After performing potentiometric titrations with **1a** and **1b**, both compounds show two basicity constants in a pH range between 2 and 12, forming species denoted as HL and H_2L (represented in Scheme 1). Both constants correspond to the protonation of the amine groups. Such protonation process was also monitored by ^{1}H-NMR spectroscopy, thus confirming that the two protonations can occur with the both of the primary amino groups.

[14] a) Marti-Centelles, V.; Kumar, D. K.; White, A. J. P.; Luis, S. V.; Vilar, R., Zinc(ii) coordination polymers with pseudopeptidic ligands. *CrystEngComm* **2011**, *13*, 6997-7008.
[15] a) Martell, A. E.; Motekaitis, R. J., Potentiometry revisited: the determination of thermodynamic equilibria in complex multicomponent systems. *Coord. Chem. Rev.* **1990**, *100*, 323-361; b) García-España, E.; Díaz, P.; Llinares, J. M.; Bianchi, A., Anion coordination chemistry in aqueous solution of polyammonium receptors. *Coord. Chem. Rev.* **2006**, *250*, 2952-2986.

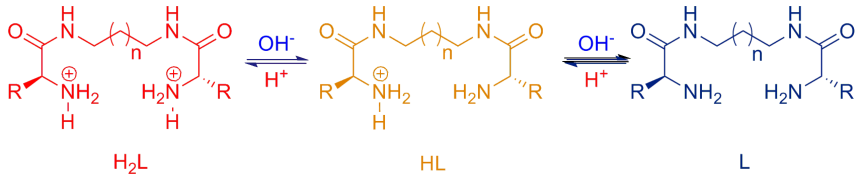

Scheme 1. Protonation process in the bis(amino amide) type of compounds.

In the following Table 1, can be seen basicity constants obtained for compounds **1a** and **1b** using different solvent mixtures. Regarding solvent effect, the reduction in the basicity constants for **1a** is about one order of magnitude in the case of the mixed solvent system. On the other hand, as can be seen the effect of the amino acid side chain can be relevant, from isopropyl to benzyl the first protonation constants for compound **1a** (log K_{H1} 7.09) and **1b** (log K_{H1} 7.17) are very close, but the second protonation constant is higher for **1a** than for **1b** (log K_{H2} 7.08 and 6.21 respectively). Most likely, this reflects the interference of the aromatic rings of the side chains with the solvation of the ammonium ions.

The corresponding distribution diagrams are presented in the main article (Chapter 4) and Annex I, showing the differences between the values of the protonation constants discussed above.

Table 1. Logarithms of cumulative and stepwise protonation constants of pseudopeptidic compounds **1a** & **1b** measured at 298.1 ± 0.1 K.

Reaction[a]	**1a**[c]	**1a**[d]	**1b**[d]
H + L ⇌ HL	8.13(2)[b]	7.09(9)	7.17(3)
2H + L ⇌ H_2L	15.02(4)	14.17(8)	13.38(2)
H + HL ⇌ H_2L	6.89(2)	7.08(9)	6.21 (3)

[a] Charges omitted for clarity. [b] Values in parentheses are the standard deviations in the last significant figure. [c] NaCl 0.1 M. [d] NaCl 0.1 M/CH_3CN 7/3 v/v.

Moreover, the studies revealed that the substitution of the ethylenic spacer by the aromatic one seems not to have any effect on the observed basicity. Even in the case of the second protonation constant, the values are comparable indicating that in both cases and appropriate separation of the two positive charges in the diammonium salt can be achieved.

3.1.1 Interaction with metals (M^{2+})

Because of the interest of developing metal-containing model systems for metalloproteins, Cu^{2+}, Zn^{2+} and Ni^{2+}complexes of the new ligands were investigated to explore their coordination chemistry. The $[MH_{-2}L]$ complexes of **1a** and **1b** with Cu^{2+}, Zn^{2+} and Ni^{2+} could be synthesized in basic media (Scheme 2).

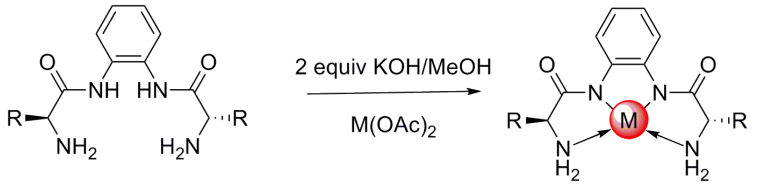

Scheme 2. Synthesis of the metal complexes (**2a-4b**) derived from bis(amino amides) **1a** and **1b**.

The formation of these complexes could be followed by FT-IR experiments by the significant shift of the C=O band to lower frequencies when the complexes were formed, confirming the deprotonation of the amide group in the formation of the corresponding complexes (Annex I).

The stability constants for the formation of Cu^{2+} (Table 2) and Zn^{2+} **(**Table 3**)** complexes were determined for a 1:1 metal-ligand ratio using potentiometric titrations.

For copper coordination studies, the results obtained, reveals that the nature of the central spacer in the ligand is critical for determining the complex speciation and the strength of the complexes formed in water. Thus, for compound **1a**, the stability of the complexes observed is several orders of magnitude higher than for the analogous containing aliphatic central spacer, the corresponding distribution diagrams differ significantly and the relative importance of the neutral [$CuH_{-2}L$] species was very different (Chapter 4 and Annex I).

Table 2. Logarithms of the formation constants (log β) for the complexes of Cu^{2+} with pseudopeptidic compounds **1a-b** at 298.1 ± 0.1 K.

Reaction[a]	**1a**[c]	**1a**[d]	**1b**[d]
$Cu + L \rightleftharpoons CuL$	8.48(9)[b]	8.83(4)	9.24(3)
$Cu + L \rightleftharpoons CuH_{-1}L + H$	–	4.80(1)	5.03(2)
$Cu + L \rightleftharpoons CuH_{-2}L + 2H$	0.17(1)	-0.69(3)	-0.54(3)
$CuL \rightleftharpoons CuH_{-1}L + H$	–	-4.03(3)	-4.21(3)
$CuH_{-1}L \rightleftharpoons CuH_{-2}L + H$	–	-5.49(1)	-5.57(1)
$CuL \rightleftharpoons CuH_{-2}L + 2H$	-8.31(1)	-9.52(4)	-9.78(3)

[a] Charges omitted for clarity. [b] Values in parentheses are the standard deviations in the last significant figure. [c] NaCl 0.1 M. [d] NaCl 0.1 M/CH_3CN 7/3 v/v.

Regarding the effect of the side chain, comparing ligands **1a** and **1b**, the data obtained in the mixed solvent shows that the formation constants were slightly lower for ligand **1a** (*i.e.* log K = 8.83 and 9.24 respectively for $[CuL]^{2+}$).

Table 3. Logarithms of the formation constants (log β) for the complexes of Zn^{2+} with pseudopeptidic compounds **1a-b** at 298.1 ± 0.1 K.

Reaction[a]	**1a**[c]	**1a**[d]	**1b**[d]
Zn + L ⇌ ZnL	–	4.05(1)[b]	3.81(4)
Zn + L ⇌ $ZnH_{-2}L$ + 2H	-12.22(8)	-10.01(1)	-10.45(3)
ZnL ⇌ $ZnH_{-2}L$ + 2H	–	-14.06(1)	-14.26(7)

[a] Charges omitted for clarity. [b] Values in parentheses are the standard deviations in the last significant figure. [c] NaCl 0.1 M. [d] NaCl 0.1 M/CH_3CN 7/3 v/v.

For Zn^{2+} complexes studies, ligands **1a** and **1b** displayed a very similar behaviour, with the formation of the [ZnL] and [$ZnH_{-2}L$] complex species. Regarding the nature of the spacer, no appreciable differences were observed and the corresponding distribution diagrams were also very similar, with the neutral complex species being formed at basic pH values. Moreover, for most nitrogenated ligands and in particular for those related to **1a** and **1b**, above Zn^{2+} complexes are significantly less stable than those for Cu^{2+} and present formation constants several orders of magnitude lower. Comparing the distribution diagrams for **1a,** the neutral species are formed at acidic pH for Cu^{2+} while in for Zn^{2+} the neutral species is predominant at pH > 8 (Figure 2).

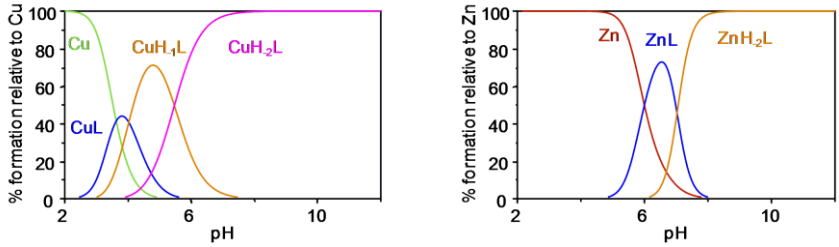

(a) (b)

Figure 2. Distribution diagrams for the ligand **1a** with Cu^{2+} (a) and Zn^{2+} (b) as a function of pH in 0.1 M NaCl/CH_3CN 7/3 v/v, at 298.1 ± 0.1 K. Charges have been omitted for clarity.

In order to gain additional information on the molecularity of the complexes formed, UV-Vis spectroscopy experiments and mass spectrometry (ESI-MS) studies were performed. The experimental data obtained by UV-Vis spectroscopy at different pHs indicates the presence of equilibria between several Cu^{2+} complexes species having different geometries. At pH > 10 an intense band slightly above 500 nm is observed in good agreement with the presence of predominant square-planar or square pyramidal geometries[16] (Chapter 4 main article).

Regarding mass spectrometry (ESI-MS), which is a complementary technique of great importance since it allows the detection of species at very low concentrations in solution, the formation of deprotonated Cu^{2+} complex species even at acidic pH regions was confirmed and for Zn^{2+} complexes the ESI-MS^{+} measured at pH 9.10 showed a peak at 345 corresponding to $[L+K]^{+}$ and a peak at 407 corresponding to the $[ZnH_{-2}L+K]^{+}$ species (Annex I).

Furthermore, the presence of the rigid aromatic central spacer significantly enhanced the possibility of getting crystals of good quality for diffraction studies. Thus, suitable crystals for X-ray diffraction analysis were obtained, in the case of ligand **1b** and for $[MH_{-2}L]$ complexes **2a**-**4a**, **2b**, and **4b**.

In Figure 3 is shown the X-Ray structure for the free ligand **1b**. Four independent molecules (A-D) participate in the asymmetric unit and the presence of the aromatic central unit preorganizes the molecules in U-shape conformations. Molecules B and C have the corresponding U-shapes aligned in the same direction, whilst molecules A and D are oriented in the opposite direction. Two main conformations are observed in the crystal lattice. There is intermolecular hydrogen bonding present between the carbonyl group of one molecule and the amine groups of two different

[16] a) Polt, R.; Kelly, B. D.; Dangel, B. D.; Tadikonda, U. B.; Ross, R. E.; Raitsimring, A. M.; Astashkin, A. V., Optically Active 4- and 5-Coordinate Transition Metal Complexes of Bifurcated Dipeptide Schiff Bases. *Inorg. Chem.* **2003**, *42*, 566-574; b) Autzen, S.; Korth, H.-G.; Boese, R.; Groot, Herbert d.; Sustmann, R., Studies of Pyridinyl-Containing 14-Membered Macrocyclic Copper(II) Complexes. *Eur. J. Inorg. Chem.* **2003**, *2003*, 1401-1410; c) Pauly, M. A.; Erwin, E. M.; Powell, D. R.; Rowe, G. T.; Yang, L., A synthetic, spectroscopic and computational study of copper(II) complexes supported by pyridylamide ligands. *Polyhedron* **2015**, *102*, 722-734.

molecules, and between the NH of one amine group and the NH of the amide of a second molecule.

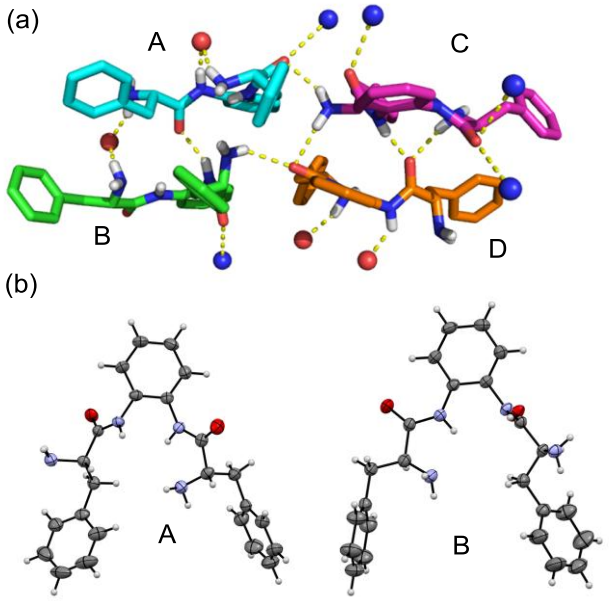

Figure 3. Schematic representation of the hydrogen bond network in the packing of the free ligand **1b** (a) and the molecular structure of the two conformations present for ligand **1b** (b).

In the case of [$CuH_{-2}L$] and [$NiH_{-2}L$] complexes, the X-Ray structures for **2a**, **2b**, **4a**, and **4b** show a square planar geometry, with the metal located essentially in the plane defined by the four nitrogen atoms of the ligand. In most cases, however, the oxygen of an amide carbonyl group of a second ligand is located at a short distance and acts as a fifth donor in these complexes. In the crystal structure obtained for **3a**, the Zn atom displays a clear square pyramidal geometry coordinated to the four nitrogen atoms of a ligand and to the carbonyl oxygen of a second ligand (Figure 4).

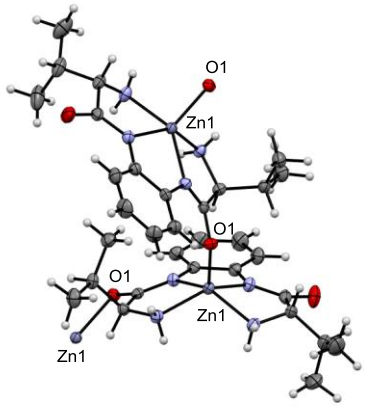

Figure 4. The molecular structure of complex **3a**. The arrangement of two consecutive molecular units displaying the interaction of the oxygen atom of one amide of the first complex with the Zn atom of the second one.

The presence of the aromatic side chains in ligand **1b** makes more difficult the coordination of the carbonyl group of the second ligand to the metal center as was observed in the crystals obtained for **2b** and **4b**.

Finally, preliminary experiments reveal the capacity of some of the former complexes to act as catalysts for the ring opening of the cyclohexene epoxide using aniline as the nucleophile in water. Interestingly, the results show that Zn^{2+} complexes act as more efficient catalysts, in particular, **3b** formed in the presence of ligand **1b**, than the related Cu^{2+} complexes. Unfortunately, the catalytic reaction took place without any observed enantiomeric induction.

3.2 Selective Cu^{2+} recognition by *N,N'*-benzylated bis(amino amides)

The detection of transition metals is very important due to their important role in various areas such as chemistry or biology and their association to key environmental concerns. Transition metals are not only required for biological functions as was mention in Chapter 3.1 but also have great potential for industrial applications. In this context, the design and synthesis of selective probes are required for the sensing of biologically and environmentally important species, being this particularly relevant for the case of transition metal ions.[17]

Among the various transition metal ions, Cu^{2+} is very important as it plays various roles in living systems as a nutrient trace element present in the active sites of some key enzymes and performing as redox catalyst or dioxygen carrier, but, at the same time, this metal can also be associated with many serious human physiological dysfunctions such as Alzheimer's and Prion type neurodegenerative diseases, amyotrophic lateral sclerosis, Wilson's diseases etc.[18]

[17] a) Wang, W.; Wen, Q.; Zhang, Y.; Fei, X.; Li, Y.; Yang, Q.; Xu, X., Simple naphthalimide-based fluorescent sensor for highly sensitive and selective detection of Cd^{2+} and Cu^{2+} in aqueous solution and living cells. *Dalton Trans.* **2013**, *42*, 1827-1833; b) Dhar, P. C.; Pal, A.; Mohanty, P.; Bag, B., Colorimetric detection of Cu(II) ion with a 1,3-bis-azachalcone derivative. *Sens. Actuators, B,* **2015**, *219*, 308-314; c) Singhal, D.; Gupta, N.; Singh, A. K., Chromogenic 'naked eye' and fluorogenic 'turn on' sensor for mercury metal ion using thiophene-based Schiff base. *RSC Adv.* **2015**, *5*, 65731-65738; d) de Silva, A. P.; Gunaratne, H. Q. N.; Gunnlaugsson, T.; Huxley, A. J. M.; McCoy, C. P.; Rademacher, J. T.; Rice, T. E., Signaling Recognition Events with Fluorescent Sensors and Switches. *Chem. Rev.* **1997**, *97*, 1515-1566; e) Pu, L., Fluorescence of Organic Molecules in Chiral Recognition. *Chem. Rev.* **2004**, *104*, 1687-1716; f) Gokel, G. W.; Leevy, W. M.; Weber, M. E., Crown Ethers: Sensors for Ions and Molecular Scaffolds for Materials and Biological Models. *Chem. Rev.* **2004**, *104*, 2723-2750; g) Beer, P. D.; Gale, P. A., Anion Recognition and Sensing: The State of the Art and Future Perspectives. *Angew. Chem., Int. Ed.* **2001**, *40*, 486-516; h) Prodi, L.; Bolletta, F.; Montalti, M.; Zaccheroni, N., Luminescent chemosensors for transition metal ions. *Coord. Chem. Rev.* **2000**, *205*, 59-83; i) Amendola, V.; Fabbrizzi, L.; Foti, F.; Licchelli, M.; Mangano, C.; Pallavicini, P.; Poggi, A.; Sacchi, D.; Taglietti, A., Light-emitting molecular devices based on transition metals. *Coord. Chem. Rev.* **2006**, *250*, 273-299.

[18] a) Gaggelli, E.; Kozlowski, H.; Valensin, D.; Valensin, G., Copper Homeostasis and Neurodegenerative Disorders (Alzheimer's, Prion, and Parkinson's Diseases and Amyotrophic Lateral Sclerosis). *Chem. Rev.* **2006**, *106*, 1995-2044; b) Mathie, A.; Sutton, G.L.; Clarke, C.E.; Veale, E.L. Zinc and copper: Pharmacological probes and endogenous modulators of neuronal excitability. *Pharmacol. Ther.* **2006**, *111*, 567-583; c) Barnham, K. J.; Masters, C. L.; Bush, A. I., Neurodegenerative diseases and oxidative stress. *Nat. Rev. Drug Discovery* **2004**, *3*, 205-214; d) Waggoner, D. J.; Bartnikas, T. B.; Gitlin, J. D., The Role of Copper in Neurodegenerative Disease. *Neurobiol. Dis.* **1999**, *6*, 221-230; e) Bruijn, L. I.; Miller, T. M.; Cleveland, D. W., Unraveling the

In order to be able to selectively detect the presence of Cu^{2+} various sensing systems have been developed following a variety of methodological approaches allowing the quantification of photophysical signals.[19] In this context, molecular probes involving a clear shift in their visible absorption or in that of the corresponding cation or the corresponding charge transfer complexes are advantageous as they provide logistics of detection through a colour change for visual perception (naked-eye detection).[20] In designing such a probe, the structural motifs of its coordination environment defining the spatial disposition of the donor atoms for effective metal ion coordination play a crucial role.

Within this context and taking into account the previous metal binding studies of our group using different bis(amino amides) with aliphatic and aromatic central spacers towards Cu^{2+} and Zn^{2+} ions.[14,21,22] We decided here to synthesize open-chain *N,N'*-benzylated bis(amino amide) ligands derived from *L*-valine (**6a**) and *L*-phenylalanine (**6b**) (Figure 5) and the study of their acid-base properties as well as their capacity to form stable complexes with metal cations, in particular Ni^{2+} and Cu^{2+} as studied by the UV-Vis absorption, CD and ESI-MS that intimate the selective recognition of Cu^{2+} by **6a** and even allowing its naked-eye selective detection in the

mechanisms involved in motor neuron degeneration in ALS. *Annu. Rev. Neurosci.* **2004**, *27*, 723-749; f) Zhao, C.; Liu, B.; Bi, X.; Liu, D.; Pan, C.; Wang, L.; Pang, Y., A novel flavonoid-based bioprobe for intracellular recognition of Cu^{2+} and its complex with Cu^{2+} for secondary sensing of pyrophosphate. *Sens. Actuators, B* **2016**, *229*, 131-137.

[19] a) Xiang, Y.; Li, Z.; Chen, X.; Tong, A., Highly sensitive and selective optical chemosensor for determination of Cu^{2+} in aqueous solution. *Talanta* **2008**, *74*, 1148-1153; b) High, B.; Bruce, D.; Richter, M. M., Determining copper ions in water using electrochemiluminescence. *Anal. Chim. Acta* **2001**, *449*, 17-22; c) Tapia, L.; Suazo, M.; Hödar, C.; Cambiazo, V.; González, M., Copper exposure modifies the content and distribution of trace metals in mammalian cultured cells. *Biometals* **2003**, *16*, 169-174; d) Chen, F.; Liu, G.; Shi, Y.; Xi, P.; Cheng, J.; Hong, J.; Shen, R.; Yao, X.; Bai, D.; Zeng, Z., A coumarin-derived fluorescent chemosensor for selectively detecting Cu^{2+}: Synthesis, DFT calculations and cell imaging applications. *Talanta* **2014**, *124*, 139-145.

[20] a) Valeur, B.; Leray, I., Design principles of fluorescent molecular sensors for cation recognition. *Coord. Chem. Rev.* **2000**, *205*, 3-40; b) Kaur, N.; Kumar, S., Colorimetric metal ion sensors. *Tetrahedron* **2011**, *67*, 9233-9264.

[21] a) Blasco, S.; Burguete, M. I.; Clares, M. P.; García-España, E.; Escorihuela, J.; Luis, S. V., Coordination of Cu^{2+} Ions to C_2 Symmetric Pseudopeptides Derived from Valine. *Inorg. Chem.* **2010**, *49*, 7841-7852; b) Marti, I.; Ferrer, A.; Escorihuela, J.; Burguete, M. I.; Luis, S. V., Copper(ii) complexes of bis(amino amide) ligands: effect of changes in the amino acid residue. *Dalton Trans.* **2012**, *41*, 6764-6776.

[22] Lingaraju Gorla, Vicente Martí-Centelles, Lena Freimuth, Belén Altava, M. Isabel Burguete and Santiago V. Luis, Cu^{2+}, Zn^{2+} and Ni^{2+} Complexes of C_2-symmetric pseudopeptides with an aromatic central spacer (Chapter 3.1 of present thesis)

submillimolar range. The Cu^{2+} complex formed to display a 1:1 stoichiometry and a square planar arrangement around the metal center according to spectroscopic data. This was also confirmed by the X-Ray crystal structures of the copper and nickel complexes obtained with ligands **6a** and **6b.** The experimental procedures for carrying out each of these studies are detailed in the article that is presented in Chapter 5 entitled *as ''Selective Cu^{2+} recognition by N,N'-benzylated bis(amino amides)''.*

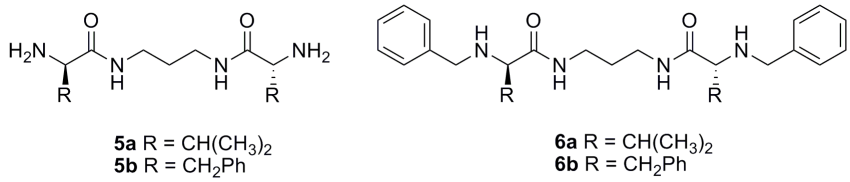

Figure 5. Bis(amino amide) ligands considered in the present work.

These compounds can be readily prepared from the corresponding *N*-Cbz protected amino acid via the initial formation of the activated ester, followed by coupling with 1,3- diamino propane and finally deprotection of the amine group following the synthetic procedures published previously from our group.[23] New *N,N'*-benzylated bis(amino amides) were synthesised by reductive amination of bis(amino amides) with benzaldehyde in methanol affording the final compounds in good yields[24] and used for the selective recognition of metal ions.

The study of acid-base properties of the new ligands revealed that *N,N'*-benzyl substitution decreases the basicity from non-substituted bis(amino amides) as expected (see table 4, *i.e.* log K_{H1} 7.77 for **5a** against log K_{H1} 6.74 for **6a**).

[23] Becerril, J.; Bolte, M.; Burguete, M. I.; Galindo, F.; García-España, E.; Luis, S. V.; Miravet, J. F., Efficient Macrocyclization of U-Turn Preorganized Peptidomimetics: The Role of Intramolecular H-Bond and Solvophobic Effects. *J. Am. Chem. Soc.* **2003**, *125*, 6677-6686.

[24] a) Alfonso, I.; Bolte, M.; Bru, M.; Burguete, M. I.; Luis, S. V.; Rubio, J., Supramolecular Control for the Modular Synthesis of Pseudopeptidic Macrocycles through an Anion-Templated Reaction. *J. Am. Chem. Soc.* **2008**, *130*, 6137-6144; b) Bru, M.; Alfonso, I.; Bolte, M.; Burguete, M. I.; Luis, S. V., Structurally disfavoured pseudopeptidic macrocycles through anion templation. *Chem. Commun.* **2011**, *47*, 283-285.

Regarding the effect of the amino acid residue, the first protonation constant obtained for compound **6a** (log K_{H1} 6.74) and **6b** (log K_{H1} 6.77) were very close, although the second protonation constant for compound **6b** (log K_{H2} 5.15) was lower than for compound **6a** (log K_{H2} 6.73) (Table 4). This is in accordance with related pseudopeptidic compounds containing aliphatic spacers where phenylalanine derivatives present lower basicity than valine analogous. The corresponding distribution diagrams also differ not too much in the species which is presented in chapter 5 main article and Annex II.

Table 4. Logarithms of cumulative and stepwise protonation constants of pseudopeptidic compounds **5a** & **6a-b** measured in NaCl 0.1M/CH_3CN 7/3 v/v at 298.1 ± 0.1 K.

Reaction[a]	**5a**	**6a**	**6b**
H + L ⇌ HL	7.77(8)[b]	6.74(9)	6.77(7)
2H + L ⇌ H_2L	14.88(7)	13.47(6)	11.92(8)
H + HL ⇌ H_2L	7.11(8)	6.73(9)	5.15(1)

[a] Charges omitted for clarity. [b] Values in parentheses are the standard deviations in the last significant figure.

3.2.1 Interaction with metals (M^{2+})

As mention above, because the interest of transition metal detection, metal complexes of the new ligands were investigated to explore their coordination chemistry by UV-VIS, ESI-Mass, CD experiments and X-ray crystallography.

Ligand **6a** was used for further selective metal recognition studies due to the higher solubility of the corresponding metal complex species in polar protic solvents, which significantly facilitated the corresponding studies and made them more relevant. This allowed the study of **6a** in a MeOH/H_2O (80/20 v/v) mixture.

In a series of initial experiments, to a set of vials containing a 2.5 mM solution (2 mL, MeOH/H_2O 80/20) of a given transition metal ion, 1,2 equivalents of ligand **6a** were added (200 μL of a 30 mM solution in the same solvent) (Figure 6a) and the corresponding UV-Vis spectra analysed. The acetate salts for Cu^{2+}, Zn^{2+}, Ni^{2+} and the chloride salts for $Co^{2+}$and Cd^{2+} were used. The pH of the metal solutions was close to neutrality in all cases and only slight changes in the pH were observed after addition of the equimolecular amount of the ligand. For the Cu^{2+} solution, a peak with an absorption maximum at 490 nm and a small peak at 750 nm were observed in the presence of ligand, along with the development of a purple colour of the solution. For the Ni^{2+} solution, two small absorption peaks at 400 and 650 nm were observed along with the development of a yellowish colour in the presence of the ligand. Only a very weak absorption at 500 nm was observed for the Co^{2+} solution when ligand **6a** was added (Figure 6b). However, as could be expected, no absorption peaks between 400 to 800 nm were observed for Zn^{2+} and Cd^{2+} solutions on the addition of 1 equivalent of ligand **6a** and both solutions remained colourless. Thus, a selective naked-eye detection of Cu^{2+} could be observed under those conditions in the mM range.

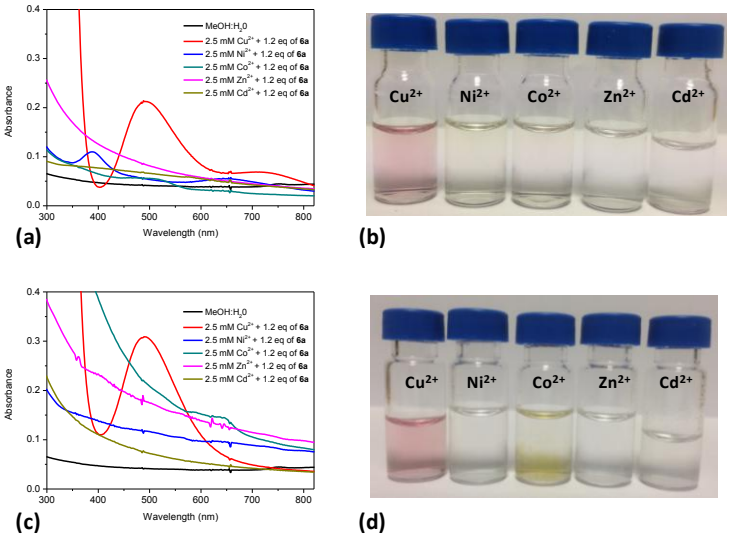

Figure 6. (a) UV–Vis spectra for 2.27 mM of M^{2+} in the presence of 1.2 equivalent of ligand **6a** in the absence of added base; (b) Colorimetric study for 2.27 mM of M^{2+} in the presence of 1.2 equivalent of ligand **6a** in the absence of added base; (c) UV–Vis spectra for 2.27 mM of M^{2+} in the presence of 1.2 equivalent of ligand **6a** in basic media; (d) Colorimetric study for 2.27 mM of M^{2+} in the presence of 1.2 equivalent of ligand **6a** in basic media.

According to literature data, the appearance of the absorption peak at 490 nm region corresponds to the complexation of ligand **6a** with Cu^{2+} with a square planar geometry whereas in the case of Ni^{2+} a new absorption peak at 460 nm was observed, even after 24 hours corresponding to the expected square planar Ni^{2+} complex, thus, the kinetic for the Ni complexes formation is slower than for the corresponding Cu^{2+} analogous.

The stoichiometry of the complex formed by **6a** and Cu^{2+} in the absence of base was determined to be 1:1 (ligand:metal) from the plot of its absorbance monitored at 490 nm as a function of the molar fraction of added Cu^{2+} in MeOH/H_2O v/v (Chapter 5 main article and Annex II).

The changes in the absorption spectra of Cu^{2+} with the gradual addition of increasing amounts of **6a** in $MeOH/H_2O$ at room temperature are shown in Figure 7a. A gradual increase in the intensity of the absorption at 490 nm and a decrease of that at 750 nm was observed as a function of the concentration of added ligand. The non-linear fitting for a 1:1 stoichiometry of this titration curve provided an apparent constant (K_{app}) of 562 M^{-1} (Figure 7b).[25] A similar titration was carried out in the presence of two equivalents of base (Figure 7c). In this case, the isosbestic point around 640 nm was better defined and the fitting of the curve for the absorption at 490 nm provided a value for K_{app} of 3350 M^{-1} (Figure 7d).

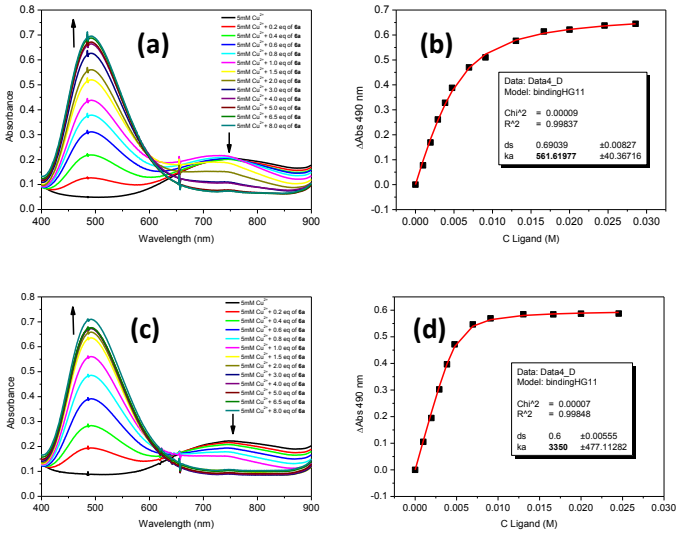

Figure 7. (a) UV-Visible spectra for Cu^{2+} (5 mM) in the presence of increasing amounts of compound **6a**; (b) Plot of the absorbance (490 nm) against the concentration of **6a**; data for the non-linear fitting have been included; (c) UV-Visible spectra for Cu^{2+} (5 mM) in the presence of increasing amounts of compound **6a** in the basic media (pH = 11.68). (d) Plot of the absorbance (490 nm) against the concentration of **6a**; data for the non-linear fitting in basic media have been included.

[25] Thordarson, P., Determining association constants from titration experiments in supramolecular chemistry. *Chem. Soc. Rev.*, 2011, **40**, 1305-1323.

Considering the chiral nature of the ligand, the complexation of **6a** with the different metal ions was also studied by CD. The CD of the free ligand **6a** shows a negative band centered at 240 nm that can be assigned to the n-π^* transitions of the amide groups (Figure 8a). Interestingly, in the presence Cu^{2+} (Figure 8b, black line) a strong negative split-Cotton effect (-, +) with a minimum at 529 nm ($\Delta\varepsilon$ = - 0.44 cm^2 $mmol^{-1}$) and a maximum at 448 nm ($\Delta\varepsilon$ = 0.23 cm^2 $mmol^{-1}$), and passing through zero at 481 nm, which is the λ_{max} for the UV band for the square planar complex. An additional Cotton effect of much lower intensity is also observed around 350 nm in correspondence with the absorption detected in the UV-Vis spectrum in this region. These bands have been generally attributed to metal-ligand charge transfer or to intraligand transitions. For the Ni^{2+} complex, a negative signal with the minimum at 463 nm and a positive one with the maximum at 284 nm were observed (Figure 8b, red line) in good correspondence with the absorption bands detected in the UV-Vis spectrum. For the other M^{2+} metal ions, only one single negative signal in the 220-250 nm regions, corresponding to intraligand transitions was obtained.

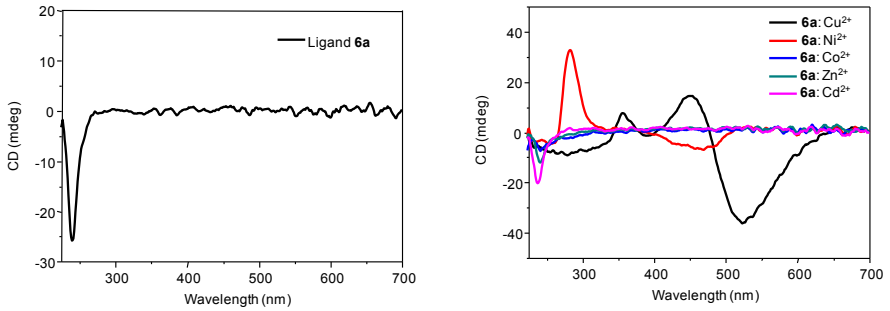

a) b)

Figure 8. (a) CD spectra for ligand **6a** in basic media (2 equiv. of NaOH). (b) CD spectra for ligand **6a** in basic media (2 equiv. of NaOH) in the presence of 1 equivalent of different M^{2+} metals.

Taking into account the selective response obtained for Cu^{2+}.**6a** complexes in the UV-Vis and CD studies, this ligand can be used for the selective detection of this metal. Thus, different additional studies were carried out in

order to check this possibility. First of all, a series of vials containing ligand **6a** and Cu^{2+} in equimolecular amounts were prepared by successive dilutions of a stock solution 10 mM in both components ($MeOH/H_2O$ 80/20, v/v). As can be seen in Figure 9, the color developed for the complex is still visible below the mM range (LOD value for the naked eye detection could be estimated to be 0.25 mM). A similar behaviour was observed when the former experiments were carried out using 2 equiv. of the base relative to the ligand.

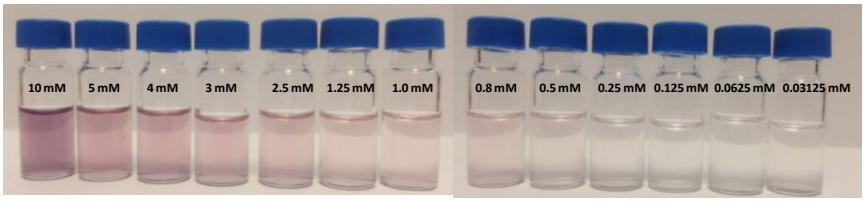

Figure 9. Naked eye color changes upon successive dilutions from a stock solution of 10 mM ligand **6a**:Cu^{2+} in neutral conditions.

A more accurate LOD determination was carried out for the same samples using the corresponding UV-Vis spectra (Figure 10a) and following the absorbance at 490 nm as a function of the L:Cu concentration and using a standard protocol (SD = 3), a detection limit of 85 μM could be established. Similar studies from CD experiments allow a detection limit of 43 μM (Figure 10b). Again, slightly lower LOD values (28 μM) were obtained from CD experiments when the experiments were carried out using 2 equiv. of the base relative to the ligand (Annex II).

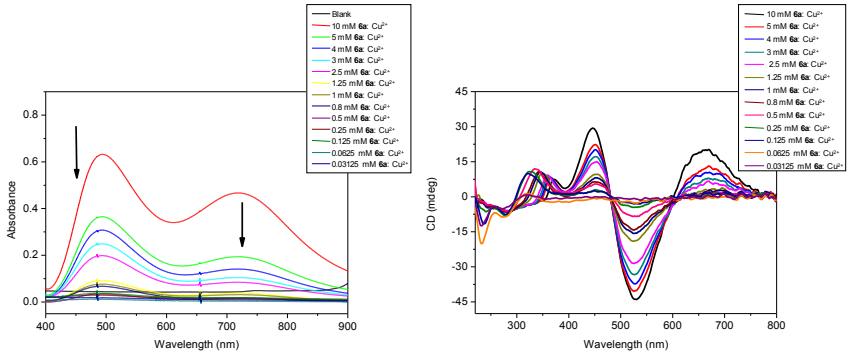

a) b)

Figure 10. UV-Visible (a) and CD (b) spectra obtained from successive dilutions from a stock solution of 10 mM ligand **6a**:Cu^{2+} in the absence of added base.

The corresponding copper(II) and nickel(II) complexes derived from ligand **6** were synthesised in MeOH with the addition of a base (Scheme 3) allowing the generation of the neutral metal complexes. The formation of these complexes could be followed by FT-IR experiments by the significant shift of the C=O band to lower frequencies when the complexes were formed, confirming the deprotonation of the amide group in the formation of the corresponding complexes (see Figure 11).

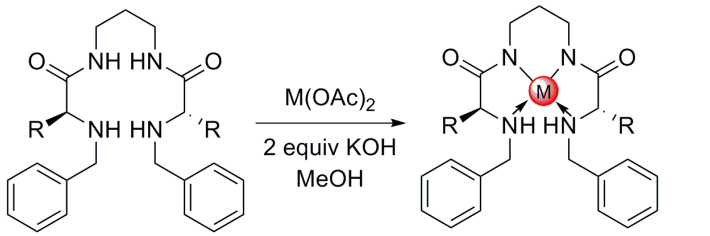

6a R = $CH(CH_3)_2$
6b R = CH_2Ph

7a R = $CH(CH_3)_2$; M = Cu
7b R = CH_2Ph ; M = Cu
8a R = $CH(CH_3)_2$; M = Ni
8b R = CH_2Ph ; M = Ni

Scheme 3. Synthesis of the metal complexes derived from *N*,*N'*-benzyl bis(amino amides) **6a** and **6b**.

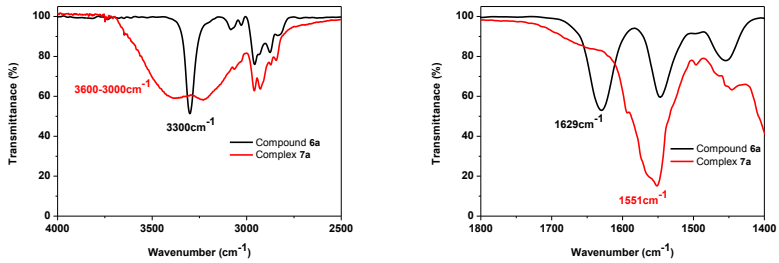

a) b)

Figure 11. IR spectra for free ligand **6a** (black line) and complex **7a** (red line). (a) Changes in NH and (b) C=O bond stretching frequencies.

The stability constants for the formation of Cu complexes were determined for a 1:1 metal-ligand ratio using potentiometric titrations using NaCl 0.1M/CH_3CN 7/3 v/v to maintain a constant ionic strength and a temperature of 298.1 ± 0.1 K (Table 5). The lower solubility of ligand **6b** with Cu^{2+} also precluded carrying out accurate potentiometric titrations.

As can be seen in table 5, significant differences can be observed between the two related ligands. The most remarkable observation is the general lower stability of the non-deprotonated, mono and di-deprotonated complex species for compound **6a**. Thus, for the neutral [$CuH_{-2}L$] species from **6a** the formation constant (log β = -6.29) was more than three orders of magnitude lower than the related formation constant for ligand **5a** (log β = -2.97). In spite of this, these neutral complex species were predominant around pH 7 for **5a** and **6a**, though [$CuH_{-2}L$] starts to be formed at slightly higher pH values for **6a** (Figure 12 a& b**)**. This confirms the formation of [$CuH_{-2}L$] species at physiologic pH for **6a**. On the other hand, the relative importance of [$CuH_{-1}L$] and [CuL] species is reversed for both ligands. For **6a**, the [$CuH_{-1}L$] species is more important at pH values around 6, while it is a minor species in the case of **5a**, and [CuL] is relatively important for **5a** at pH values close to 5, whereas it is very minor for **6a**.

Table 5. Logarithms of the formation constants (log β) for the complexes of Cu^{2+} with pseudopeptidic compounds **5a** and **6a** measured in 0.1M NaCl/ ACN 7/3 v/v mixture at 298.1 ± 0.1 K.

Reaction[a]	**5a**	**6a**
Cu + L ⇌ CuL	6.99(7)[b]	4.39(9)
Cu + L ⇌ $CuH_{-1}L$ + H	1.53(7)	-0.66(3)
Cu + L ⇌ $CuH_{-2}L$ + 2H	-2.97(1)	-6.29(1)
CuL ⇌ $CuH_{-1}L$ + H	-5.46(9)	-5.05(9)
$CuH_{-1}L$ ⇌ $CuH_{-2}L$ + H	-4.50(1)	-5.63(2)
CuL ⇌ $CuH_{-2}L$ + 2H	-9.96(9)	-10.68(9)

[a] Charges omitted for clarity. [b] Values in parentheses are the standard deviations in the last significant figure.

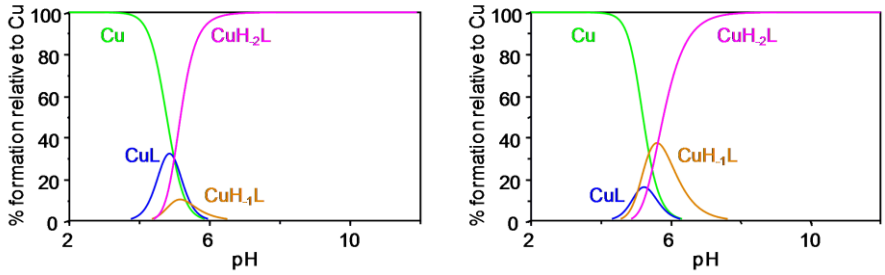

a) b)

Figure 12. Distribution diagrams for ligands **5a** (a) and **6a** (b) with Cu^{2+} as a function of pH in 0.1 M NaCl/CH_3CN 7/3 v/v, at 298.1 ± 0.1 K. Charges have been omitted for clarity.

ESI-MS experiments also allow us that the ligand **6a** obtained after addition of M^{2+} ions also supported the different binding pattern of Cu^{2+} in comparison to that with other metal ions. The ESI mass spectrum for ligand **6a** in the presence of 1 eq. of $Cu(OAc)_2$, displayed peaks at 514.4 and at 574.3 associated to $[CuH_{-2}L+H]^+$ and to $[CuH_{-1}L+AcOH]^+$ species

respectively, supporting a 1:1 complexation stoichiometry and the formation of mono- and bisdeprotonated complexes (Chapter 5 main article and Annex II).

The stoichiometry and the geometry of the M^{2+} complexes were again confirmed by X-ray crystallography with the crystals suitable for single-crystal X-ray diffraction analysis obtained.

The X-ray crystal structure of the copper and nickel complexes **7a-8b** are presented in Figure 13 and Figure 14. X-ray diffraction data confirm the formation of the metal complexes with a 1:1 stoichiometry. The crystal structures obtained for complexes **6a** and **6b** show distorted square planar geometries for Cu^{2+} and Ni^{2+}.

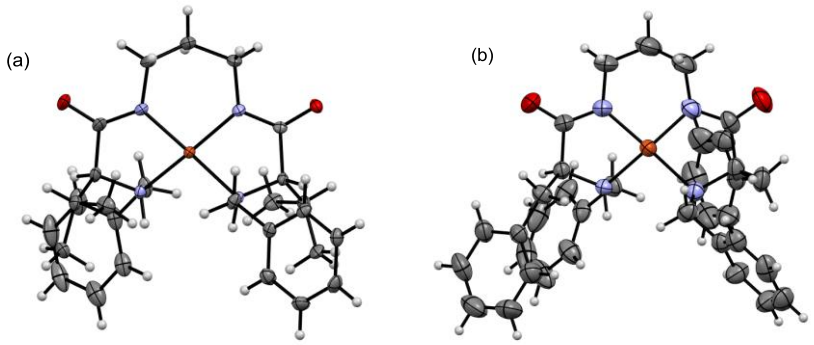

Figure 13. X-ray crystal structure of Cu^{2+} complexes **7a** (a) and **8a** (b). Ellipsoids represented at the 50% probability level.

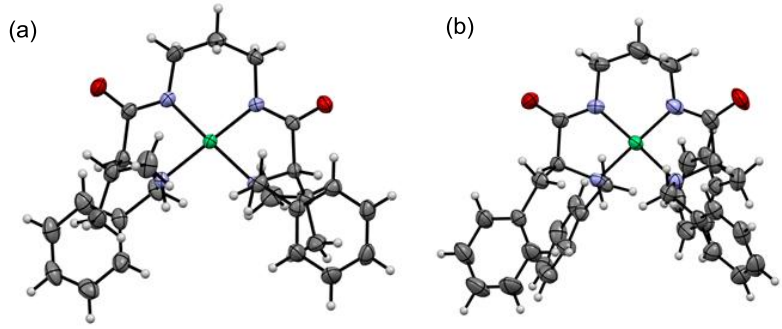

Figure 14. X-ray crystal structure of Ni^{2+} complexes **7b** (a) and **8b** (b). Ellipsoids represented at the 50% probability level.

3.3 Coordination behaviour of new open chain and macrocyclic peptidomimetic compounds with Cu^{2+}

Macrocyclic metal complexes have attracted significant and increasing interest due to the role they play in facilitating an understanding of the molecular processes occurring in biochemistry, materials science, catalysis, encapsulation, activation, transport, separation phenomena and hydrometallurgy.[26] Many ligand systems have been designed to mimic the function of natural carriers in recognizing and transporting specific metal ions, anions or neutral molecules and for understanding and reproducing the catalytic activity of metalloenzymes and proteins.[27] By another side, macrocyclic ligands can have their structures extended through the attachment of pendant donor groups and the resulting metal complexes have found considerable significance.[28] Arms bearing additional potential ligating groups have been introduced at both carbon and nitrogen atoms of macrocycles, which commonly have polyaza- or polyoxa-donor sets. A significant development in this area derives from the concept that the presence of two or more pendant arms, attached at appropriate positions on

[26] a) Curtis, N. F., Macrocyclic coordination compounds formed by condensation of metal-amine complexes with aliphatic carbonyl compounds. *Coord. Chem. Rev.* **1968**, *3*, 3-47; b) Ōkawa, H.; Furutachi, H.; Fenton, D. E., Heterodinuclear metal complexes of phenol-based compartmental macrocycles. *Coord. Chem. Rev.* **1998**, *174*, 51-75; c) Martell, A. E.; Perutka, J.; Kong, D., Dinuclear metal complexes and ligands: stabilities and catalytic effects. *Coord. Chem. Rev.* **2001**, *216–217*, 55-63; d) Rezaeivala, M.; Keypour, H., Schiff base and non-Schiff base macrocyclic ligands and complexes incorporating the pyridine moiety - The first 50 years. *Coord. Chem. Rev.* **2014**, *280*, 203-253.

[27] Vigato, P. A.; Tamburini, S., The challenge of cyclic and acyclic schiff bases and related derivatives. *Coord. Chem. Rev.* **2004**, *248*, 1717-2128.

[28] a) Kaden, T. A., Synthesis and metal complexes of aza-macrocycles with pendant arms having additional ligating groups. In *Host Guest Complex Chemistry III*, Vögtle, F.; Weber, E., Eds. Springer Berlin Heidelberg: Berlin, Heidelberg, 1984; pp 157-179; b) Alcock, N. W.; Balakrishnan, K. P.; Moore, P.; Pike, G. A., Synthesis of pyridine-containing tetra-aza macrocycles: 3,7,11,17-tetra-azabicyclo[11.3.1]heptadeca-1(17),13,15-triene (L^1), its 3,11-dibenzyl (L^2) and 3,7,11-tribenzyl (L^3) derivatives, and their nickel(II), copper(II), and zinc(II) complexes: crystal structures of L^2.HCL and $[Ni(L^2)Cl]ClO_4.H_2O$. *J. Chem. Soc., Dalton Trans.* **1987**, 889-894; c) Adams, H.; R. J. Elsegood, M.; E. Fenton, D.; L. Heath, S.; J. Ryan, S., Dinuclear silver(I) complexes of bibracchial tetraimine Schiff base macrocycles derived from pyrrole-2,5-dicarbaldehyde. *J. Chem. Soc., Dalton Trans.* **1999**, 2031-2038; d) Benniston, A. C.; Ellis, D.; Farrugia, L. J.; Kennedy, R.; Peacock, R. D.; Walker, S., The synthesis of small azamacrocycles bearing pendant aromatic functionalities. The crystal structures of $[Cu(L_1)_2](PF_6)_2$, $[(L_1)CuCl_2]$, $[Cu(L_6)(NO_3)_2]$ and $[Cu_2(L_7–H)_2(OH_2)_2](PF_6)_2 \cdot 3H_2O$ (L_1 = N-(mesitylethyl)-1,4,7-triazacyclononane, L_6=N-(4-hydroxymethylbenzyl)-1,4,7-triazacylcononane, L_7=N-(4-benzylcarboxylic acid)-1,4,7-triazacylcononane) *Polyhedron* **2002**, *21*, 333-342; e) Keypour, H.; Salehzadeh, S.; Pritchard, R. G.; Parish, R. V., Synthesis and Crystal Structure Determination of Some Asymmetrical and Symmetrical CR-Type Macrocyclic Schiff Base Complexes, with a Single Pendant Coordinating 2-Aminoethyl Arm. *Inorg. Chem.* **2000**, *39*, 5787-5790.

a macrocyclic framework can create a pseudo-enclosed environment suitable for the formation of supramolecular, molecular receptor species.[29]

In this regard, as was mention in Chapter 1.2, our group has been working with different families of macrocyclic pseudopeptidic systems. In this regard here, we have designed open-chain bis(amino amide) and its macrocyclic pseudopeptide containing a pendant carboxylic group with diethylenetriamine as spacer group (Figure 15). In such systems, besides the inclusion of additional donor group, the presence of the carboxylic group can provide an important contribution to the water solubility of the resulting ligand, allowing its study under aqueous conditions of biological relevance. The experimental procedures for carrying out each of these studies are detailed in the article that is presented in Chapter 6 entitled as *''Coordination behaviour of new open chain and macrocyclic peptidomimetic compounds with* Cu^{2+}*''*.

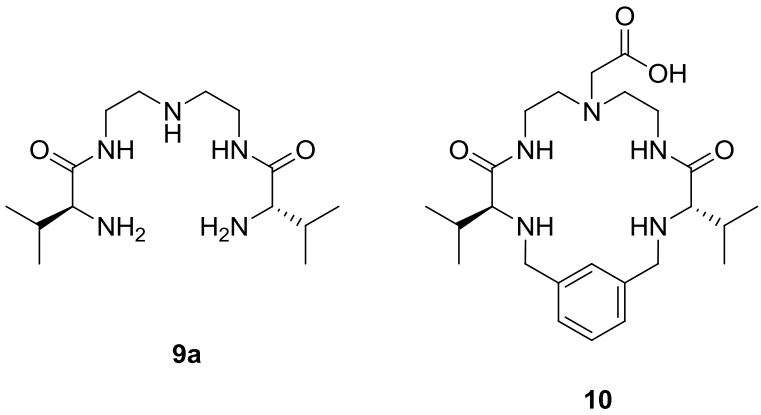

Figure 15. Bis(amino amide) ligands studied in this work.

[29] a) Wainwright, K. P., Applications for polyaza macrocycles with nitrogen-attached pendant arms. In *Advances in Inorganic Chemistry*, Academic Press: 2001; Vol. Volume 52, pp 293-334; b) Smith, C. B.; Stephens, A. K. W.; Wallwork, K. S.; Lincoln, S. F.; Taylor, M. R.; Wainwright, K. P., Metal Ion-Dependent Molecular Inclusion Chemistry: Inclusion of Aromatic Anions by Coordinated 1,4,7,10-Tetrakis((S)-2-hydroxy-3-phenoxypropyl)-1,4,7,10-tetraazacyclododecane. *Inorg. Chem.* **2002**, *41*, 1093-1100.

The open-chain bis(amino amide) compound **9a** can be easily prepared starting from *N*-Cbz protected valine through the initial formation of the corresponding activated *N*-hydroxysuccinimide ester, coupling with diethylenetriamine and final *N*-deprotection. The *N*-Cbz protected compound **9a** was also a key intermediate for the synthesis of the macrocyclic compound **10**. The open-chain *N*-Cbz protected intermediate **9a** was reacted with methyl-2-bromoacetate in DMF at 50 °C for 24 h, using K_2CO_3 as the base, to introduce the ester functionalized pendant arm. Then, deprotection of the Cbz group was carried out by hydrogenolysis, followed by reaction with 1,3-bis(bromomethyl)benzene provided the macrocyclic structure from which, after hydrolysis of the ester group using lithium hydroxide in a 2:1 THF–H_2O mixture, the desired cyclic pseudopeptide **10** was obtained in good yield. The resulting pseudopeptide is a highly functional macrocycle with a relatively large and flexible cavity, which increases its potential for the interaction with metal cations and its water solubility. The new compounds were fully characterized by ^{1}H NMR, ^{13}C NMR, FT-IR, and ESI-MS techniques (Chapter 6 main article and Annex III).

The acid-base properties of **9a** and **10** were studied using potentiometric titrations (Table 6). Macrocyclic compound **10** displays the higher constant ($\log K = 10.01$) for the formation of the [HL] species. This first protonation can be assigned to the carboxylate group or to one of the amine groups, leading to the formation of a neutral or a zwitterionic species. The results suggest that the [H_2L] species for **9a** and **10** involves the preferential protonation at the two more distant amine nitrogen atoms to reduce the electrostatic repulsion.

Table 6. Logarithms of the stepwise protonation constants of pseudopeptidic compounds **9a** & **10** determined in NaCl 0.1M at 298.1 ± 0.1 K.

Reaction[a]	**9a**	**10**
$H + L \rightleftharpoons HL$	9.02(1)[b]	10.01(1)
$H + HL \rightleftharpoons H_2L$	7.86(1)	7.95(1)
$H + H_2L \rightleftharpoons H_3L$	6.93(1)	6.45(1)
$H + H_3L \rightleftharpoons H_4L$	–	5.87(2)

[a] Charges omitted for clarity. [b] Values in parentheses are the standard deviations in the last significant figure.

The distribution diagrams shows the predominance of non-protonated species (L) at pH values slightly higher than 10 for compound **9a,** while for compound **10**, the anionic species (L), corresponding to the presence of a carboxylate group and non-protonated amino groups, predominates in the very basic region (pH > 10), while the neutral species (HL), is prevalent at the pH range 8-10 (Chapter 6 main article).

^{1}H NMR studies were also carried out at different pH values in D_2O, and the results obtained are in agreement with the distribution diagrams observed and suggest that all the different nitrogen atoms are protonated, at some extent, in the different [H_xL] species. Moreover, the formation of the zwitterionic species seems to involve the protonation of one of the benzylic nitrogen atoms from pH 11.4 to 8.3 (Chapter 6 main article).

3.3.1 Determination of the Cu^{2+} complexes formation constants

The interaction of Cu^{2+} with ligands **9a** and **10** was systematically studied by potentiometric titrations in aqueous solution over the 2–11 pH range. The stability constants for the formation of Cu^{2+} complexes were determined in water for a 1:1 metal-ligand ratio, using 0.1 M NaCl to maintain a constant ionic strength and a temperature of 298.1 ± 0.1 K. The results obtained are presented in Table 7.

Table 7. Logarithms of the cumulative and stepwise formation constants (log β) for the complexes of Cu^{2+} with pseudopeptidic compounds determined in 0.1 M NaCl at 298.1 ± 0.1 K.

Reaction[a]	**9a**	**10**
$Cu + L \rightleftharpoons CuL$	11.03(1)[b]	12.19(2)
$Cu + L + H \rightleftharpoons CuHL$	16.46(1)	19.29(3)
$Cu + L + 2H \rightleftharpoons CuH_2L$	–	23.73(3)
$Cu + L \rightleftharpoons CuH_{-1}L + H$	3.052(2)	2.44(1)
$Cu + L \rightleftharpoons CuH_{-2}L + 2H$	6.457(2)	7.05(1)
$Cu + L \rightleftharpoons CuH_{-3}L + 3H$	16.96(4)	–

[a] Charges omitted for clarity. [b] Values in parentheses are the standard deviations in the last significant figure.

The presence of an additional nitrogen donor atom in the central spacer provides the formation of significantly more stable complexes. This is clearly observed when comparing the values of the constants for the open chain pseudopeptides **9a** with its analogous A5Val (*i.e.* for [CuL] species log *K* = 11.03 and 6.76 for compound **9a** and A5Val respectively).[21a] In the case of compound **9a**, the formation of a monoanionic complex species, $[CuH_{-3}L]$ is detected, which should correspond to the deprotonation of a coordinated water molecule to form the corresponding hydroxide. Such a complex has not been detected for A5Val, revealing the important structural differences associated with the presence of the third amino group in the spacer.

The existence of an additional carboxylate donor group as in **10** provides [CuL] formation constants significantly higher for this ligand. However, for the neutral ligands, the situation is different. Thus, the value of the constant for the formation of the [CuL] dicationic species for **9a** (log *K* = 11.03) can be compared to that for the discharged [CuHL] species for **10** (log *K* = 9.28). This seems to preclude a relevant contribution of the macrocyclic

effect, in this case, most likely for it is counterbalanced by the increase in structural stress associated with the presence of the rigid aromatic ring.

In both cases, from the distribution diagrams, the monocationic and dicationic complexes ([$CuH_{-1}L$] and [CuL] for **9a** and [CuL] and [CuHL] for **10**) are the major species identified around neutral pH values. The macrocyclic ligand **10** represents the first example of this family of pseudopeptidic cyclophanes being able to display a significant capacity to form stable copper complexes in aqueous solutions and for a broad range of pH values (Chapter 6 main article).

UV-Vis spectroscopy experiments and mass spectrometry (ESI-MS) studies were also performed.

Regarding ESI-MS, at basic pH values (pH range 9–11) a peak at 403 was clearly detectable for ligand **9a**. This peak can be assigned to a solvated (H_2O) sodium ion adduct of the neutral species [$CuH_{-2}L$], [$CuH_{-2}L+H_2O+Na^+]^+$. The base peak appears at 363 corresponding to the monocationic species [$CuH_{-2}L+H^+]^+$ obtained from the neutral complex [$CuH_{-2}L$], or directly from the monocationic species [$CuH_{-1}L$]. A peak at 385 was also detectable and can be assigned to [$CuH_{-2}L+Na^+]^+$, whose $+H_2O$ and $+2H_2O$ species are [$CuH_{-2}L+H_2O+Na^+]^+$ (403) and [$CuH_{-2}L+H_2O+Na^+]^+$ (421), respectively. The second most intense peak appears at 302, corresponding to the protonated free ligand [HL].

The ESI^+-MS spectra for the Cu^{2+} complexes with **10** at pH =11.5 presents a base peak at 545. Taking into account that L has been defined for **10** as monoanionic, this peak can be assigned to the monocationic [$CuH_{-2}L+H^++Na^+]^+$ species, while the peak at 561 should correspond to the monocationic [$CuH_{-2}L+H^++K^+]^+$ species, in good agreement with the distribution diagram (Chapter 6 main article and Annex III).

UV studies at different pH values (Figure 16) reveal that the geometry of these complexes, having different protonation states, seems to be very similar, most likely from square planar to square-pyramidal, a behaviour

clearly divergent from the one found for ligand A5Val and related compounds.

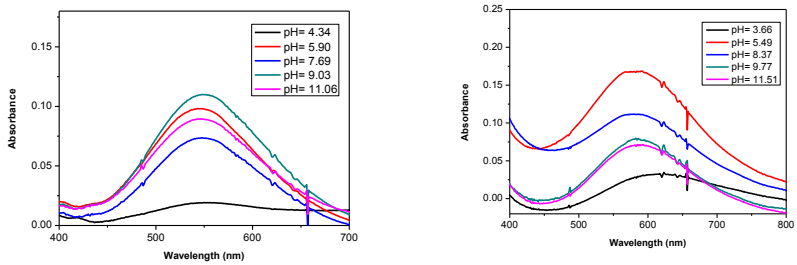

a) b)

Figure 16. UV-Visible spectra obtained for 1:1 Cu:L mixtures for ligands **9a** (a) and **10** (b) at different pH values.

For compound **9a**, the square planar base can be easily formed by the two amides and two amine groups from the amino acid moieties, while the additional nitrogen atom or, in basic media, a hydroxide anion could occupy the apical position while compound **10** can lead to distorted square pyramidal complexes or distorted square planar complexes as the transition from square pyramidal to trigonal bipyramidal has been observed to be associated with a bathochromic shift from around 550 to *ca*. 600 nm.

3.4 Self-assembly of pseudopeptidic systems

Self-assembly processes exist widely in nature that uses them to generate functional complex systems, being amino acids the basic element for the construction of such systems. As was mention before (Chapter 1.4) self-assembly has been applied to a large number of different systems in supramolecular chemistry. In this regard, synthetic receptors containing amine and amide functionalities, by virtue of their H-bonding ability, are able to self-assemble into more complex structures. However, still much research work needs to be focused on such processes to generate well-defined structures and materials with new properties and functionalities.

As was mention in Chapter 1.2 our group has been working with different families of pseudopeptidic systems, most of them open chain pseudopeptides with C_2 symmetry containing aliphatic or aromatic spacers (Figure 17).

Despite we have studied previously the behaviour of the architecture of some of these systems on solid and solution state, in order to gain more information on the nature of the intermolecular interactions in the network formed, we attempted here to obtain crystals suitable for X-ray diffraction studies of open C_2-pseudopeptidic compounds derived from *L*-Valine and *L*-Phenyl alanine and study the role of the amino acid residue, the length and nature of the spacer and the *N*-substitution in the self-assembly of these systems. In this regard, the study of the self-assembly of the crystalline structure of these compounds can provide important information for future designs of pseudopeptidic building blocks for tailored functions.

Pseudopeptidic compounds can be prepared very efficiently in three steps as has been mention in Chapter 3.2, starting from commercially available *N*-Cbz protected amino acids, following the procedures previously reported for similar compounds from our group in good yields (*ca*. 80% overall yields).[23]

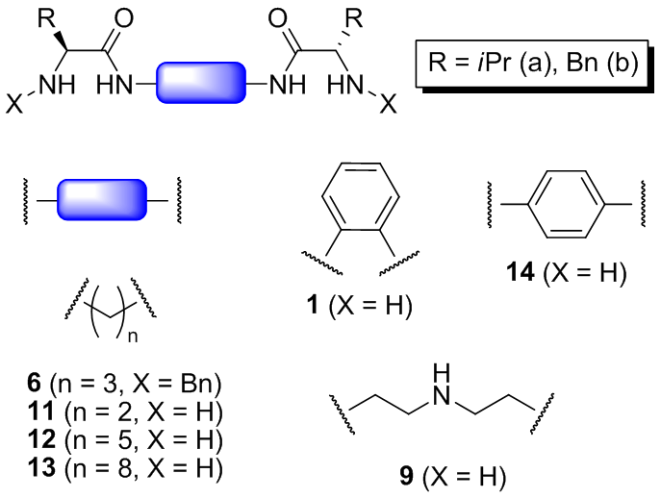

Figure 17. The general structure of pseudopeptidic compounds used in this study.

To obtain suitable crystals for X-ray diffraction studies of open C_2-pseudopeptidic compounds derived from *L*-Valine and *L*-Phenyl alanine, simple traditional crystallisation method as solvent evaporation did not allow to obtain suitable crystals in a broad range of solvents. Nevertheless, suitable crystals were obtained in most of the cases by slow vapour diffusion method in Toluene or DCM. Thus, we have analysed in detail the assembly pattern in crystal structure for C_2-open chain pseudopeptidic compounds displayed in Figure 17. The crystal structures of compounds **1b**, **6b**, **11b**, **14a**, and **14b**, have been described previously in the literature.[22,30]

The results obtained in the solid state, suggest the formation of very different patterns in the self-assembly as a function of the length of the spacer and the nature of the aminoacid residue. Thus, for *L*-valine

[30] a) Becerril, J.; Bolte, M.; Burguete, M. I.; Escorihuela, J.; Galindo, F.; Luis, S. V., A simple peptidomimetic that self-associates on the solid state to form a nanoporous architecture containing chiral p-channels. *CrystEngComm*, **2010**, *12*, 1722-1725; b) Marti-Centelles, V.; Kumar, D. K.; White, A. J. P.; Luis, S. V.; Vilar, R., Zinc(ii) coordination polymers with pseudopeptidic ligands. *CrystEngComm* **2011**, *13*, 6997-7008.

derivatives containing an even number of atoms in the central aliphatic spacer (**11a** and **13a**) the amide groups were oriented in *anti* disposition while the analogous compounds containing an odd number of atoms (**12a** and **9a**) the amide groups were oriented in *syn* position. However, the opposite behaviour was observed for *L*-phenylalanine pseudopeptidic derivatives, for a compound with an even number of atoms in the central spacer (**11b**) the amide groups was oriented in *syn* disposition. While for compounds **12b** and **9b** (odd number of atoms in the central spacer) the amide groups were oriented in *anti* disposition (Figure 18). The different conformation observed for the amide units leads to a different packing motif (Chapter 7 main article).

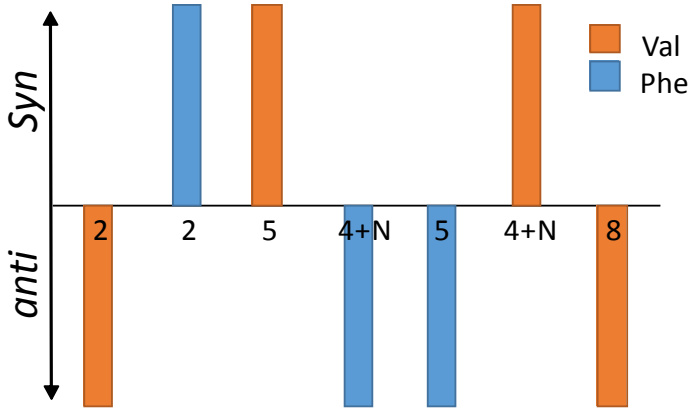

Figure 18. Parallel and antiparallel pseudopeptidic structures against the number of atoms of the central spacer.

Thus, in the case of C_2 pseudopeptidic compounds containing an amine group in the aliphatic spacer **12a** and **12b**, the molecular structure and packing obtained are displayed in Figure 19 and 20.

Compound **12a** showed an extended conformation with amide groups oriented in *syn* disposition with plane angles of 79º (Figure 19). All the amide groups display the expected almost perfect *anti*-coplanar arrangement with O-C-N-H torsion angles between 177º and 178º. The crystal lattice is formed by four molecules of **12a** and six molecules of

water. The network is stabilized by hydrogen bonds involving the oxygen atoms of the carbonyl groups and the hydrogen atom of the amide groups (average N---O distances of 2.827 Å). Moreover, water molecules play a key role in defining the intermolecular interactions leading to the stabilization of the three-dimensional structure observed in the crystal packing. Thus, each water molecule acts as hydrogen bond donor with the nitrogen atom of the NH_2 and the central NH atom.

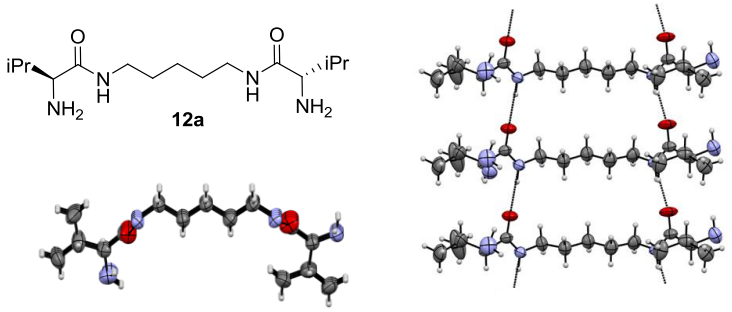

Figure 19. The molecular structure of **12a** and packing showing amide-amide hydrogen bonds.

On the contrary different pattern was observed for compound **12b**, containing phenylalanine as an amino acid side chain (Figure 20). Compound **12b** presented an almost extended conformation with amide groups oriented in *anti* disposition with almost perpendicular planes (85°). Moreover, the aromatic amino acid side chain is oriented toward the cavity defined by the molecular folding able to interact through the edge to face π-π intramolecular interactions (aromatic centroid–Har distance of 2.972 Å), this folding conformation is analogous to the one observed for **11b**. The primary amine groups are oriented in opposite directions outside the folding able to interact through intermolecular hydrogen bonds while the central NH is oriented inside the cleft unable to participate in intermolecular hydrogen bonds. The three-dimensional structure is stabilized by the polar intermolecular hydrogen bonds between the hydrogen atom of amide groups and the oxygen of the carbonyl group (N---O average distances 2.902 Å). Moreover, the intermolecular hydrogen

bonds involving four amine groups from four different molecules (N---H distances 2.583, 2.409, 2.657, and 2.660 Å) lead to stabilized the 3D structure. Finally, the self-assembled structure is also stabilized by π-π interactions involving aromatic side chains with Har---Har distances of 2.400 Å.

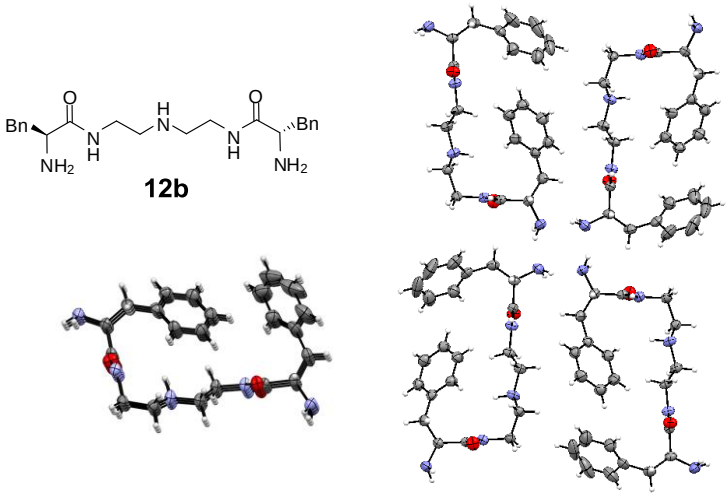

Figure 20. The molecular structure of **12b** and crystal packing stabilized by amine amine hydrogen bonds.

Regarding intermolecular amide-amide H-bond distances, the hydrogen bond distances for *L*-phenylalanine derivatives are larger than for the *L*-valine analogous, this behaviour can be ascribed to the folding conformation observed for phenylalanine systems considered here **12b**, **9b**. Moreover, for pseudopeptidic compound **11b** derived from L-phenylalanine and n = 2, no intermolecular amide-amide hydrogen bond was observed. By another side, as longer is the aliphatic spacer, larger is the amide-amide N---O distances following the order **11a<9a<12a<13a** for valine derivatives.

All systems, except **11a**, preferred an extended conformation and regarding aminoacid residue, *L*-Val pseudopeptidic compounds assembled into a β–sheet-like structure stabilized by polar intermolecular interactions while

L-phenylalanine pseudopeptidic compounds with long aliphatic spacer lead to display folding conformation of the side chain stabilized by π–π intramolecular interactions.

Finally, when plotting the occurrence of the observed N---O intermolecular distances considering compounds **1-14**, (Figure 21), we obtained a distribution with a maximum at 2.85 Å, which is within the range of the natural peptides. Nevertheless as we mention above N---O distances are shorter for pseudopeptidic compounds derived from *L*-valine suggesting a stronger interaction in their supramolecular network.

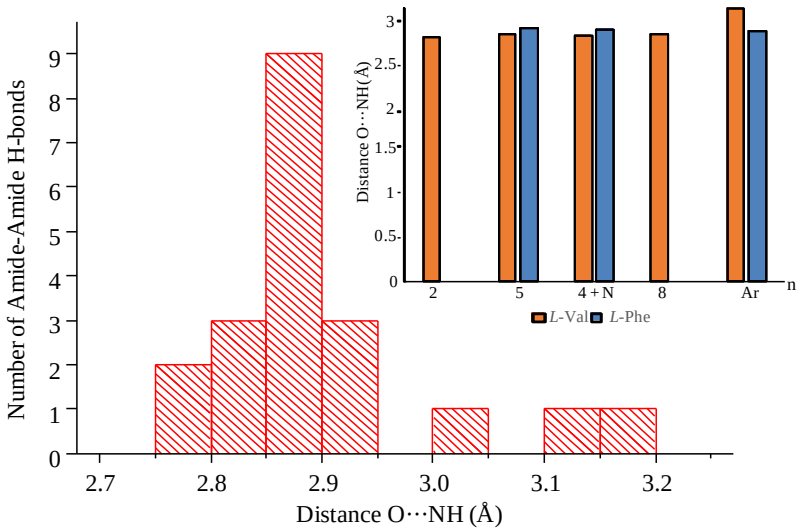

Figure 21. Histogram of the amide bond distances found in the crystal packing of the pseudopeptidic compounds **1-14** (Figure inset, O—NH distances against the number of carbons (n) for **3, 5, 7** and (Ar) for **1**.

Chapter IV

Cu^{2+}, Zn^{2+} and Ni^{2+} Complexes of C_2-symmetric pseudopeptides with an aromatic central spacer

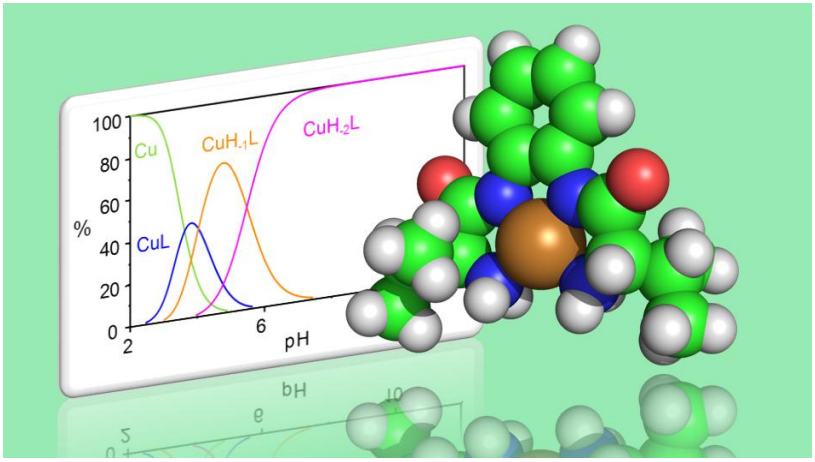

Manuscript submitted in Inorganic Chemistry

Cu^{2+}, Zn^{2+} and Ni^{2+} Complexes of C_2-symmetric pseudopeptides with an aromatic central spacer

Lingaraju Gorla, Vicente Martí-Centelles, Lena Freimuth, Belén Altava, M. Isabel Burguete and Santiago V. Luis**

Departamento de Química Inorgánica y Orgánica, Universitat Jaume I, Av. de Vicent Sos Baynat, s/n 12071, Castellón, Spain

KEYWORDS Phenyl-bridged pseudopeptidic compounds, Cu^{2+}, Zn^{2+} and Ni^{2+} complexes, crystal structures

ABSTRACT: Two new tetradentate C_2-symmetric pseudopeptidic ligands derived from Val and Phe containing two amino and two amido groups and a central *o*-substituted aromatic spacer have been prepared. Their complexes with Cu^{2+}, Zn^{2+} and Ni^{2+} have been studied by potentiometry, UV-Vis spectrophotometry, FT-IR, and ESI-MS. The presence of the aromatic spacer provides Cu^{2+} complexes with stability constants several orders of magnitude higher than those observed for related ligands containing aliphatic central spacers. Besides, the formation of $[MH_{-2}L]$ complex species is favored. Crystal structures for the corresponding Cu^{2+} and Ni^{2+} have been obtained revealing the metal atom in an essentially square planar geometry, although in several instances, the oxygen atom of an amide carbonyl can act as a fifth coordination site. In the case of Zn^{2+}, the only crystal structure obtained displays a square-pyramidal arrangement of the metal center. Finally, preliminary experiments show the catalytic activity of some of these

complexes, in particular, Zn^{2+} complexes, for epoxide ring opening with using aniline as the nucleophile in a ligand accelerated the process.

INTRODUCTION

Metal chelation is involved in many biological processes. Thus, copper is responsible for the normal function of many tissues, including immune, nervous and cardiovascular systems.[1] Moreover, in recent years, metal-related drugs have gained much importance in medicinal chemistry. They are currently in use as medicines for the treatment of diabetes and cancer, as anti-inflammatory and antimicrobial and for cardiovascular diseases.[2,3,4,5] A large variety of ligands have been explored in coordination chemistry,[6,7,8] and the inclusion of amino acid residues in their structure is an important strategy, not only for their strong coordinating ability for a variety of metal ions but also because they provide coordination environments similar to those found in metalloproteins with multiple binding sites.[9] In this context, amino acid derived open-chain and macrocyclic compounds have recently drawn much attention in very different fields like synthetic,[10] bioorganic,[11] medicinal,[12] and supramolecular chemistry,[13] or in catalysis.[14] In this context, symmetrical tetra-coordinated Schiff-base metal complexes derived from amino acids, containing aromatic central spacers, have been studied as catalysts for Et_2Zn addition reactions and as chiral porphyrin mimics.[15] Furthermore, recent contributions from our group have shown how minimalistic pseudopeptides derived from simple natural amino acids, with the general structures I-III (Chart 1) can have important applications,[16] and have been reported as chiral solvating agents or selective receptors for substrates of biological relevance,[17] as minimalistic molecular machines,[18] as organogelators,[19] acting as '*in vivo*' fluorescent pH probes,[20] and as ligands for the preparation of enantioselective catalysts.[21]

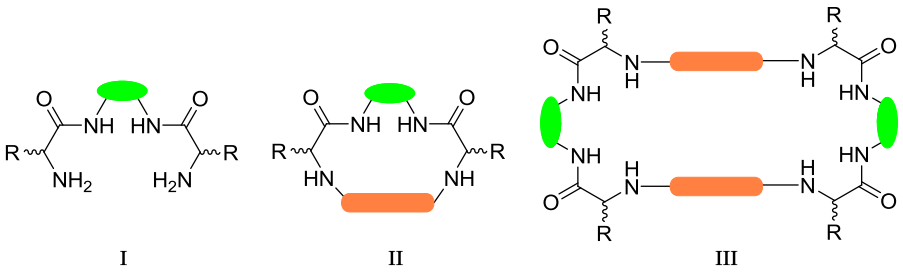

Chart 1. General structure of pseudopeptides.

Regarding metal complexation, our group has recently studied the coordination ability of some C_2- symmetrical bis(amino amides) derived from amino acids with the general structure I and possessing an aliphatic central spacer (-$(CH_2)_n$-) towards Cu^{2+} and Zn^{2+} ions.[22] The obtained results revealed that both the nature of the constituent amino acid (R in I) and the length of the aliphatic spacer (n in -$(CH_2)_n$-) were of importance in determining the complexes formed and their stability. Taking this into account, the substitution of the flexible aliphatic central spacer in I by a rigid aromatic spacer derived from *o*-diamino benzene seems to be a logical step forward for a proper understanding of the coordination properties of this family of ligands. This aromatic spacer should not only provide a geometrically more defined coordination environment, but also a modification of the acidity of the N–H of the amide group and, accordingly, of its involvement in the coordination of metal centers.

In this context, here we present the synthesis, characterization, and study of a family of bis(amino amide) ligands I derived from *L*-valine and *L*-phenylalanine with an aromatic central spacer associated to *o*-diamino benzene, as well as the analysis of their binding ability towards Cu^{2+}, Zn^{2+}, and Ni^{2+}. Moreover, preliminary studies on the catalytic properties of some of the complexes prepared have been carried out.

Results and Discussion

Syntheses Open-chain pseudopeptides **5** and **6** derived from *L*-valine and *L*-phenylalanine, respectively, could be easily prepared starting from the corresponding *N*-Cbz protected amino acid (**1** and **2**) through the initial formation of the corresponding *N*-protected bis(amino amide) (**3** and **4**) by reaction with *o*-phenylene diamine and its *N*-deprotection by hydrogenolysis, following previously reported procedures for related compounds (Scheme 1).[23] Overall yields for the preparation of compounds **5-6** after the final deprotection step were in the 53-66% range. These bis(amino amides) were fully characterized by ^{1}H NMR, ^{13}C NMR, FT-IR, and ESI-MS techniques (Figures S1-S6).

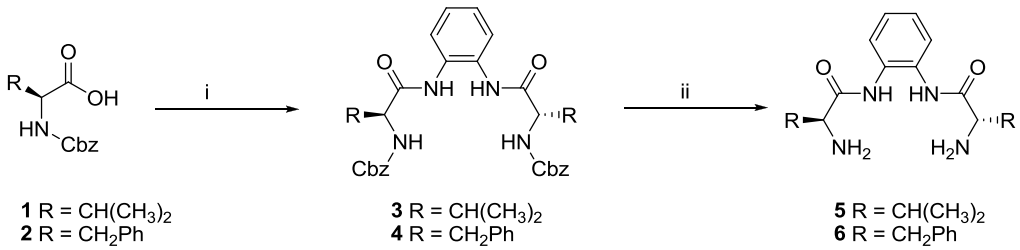

Scheme 1. Synthesis of chiral bis(amino amide) ligands. Reagents: i) Et_3N, ClCOOEt, *o*-phenylene diamine, -10 ºC 2 h, then rt, 24 h, THF, 39-57%; ii) H_2/Pd-C, MeOH, rt, 8 h, 53-66%.

Acid-Base Properties The proper determination of the acid-base properties of nitrogenated compounds is essential for understanding their coordination properties.[24,25] Thus, the protonation constants of bis(amino amides) **5** and **6** were determined by potentiometric titrations. Although compound **5** was soluble enough to carry out the corresponding studies in 0.1 M NaCl, the low solubility of **6** in 0.1 M NaCl required the use of a mixed solvent (0.1 M NaCl/CH_3CN 7/3 v/v) for the corresponding studies. All the titrations were carried out as is fully described in the

Experimental Section, at 298.1 ± 0.1 K, using 0.1 M NaCl or 0.1 M NaCl/CH_3CN 7/3 v/v to maintain a constant ionic strength. The cumulative and stepwise stability constants for the protonation of these pseudopeptidic derivatives obtained following this methodology and using the program HYPERQUAD[26] are presented in Table 1. For the potentiometric studies in 0.1 M NaCl/CH_3CN 7/3 v/v, the value used for pK_w was determined to be 14.6.[27] The constants previously obtained for the related valine and phenylalanine bis(amino amides) with an ethylenic central spacer **7** and **8** (Chart 2) have also been included for comparison.[22]

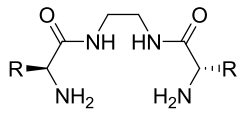

7 R = $CH(CH_3)_2$
8 R = CH_2Ph

Chart 2. The pseudopeptidic ligands (**7**–**8**) previously prepared related to compounds **5** and **6**.

The comparison of the constants obtained in 0.1 M NaCl for ligands **5** and **7** derived from Val reveal that the substitution of the ethylenic spacer by the aromatic one seems to have no effect on the observed basicity. Even in the case of the second protonation constant, the values are comparable indicating that in both cases an appropriate separation of the two positive charges in the diammonium salt occurs. The change in the solvent system to 0.1 M NaCl/CH_3CN 7/3 v/v is accompanied, for ligand **5**, by a reduction in the first basicity constant of about one order of magnitude. The change in the side chain from isopropyl to benzyl also has some effects. Thus, the first protonation constants for **5** (log K_{H1} 7.09) and **6** (log K_{H1} 7.17) are very close, but the second protonation constant is higher for **5** than for **6** (log K_{H2} 7.08 and 6.21 respectively). Most likely, this reflects the interference of the aromatic rings of the side chains with the solvation of

the ammonium ions. As can be observed in Table 1, a small reduction in the basicity constants was also observed in **8**, also derived from Phe, when compared with the structurally related pseudopeptide **7**.[22]

The distribution diagrams for **5** and **6** in the mixed solvent (Figure 1, see Figure S7 for the distribution diagram of **5** in 0.1 M NaCl) revealed the presence of HL^+ species at pH 7 for both ligands (being the major species for **6**) while H_2L^{2+} species predominate for the pH regions below **7** (ligand **5**) and 6 (ligand **6**), being the only species present below pH 5 and 4 respectively. Neutral L species start to predominate for both ligands at pH > 7.

Table 1. Logarithms of cumulative and stepwise basicity constants of ligands **5-8** determined at 298.1 ± 0.1 K.

Reaction[a]	**5**[c]	**7**[d,f]	**8**[c,g]	**5**[e]	**6**[e]
$H + L \rightleftharpoons HL$	8.13(3)[b]	7.94(1)	7.57(1)	7.09(9)	7.17(3)
$H + HL \rightleftharpoons H_2L$	6.89(3)	6.96(1)	6.70(1)	7.08(9)	6.21 (3)

[a] Charges omitted for clarity. [b] Values in parentheses are the standard deviations in the last significant figure. [c] 0.1 M NaCl. [d] 0.15 M $NaClO_4$ (Ref. 22a). [e] 0.1M NaCl/CH_3CN 7/3 v/v. [f] Ref. 22a. [g] Ref. 22b.

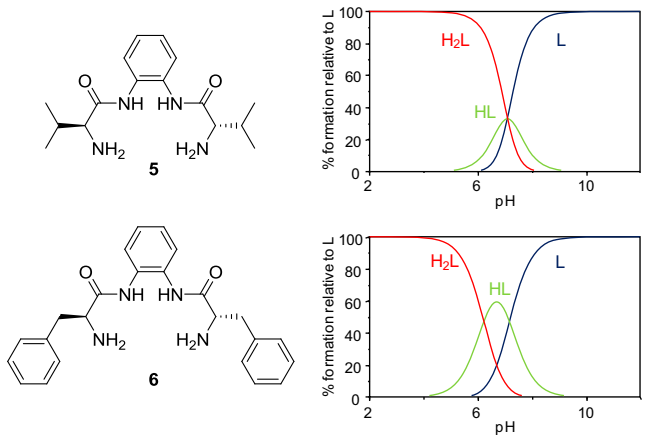

Figure 1. Distribution diagrams for the protonated species of compounds **5** and **6** as a function of pH in 0.1 M NaCl/CH_3CN 7/3 v/v at 298 K. Charges have been omitted for clarity.

The protonation of ligand **5** was also monitored by ^1H NMR spectroscopy.[28] For this purpose, ^1H NMR spectra were obtained at basic, neutral and acidic CD_3CN/D_2O 7/3 v/v. Figure 2 shows the chemical shift changes observed for H_{A-D} protons against pH (see also Figure S8). At pH values above 8, no changes were observed for protons H_{A-D}. At lower pH, small chemical shifts variations were observed for H_A protons, while significant variations were observed for H_B, Hc, and H_D, confirming the protonation of the amine groups at pH < 6.0. The protonation seems to be complete at pH values around 4, in good agreement with potentiometric studies.

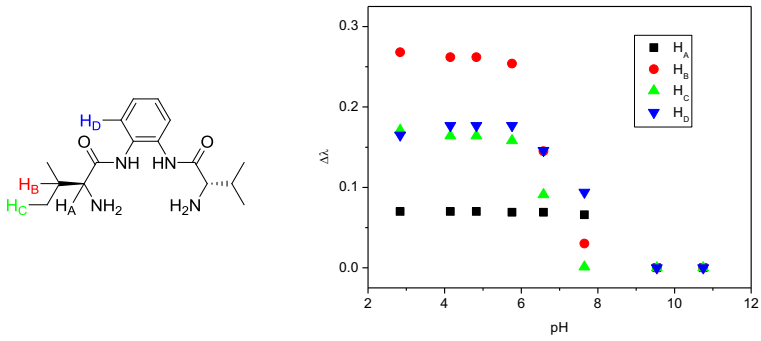

Figure 2. ^{1}H NMR chemical shift variation against pH for compound **5**.

Determination of the Cu^{2+} and Zn^{2+} Complexes Formation Constants

Because of the interest of developing metal-containing model systems for metalloproteins, and taking into account our previous experience in this field, the copper, zinc and nickel complexes of the new ligands were investigated to explore their coordination chemistry. The interaction of ligands **5** and **6** with Cu^{2+} and Zn^{2+} was studied by potentiometric titrations in 0.1 M NaCl and 0.1 M NaCl/CH_3CN 7/3 v/v over the 2-12 pH range at 298.1 ± 0.1 K. The stability constants for the formation of complexes were determined for a 1:1 metal-ligand ratio. As in the case of the protonation constants, accurate results for **6** could only be obtained in the mixed solvent because of its limited solubility in water. Results obtained are presented in Tables 2 and 3 and the corresponding distribution diagrams are displayed in Figures 3 and 4. The values obtained previously for the related ligands **7** and **8** have also been included for comparison.[22a]

As seen in Table 2, the comparison between ligands **5** and **7** in water highlights the importance of the nature of the central spacer. The stability of the complexes detected is several orders of magnitude higher in the case of the ligand with the central aromatic spacer (**5**). Moreover, for **5**

only two complex species (non-deprotonated and bis-deprotonated) were detected, while the mono-deprotonated $[CuH_{-1}L]^+$ species was also detected for **7** around neutrality.[22a] In this regard, the corresponding distribution diagrams differ significantly and the relative importance of the neutral $[CuH_{-2}L]$ species was very different (Figure S9 for the distribution diagram of **5** with Cu^{2+} in 0.1 M NaCl). For **7** this complex species starts to be formed at pH values slightly below 6, becoming the major species in the basic region from *ca.* pH>7. On the contrary, for **5**, the $[CuH_{-2}L]$ species is formed at pH values slightly below 4 and becomes predominant above pH 4. For compound **5**, the free cation is only the major species at the very acidic regions below pH 4, while for **7** predominates below pH 6.[22a]

As mentioned above, the comparison of **5** and **6** required a mixed solvent (0.1M NaCl/CH_3CN 7/3 v/v). When comparing the data for **5** in both solvents, it can be observed that the dicationic complex $[CuL]^{2+}$ is slightly more stable in the mixed solvent, but the neutral complex $[CuH_{-2}L]$ is one order of magnitude less stable. This can be associated with the presence of CH_3CN in the solvent mixture that could participate to a higher extent in the coordination to the $[CuL]^{2+}$ species. On the other hand, the mixed solvent can reduce the basicity of the amide groups. This allows the observation of $[CuH_{-1}L]^+$ as an important species that becomes predominant at *ca.* pH 5.5 (Figure 3). In any case, the values of the stability constants continue being several orders of magnitude higher than those measured for ligand **7**, containing a central ethylenic spacer, in water. In this mixed solvent, the values of the formation constants were slightly lower for ligand **5** (*i.e.,* log K = 8.83 and 9.24 respectively for $[CuL]^{2+}$). The corresponding distribution diagrams (Figure 3) display similar trends for both ligands and are in line with the distribution diagram observed for **5** in 0.1M NaCl (Figure S9) except for the presence of the $[CuH_{-1}L]^+$ complex species that predominate around pH 5. Thus, the $[CuH_{-2}L]$ species start to be formed at pH

values above 4 and become the major species above pH 6. On the other hand, the [CuL] species are present at pH values around 4 and are particularly relevant for ligand **6**. This makes that free Cu^{2+} species are only predominant at the very acidic pH regions, below pH 3.5 for **5** and below pH 3 for **6**.

Table 2. Logarithms of the formation constants (log β) for the Cu^{2+} complexes with pseudopeptidic ligands at 298.1 ± 0.1 K.

Reaction[a]	**5**[c]	**7**[d,f]	**8**[c,g]	**5**[e]	**6**[e]
Cu + L ⇌ CuL	8.48(9)[b]	6.09(4)	-	8.83(4)	9.24(3)
Cu + L ⇌ $CuH_{-1}L$ + H	-	0.67(1)	1.11(1)	4.8(1)	5.03(2)
Cu + L ⇌ $CuH_{-2}L$ + 2H	0.17(1)	-6.48(1)	-6.27(1)	-0.69(3)	-0.54(3)

[a] Charges omitted for clarity. [b] Values in parentheses are the standard deviations in the last significant figure. [c] 0.1 M NaCl. [d] 0.15 M NaClO4 (Ref. 22a). [e] 0.1M NaCl/CH_3CN 7/3 v/v. [f] Ref. 22a. [g] Ref. 22b

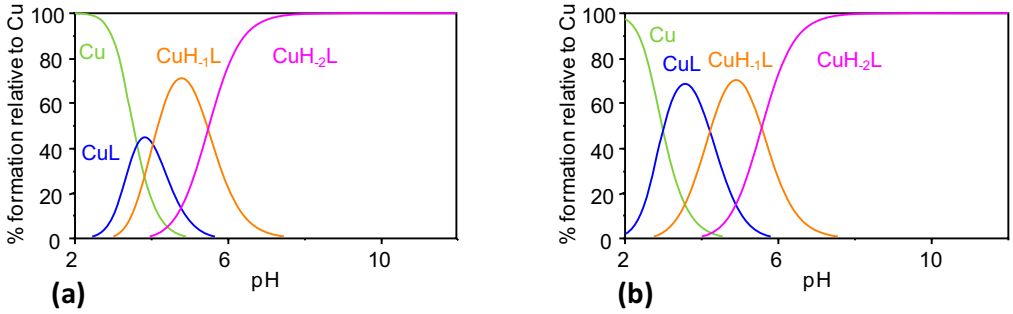

Figure 3. Distribution diagrams for ligands **5** (a) and **6** (b) with Cu^{2+} as a function of pH in 0.1 M NaCl/CH_3CN 7/3 v/v, at 298.1 ± 0.1 K. Charges have been omitted for clarity. Determined in 0.1 M NaCl/CH_3CN 7/3 v/v using 50 mL solution of a 0.1 mM ligand and $Cu(OAc)_2$.

A similar study was carried out in the case of the Zn^{2+} cation (Table 3). As has been observed for most nitrogenated ligands and in particular for those related to **5** and **6**, the Zn^{2+} complexes are significantly less stable than those for Cu^{2+} with formation constants several orders of magnitude

lower. In this case, no appreciable differences were obtained as a consequence of the change in the central spacer and similar values were calculated in water for the formation constants of the $[ZnH_{-2}L]$ species for **5** and **7**, being this one the only complex species detected. The corresponding distribution diagrams were also very similar, with the neutral complex species being formed at basic pH values and becoming the major species at about pH 8 (Figure S9).[22a]

In the mixed solvent, ligands **5** and **6** displayed a very similar behavior, with the formation of [ZnL] and $[ZnH_{-2}L]$ complex species. Interestingly, [ZnL] species are only detected in this medium revealing a higher stability of these complexes. The formation constants observed for the $[ZnH_{-2}L]$ species are two orders of magnitude higher in this medium. The corresponding distribution diagrams are shown in Figure 4. For both ligands, the neutral complex $[ZnH_{-2}L]$ start to be formed at pH values above 6 and becomes the dominant species in both systems at pH > 7.5 while the $[ZnL]^{2+}$ species predominates at neutrality and the Zn^{2+} ion start to be the dominant zinc species slightly below pH 6. The slow kinetics usually associated with the formation of Ni^{2+} complexes hindered the study of those complexes by potentiometric techniques.

Table 3. Logarithms of the formation constants (log β) for the complexes of Zn^{2+} with pseudopeptidic ligands at 298.1 ± 0.1 K.

Reaction[a]	**5**[c]	**7**[d]	**5**[e]	**6**[e]
Zn + L ⇌ ZnL	-	-	4.05(1)	3.81(4)
Zn + L ⇌ $ZnH_{-2}L$ + 2H	-12.22(8)[b]	-12.44(1)	-10.01(1)	-10.45(3)

[a] Charges omitted for clarity. [b] Values in parentheses are the standard deviations in the last significant figure. [c] 0.1 M NaCl. [d] 0.15 M $NaClO_4$ (Ref. 22a). [e] 0.1 M NaCl/CH_3CN 7/3 v/v.

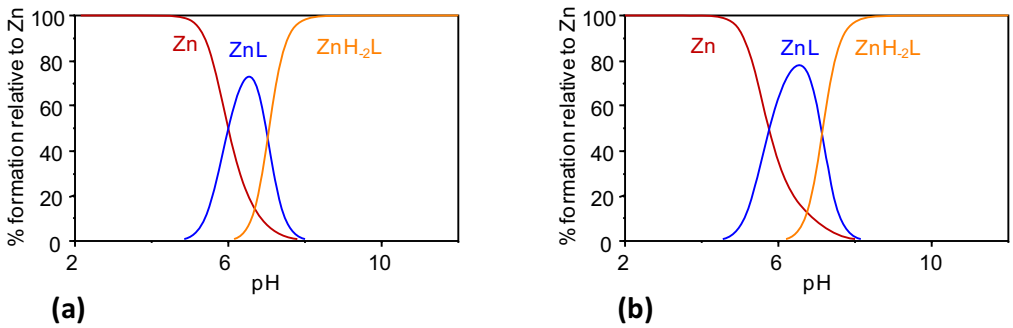

Figure 4. Distribution diagrams for ligands **5** (a) and **6** (b) with Zn^{2+} as a function of pH in 0.1 M NaCl/CH_3CN 7/3 v/v, at 298.1 ± 0.1 K. Charges have been omitted for clarity. Determined in 0.1 M NaCl/CH_3CN 7/3 v/v using 50 mL solution of a 0.1 mM ligand and $Zn(OAc)_2$.

Spectroscopic and Mass Spectrometry studies

The $[MH_{-2}L]$ complexes of **5** and **6** with Cu^{2+}, Zn^{2+} and Ni^{2+} were synthesized in MeOH with the addition of two equivalents of KOH (Scheme 2). The process was accompanied by a change in color from blue to purple for the two Cu^{2+} complexes and from green to yellow for the Ni^{2+} complexes, while, as could be expected colorless complexes were formed in the case of Zn^{2+}. Moreover, their formation could be followed by FT-IR experiments by a significant shift of the C=O band to lower frequencies (*i.e* 1551 cm^{-1} for **9a** against 1661 cm^{-1} for **5**, Figure S10), confirming the deprotonation of the amide group.[22]

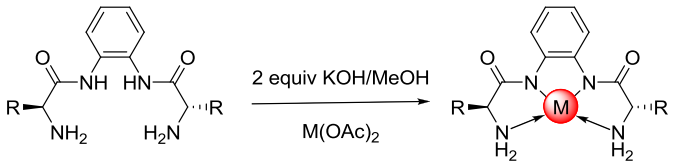

5, 6

9a R = $CH(CH_3)_2$; M = Cu
10a R = CH_2Ph ; M = Cu
9b R = $CH(CH_3)_2$; M = Zn
10b R = CH_2Ph ; M = Zn
9c R = $CH(CH_3)_2$; M = Ni
10c R = CH_2Ph ; M = Ni

Scheme 2. Synthesis of metal complexes derived from bis(amino amides) **5** and **6**.

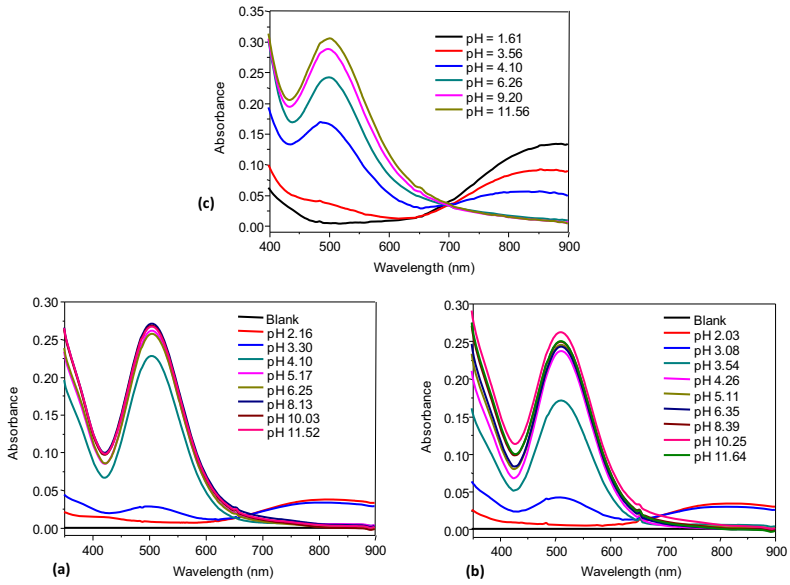

Figure 5. UV-Vis spectra in 0.1 M NaCl/CH_3CN 7/3 v/v for the systems: a) Cu^{2+}-**5**; b) Cu^{2+}-**6**; and for c) Cu^{2+}-**5** in MeOH (*ca.* 0.1 mM in the ligand and in $Cu(OAc)_2$) at different pH values.

In order to gain a more detailed insight into the nature of the metal complexes formed with ligands **5** and **6**, UV-Vis spectroscopic studies were carried out, in the case of Cu^{2+}, by selecting

preferentially those pH regions at which one of the complex species is dominant. For this purpose, the pH of a 0.1 mM solution (50 mL) of the ligand and $Cu(OAc)_2$ in 0.1 M NaCl /CH_3CN 7/3 v/v was adjusted to *ca*. 2 by the addition of 50 μL of concentrated HCl. This sample was titrated exactly under the same conditions used for the potentiometric titrations described above using a 0.1 M NaOH solution in water. Aliquots of 2 mL were taken for UV-Vis analysis at the selected pH values and the resulting spectra are presented in Figures 5a and b. In the more acidic pH regions where the presence of $[CuL]^{2+}$ or the uncomplexed cation is relevant, an ill-defined broad band with the maximum above 700 nm is observed and can be assigned to the d-d transitions associated to octahedral Cu^{2+} complexes. However, it must be taken into account that based on crystallographic studies, hardly supported six-coordinated complexes have been shown to be pentacoordinated.[29] This band is more clearly visible for ligand **5** in MeOH (Figure 5c), displaying at acidic pH values an intense band with its maximum above 800 nm (*i.e.* 880 nm at pH 1.6). The formation of deprotonated $[CuH_{-x}L]$ complexes is accompanied by an important bathochromic shift for this transition that appears as an intense band slightly above 500 nm (at pH > 10, 505 and 510 nm for **5** and **6** respectively). This is in good agreement with the predominance of square-planar or square pyramidal geometries.[15,30]

The complex species formed by **5** and **6** with Cu^{2+} and Zn^{2+} were also studied by mass spectrometry in methanol at the acidic and basic regions. Again, the slow kinetics associated to Ni^{2+} precluded the study of the corresponding complexes. The ESI-MS technique allows the detection in a solution of species at low concentration, and this makes it attractive to analyze complexation processes.[31] This allowed confirming the formation of deprotonated complex species even at acidic pH regions. Thus, for instance, the ESI-MS spectrum, in the positive mode of analysis, of the Cu^{2+}-**5** system at pH 4 showed a major peak corresponding to $[\mathbf{5}+H]^+$ at 307

and a peak at 368 corresponding to the one expected for the $[CuH_{-1}L]^+$ species. Full isotopic analysis showed a perfect agreement between simulated and experimental mass spectra (Figure S11). It must be noted that the peak at 368 can also correspond to the ion $[CuH_{-2}L+H]^+$ taking into consideration that the $[CuH_{-2}L]$ species is neutral and for being observed in the ESI-MS^+ mode requires the interaction with an additional positively charged species (H^+, Na^+, K^+ or other species depending on experimental conditions). This is confirmed by the observation of a smaller peak, with the correct isotopic pattern, at 406 corresponding to the $[CuH_{-2}L+K]^+$ species.

The observation of the bis deprotonated complex species $[MH_{-2}L]^+$ is easier at basic pH values. Thus, for Zn^{2+} complexes formed with **5**, the ESI-MS^+ measured at pH 9.1 showed a peak at 345 corresponding to $[\mathbf{5}+K]^+$ and a peak at 407 corresponding to the $[ZnH_{-2}L+K]^+$ species (Figure S11). Peaks with the correct isotopic pattern were also observed at 439 and 505 corresponding to the formation of the $[ZnH_{-2}L+K+CH_3OH]^+$ and $[ZnH_{-2}L+K+2NaOH+H_2O]^+$ clusters.

Single-crystal X-ray diffraction studies

The presence of the rigid aromatic central spacer significantly enhanced the possibility of obtaining crystals of good quality for diffraction studies. In many instances, crystals were formed directly in the samples obtained from potentiometric titrations at basic pH values. X-Ray quality single crystals for the complexes were grown by layering an ethanolic solution of the pseudopeptidic ligand over an aqueous solution of $Cu(OAc)_2$, $Zn(OAc)_2$ and $Ni(OAc)_2$ respectively. Thus, suitable crystals for X-ray diffraction analysis were obtained, in the case of ligand **5** for the three $[MH_{-2}L]$ complexes **9a-c**. For ligand **6**, appropriate crystals were obtained for the ligand itself and for its Cu^{2+} and Ni^{2+} complexes, **10a**, and **10c**.

The main features of the X-Ray structure for the free ligand **6** are shown in Figure 6 (see also Tables S2 and S3). Four independent molecules (A-D) participate in the asymmetric unit. The presence of the aromatic central unit preorganizes the molecules in U-shape conformations. Molecules B and C have the corresponding U-shapes aligned in the same direction, whilst molecules A and D are oriented in the opposite direction. Two main conformations are observed. For molecules A and D, one of the amide groups is coplanar with the central aromatic ring (8.8º C–C–N–H torsion angle) and the second one is almost perpendicular (83.1º and 91.1º C–C–N–H torsion angles for A and D respectively). In molecules B and C, none of the amide groups is coplanar with the aromatic ring, defining torsion angles ranging from 31.9º to 56.5º. All the amide groups display the expected almost perfect anti-coplanar arrangement with O–C–N–H torsion angles between 170.8º and 177.9º. Amide N-H fragments are always oriented toward the cavity defined by the molecular cleft facilitating the convergence of the nitrogen atoms (three for B and C and the four for A and D) on this cleft.[32] This also favors the participation of the oxygen atoms of the carbonyl groups in the formation of an extensive networks of intermolecular hydrogen bonding, in particular in the case of molecules B and C for which the two amide groups show an anti-disposition in two planes displaying 33.8º and 37º angles, leading to the formation of hydrogen bonds with adjacent molecules located in opposite directions. Besides, the aromatic groups of the side chains display edge-to-face arrangements with neighboring aromatic rings from other side chains or from the central spacer. These π-π interactions are characterized by the presence of H$\cdots$C$_{ar}$ distances < 3 Å (up to 2.86 Å) representing %vd$_W$H,C <100.[33]

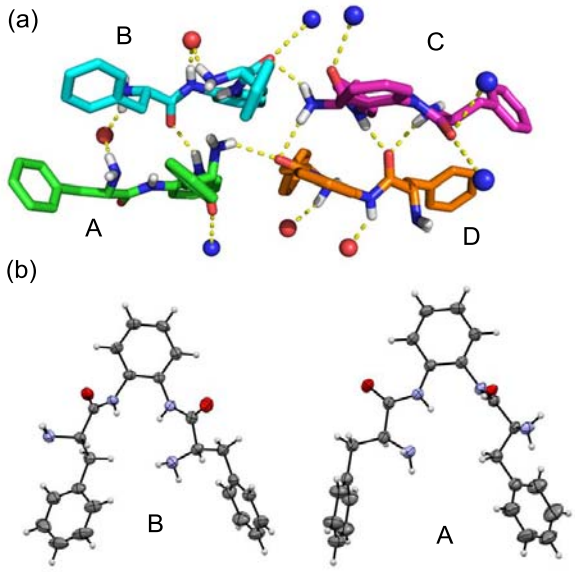

Figure 6. Schematic representation of the hydrogen bond network in the packing of the free ligand **6** (a) and the molecular structure of the two conformations present for ligand **6** (b).

In the case of the [$CuH_{-2}L$] complex formed by ligand **5** (**9a**), two [$CuH_{-2}L$] units form the asymmetric unit in the crystalline structure (Figure 7a). In one of those units, the coordination environment around the copper presents a slightly distorted square-pyramidal geometry in which the square base is formed by the four nitrogen atoms of a bis deprotonated ligand. The oxygen atom from a carbonyl group of the second molecule provides the fifth axial coordination being the Cu–O distance (2.663 Å) significantly longer that those corresponding to Cu–N distances that range from 1.912 to 2.013 Å . The copper atom is essentially located in the plane defined by the four nitrogen atoms, although a small distortion is observed with the Cu-plane distance being 0.047 Å. The OCuN angles defined are 82.3º and 82.7º for the amide nitrogen atoms and 104.2º and 100.6º for the amino nitrogen atoms. The bite angles for the five chelate rings range from

84.3º to 89.1º, indicative of a tight chelation. In concordance, the N_{amine}–Cu–N_{amine} bite angle is 104.2º. The coordination geometry around the Cu^{2+} for the second molecule is square planar, with the copper atom located at 0.015 Å from the plane defined by the four nitrogen atoms. In this case, the Cu–N distances range from 1.905 to 2.004 Å, slightly shorter as could be expected from the absence of the fifth donor atom. The bite angles for the five chelate rings range from 84.2º to 84.8º, in this case, with the N_{amine}–Cu–N_{amine} bite angle being 106.7º. In both molecules the Cu–N_{amide} distances are shorter than the ones corresponding Cu–N_{amine}, being 1.912 and 1.995 Å on average, respectively. The latter was previously observed for analogous Cu–pseudopeptidic complexes and was attributed to the anionic coordination from the deprotonated N_{amide} donors instead of the neutral donation from the N_{amine} groups.[22b]

The unit cell for complex **9a** contains four of such pairs of [$CuH_{-2}L$] units and, besides, two water molecules are present for each [$CuH_{-2}L$] unit. These water molecules play a key role in the hydrogen bonding network present in the crystal structure (Figure S12). For the [$CuH_{-2}L$] unit containing the square pyramidal copper ion, each of the oxygen atoms of the deprotonated amide groups acts as hydrogen bond acceptor with one molecule of water and one amino group of a different molecule and only one of its amino groups acts as a hydrogen donor with a third water molecule. For the square planar [$CuH_{-2}L$] unit the non-coordinated amide carbonyl is hydrogen bonded to a water molecule while the amino groups form hydrogen bonds with the oxygen atoms from the amide groups of two different molecules and one of them also acts as hydrogen donor with a water molecule.

The crystal structure of the Ni^{2+} complex with the bis deprotonated ligand **5** (**9c**) displays some common features with the one analyzed for the Cu^{2+} complex **9a**. The asymmetric unit for

complex **9c** (Figure 7b) is also formed by two [NiH$_{-2}$L] units defining almost perpendicular main planes (87.6º). In one of these units, the nickel presents an almost perfect square-planar geometry. The four Ni−N distances are 1.827 Å for both Ni–N_{amide} and 1.912 and 1.921 Å for Ni–N_{amine}. The three bite angles for the chelate rings are very close to 86º, higher than in the case of Cu^{2+}. The Ni atom is located at 0.013 Å from the plane defined by the nitrogen atoms. In the second [NiH$_{-2}$L] unit the nickel atom displays a more distorted square planar geometry becoming intermediate with the one for a square pyramidal coordination. In this regard, the oxygen atom of one amide group of the other unit is located at 2.970 Å from the nickel atom. Besides this long distance, it must be noted that the oxygen atom is significantly displaced from the vertical, defining OCuN angles of 100.9º and 109.8º for the amide nitrogen atoms and 69.1º and 78.4º for the amino nitrogen atoms. The unit cell for complex **9c** contains eight [NiH$_{-2}$L] units, grouped in four pairs, and eight water molecules. Moreover, an extensive network of intermolecular hydrogen-bonding interactions can be observed between the O atoms of the carbonyl groups and the H atom of the amine groups and/or the water molecules. The amino groups also participate as hydrogen bond donors with water molecules (Figure S13).

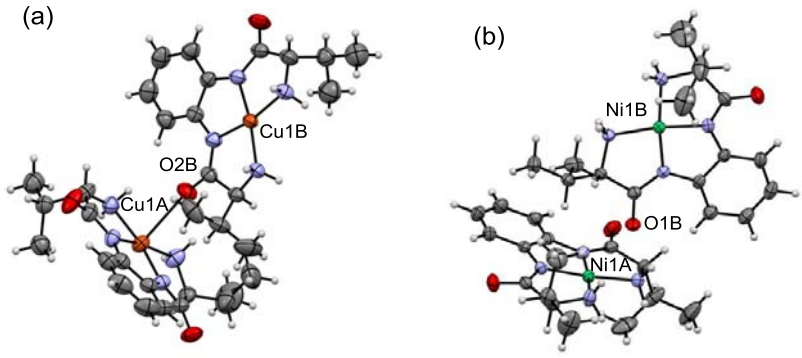

Figure 7. The molecular structure for complexes **9a** (a) and **9c** (b) in their crystal structures.

In the case of the Zn complex (**9b**), only one [$ZnH_{-2}L$] species contribute to the asymmetric unit along with a molecule of isopropanol (Figure 8). In the corresponding molecular structure, the Zn atom displays a distorted square pyramidal geometry in which the square base is formed by the terminal amine and the deprotonated amide nitrogen atoms of the ligand **6**. The oxygen atom from a carbonyl group of a second molecule occupies the apical coordination position of the square pyramidal geometry. The metal center lies above the mean plane of the coordinated nitrogens by 0.603 Å. The Zn–N_{amine} distances average 2.123 Å and the Zn–N_{amide} 2.051 Å, being the Zn–O distance 1.996 Å. The distortion in the square pyramidal geometry is clearly reflected in the O–Zn–N angles present. The two angles involving the N_{amide} atoms are 116.1º and 114.4º while the two involving the N_{amine} atoms are 99.5º and 100.3º. The bite angles for the three chelate rings are very similar and slightly below 80º (79.7º, 79.2º, and 78.9º), providing a N_{amine}–Cu–N_{amine} bite angle of 102.8º. Four independent [$ZnH_{-2}L$] units and four *i*-PrOH molecules define the unit cell. The association of contiguous [$ZnH_{-2}L$] units through O–Zn bonds provides the formation of unidimensional polymeric chains. The contiguous units are not parallel but their main plains, as defined by the aromatic carbons and the four nitrogen atoms, are tilted by ca. 41º and the aromatic fragments are located at opposite sites. The *i*-PrOH molecules play a key role in defining the intermolecular interactions leading to the stabilization of the three-dimensional structure observed in the crystal packing. Each *i*-PrOH molecule acts as hydrogen bond acceptor with one hydrogen atom of the NH_2 group closer to the carbonyl group bound to Zn (NH⋯O distance 2.189 Å) of a [$ZnH_{-2}L$] unit and is also within a short distance of one hydrogen atom of the second NH_2 group of the same unit (2.390 Å). Besides, it acts as a hydrogen bond donor with the oxygen atom of the amide carbonyl not bound to Zn of a [$ZnH_{-2}L$]

unit belonging to a second chain. As *i*-PrOH molecules associated with consecutive units are located at opposite sides of the chain, this defines a 3D hydrogen bond network (Figure S14).

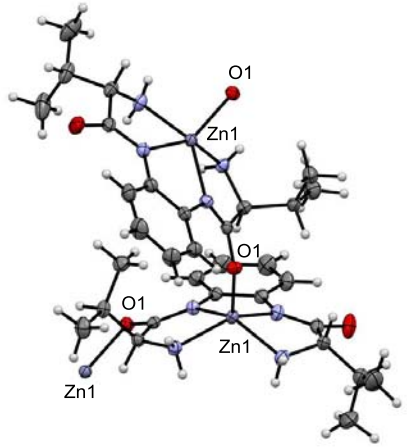

Figure 8. Molecular structure for complex **9b**. The arrangement of two consecutive molecular units displaying the interaction of the oxygen atom of one amide of the first complex with the Zn atom of the second one.

The effect of the substitution of the valine fragment by the one corresponding to phenylalanine can be analyzed comparing the molecular structures of complexes **9a** and **10a** (Figures 7a and 9a). Also, in the case of **10a** two [$CuH_{-2}L$] units are involved in the asymmetric unit (Figure 9a). The coordination environments of the two copper ions are very similar to those described in **9a**, with the metal coordinated to the four nitrogen atoms of ligand **6** (two amines and two deprotonated amides) in a formal square-planar geometry.

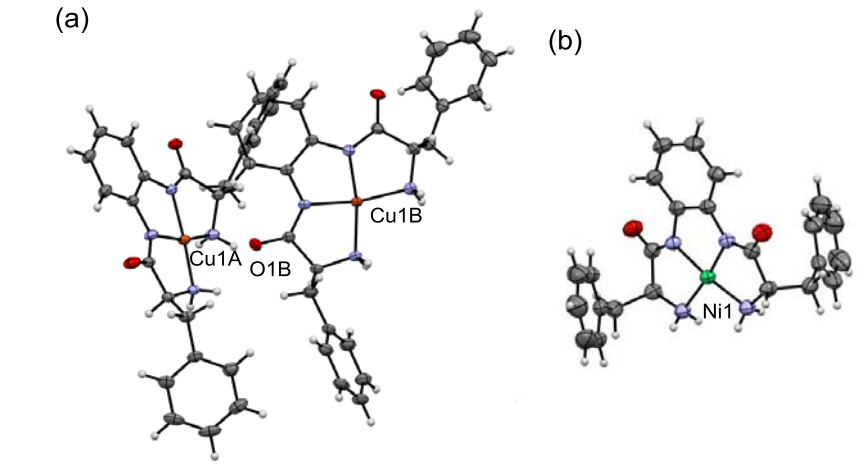

Figure 9. Molecular structure for complexes **10a** (a) and **10c** (b) in their crystal structures.

Again, the Cu–N_{amide} distances are slightly shorter than these for Cu–N_{amine}, being 2.006 and 1.912 Å on average, respectively. Bite angles are very similar to those found in **9a**. Also, in this case, one of the carbonyl groups of one molecule is oriented towards the metal center of the second one, suggesting an actual five coordinated distorted square-pyramidal arrangement. Nevertheless, the resulting Cu–O distance is significantly larger now (2.835 vs. 2.663 Å) and the disposition is similar to that found for the Cu^{2+} complex of the Phegly derived ligand containing an ethylenic central spacer.[22b] The square-planar geometry is essentially coplanar with the aromatic central spacer with the angles between the corresponding mean planes being 1.4º and 7.5º in both units. The two deprotonated amide moieties are more coplanar in **10a** than in **9a**, defining angles between their mean planes of 4.3º and 7.2º instead of the values of 14.6º and 18.5º found in **9a**. The presence of the additional aromatic units in **10a** is important to define the resulting packing (Figure S15). The dispositions of the two [$CuH_{-2}L$] units of the asymmetric unit are different in **9a** and **10a**. In **10a** the two central aromatic spacers and the aromatic unit of

one side chain converge displaying edge-to-face dispositions in which the shorter H-C distances are 3.137 and 3.148 Å between the central spacers and 2.977 and 3.072 Å between the aromatic side chain and the central spacer of the second molecule (in this case the shorter H-centroid distance is 2.984 Å).

The change in the component amino acid is more relevant in the crystal structure of the corresponding Ni^{2+} complexes. For complex **10c**, all the [$NiH_{-2}L$] units present the same molecular structure displaying a perfect C_2 symmetry (Figure 9b). As a matter of fact, only half a unit is required to define the asymmetric unit, with the unit cell involving five [$NiH_{-2}L$] structures (Figure S16). The coordination environment around the nickel shows a perfect square-planar geometry with the Ni atom in the plane defined by the four nitrogen atoms (Ni-plane distance is 0.000 Å) and Ni–N_{amide} and Ni–N_{amine} distances being 1.829 and 1.909 Å, respectively. Bite angles are very similar to those found in **9c**. The aromatic ring of the spacer and the four nitrogen atoms, along with the metal center, define essentially a single plane (deviation is 1.2º). In the molecular structure, the two aromatic rings of the side chains partly cover the space above and below the plane defined by the four nitrogen atoms and the Ni and this seem to preclude a close approaching of an additional [$NiH_{-2}L$] unit as to allow the additional coordination of the oxygen of one amide carbonyl to the metal, as observed in **9c**. In the packing, each [$NiH_{-2}L$] unit has two additional units located close to its NH_2 fragments, displaying NH⋯O distances of 2.387 Å. The main plain of both molecules is almost perpendicular to the one of the first unit (85.9º), one being located above this plane and the second one located below and maintaining the C_2 symmetry defined by the C_2 axis of the first [$NiH_{-2}L$] unit. Aromatic interactions are important. Each of the aromatic rings of the side chain of this first unit shows an edge-to-face arrangement with the central aromatic spacer one of these contiguous units with the

$C_{ar}H\cdots C_{ar}$ shorter distance being 2.853 Å. This aromatic side chain also shows a displaced face-to-face arrangement with one of the aromatic side chains of the same molecule with the $C_{ar}H\cdots$Centroid shorter distance being 3.434 Å.

Catalytic studies

Different metal complexes of pseudopeptidic ligands have shown to be catalytically active for a variety of organic transformations.[14,15,21,34] In this regard, the ring-opening of epoxides with an amine as the nucleophile is an important but challenging route for the synthesis of β-amino alcohols.[35,36] Some of the existing methods have limitations, including the failure of less basic amines to open epoxides under ambient conditions, the requirement of high catalyst loading, the need of using air and moisture sensitive catalysts, non-environmentally friendly solvents or long reaction times.[37] Taking this into account and in order to obtain information on the potential catalytic activity of the considered metal complexes, preliminary studies were carried out on the use of the corresponding Cu^{2+}, Zn^{2+}, and Ni^{2+} complexes with ligands **5** and **6** for the ring opening of cyclohexene oxide with aniline using water, and EtOH as environmentally friendly solvents (Scheme 3).[38]

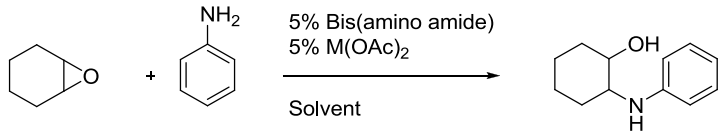

Scheme 3. Epoxide ring opening reaction studied.

Table 4. Yields obtained in the ring opening epoxide reaction between cyclohexene oxide and aniline.

Entry	Ligand	Metal	Solvent	Yield[a]
1	**5**	$Cu(OAc)_2$	EtOH	12.2
2	**5**	$Cu(OAc)_2$	H_2O	33.5
3	**6**	$Cu(OAc)_2$	EtOH	26.6
4	**6**	$Cu(OAc)_2$	H_2O	54.4
5	**5**	$Zn(OAc)_2$	EtOH	30.8
6	**5**	$Zn(OAc)_2$	H_2O	56.8
7	**6**	$Zn(OAc)_2$	EtOH	25.3
8	**6**	$Zn(OAc)_2$	H_2O	81.4
9	**5**	$Ni(OAc)_2$	EtOH	46.8
10	**5**	$Ni(OAc)_2$	H_2O	69.6
11	**6**	$Ni(OAc)_2$	EtOH	18.4
12	**6**	$Ni(OAc)_2$	H_2O	65.6
13	**---**	$Cu(OAc)_2$	H_2O	5.6
14	**---**	$Zn(OAc)_2$	H_2O	34.9
15	**---**	$Ni(OAc)_2$	H_2O	64.9
16	**---**	$Cu(OAc)_2$	EtOH	3.9
17	**---**	$Zn(OAc)_2$	EtOH	15.7
18	**---**	$Ni(OAc)_2$	EtOH	4.1
19	**---**	---	EtOH	15.9
20	**---**	---	H_2O	26.2

Reaction conditions: 5 mol % of ligand and 5 mol % of $M(OAc)_2$, 16 h, rt. [a] Isolated yields.

The results obtained are summarized in Table 4. In general, better yields were obtained using water as a solvent. It must be noted that in water the background reaction in the absence of any catalyst is relatively important (entry 20). [39] The addition of $Zn(OAc)_2$ slightly accelerates this reaction (entry 14) but, on the contrary, the addition of $Cu(OAc)_2$ seems to inhibit the process (entry 13), most likely through the strong coordination of copper to the amino groups. The addition of $Ni(OAc)_2$ accelerates the process to a significant extent. The formation of the corresponding complexes with ligands **5** and **6** led to an acceleration of the reaction for both Zn^{2+} and Cu^{2+} complexes while for Ni^{2+} complexes seem to have no effect. Again the slow kinetics observed for the formation of nickel complexes can be important in this regard. This is

interesting for future applications as reveals this to be a ligand accelerated process for copper and zinc complexes. In any case, copper complexes were less active than zinc complexes. For both metals, complexes formed with ligand **6** derived from Phe were more active than those from ligand **5** derived from Val (compare entries 2 and 4, 6 and 8). The best results were obtained using ligand **6** and $Zn(OAc)_2$ (81.4% yield, entry 8). In general, higher reaction times are needed to afford good yields when the reaction is carried out in the presence of catalysts.[38,40] Unfortunately, no enantiomeric excesses were detected in any case.

CONCLUSIONS

The substitution of an aliphatic central spacer by an aromatic spacer derived from *o*-diaminobenzene in pseudopetidic structures I afford tetradentate ligands **5** and **6** providing some interesting properties in their interaction with Cu^{2+}, Zn^{2+}, and Ni^{2+}. Potentiometric studies reveal that the stability of the complexes formed with Cu^{2+} is several orders of magnitude higher when compared to those formed by the related ligand containing an ethylenic central spacer. This is particularly relevant for the formation of the $[CuH_{-2}L]$ species, leading, as shown in the corresponding distribution diagrams, to the formation of such species even in relatively acidic regions. The preorganization of the ligands in a U-shape conformation favored by the *o*-substitution of the aromatic spacer and the increase in acidity of the amido groups bound to the aromatic fragments can be responsible for this behavior. The differences are, however, less relevant for Zn^{2+} complexes. The rigidity of the central aromatic spacer also seems to facilitate obtaining crystals suitable for X-Ray diffraction. Crystal structures for ligand **6** and $[MH_{-2}L]$ complexes Cu-**5** (**9a**), Cu-**6** (**10a**), Zn-**5** (**9b**), Ni-**5** (**9c**) and Ni-**6** (**10c**) were obtained. In the case of Cu^{2+} and Ni^{2+}, the square planar geometry dominates, with the metal located essentially in the plane defined by the four nitrogen atoms of the ligand. This square planar geometry is in agreement with the spectroscopic data obtained in solution for the Cu^{2+} complexes. In most

cases, however, the oxygen of an amide carbonyl group of a second ligand is located at a short distance and acts as a fifth donor in these complexes. In the crystal obtained for **9b**, the Zn atom displays a clear square pyramidal geometry coordinated to the four nitrogen atoms of a ligand and to the carbonyl oxygen of a second ligand. As observed in other C_2- symmetric pseudopeptidic ligands, the nature of the side chain of the component amino acid plays an important role in the fine-tuning of the properties of the corresponding complexes, affecting both to the stability constants and to the structural arrangement presented. Thus, for instance, the presence of the aromatic side chains in ligand **6** makes more difficult the coordination of the carbonyl group of the second ligand to the metal center in complexes **10a** and **10c**.

Finally, preliminary experiments reveal the capacity of some of the former complexes to act as catalysts for the ring opening of the cyclohexene epoxide using aniline as the nucleophile in water. Interestingly, the results show that this is a ligand accelerated the catalytic process and Zn^{2+} complexes act as more efficient catalysts, in particular, **10b** formed in the presence of ligand **6**, than the related Cu^{2+} complexes. Unfortunately, the catalytic reaction took place without any observed enantiomeric induction.

ASSOCIATED CONTENT

Supporting Information

The Supporting Information material is available free of charge on the ACS Publications Web site. at DOI:

Characterization of the compounds **5** and **6** , ^{1}H NMR titration of compound **5** at different pD values, potentiometric distribution diagrams, FT-IR spectroscopy, ESI-MS spectra, X-ray crystal structures data.

AUTHOR INFORMATION

Corresponding Authors

Email: luiss@uji.es

Email: altava@uji.es

Notes

The authors declare no competing financial interests.

ACKNOWLEDGMENT

This research work was supported by the Spanish MINECO (CTQ2015-68429-R), Generalitat Valenciana (PROMETEO/2012/020) and PPI-UJI (P1-1B-2013-38). L.G thanks, Generalitat Valenciana for a Santiago Grisolia fellowship (GRISOLIA 2012/015). The support of the SCIC for the different instrumental techniques at Universitat Jaume I is acknowledged.

Experimental section

All reagents and solvents were obtained from commercial sources and used as received unless otherwise stated. Deionized water was used from a “Milli-Q® Integral Water Purification System” by Millipore. Microanalyses were performed on an elemental analyzer equipped with an

oxygen module. Rotatory power was determined with a digital polarimeter (Na: 589 nm). Melting points were measured using a standard apparatus and are uncorrected.

^{1}H NMR experiments

^{1}H spectra were recorded on a Varian INOVA 500 spectrometer (500 and 125 MHz for ^{1}H and ^{13}C NMR, respectively). The solvent signal was used as a reference standard. Additional experiments were carried out using CD_3CN/D_2O 7/3 v/v using the standard solvent suppression pulse sequence.

Electromotive force measurements and UV-Vis experiments

The potentiometric titrations were carried out at 298.1 ± 0.1 K using 0.1 M NaCl as the supporting electrolyte. The experimental procedure (burette, potentiometer, cell, stirrer, micro-computer, etc.) has been fully described elsewhere.[41] The acquisition of the emf data was performed with the computer program CrisonCapture. The reference electrode was an Ag/AgCl electrode in saturated KCl solution. The glass electrode was calibrated as a hydrogen-ion concentration probe by titration of previously standardized amounts of HCl with CO_2-free NaOH solutions and the equivalence point determined by the Gran's method,[42] which gives the standard potential, E°′, and the ionic product of water 13.78, whereas in the case of the water/ACN mixture used this value was 14.6.[27] The computer program HYPERQUAD[26] was used to calculate the protonation and stability constants, and the HySS29[43] program was used to obtain the distribution diagrams. The pH range investigated was 2.0-12.0 and the concentration of the metal ions and of the ligands 0.1 mM with M^{2+}:L molar ratios as 1:1. The different titration curves for each system (at least two) were treated either as a single set or as separated curves

without significant variations in the values of the stability constants. Finally, the sets of data were merged together and treated simultaneously to give the final stability constants.

UV-Vis absorption spectra were recorded using a Hewlett-Packard 8453 device, using solutions of 0.1 mM at different pH values containing 1:1 M^{2+}:L molar ratios. Additional experiments were carried out in 0.1 M NaCl solutions. Only minimal differences were observed in this case.

Mass spectrometry

Mass spectra were recorded on a Q-TOF Premier mass spectrometer with an orthogonal Z-spray electrospray interface (Micromass, Manchester, UK) either by electrospray positive mode (ES^+) or by electrospray negative mode (ES^-). The desolvation gas, as well as nebulizing gas, was nitrogen at a flow of 700 L/h and 20 L/h, respectively. The temperature of the source block was set to 120 °C and the desolvation temperature to 150 °C. A capillary voltage of 3.5 and 3.3 kV was used in the positive and negative scan mode, respectively. The cone voltage was typically set to 20 V to control the extent of fragmentation of the identified ions. Sample solutions were infused via syringe pump directly connected to the ESI source at a flow rate of 10 mL/min. The observed isotopic pattern of each intermediate perfectly matched the theoretical isotope pattern calculated from their elemental composition using the MassLynx 4.0 program.[44]

IR spectroscopy

FT-IR spectra were acquired on a JASCO 6200 equipment with a MIRacle single reflection ATR diamond/ZnSe accessory. The raw IR spectral data were processed with the JASCO spectral manager software.

Crystallography

Single crystals of ligand **6** and complexes **9a-c** and **10a**, **10c** were obtained. A suitable crystal was selected and measured on a single crystal X-Ray diffractometer. Using Olex2,[45] all the structures were solved with the ShelXS 2014[46] structure solution program using Direct Methods and refined with the ShelXL 2014[46] refinement package using Least Squares minimization. The program MERCURY[47] and PyMOL[48] were used to prepare artwork representations. Crystallographic data and refinement parameters are summarized in Table S1–S2. Hydrogen bonds for the compounds are grouped in S3–S7. Crystallographic details are available in the Supporting Information in CIF format. CCDC numbers 1474242 (**9b**), 1474243 (**10a**), 1474244 (**6**), 1474245 (**10c**), 1474246 (**9c**), 1474247 (**9a**).

Synthesis of compounds

Compound 3. Cbz-Val-OH (10.0 g, 39.0 mmol) and triethyl amine (5.48 mL, 39.0 mmol) were dissolved, under a nitrogen atmosphere, in dry THF (200 mL). The reaction mixture was cooled with an ice bath and NaCl to -10 ^{o}C. Previously cooled ethyl chloroformate (3.84 mL, 39.0 mmol) was then added dropwise and the reaction mixture stirred for 30 min at -10 ^{o}C. Afterwards, 1,2-phenylene diamine (2.13 g, 19.5 mmol) dissolved in 25 mL of dry THF was added dropwise, avoiding any increase of the temperature. After stirring for an additional 2 h at this temperature, it was left to warm up to room temperature, the stirring being continued for 24 h. The white precipitate formed was filtered, washed with water and vacuum dried. Yield 57% (6.53 g, 11.37 mmol); mp 206-208 ^{o}C; $[\alpha]_D^{25}$ + 3.08 (c = 0.01, DMSO); IR (ATR) 3289, 2961, 1690, 1652, 1594, 1533, 1497, 1454 cm^{-1}; ^{1}H NMR (500 MHz, DMSO-d_6) δ 9.44 (s, 2H), 7.52 (s, 2H), 7.46 (d, *J* = 7.5 Hz, 2H), 7.38 – 7.27 (m, 10H), 7.18 (dd, *J* = 5.9, 3.5 Hz, 2H), 5.11 –

5.01 (m, 4H), 4.01 (t, *J* = 7.2 Hz, 2H), 2.09 (d, *J* = 6.4 Hz, 2H), 0.91 (t, *J* = 6.0 Hz, 12H); ^{13}C NMR (75 MHz, DMSO-*d*$_6$) δ 170.9, 156.7, 137.2, 130.5, 128.8, 127.9, 125.2, 65.9, 61.5, 30.5, 19.4, 18.6; Anal. Calcd. (%) for $C_{32}H_{38}N_4O_6$: C, 66.88; H, 6.67; N, 9.75. Found: C, 66.30; H, 6.50; N, 9.81.

Compound 5. To a solution of compound **3** (1.20 g, 2.09 mmol) in dry MeOH in a two necked round bottom flask, 10 mol % of the catalyst (5 wt % Pd on activated carbon) was added. The system was purged to remove the air and connected to an H_2 atmosphere (H_2 balloon) and stirred at room temperature for 8 h. The grey suspension turned black and the precipitate was filtered off through a Celite® bed and washed with MeOH. Evaporation of the solvent under vacuum yielded the compound **5** as a white solid. Yield 66% (0.420 g, 1.37 mmol); mp 70-72 ^{o}C; $[\alpha]_D^{25}$ -15.34 (c = 0.01, $CHCl_3$); IR (ATR) 3298, 2959, 2930, 2872, 1661, 1599, 1506, 1465 cm^{-1}; ^{1}H NMR (500 MHz, $CDCl_3$) δ 9.55 (s, 2H), 7.61 (dd, *J* = 5.9, 3.6 Hz, 2H), 7.19 (dd, *J* = 6.0, 3.5 Hz, 2H), 3.39 (s, 2H), 2.44 – 2.33 (m, 2H), 1.07 (d, *J* = 7.0 Hz, 6H), 0.93 (d, *J* = 6.9 Hz, 6H); ^{13}C NMR (75 MHz, $CDCl_3$) δ 173.5, 130.0, 126.0, 124.5, 61.0, 31.4, 19.7, 16.3; HRMS (ESI-TOF)$^+$ Calcd. for $C_{16}H_{26}N_4O_2$ ($M+H^+$) 307.2134. Found 307.2131; Anal. Calcd. (%) for $C_{16}H_{26}N_4O_2 \cdot 0.5\ H_2O$: C, 60.93; H, 8.60; N, 17.76. Found: C, 61.54; H, 8.13; N, 17.41.

Compound 4. Prepared using the same protocol described for **3** but starting from Cbz-Phe-OH. Yield 39% (4.39 g, 6.55 mmol); mp 201-203 ^{o}C; $[\alpha]_D^{25}$ + 4.84 (c = 0.01, DMSO); IR (ATR) 3302, 3256, 3062, 2918, 1652, 1527, 1255 cm^{-1}; ^{1}H NMR (500 MHz, DMSO-*d*$_6$) δ 9.55 (s, 2H), 7.65 (d, *J* = 7.4 Hz, 1H), 7.49 (s, 1H), 7.32 – 7.02 (m, 10H), 4.93 (dd, *J* = 51.5, 12.6 Hz, 4H), 4.44 (s, 2H), 3.01 – 2.84 (m, 2H); ^{13}C NMR (75 MHz, DMSO-*d*$_6$) δ 171.1, 138.3, 137.3, 130.8, 129.7, 128.7, 128.5, 128.1, 127.9, 126.8, 125.8, 125.3, 65.9, 57.3, 37.6; Anal. Calcd. (%) for $C_{40}H_{38}N_4O_6 \cdot 0.5\ H_2O$: C, 70.68; H, 5.78; N, 8.24. Found: C, 70.42; H, 5.59; N, 7.93.

Compound 6. Prepared using the same protocol described for **5** but starting from **4**. Yield 53% (0.324 g, 0.81 mmol); mp 110-113 ^{o}C; $[\alpha]_D^{25}$ + 111.13 (c = 0.01, $CHCl_3$); IR (ATR) 3373, 3298, 3026, 2918, 1671, 1509, 1452 cm^{-1}; ^{1}H NMR (500 MHz, $CDCl_3$) δ 9.47 (s, 1H), 7.61 (dd, *J* = 5.9, 3.6 Hz, 2H), 7.32 (dd, *J* = 20.0, 12.5 Hz, 4H), 7.27 – 7.20 (m, 6H), 3.76 (dd, *J* = 9.2, 4.1 Hz, 2H), 3.34 (dd, *J* = 13.7, 4.0 Hz, 2H), 2.80 (dd, *J* = 13.7, 9.2 Hz, 2H); ^{13}C NMR (75 MHz, $CDCl_3$) δ 172.8, 137.4, 129.8, 129.3, 128.8, 126.8, 126.0, 124.5, 56.9, 40.9; HRMS (ESI-TOF)$^{+}$ Calcd. for $C_{24}H_{26}N_4O_2$ ($M+H^+$) 403.2134. Found 403.2139; Anal. Calcd. (%) for $C_{24}H_{26}N_4O_2 \cdot 0.2\ H_2O$: C, 70.98; H, 6.55; N, 13.80. Found: C, 70.93; H, 6.28; N, 13.46.

General procedure for the synthesis of Cu^{2+} complexes

Complex 9a. A solution of $Cu(OAc)_2$ (1 equiv.) in MeOH (*ca*. 10^{-2} M) was added to a solution of compound **5** (1 equiv) in MeOH (ca. 10^{-2} M). After stirring the mixture for 30 min at room temperature, KOH (*ca*. 2 equiv) 1 M in methanol was added and the solution was maintained at room temperature overnight. The precipitate formed was isolated by filtration and washed with dichloromethane, to yield a purple powder. Yield 73% (101.2 mg, 0.28 mmol); (IR) ATR 3600-3000, 2963, 2960, 1591, 1537, 1469, 1395 cm^{-1}; Anal. Calcd. (%) for $C_{16}H_{24}N_4O_2Cu \cdot H_2O$: C, 49.79; H, 6.79; N, 14.52. Found: C, 49.28; H, 6.75; N, 14.38.

Complex 10a. Yield 84% (76.2 mg, 0.16 mmol); (IR) ATR 3600-3000, 2963, 1594, 1541, 1471 cm^{-1}; Anal. Calcd. (%) for $C_{24}H_{24}N_4O_2Cu$: C, 62.12; H, 5.21; N, 12.07. Found: C, 62.11, H, 5.28, N, 11.96.

General procedure for the synthesis of Zn^{2+} complexes

Complex 9b. A solution of $Zn(OAc)_2$ (1 equiv) in MeOH (*ca.* 10^{-2} M) was added to a solution of compound **5** (1 equiv) in MeOH (*ca.* 10^{-2} M). After stirring the mixture for 30 min at room temperature, KOH (ca. 2 equiv) 1 M in methanol was added and the solution was maintained at room temperature overnight. The precipitate formed was isolated by filtration and washed with dichloromethane to yield a white solid. Yield 54% (434 mg, 1.17 mmol); (IR) ATR 3600-3000, 1591, 1523, 1473 cm^{-1}; Anal. Calcd (%) for $C_{16}H_{24}N_4O_2Zn \cdot 3\ H_2O$: C, 45.34; H, 7.13; N, 13.22. Found C, 45.64; H, 6.75; N, 13.12.

Complex 10b. Yield 41% (143 mg, 0.31 mmol); (IR) ATR 3352-3308, 3248, 3144, 2963, 2960, 1591, 1537, 1469, 1395 cm^{-1}; Anal. Calcd. (%) for $C_{24}H_{24}N_4O_2Zn \cdot 0.1\ H_2O$: C, 61.63; H, 5.22; N, 11.98. Found C, 61.34, H, 5.25; N, 11.75.

General procedure for the synthesis of Ni^{2+} complexes

Complex 9c. To a solution of $Ni(OAc)_2$ (1 equiv) in MeOH (*ca.* 10^{-2} M) was added to a solution of compound 5 (1 equiv) in MeOH (ca. 10^{-2} M). After stirring the mixture for 30 min at room temperature, KOH (ca. 2 equiv) 1 M in methanol was added and the solution was maintained at room temperature overnight. The precipitate formed was isolated by filtration and washed with dichloromethane to yield a yellow solid. Yield 67% (91.4 mg, 0.25 mmol); (IR) ATR 3396-3274, 2961, 1594, 1551, 1494 cm^{-1}; Anal. Calcd. (%) for $C_{16}H_{24}N_4O_2Ni \cdot C_2H_5OH$: C, 52.84; H, 7.39; N, 13.69. Found: C, 52.81; H, 7.29; N, 13.66.

Complex 10c. Yield 78% (66.5 mg, 0.14 mmol); (IR) ATR 3281-3026, 2940, 2918, 1597, 1551, 1476, 1452, 1275 cm^{-1}; Anal. Calcd. (%) for $C_{24}H_{24}N_4O_2Ni \cdot H_2O$: C, 60.41; H, 5.49; N, 11.74. Found: C, 60.59, H, 5.25, N, 11.67.

Typical procedure for ring opening of epoxide reaction

In an oven dried 5 mL vial, the bis(amino amide) (0.05 mmol) and the metal acetate (0.05 mmol) were dissolved in 2 mL of solvent and the vial closed. After 30 minutes stirring, cyclohexene oxide (103 μL, 1 mmol) was added. After 1 h stirring at room temperature, aniline (92 μL, 1 mmol) was added and the mixture stirred for 12 h. The solvent was evaporated to dryness, the residue dissolved in water (5 mL) and extracted with DCM (3 x 5 mL). The organic phases were collected and dried over anhydrous $MgSO_4$ and evaporated to give pure 2-phenyl amino cyclohexanol. ^{1}H NMR (500 MHz, $CDCl_3$) δ 7.22 – 7.11 (m, 2H), 6.80 – 6.63 (m, 3H), 3.38 – 3.32 (m, 1H), 3.15 (ddd, J = 11.2, 9.2, 4.0 Hz, 1H), 2.20 – 2.03 (m, 2H), 1.83 – 1.63 (m, 2H), 1.47 – 1.21 (m, 3H), 1.06 (ddd, J = 24.1, 12.8, 3.7 Hz, 1H).

REFERENCES

1 a) Multhaup, G.; Schlicksupp, A.; Hesse, L.; Beher, D.; Ruppert, T.; Masters, C. L.; Beyreuther, K., *Science* **1996**, *271*, 1406-1409. (b) Sen, C. K.; Khanna, S.; Venojarvi, M.; Trikha, P.; Ellison, E. C.; Hunt, T. K.; Roy, S., *Am. J. Physiol. Heart Circ. Physiol.* **2002**, *282*, H1821-H1827. (c) Grubman, A. ; White, A. R., *Expert Rev. Mol. Med.* **2014**, *16*, e11. (d) Scheiber, I. F.; Mercer, J. F. B.; Dringen, R., *Prog. Neurobiol.* **2014**, *116*, 33-57. (e) Bellingham, S. A.; Guo, B.; Hill, A. F., *Biol. Cell* **2015**, *107*, 389-418.

2 (a) Fricker, S. P., *Dalton Trans.* **2007**, 4903-4917. (b) Mjos, K. D.; Orvig, C., *Chem. Rev.* **2014**, *114*, 4540-4563. (c) Medici, S.; Peana, M.; Nurchi, V. M.; Lachowicz, J. I.; Crisponi, G.; Zoroddu, M. A., *Coord. Chem. Rev.* **2015**, *284*, 329-350.

3 (a) Crichton, R. R.; Dexter, D. T.; Ward, R. J., *Coord. Chem. Rev.* **2008**, *252*, 1189-1199. (b) Ward, R. J.; Dexter, D. T.; Crichton, R. R., *Curr. Med. Chem.* **2012**, *19,* 2760-2772.

4 (a) Cini, R.; Tamasi, G.; Defazio, S.; Hursthouse, M. B., *J. Inorg. Biochem.* **2007**, *101*, 1140-1152. (b) Marzano, C.; Pellei, M.; Tisato, F.; Santini, C., *Anti-Cancer Agents Med. Chem.* **2009**, *9*, 185-211.

5 (a) Sousa, I.; Claro, V.; Pereira, J. L.; Amaral, A. L.; Cunha-Silva, L.; de Castro, B.; Feio, M. J.; Pereira, E.; Gameiro, P., *J. Inorg. Biochem.* **2012**, *110*, 64-71. (b) Dorotikova, S.; Koziskova, J.; Malcek, M.; Jomova, K.; Herich, P.; Plevova, K.; Briestenska, K.; Chalupkova, A.; Mistrikova, J.; Milata, V.; Dvoranova, D.; Bucinsky, L., *J. Inorg., Biochem.* **2015**, *150*, 160-173.

6 Sönmez, M.; Levent, A.; Şekerci, M., *Russ. J. Coord. Chem.* **2004**, *30*, 655-660.

7 (a) Miyake, H.; Kojima, Y., *Coord. Chem. Rev.* **1996**, *148*, 301-314. (b) Wende, C.; Lüdtke, C.; Kulak, N., *Eur. J. Inorg. Chem.* **2014**, *2014*, 2597-2612. (c) Quintanova, C.; Keri, R. S.; Chaves, S.; Santos, M. A., *J. Inorg. Biochem.* **2015**, *151*, 58-66. (d) Skalamera, D.; Sanders, E.; Vianello, R.; Marsavelski, A.; Pevec, A.; Turel, I.; Kirin, S. I., *Dalton Trans.* **2016**, *45*, 2845-2858.

8 (a) Karlin, K., *Science* **1993**, *261*, 701-708. (b) Roat-Malone, R. M., *Bioinorganic Chemistry: A Short Course*, 2nd Edition, John Wiley & Sons, Inc.: Hoboken, NJ, 2007. (c) Gray, H. B.; Stiefel, E. I.; Valentine, J. S.; Bertini, I., *Biological Inorganic Chemistry: Structure and Reactivity 1st Edition*, University Science Books,

Sausalito, CA, 2007. (d) Gramage-Doria, R.; Armspach, D.; Matt, D., *Coord. Chem. Rev.* **2013**, *257*, 776-816. (e) Bistri, O.; Reinaud, O., *Org. Biomol. Chem.* **2015**, *13*, 2849-2865.
9 (a) Hechavarría Fonseca, M.; König, B., *Adv. Synth. Catal.* **2003**, *345*, 1173-1185. (b) Green, B. J.; Tesfai, T. M.; Xie, Y.; Margerum, D. W., *Inorg. Chem*. **2004**, *43*, 1463-1471. (c) Tesfai, T. M.; Green, B. J.; Margerum, D. W., *Inorg. Chem*. **2004**, *43*, 6726-6733. (d) Prell, J. S.; Flick, T. G.; Oomens, J.; Berden, G.; Williams, E. R., *J. Phys. Chem. A* **2010**, *114*, 854-860. (e) Dokorou, V. N.; Milios, C. J.; Tsipis, A. C.; Haukka, M.; Weidler, P. G.; Powell, A. K.; Kostakis, G. E., *Dalton Trans.* **2012**, *41*, 12501-12513. (f) Dennis, C. R.; Swarts, J. C.; Margerum, D. W., *React. Kinet., Mech. Catal.* **2012**, *107*, 27-38. (g) Dong, J.; Wang, Y.; Xiang, Q.; Lv, X.; Weng, W.; Zeng, Q., *Adv. Synth. Catal.* **2013**, *355*, 692-696.
10 (a) Locardi, E.; Stöckle, M.; Gruner, S.; Kessler, H., *J. Am. Chem. Soc.* **2001**, *123*, 8189-8196. (b) Gibson, S. E.; Lecci, C., *Angew. Chem., Int. Ed.* **2006**, *45*, 1364-1377. (c) White, C. J.; Yudin, A. K., *Nat. Chem.* **2011**, *3*, 509-524. (d) Lewandowski, B.; De Bo, G.; Ward, J. W.; Papmeyer, M.; Kuschel, S.; Aldegunde, M. J.; Gramlich, P. M. E.; Heckmann, D.; Goldup, S. M.; D'Souza, D. M.; Fernandes, A. E.; Leigh, D. A., *Science* **2013**, *339*, 189-193.
11 (a) Fernandez-Lopez, S.; Kim, H.-S.; Choi, E. C.; Delgado, M.; Granja, J. R.; Khasanov, A.; Kraehenbuehl, K.; Long, G.; Weinberger, D. A.; Wilcoxen, K. M.; Ghadiri, M. R., *Nature* **2001**, *412*, 452-455. (b) Kubik, S., *Chem. Soc. Rev.* **2009**, *38*, 585-605. (c) Klemm, K.; Radić Stojković, M.; Horvat, G.; Tomišić, V.; Piantanida, I.; Schmuck, C., *Chem. - Eur. J.* **2012**, *18*, 1352-1363.
12 (a) Hu, X.; Nguyen, K. T.; Verlinde, C. L. M. J.; Hol, W. G. J.; Pei, D., *J. Med. Chem.* **2003**, *46*, 3771-3774. (b) Loughlin, W. A.; Tyndall, J. D. A.; Glenn, M. P.; Fairlie, D. P., *Chem. Rev.* **2004**, *104*, 6085-6118. (c) Silva, G. A.; Czeisler, C.; Niece, K. L.; Beniash, E.; Harrington, D. A.; Kessler, J. A.; Stupp, S. I., *Science* **2004**, *303*, 1352-1355.
13 (a) Choi, K.; Hamilton, A. D., *Coord. Chem. Rev.* **2003**, *240*, 101-110. (b) Wu, Y.-D.; Gellman, S., *Acc. Chem. Res.* **2008**, *41*, 1231-1232. (c) Nowick, J. S., *Acc. Chem. Res.* **2008**, *41*, 1319-1330. (d) Suzuki, M.; Hanabusa, K., *Chem. Soc. Rev*. **2009**, *38*, 967-975. (e) Brea, R. J.; Reiriz, C.; Granja, J. R., *Chem. Soc. Rev.* **2010**, *39*, 1448-1456. (f) Ke, D.; Zhan, C.; Li, A. D. Q.; Yao, J., *Angew. Chem., Int. Ed*. **2011**, *50*, 3715-3719. (g) Das, D.; Maiti, S.; Brahmachari, S.; Das, P. K., *Soft Matter* **2011**, *7*, 7291-7303.
14 (a) Merschky, M.; Schmuck, C., *Org. Biomol. Chem.* **2009**, *7*, 4895-4903. (b) Weseliński, Ł.; Słyk, E.; Jurczak, J., *Tetrahedron Lett.* **2011**, *52*, 381-384. (c) Paradowska, J.; Pasternak, M.; Gut, B.; Gryzło, B.; Mlynarski, J., *J. Org. Chem*. **2012**, *77*, 173-187.
15 (a) Dangel, B.; Clarke, M.; Haley, J.; Sames, D.; Polt, R., *J. Am. Chem. Soc.* **1997**, *119*, 10865-10866. (b) Dangel, B. D.; Polt, R., *Org. Lett.* **2000**, *2*, 3003-3006. (c) Polt, R.; Kelly, B. D.; Dangel, B. D.; Tadikonda, U. B.; Ross, R. E.; Raitsimring, A. M.; Astashkin, A. V., *Inorg. Chem.* **2003**, *42*, 566-574.
16 (a) Luis, S. V.; Alfonso, I., *Acc. Chem. Res.* **2014**, *47*, 112-124.
17 (a) Galindo, F.; Becerril, J.; Isabel Burguete, M.; Luis, S. V.; Vigara, L., *Tetrahedron Lett.* **2004**, *45*, 1659-1662. (b) Alfonso, I.; Burguete, M. I.; Galindo, F.; Luis, S. V.; Vigara, L., *J. Org. Chem.* **2009**, *74*, 6130-6142. (c) Altava, B.; Burguete, M. I.; Carbó, N.; Escorihuela, J.; Luis, S. V., *Tetrahedron: Asymmetry* **2010**, *21*, 982-989. (d) Martí-Centelles, V.; Izquierdo, M. A.; Burguete, M. I.; Galindo, F.; Luis, S. V., *Chem. - Eur. J.* **2014**, *20*, 7465-7478. (e) Faggi, E.; Moure, A.; Bolte, M.; Vicent, C.; Luis, S. V.; Alfonso, I., *J. Org. Chem.* **2014**, *79*, 4590-4601.
18 (a) Alfonso, I.; Burguete, M. I.; Luis, S. V., *J. Org. Chem.* **2006**, *71*, 2242-2250. (b) Alfonso, I.; Burguete, M. I.; Galindo, F.; Luis, S. V.; Vigara, L., *J. Org. Chem.* **2007**, *72*, 7947-7956. (c) Faggi, E.; Luis, S. V.; Alfonso, I., *RSC Adv.* **2013**, *3*, 11556-11565.
19 (a) Becerril, J.; Burguete, M. I.; Escuder, B.; Galindo, F.; Gavara, R.; Miravet, J. F.; Luis, S. V.; Peris, G., *Chem. - Eur. J.* **2004**, *10*, 3879-3890. (b) Becerril, J.; Escuder, B.; Miravet, J. F.; Gavara, R.; Luis, S. V., *Eur. J. Org. Chem.* **2005**, *2005*, 481-485. (c) Wadhavane, P. D.; Galian, R. E.; Izquierdo, M. A.; Aguilera-Sigalat, J.; Galindo, F.; Schmidt, L.; Burguete, M. I.; Perez-Prieto, J.; Luis, S. V., *J. Am. Chem. Soc.* **2012**, *34*, 20554-20563. (d) Rubio, J.; Martí-Centelles, V.; Burguete, M. I.; Luis, S. V., *Tetrahedron* **2013**, *69*, 2302-2308.
20 (a) Galindo, F.; Burguete, M. I.; Vigara, L.; Luis, S. V.; Kabir, N.; Gavrilovic, J.; Russell, D. A., *Angew. Chem., Int. Ed.* **2005**, *44*, 6504-6508. (b) Wadhavane, P. D.; Izquierdo, M. A.; Lutters, D.; Burguete, M. I.; Marin, M. J.; Russell, D. A.; Galindo, F.; Luis, S. V., *Org. Biomol. Chem.* **2014**, *12*, 823-831.
21 Adrián, F.; Burguete, M. I.; Fraile, J. M.; García, J. I.; García, J.; García-España, E.; Luis, S. V.; Mayoral, J. A.; Royo, A. J.; Sánchez, M. C., *Eur. J. Inorg. Chem.* **1999**, *1999*, 2347-2354.
22 (a) Blasco, S.; Burguete, M. I.; Clares, M. P.; García-España, E.; Escorihuela, J.; Luis, S. V., *Inorg. Chem.* **2010**, *49*, 7841-7852. (b) Marti, I.; Ferrer, A.; Escorihuela, J.; Burguete, M. I.; Luis, S. V., *Dalton Trans.* **2012**, *41*,

6764-6776. (c) Wadhavane, P. D.; Gorla, L.; Ferrer, A.; Altava, B.; Burguete, M. I.; Izquierdo, M. A.; Luis, S. V., *RSC Adv.* **2015**, *5*, 72579-72589.
23 Marti-Centelles, V.; Kumar, D. K.; White, A. J. P.; Luis, S. V.; Vilar, R., *CrystEngComm* **2011**, *13*, 6997-7008.
24 Martell, A. E.; Motekaitis, R. J., *Coord. Chem. Rev.* **1990**, *100*, 323-361.
25 García-España, E.; Díaz, P.; Llinares, J. M.; Bianchi, A., *Coord. Chem. Rev.* **2006**, *250*, 2952-2986.
26 Gans, P.; Sabatini, A.; Vacca, A., *Talanta* **1996**, *43*, 1739-1753.
27 Herrador, M. Á.; González, A. G., *Talanta* **2002**, *56*, 769-775.
28 (a) Bianchi, A.; Escuder, B.; Garcia-España, E.; Luis, S. V.; Marcelino, V.; Miravet, J. F.; Ramirez, J. A., *J. Chem. Soc., Perkin Trans. 2* **1994**, 1253-1259. (b) Aguilar, J. A.; García-España, E.; Guerrero, J.; Luis, S. V.; Llinares, J.; Ramírez, J.; Soriano, C., *Inorg. Chim. Acta* **1996**, *246*, 287-294. (c) Arán, V. J.; Kumar, M.; Molina, J.; Lamarque, L.; Navarro, P.; García-España, E.; Ramírez, J. A.; Luis, S. V.; Escuder, B., J. Org. Chem. **1999**, *64*, 6135-6146.
29 (a) Constable, E. C.; Housecroft, C. E.; Price, J. R.; Zampese, J. A., *CrystEngComm* **2010**, *12*, 3163-3171. (b) Abdi, K.; Hadadzadeh, H.; Weil, M.; Salimi, M., *Polyhedron* **2012**, *31*, 638-648. (c) Bukharov, M. S.; Shtyrlin, V. G.; Mamin, G. V.; Stapf, S.; Mattea, C.; Mukhtarov, A. S.; Serov, N. Y.; Gilyazetdinov, E. M., *Inorg. Chem.* **2015**, *54*, 9777-9784.
30 (a) Autzen, S.; Korth, H.-G.; Boese, R.; de Groot, H.; Sustmann, R., *Eur. J. Inorg. Chem.* **2003**, *2003*, 1401-1410. (b) Pauly, M. A.; Erwin, E. M.; Powell, D. R.; Rowe, G. T.; Yang, L., *Polyhedron* **2014**, *102*, 722-734.
31 (a) Schug, K.; Fryčák, P.; Maier, N. M.; Lindner, W., *Anal. Chem.* **2005**, *77*, 3660-3670. (b) Di Tullio, A.; Reale, S.; De Angelis, F., *J. Mass Spectrom.* **2005**, *40*, 845-865. (c) Baytekin, B.; Baytekin, H. T.; Schalley, C. A., *Org. Biomol. Chem.* **2006**, *4*, 2825-2841. (d) Beattie, J. W.; White, D. S.; Bheemaraju, A.; Martin, P. D.; Groysman, S., *Dalton Trans.* **2014**, *43*, 7979-7986.
32 (a) Rebek, J., *Science* **1987**, *235*, 1478-1484. (b) Rebek, J., *Acc. Chem. Res.* **1990**, *23*, 399-404.
33 (a) Dance, I., *New J. Chem.* **2003**, *27*, 22-27. (b) Álvarez, S., *Dalton Trans.* **2013**, *42*, 8617-8636. (c) White, N. G.; Serpell, C. J.; Beer, P. D., *Cryst. Growth Des.* **2014**, *14*, 3472-3479.
34 (a) Alcón, M. J.; Iglesias, M.; Sánchez, F.; Viani, I., *J. Organomet. Chem.* **2000**, *601*, 284-292. (b) Burguete, M. I.; Collado, M.; Escorihuela, J.; Galindo, F.; García-Verdugo, E.; Luis, S. V.; Vicent, M. J., *Tetrahedron Lett.* **2003**, *44*, 6891-6894. (c) Xiong, Y.; Huang, X.; Gou, S.; Huang, J.; Wen, Y.; Feng, X., *Adv. Synth. Catal.* **2006**, *348*, 538-544. (d) Burguete, M. I.; Collado, M.; Escorihuela, J.; Luis, S. V., *Angew. Chem. Int. Ed.* **2007**, *46*, 9002-9005. (e) Xu, Z.; Daka, P.; Wang, H., *Chem. Commun*. **2009**, 6825-6827. (f) Albada, H. B.; Rosati, F.; Coquière, D.; Roelfes, G.; Liskamp, R. M. J., *Eur. J. Org. Chem.* **2011**, *2011*, 1714-1720.
35 (a) Barbaro, P.; Bianchini, C.; Sernau, V., *Tetrahedron: Asymmetry* **1996**, *7*, 843-850. (b) Azizi, N.; Saidi, M. R., *Org. Lett.* **2005**, *7*, 3649-3651. (c) Bonollo, S.; Fringuelli, F.; Pizzo, F.; Vaccaro, L., *Green Chem.* **2006**, *8*, 960-964.
36 (a) Sekar, G.; Singh, V. K., *J. Org. Chem.* **1999**, *64*, 287-289. (b) Yadav, J. S.; Reddy, A. R.; Narsaiah, A. V.; Reddy, B. V. S., *J. Mol. Catal. A: Chem.* **2007**, *261*, 207-212. (c) Shivani; Pujala, B.; Chakraborti, A. K., *J. Org. Chem.* **2007**, *72*, 3713-3722. (d) Bhanushali, M. J.; Nandurkar, N. S.; Bhor, M. D.; Bhanage, B. M., *Tetrahedron Lett.* **2008**, *49*, 3672-3676. (e) Li, Y.; Tan, Y.; Herdtweck, E.; Cokoja, M.; Kühn, F. E., *Appl. Catal., A* **2010**, *384*, 171-176. (f) Pujala, B.; Rana, S.; Chakraborti, A. K., *J. Org. Chem.* **2011**, *76*, 8768-8780. (g) Narsaiah, A. V.; Wadavrao, S. B.; Reddy, A. R.; Yadav, J. S., *Synthesis* **2011**, *3*, 485-489. (h) Lu, H.-F.; Sun, L.-L.; Le, W.-J.; Yang, F.-F.; Zhou, J.-T.; Gao, Y.-H., *Tetrahedron Lett.* **2012**, *53*, 4267-4272. (i) Pathare, S. P.; Akamanchi, K. G., *Tetrahedron Lett.* **2013**, *54*, 6455-6459.
37 (a) Schneider, C.; Sreekanth, A. R.; Mai, E., *Angew. Chem.* **2004**, *116*, 5809-5812. (b) Tschöp, A.; Marx, A.; Sreekanth, A. R.; Schneider, C., *Eur. J. Inorg. Chem.* **2007**, *2007*, 2318-2327.
38 Bonollo, S.; Lanari, D.; Vaccaro, L., *Eur. J. Org. Chem.* **2011**, *2011*, 2587-2598.
39 Bonollo, S.; Fringuelli, F.; Pizzo, F.; Vaccaro, L., *Green Chem.* **2006**, *8*, 960-964.
40 Kokubo, M.; Naito, T.; Kobayashi, S., *Tetrahedron* **2010**, *66*, 1111-1118.
41 Garcia- España, E.; Ballester, M.-J.; Lloret, F.; Moratal, J. M.; Faus, J.; Bianchi, A., *J. Chem. Soc., Dalton Trans.* **1988**, 101-104.
42 (a) Gran, G. *Analyst* **1952**, *77*, 661-671. (b) Rossotti, F. J. C.; Rossotti, H. J. *Chem. Educ.* **1965**, *42*, 375-378.

43 Alderighi, L.; Gans, P.; Ienco, A.; Peters, D.; Sabatini, A.; Vacca, A., *Coord. Chem. Rev.* **1999**, *184*, 311-318.
44 (a) MassLynx Software, version 4.0 (b) Moco, S.; Bino, R. J.; Vorst, O.; Verhoeven, H. A.; de Groot, J.; van Beek, T. A.; Vervoort, J.; de Vos, C. H. R., *Plant Physiol.* **2006**, *141*, 1205-1218.
45 Dolomanov, O. V.; Bourhis, L. J.; Gildea, R. J.; Howard, J. A. K.; Puschmann, H. J. *Appl. Cryst.* **2009**, *42*, 339-341.
46 Sheldrick, G. M. *Acta Cryst.* **2008**, *A64*, 112-122.
47 Macrae, C. F.; Bruno, I. J.; Chisholm, J. A.; Edgington, P. R.; McCabe, P.; Pidcock, E.; Rodriguez-Monge, L.; Taylor, R.; van de Streek, J.; Wood, P. A., *J. Appl. Crystallogr.* **2008**, *41*, 466-470.
48 Delano, W. L. The PyMOL Molecular Graphics System. http://www.pymol.org

Chapter V

Selective Cu^{2+} recognition by *N,N′*-benzylated bis(amino amides)

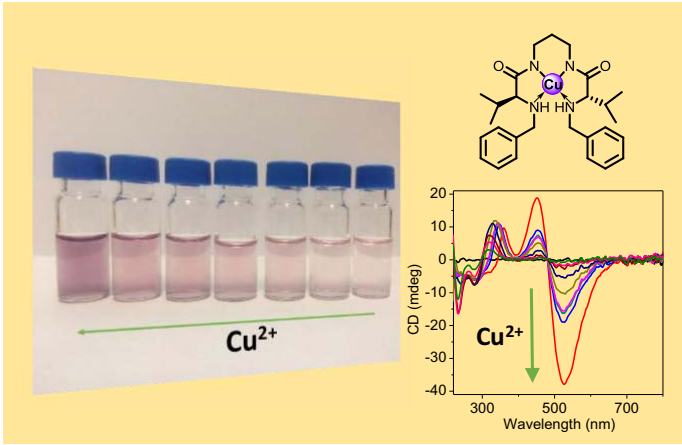

Manuscript to be submitted in Dalton Transactions

Selective Cu^{2+} recognition by *N,N′*-benzylated bis(amino amides)

Lingaraju Gorla, Vicente Martí-Centelles, Belén Altava, M. Isabel Burguete and Santiago V. Luis**

Departamento de Química Inorgánica y Orgánica, Universitat Jaume I, Avda. Sos Baynat s/n., 12071 Castellón, Spain, Tel: +34 964728239, Fax: +34 964728214; E-mail: altava@uji.es, luiss@uji.es

KEYWORDS: pseudopeptides, metal complexes, selective metal recognition, crystal structures

Abstract: Two C_2-symmetric *N,N′*-benzylated bis(amino amides) have been synthesised and their interaction with different transition metals was studied using a variety of techniques including UV-Vis and CD spectroscopy or ESI-MS. The determination of the corresponding stability constants with Cu^{2+} has been possible, in MeOH/H_2O, with one of these ligands (**4**) using potentiometric titrations. The results obtained reveal that *N*-benzylation is accompanied by an appreciable decrease in the corresponding stability constants with metals. However, this seems to produce an increase in the selectivity in the interaction with the different metal cations. This, along with the low kinetics associated to Ni^{2+}, facilitates the selective recognition of Cu^{2+} by **4**, even allowing its naked-eye selective detection in the submillimolar range. The intense CD curve observed for the corresponding Cu^{2+} complex can be used for the selective detection of this cation with a LOD value below 50 μM. The formation by both ligands (**3** and **4**) of square planar complexes with Cu^{2+} and Ni^{2+} displaying a 1:1 stoichiometry was confirmed by their X-Ray crystal structures.

Introduction

The detection of transition metals is very important due to their important role in various areas such as chemistry or biology and their association to key environmental concerns. Transition metals are not only required for biological functions but also have great potential for industrial applications. In this context, the design and synthesis of selective probes are required for the sensing of biologically and environmentally

important species, being this particularly relevant for the case of transition metal ions.[1] Among the various transition metal ions, Cu^{2+} is very important as it plays various roles in living systems as a nutrient trace element present in the active sites of some key enzymes and performing as redox catalyst or dioxygen carrier, but, at the same time, this metal can also be associated with many serious human physiological dysfunctions such as Alzheimer's and Prion type neurodegenerative diseases, amyotrophic lateral sclerosis, Wilson's diseases etc.[2]

In order to be able to selectively detect the presence of Cu^{2+} various sensing systems have been developed following a variety of methodological approaches allowing the quantification of photophysical signals.[3] In this context, molecular probes involving a clear shift in the visible absorption bands of the components are advantageous as they provide logistics of detection through a colour change for visual perception (naked-eye detection).[4] In designing such a probe, the structural motifs of its coordination environment defining the spatial disposition of the donor atoms for effective metal ion coordination play a crucial role.

In this regard, nitrogen binding sites are commonly used as donor atoms.[5] Thus, amino acid derivatives are interesting ligands able to bind with metals to form stable complexes.[6] Recent contributions from our group have shown how C_2-symmetrical bis(amino amides) derived from amino acids can form stable complexes with Cu^{2+}, Zn^{2+} and Ni^{2+} ions.[7] These previous results have shown the importance of the different structural factors (nature of the central spacer and the side chain of the constituent amino acid) in the resulting capacity of these bis(amino amides) to interact with cations and have suggested that the presence of aromatic rings at different positions can be a key structural factor. In particular, the inclusion of benzyl and related groups can be very relevant for the properties of the resulting ligands as has been highlighted by the contributions of Dangel *et al.* and Polt *et al.* in catalytic applications,[6] and more recently by *Alfonso et al.* in cascade-systems for the recognition of dicarboxylates.[8] Herein, we present the synthesis of two open-chain *N,N'*-benzylated bis(amino amide) ligands derived from *L*-phenylalanine (**3**) and *L*-valine (**4**) and the study of their acid-base properties as well as their capacity to form stable complexes with metal cations, in particular Ni^{2+} and Cu^{2+} as studied by a variety of techniques.

Results and discussion

Synthesis, characterization and acid-base properties of the ligands

The general synthetic pathway for the preparation of the desired ligands is displayed in Scheme 1. Bis(amino amides) **1** and **2**, derived from *L*-phenylalanine and *L*-valine, were prepared starting from the corresponding *N*-Cbz protected amino acid *N*-hydroxysuccinimide ester, *via* coupling with 1,3-diaminopropane and final *N*-deprotection using HBr/AcOH, following previously reported procedures.[9] Then, bis(amino amides) **1** and **2** were subjected to a reductive amination process with benzaldehyde in methanol, affording the ligands **3** and **4** in good yields.[10] The selection of the central spacer containing three methylene groups was based on the results previously obtained with related ligands, showing that this spacer is very well suited to favour the formation of strong 1:1 metal complexes with the bisdeprotonated ligand.[7a,b]

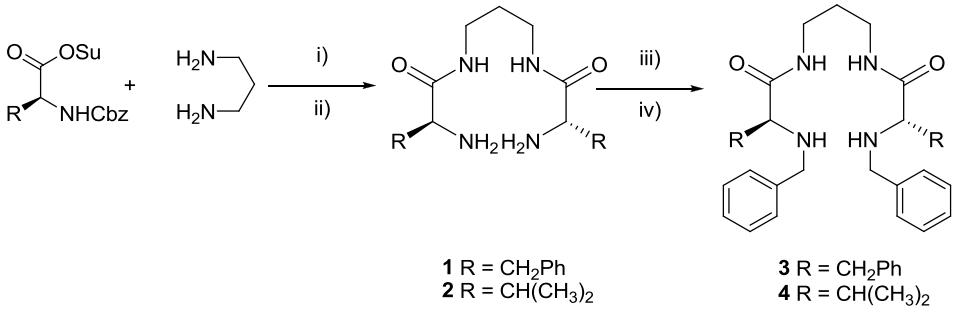

Scheme 1. Synthesis of ligands **3** and **4**. i) DME, 20 h, r.t., 70–80%; ii) HBr/AcOH 8h, NaOH, r.t., 60–70%; iii) benzaldehyde, methanol, 2 h, r.t; iv) sodium borohydride, 18 h, r.t., 70–80%.

Ligands **3** and **4** were fully characterised using standard techniques (^{1}H-NMR, ^{13}C-NMR, ESI-MS, and FT-IR), and in the case of **3**, crystals suitable for single-crystal X-ray diffraction analysis were obtained.

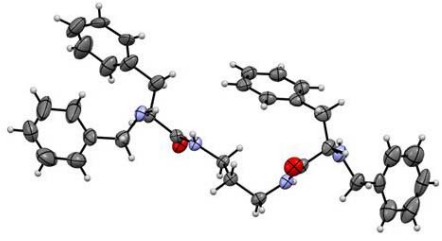

Figure 1. X-ray crystal structure of ligand **3**.

The crystal lattice for **3** (ESI Figure S1) highlights the potential of this ligand to self-associate through well-defined directional supramolecular interactions and the importance of the aromatic rings in this regard. The most prominent feature for this organization is that a defined set of H-bonds induce a global parallel disposition of the molecules (a β-sheet-like arrangement) with carbonyl groups from the two amides of each molecule located in *anti* position (Figure 1), pointing to opposite directions and H-bonding to the amide groups of two additional molecules located at the two opposite sites. It must be noted that a different pattern was observed for the analogous compound with a shorter aliphatic spacer, displaying a *syn* disposition of the carbonyl groups from amides and both aromatic amino acid side chain in opposite directions.[8]

The proper determination of the acid–base properties of nitrogenated compounds is essential for understanding their coordination properties.[11,12] Thus, the protonation constants of bis(amino amides) **3** and **4** were determined by potentiometric titrations. The presence of some CH_3CN as co-solvent was required to guarantee the solubility of the ligands. Thus, all the titrations were carried out at 298.1 K, using 0.1 M NaCl/CH_3CN 7/3 v/v to maintain a constant ionic strength. The cumulative and stepwise stability constants for the protonation of these pseudopeptidic derivatives using the program HYPERQUAD[13] are presented in Table 1. For the potentiometric studies in 0.1 M NaCl/CH_3CN 7/3 v/v, the value used for pK_w was determined to be 14.6.[14] The acid-base properties of the starting bis(amino amides) **1** and **2** had been studied previously by our group in 0.15 or 0.10 M NaCl[7a,b]. To facilitate a proper comparison, here we have also studied the acid-base properties of **2** in 0.1 M NaCl/CH_3CN 7/3 v/v.

Table 1. Logarithms of cumulative and stepwise basicity constants of ligands **1-4** determined at 298.1 ± 0.1 K.

Reaction[a]	**1**[c,f]	**2**[d,g]	**2**[e]	**3**[e]	**4**[e]
H + L ⇌ HL	7.57(1)[b]	8.01(5)	7.77(8)	6.77(7)	6.74(9)
2H + L ⇌ H_2L	14.27(1)	14.97(7)	14.88(7)	11.92(8)	13.47(6)
H + HL ⇌ H_2L	6.70(1)	6.96(7)	7.11(8)	5.15(1)	6.73(9)

[a] Charges omitted for clarity. [b] Values in parentheses are the standard deviations in the last significant figure. [c] determined in 0.1 M NaCl. [d] determined in 0.15 M NaCl. [e] 0.1M NaCl/CH_3CN 7/3 v/v. [f] data taken from reference 7b. [g] data taken from reference 7a.

As can be seen in Table 1, the change in the solvent seems to have only a minor effect on the protonation constants for **2**. As expected, the double *N*-benzyl substitution decreases the basicity of the resulting bis(amino amides), (*i.e.* log K_{H1} 7.77 for **2** against log K_{H1} 6.74 for **4**). Regarding the effect of the amino acid residue, the first protonation constant obtained for compound **3** (log K_{H1} 6.77) and **4** (log K_{H1} 6.74) were very close, although the second protonation constant for compound **3** (log K_{H2} 5.15) was more than one order of magnitude lower than for compound **4** (log *K* K_{H2} 6.73) (Table 1). This is in accordance with related pseudopeptidic compounds containing aliphatic spacers where phenylalanine derivatives present lower basicity than valine analogous.[7b] The distribution diagrams (ESI Figure S2) revealed the presence of H_2L^{2+} as the predominant species at pH values lower than 5 and 4 for ligands **3** and **4** respectively while the neutral species were predominant for both ligands at pH > 8. The most relevant difference is related to the monoprotonated species HL. The lower value of the second protonation constant for **3** is reflected in the presence of HL as a more important species at pH values close to neutrality, being the major species at pH 6.

Interaction of ligands 3 and 4 with M^{2+}species

Synthesis and characterization of Cu^{2+} and Ni^{2+} complexes

The corresponding copper(II) and nickel(II) complexes derived from ligands **3** and **4** were synthesised in MeOH with the addition of a base (Scheme 2) allowing the generation of the neutral metal complexes. This was evidenced by the change of colour from blue to orange for the two copper complexes **5a** and **6a** and from green to maroon for the two nickel complexes **5b** and **6b**. Moreover, the formation of the complexes could be followed by FT-IR through the significant shift of the C=O band to lower frequencies when the complexes were formed (*i.e.* 1551 cm^{-1} for **6a** against 1629 cm^{-1} for **4**, ESI Figure S3) indicative of the deprotonation of the N-H amide groups.

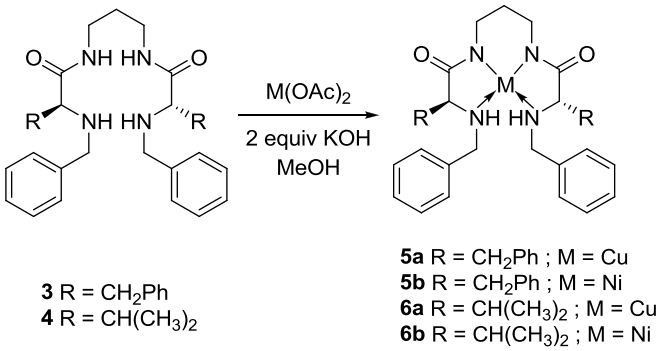

Scheme 2. Synthesis of the metal complexes derived from bis(amino amides) **3** and **4**.

UV-Vis and CD studies

Ligand **4** was used for further metal recognition studies due to the higher solubility of the corresponding metal complex species in polar protic solvents, which significantly facilitated the corresponding studies and made them more relevant. This allowed the study of **4** in a MeOH/H_2O 80/20 v/v mixture. It is worth mentioning, however, that not significant differences were observed, for instance, for the UV-Vis spectra of **4** and Cu^{2+} in this solvent and in H_2O/ACN (7/3 v/v).

In a series of initial experiments, to a set of vials containing a 2.5 mM solution (2 mL, MeOH/H_2O 80/20 v/v) of a given transition metal ion, 1.2 equivalents of ligand **4** were added (200 μL of a 30 mM solution in the same solvent) (Figure 2a) and the corresponding UV-Vis spectra analysed. The acetate salts for Cu^{2+}, Zn^{2+}, Ni^{2+} and the chloride salts for $Co^{2+}$and Cd^{2+} were used. The pH of the metal solutions was close to neutrality in all cases (6.0-7.3) and only slight changes in the pH were observed after addition of the equimolecular amount of the ligand (6.2-7.1) (ESI Table S2) For the Cu^{2+} solution, a peak with an absorption maximum at 490 nm and a small peak at 750 nm were observed in the presence of ligand, along with the development of a purple colour of the solution. For the Ni^{2+} solution, two small absorption peaks at 400 and 650 nm were observed along with the development of a yellowish colour in the presence of the ligand. Only a very weak absorption at 500 nm was observed for the Co^{2+} solution when ligand **4** was added (Figure 2b).[15] However, as could be expected, no absorption peaks between 400 to 800 nm were observed for Zn^{2+} and Cd^{2+} solutions on the addition of 1 equivalent of ligand **4** and both solutions remained colourless. Thus, a selective naked-eye detection of Cu^{2+} could be observed under those conditions in the mM range.

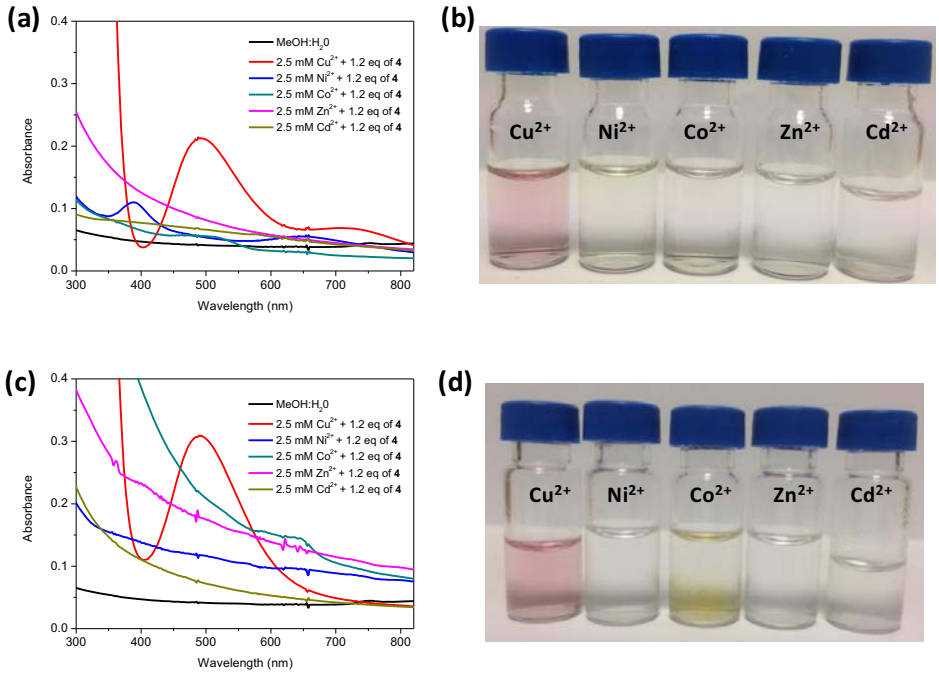

Figure 2. (a) UV–Vis spectra for solutions of M^{2+} (2.27 mM in MeOH/H_2O 80/20 v/v) in the presence of 1.2 equivalents of ligand **4** in the absence of added base; (b) pictures of vials containing the solutions for spectra in a; (c) Same as in a but after addition of base (see Table S2, ESI for pH values); (d) pictures of vials containing the solutions for spectra in c.

According to literature data, the appearance of an absorption peak at 490 nm for the Cu^{2+}·**4** system corresponds to the formation of a complex with a square planar geometry, while the peak at 750 nm must correspond to the cation in an octahedral environment.[16] For the Ni^{2+}·**4** system, the absorption peaks around 400 and 650 nm indicate the presence of an octahedral structure similar to the one in $[Ni(H_2O)_6]^{2+}$ and related systems.[17] Taking into consideration the slight changes observed after addition of the ligand for the Ni^{2+}·**4** system, as well as the slow kinetics usually associated to this metal cation,[18] the UV-Vis spectrum for this system was again measured after 24 hours, revealing the appearance of a new absorption peak at 460 nm, corresponding to the formation of the expected square planar Ni^{2+} complex,[19] evidencing that also here the kinetic for Ni complexation is slower than the one for Cu^{2+} (ESI Figure S4). For the Co^{2+}·**4** system, the small absorption observed at 500 nm suggests the occurrence of an octahedral structure.[17a]

When *ca.* 2 equiv. of a 0.1 M NaOH solution in water were added to these vials containing the 1:1 M^{2+}·**4** systems (MeOH/H_2O 80/20 v/v, *ca.* 2.3 mM in the metal) the corresponding vials reached pH values of 9.1-9.8 (ESI Table S2). Under these conditions, some turbidity was observed except for Cu^{2+}, for which the color became more intense (ESI Figure S5). For this system, the UV-Vis (Figure 2c) showed the disappearance of the band corresponding to the octahedral complex and the increase in the intensity of the absorption at 490 nm (ε = 123 M^{-1} cm^{-1}) for the square planar complex.

The stoichiometry of the complex formed by **4** and Cu^{2+} in the absence of base, at 5 mM concentration, was determined to be 1:1 (ligand:metal) from the Job plot of its absorbance monitored at 490 nm as a function of the molar fraction of added Cu^{2+} in MeOH/H_2O (ESI Figure S6).[20] Individual measurements were taken after an equilibration period of 5 min, taking into consideration that the complexation seems to be very fast and needs less than 1 min to be complete. The same stoichiometry was observed in the presence of two equivalents of base (ESI Figure S6).

The changes in the absorption spectra of Cu^{2+} with the gradual addition of increasing amounts of **4** in MeOH/H_2O at room temperature, in the absence of added base, are shown in Figure 3a. A gradual increase in the intensity of the absorption at 490 nm and a decrease of that at 750 nm was observed as a function of the concentration of added ligand. The non-linear fitting for a 1:1 stoichiometry of this titration curve provided an apparent constant (K_{app}) of 562 M^{-1} (Figure 3b).[21] A similar titration was carried out in the presence of two equivalents of base (Figure 3c). In this case, the isosbestic point around 640 nm was better defined and the fitting of the curve for the absorption at 490 nm provided a value for K_{app} of 3350 M^{-1} (Figure 3d).

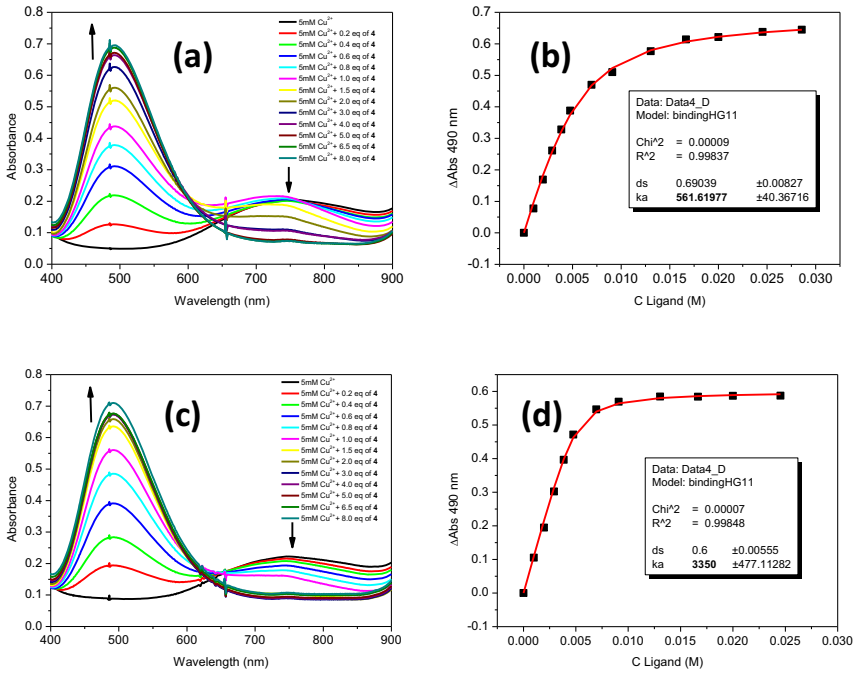

Figure 3. (a) UV-Visible spectra for Cu^{2+} (5 mM) in the presence of increasing amounts of ligand **4**. (b) Plot of the absorbance at 490 nm against the concentration of **4**; data for the non-linear fitting have been included; (c) UV-Visible spectra for Cu^{2+} (5 mM) in the presence of increasing amounts of compound **4** in basic medium (pH = 11.68). (d) Plot of the absorbance (490 nm) against the concentration of **4**; data for the non-linear fitting in basic media have been included.

Similar results were obtained when $CuCl_2$ and $CuNO_3$ were used instead of $Cu(OAc)_2$ as the source of Cu^{2+}. In both cases, the pH of the resulting solutions was close to 7 (in the absence of added base) and the formation of the complexes was also fast (less than 2 min) with the development of an intense absorption at 490 nm (ESI Figure S7).

Considering the chiral nature of the ligand, the complexation of **4** with the different metal ions was also studied by CD. For this purpose, a 2.5 mM solution ($MeOH/H_2O$ 80/20 v/v) containing an equimolecular mixture of **4** and the corresponding M^{2+} and two equivalents of added base was kept stirring for 24 hours. The CD of the free ligand **4** shows a negative band centered at 240 nm that can be assigned to the n-π^* transitions of the amide groups (Figure 4a). Interestingly, in the presence Cu^{2+} (Figure 4b, black line) a strong negative split-Cotton effect (-, +) with a minimum at 529 nm ($\Delta\varepsilon$ = - 0.44 cm^2 $mmol^{-1}$) and a maximum at 448 nm ($\Delta\varepsilon$ = 0.23 cm^2 $mmol^{-1}$), and passing through zero at

481 nm, which is the λ_{max} for the UV band for the square planar complex. An additional Cotton effect of much lower intensity is also observed around 350 nm in correspondence with the absorption detected in the UV-Vis spectrum in this region. These bands have been generally attributed to metal-ligand charge transfer or to intraligand transitions.[22] In the absence of added base, an additional signal is observed in the 600-800 nm regions, most likely associated with the octahedral species present (ESI, Figure 6). For the Ni^{2+} complex, a negative signal with the minimum at 463 nm and a positive one with the maximum at 284 nm were observed (Figure 4b, red line) in good correspondence with the absorption bands detected in the UV-Vis spectrum. For the other M^{2+} metal ions, only one single negative signal in the 220-250 nm regions, corresponding to intraligand transitions was obtained.

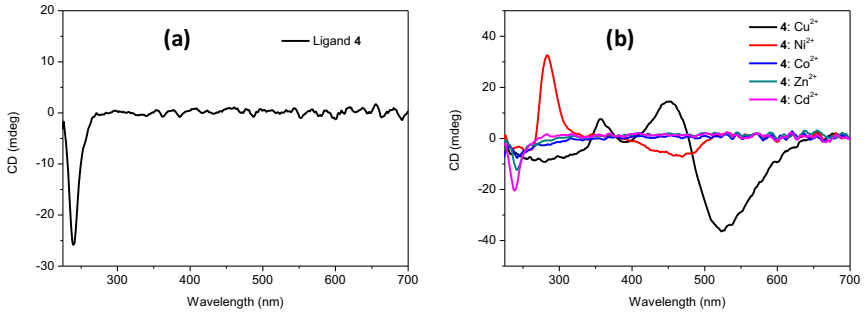

Figure 4. (a) CD spectra for ligand **4** in basic media (2 equiv. of NaOH). (b) CD spectra for ligand **4** in basic media (2 equiv. of NaOH) in the presence of 1 equivalent of different M^{2+} metals. In both cases, the solvent was MeOH/H_2O 80/20 (v/v).

Taking into account the selective response obtained for Cu^{2+}.**4** complexes in the UV-Vis and CD studies, this ligand can be used for the selective detection of this metal.[23] Thus, different additional studies were carried out in order to check this possibility. First of all, a series of vials containing ligand **4** and Cu^{2+} in equimolecular amounts were prepared by successive dilutions of a stock solution 10 mM in both components (MeOH/H_2O 80/20, v/v). As can be seen in Figure 5, the color developed for the complex is still visible below the mM range. A similar behaviour was observed when the former experiments were carried out using 2 equiv. of the base relative to the ligand (Figure S8, ESI). An approximated LOD value for the naked eye detection of this complex, under those conditions, could be estimated to be 0.25 mM.

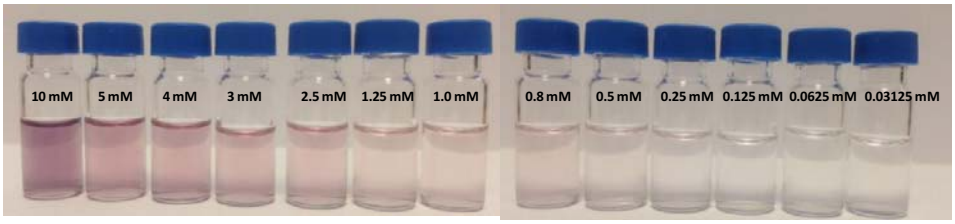

Figure 5. Naked eye color changes upon successive dilutions from a stock solution of 10 mM ligand **4**:Cu^{2+} in neutral conditions.

A more accurate LOD determination was carried out for the same samples using the corresponding UV-Vis spectra (Figure 6) and following the absorbance at 490 nm as a function of the L:Cu concentration and using a standard protocol (SD = 3).[24] In this case, a detection limit of 85 μM could be established (Figure S9, ESI). A very similar value (91 μM) was obtained from titration experiments starting from a 1 mM solution of ligand and adding variable amounts of Cu^{2+} (Figure S10, ESI). Slightly lower LOD values were obtained again when the former titration experiments were carried out using 2 equiv. of the base relative to the ligand, obtaining a value of 79 μM (Figure S11, ESI). Interestingly, the intense bands developed by this complex in the CD spectra for the different samples prepared (see, for instance, Figure 6) also allowed their use for the determination of Cu^{2+}. Following the variation of the amplitude of the Cotton effect ($\Delta CD = CD_{440nm}-CD_{520nm}$) as a function of L:Cu concentrations, the LOD obtained was 43 μM (Figure S12, ESI).[25] Again, slightly lower LOD values (28 μM) were obtained when the former experiments were carried out using 2 equiv. of the base relative to the ligand (Figure S13, ESI). Both in the UV-Vis and in the CD experiments, the linearity in the millimolar and submillimolar range was excellent. No interference by the other metals assayed was observed and the concentration of a sample of Cu^{2+} could be determined with accuracy in the presence of other cations (Figure S14, ESI)

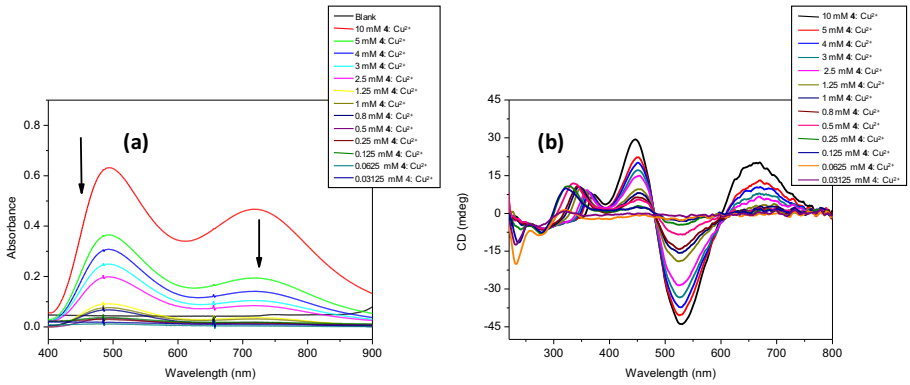

Figure 6. UV-Visible (a) and CD (b) spectra obtained from successive dilutions from a stock solution of 10 mM ligand **4**:Cu^{2+} in the absence of added base.

ESI-MS studies of the metal complexes

ESI-MS experiments with ligand **4** in the presence of M^{2+} ions also supported its selective binding to Cu^{2+}. The ESI^{+} mass spectrum for ligand **4** in the presence of 1 eq. of $Cu(AcO)_2$, displayed peaks at 514.4 and at 574.3 associated to $[CuH_{-2}L+H]^{+}$ and to $[CuH_{-1}L+AcOH]^{+}$ species respectively, supporting a 1:1 complexation stoichiometry and the formation of mono- and bisdeprotonated complexes (Figure 7).

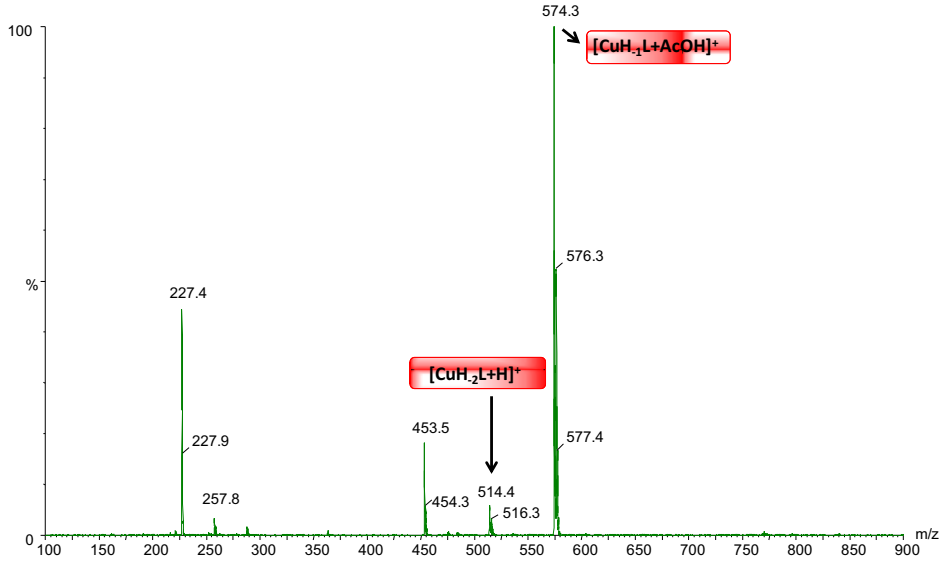

Figure 7. ESI^{+}-Mass of compound **4** (5 mM) in the presence of 1 eq. of $Cu(OAc)_2$.

In the case of Ni^{2+}, Cd^{2+}, Co^{2+}, Zn^{2+} metals, the corresponding peaks associated to $[MH_{-2}L+H]^+$ species were not observed, although the peak associated with the $[MH_{-1}L+AcOH]^+$ species was always present. However, for Ni^{2+}, the intensity of this peak was 30% of the base peak while for Cd^{2+}, Zn^{2+}, and Co^{2+} its intensity was <2% (ESI Figure S15, ESI). For Co^{2+} and Cd^{2+} very minor species (<2%) presumably corresponding to $[2L+M]^{2+}$ and $[L+M+Cl]^+$ were also observed.

Potentiometric studies for Cu^{2+} complexes

Finally, the interaction of ligand **4** with Cu^{2+} was studied by potentiometric titrations over the 2-12 pH range. The stability constants for the formation of complexes were determined for a 1:1 metal-ligand ratio, using NaCl 0.1M/CH_3CN 7/3 v/v to maintain a constant ionic strength and a temperature of 298.1 K. Though the same solvent mixture used for spectroscopic measurements was also assayed here (MeOH/H_2O 80/20 v/v), its use was not satisfactory and led to non-stable measurements. The results obtained are presented in Table 2 and the corresponding distribution diagrams are displayed in Figure 7. Again, the interaction properties of the starting bis(amino amide) **2** with Cu^{2+} were also studied by potentiometric titrations using the same medium to provide a proper comparison. The lower solubility of ligand **3** with Cu^{2+} also precluded carrying out accurate potentiometric titrations. When comparing the values obtained for **2** in both solvents it can be seen that the solvent plays, in this case, an important role. The formation of complex species seems to be favoured in the mixed solvent.[7a]

As can be seen in Table 2, significant differences can be observed between the two related ligands. The most remarkable observation is the general lower stability of the non-deprotonated, mono and di-deprotonated complex species for compound **4**. Thus, for the neutral $[CuH_{-2}L]$ species from **4** the formation constant ($\log \beta = -6.29$) was more than three orders of magnitude lower than the related formation constant for ligand **2** ($\log \beta = -2.97$). In spite of this, these neutral complex species were predominant around pH 7 for **2** and **4**, though $[CuH_{-2}L]$ starts to be formed at slightly higher pH values for **4**. This confirms the formation of $[CuH_{-2}L]$ species at physiologic pH for **4** (Figure 8). On the other hand, the relative importance of $[CuH_{-1}L]$ and [CuL] species is reversed for both ligands. For **4**, the $[CuH_{-1}L]$ species is more important at pH values around 6, while it is a minor species in the case of **2**, and [CuL] is relatively important for **2** at pH values close to 5, whereas it is very minor for **4**.

Table 2. Logarithms of the formation constants (log β) for the Cu^{2+} complexes with ligands **2** and **4** at 298.1 ± 0.1 K.

Reaction[a]	**2**[c,d]	**2**[e]	**4**[e]
Cu + L ⇌ CuL	5.99(3)[b]	6.99(7)	4.39(9)
Cu + L ⇌ $CuH_{-1}L$ + H	0.53(1)	1.53(7)	-0.66(3)
Cu + L ⇌ $CuH_{-2}L$ + 2H	-6.66(1)	-2.97(1)	-6.29(1)
CuL ⇌ $CuH_{-1}L$ + H	-5.46(3)	-5.46(9)	-5.05(9)
$CuH_{-1}L$ ⇌ $CuH_{-2}L$ + H	-7.19(1)	-4.50(1)	-5.63(2)
CuL ⇌ $CuH_{-2}L$ + 2H	-12.65(3)	-9.96(9)	-10.68(9)

[a] Charges omitted for clarity. [b] Values in parentheses are the standard deviations in the last significant figure. [c] determined in 0.15 M NaCl. [d] data taken from reference 7a. [e] 0.1M NaCl/CH_3CN 7/3 v/v.

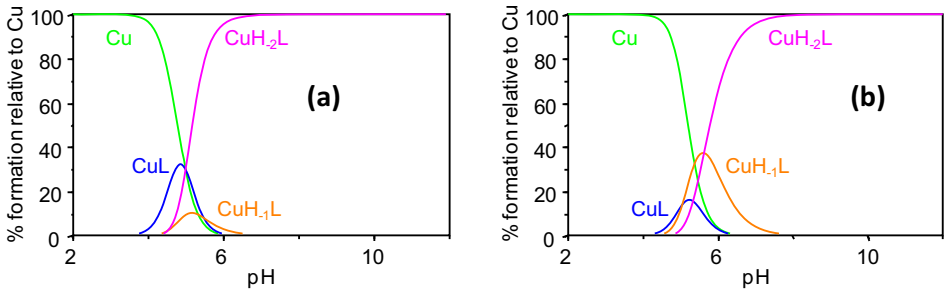

Figure 8. Distribution diagrams for ligands **2** (a) and **4** (b) with Cu^{2+} as a function of pH in 0.1 M NaCl/CH_3CN 7/3 v/v, at 298.1 ± 0.1 K. Charges have been omitted for clarity.

Single-crystal X-ray diffraction studies

The formation of the corresponding bisdeprotonated complexes of **3** and **4** with Cu^{2+} and Ni^{2+} and their stoichiometry and geometry were confirmed by X-ray crystallography. Crystals suitable for single-crystal X-ray diffraction analysis were obtained for all the metal complexes by the layering of a methanolic solution of the pseudopeptidic ligand over a basic aqueous solution of $Cu(OAc)_2$ and $Ni(OAc)_2$.

The X-ray crystal structure of the copper complexes **5a** and **6a** are presented in Figure 9. X-ray diffraction data confirm the formation of the metal complexes with a 1:1 stoichiometry.

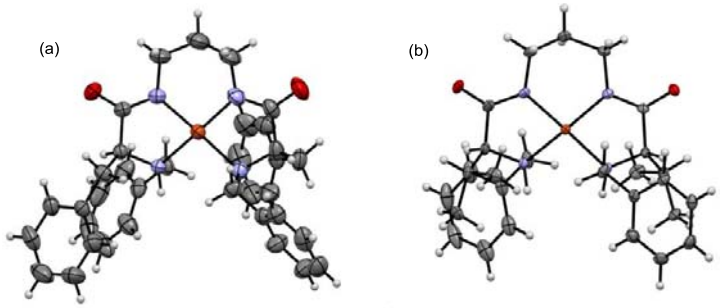

Figure 9. (a) X-ray crystal structure of Cu^{2+} complexes **5a** (a) and **6a** (b)**.** Ellipsoids represented at the 50% probability level.

The Cu^{2+} cation in **5a** is coordinated by two amine groups and two deprotonated amide groups, in a distorted square-planar geometry, and displays a torsion angle of 13.8° between the N_{amine}–Cu–N_{amide} planes. The Cu–N_{amide} distances are slightly shorter than the Cu–N_{amine} ones, being 1.921 and 2.052 Å on average, respectively.[7b] The N–Cu–N angles contained in the two five-membered rings N_{amine}–Cu–N_{amide} are *ca.* 13° smaller than the N–Cu–N angles contained in the N_{amide}–Cu–N_{amide} six-membered ring, as expected for a smaller ring size with a tighter environment. The Cu^{2+} cation in **6a** is also coordinated by two amine groups and two deprotonated amide groups, in a distorted square-planar geometry, but displays a torsion angle of 29.9°. Again the Cu–N_{amide} distances are slightly shorter than the ones for Cu–N_{amine}, being 1.912 and 2.034 Å on average, respectively, and both slightly shorter than in **5a.** The N–Cu–N angles contained in the two five-membered rings (N_{amine}–Cu–N_{amide}) are *ca.* 14° smaller than those in the six member ring (N_{amide}–Cu–N_{amide}).

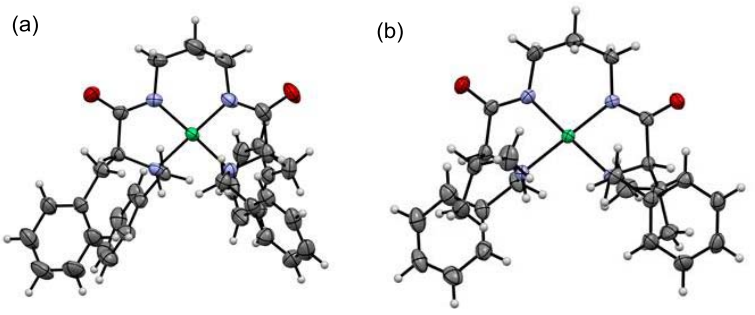

Figure 10. X-ray crystal structure of Ni^{2+} complexes **5b** (a) and **6b** (b). Ellipsoids represented at the 50% probability level.

The X-ray crystal structures for the Ni^{2+} complexes **5b** and **6b** are presented in Figure 10. Also for **5b** and **6b** the Ni^{2+} cation is coordinated by two amine groups and two deprotonated amide groups, in a distorted square-planar geometry displaying torsion angles of 12.9° and 14.8° respectively. In both complexes the $Ni–N_{amide}$ distances are slightly shorter than the corresponding $Ni–N_{amine}$ and the N–Ni–N angles contained in the five-membered rings are smaller than the angles contained in the six-membered ring (*ca.* 15° for **6b**).

Conclusions

N-benzylation of the terminal amino nitrogens in C_2-symmetric pseudopeptides containing an aliphatic central spacer provides significant changes in their properties as ligands. Thus, the solubility of **3** and **4** and their respective metal complexes in water decreases, in particular for the phenylalanine derivative (**3**), which precludes a more detailed analysis of its coordination chemistry. The corresponding spectroscopic, spectrometric and potentiometric studies could be carried out with the valine derivative **4**, in particular in aqueous mixed solvents, revealing that these bis(amino amides) are able to provide efficient tetradentate coordination for metal cations, in particular, Cu^{+2}. The resulting Cu^{2+} and Ni^{2+} bisdeprotonated complexes seem to represent the most important complex species for both cations, even at slightly acidic pH regions at least for the system Cu^{2+}·**4** and display 1:1 stoichiometries and square planar arrangements around the metal centre, as confirmed by the corresponding X-Ray structures. The presence of the additional benzyl groups in the terminal amino groups can significantly reduce the stability of the corresponding metal complexes, as has been observed when comparing the stability constants obtained potentiometrically for the system Cu^{2+}·**4** and those obtained for the non-benzylated analogue **2**. This, however, is accompanied by a strong selectivity in the interaction of **4** with Cu^{2+}, in particular at short times, in such a way that ligand **4** can act as a chemosensor and detect Cu^{+2} with high selectivity against other metals and a good sensitivity. Naked-eye detection is possible at concentrations in the submillimolar range (0.25 mM) and the LOD can reach values of 85 μM from UV-Vis measurements and 28 μM from CD experiments. The response time of **4** to Cu^{2+} was less than 2 min, indicating that this chemosensor can be used for real-time tracing of Cu^{2+} in a test system.

Experimental section

All reagents and solvents were obtained from commercial sources and used as received unless otherwise stated. Deionized water was used from a "Milli-Q® Integral Water Purification System" by Millipore. Microanalyses were performed on an elemental analyzer equipped with an oxygen module. Rotatory power was determined with a digital polarimeter (Na: 589 nm). Melting points were measured using a standard apparatus and are uncorrected.

General procedure for the synthesis of *N,N′*-benzylated bis(amino amides)

Compound 3

Compound **1** (3.01 g, 8.17 mmol) was dissolved in methanol (50 mL) and the solution added to a solution of benzaldehyde (2.013 mL, 17.97 mmol) in methanol (10 mL) in a 100 mL two necked round bottom flask, under a nitrogen atmosphere. After stirring at room temperature for 3 h, the reaction mixture was treated with a 50 mL methanolic solution of $NaBH_4$ (1.24g, 32.68 mmol) and further stirred overnight. The solvent was evaporated and the crude product was dissolved in basic water (pH=10-11) and extracted with $CHCl_3$ (3x50 mL). The organic phase was dried over anhydrous $MgSO_4$, and vacuum evaporated. The final pure product was obtained after washing with hexane as a white solid (3.418 g, 6.23 mmol, 76% Yield**):** mp 101-103 ºC; $[\alpha]_D^{25}$ = -83.57(c = 0.01, $CHCl_3$); IR (ATR) 3343, 3321, 2936, 1636, 1528, 1452cm^{-1}; ^{1}H NMR (500 MHz, $CDCl_3$) δ 7.46 (t, *J* = 6.2 Hz, 2H), 7.24 – 7.13 (m, 7H), 7.09 (d, *J* = 7.0 Hz, 2H), 7.03 (d, *J* = 6.6 Hz, 2H), 3.66 (d, *J* = 13.4 Hz, 2H), 3.49 (d, *J* = 13.4 Hz, 2H), 3.31 (dd, *J* = 9.2, 4.4 Hz, 2H), 3.11 (dt, *J* = 15.3, 5.7 Hz, 4H), 2.69 (dd, *J* = 13.8, 9.3 Hz, 2H), 1.51 – 1.47 (m, 2H); ^{13}C NMR (126 MHz, $CDCl_3$) δ 173.3, 137.2, 129.2, 128.7, 128.5, 128.2, 127.4, 126.9, 63.1, 52.5, 39.0, 35.7, 29.8; HRMS (ESI-TOF)$^+$ Calcd for $C_{35}H_{41}N_4O_2$ $(M+H)^+$: 549.3230; found 549.3235; Anal. Calcd for $C_{35}H_{40}N_4O_2$: C, 76.61; H, 7.35; N, 10.21. Found: C, 76.2; H, 7.1; N, 10.0.

Compound 4

2.380 g, 8.74 mmol, 87% Yield; mp 87-89 ^{o}C; $[\alpha]_D^{25}$ = -46.27(c = 0.01, $CHCl_3$); IR (ATR) 3301, 2958, 2940, 2933, 2898, 2877, 1629, 1546 cm^{-1}; ^{1}H NMR (500 MHz, $CDCl_3$) δ 7.52 (s, 2H), 7.33 (s, 6H), 3.80 (d, *J* = 13.0 Hz, 2H), 3.66 (d, *J* = 13.1 Hz, 2H), 3.35 – 3.24 (m, 4H), 2.97 (d, J = 3.8 Hz, 2H), 2.12 (d, *J* = 5.6 Hz, 2H), 1.67 – 1.62 (m, 2H), 0.94 (dd, *J* = 29.5, 6.6 Hz, 12H); ^{13}C NMR (126 MHz, $CDCl_3$) δ 174.1, 139.8,

128.5, 128.2, 127.2, 77.3, 77.0, 76.77, 68.1, 53.5, 35.7, 31.4, 30.3, 19.7, 17.9; HRMS (ESI-TOF)$^{+}$ Calcd for $C_{27}H_{41}N_4O_2$ $(M + H)^{+}$: 453.3230, found 453.3227; Anal. Calcd for $C_{27}H_{40}N_4O_2$: C, 71.65; H, 8.91; N, 12.38; O, 7.07. Found: C, 71.5; H, 8.7; N, 12.2.

General procedure for the synthesis of M^{2+} complexes

Compound **3** (100 mg, 0.182 mmol) was dissolved in dry MeOH (5mL) in a 25 mL round bottom flask and maintained under a nitrogen atmosphere. $Cu(OAc)_2$ (36.38 mg, 0.182mmol) dissolved in dry MeOH (5 mL) methanol was then added and the mixture stirred for 30 min at room temperature. 1 M KOH in methanol (3.3 mL, 0.364 mmol) was added and the solution was maintained at room temperature overnight. The solvent was vacuum evaporated to dryness and the residue washed with diethyl ether to afford the corresponding metal complex.

Complex 5a

70.6 mg, 0.116 mmol, 64% Yield; FT-IR: 3500-3000, 2920, 1571, 1454, 1392 cm^{-1}; Anal. Calcd. (%) for $C_{35}H_{38}N_4O_2Cu$ 2 H_2O: C, 65.05, H, 6.55, N, 8.67; found: C, 65.1, H, 6. 5, N, 8.5.

Complex 5b

73.5 mg, 0.1214 mmol, 67% Yield; FT-IR: 3600-3000, 2931, 1573, 1452, 1398 cm^{-1}; Anal. Calcd. (%) for $C_{35}H_{38}N_4O_2Ni$ 2 H_2O: C, 65.54, H, 6.60, N, 8.73; found: C, 65.4, H, 6.2, N, 8.6.

Complex 6a

47.7 mg, 0.093 mmol, 42% Yield; FT-IR: 3600-3000, 1592, 1551, 1396 cm^{-1}; Anal. Calcd. (%) for $C_{27}H_{38}N_4O_2Cu$ 1.7 H_2O: C, 59.53, H, 7.66, N, 10.28; found: C, 59.5, H, 7.4, N, 10.2.

Complex 6b

51.2 mg, 0.101 mmol, 45.5% Yield; FT-IR: 3600-3000, 1649, 1569, 1453 cm^{-1}; Anal. Calcd. (%) for $C_{27}H_{38}N_4O_2Ni$ 3.5 H_2O: C, 56.67, H, 7.87, N, 9.80; found: C, 56.3, H, 7.1, N, 9.7.

Electromotive force measurements

The potentiometric titrations were carried out at 298.1 ± 0.1 K using 0.1 M NaCl as the supporting electrolyte. The experimental procedure (burette, potentiometer, cell, stirrer,

micro-computer, etc.) has been fully described elsewhere. The acquisition of the emf data was performed with the computer program CrisonCapture. The reference electrode was an Ag/AgCl electrode in saturated KCl solution. The glass electrode was calibrated as a hydrogen-ion concentration probe by titration of previously standardized amounts of HCl with CO_2-free NaOH solutions and the equivalence point determined by the Gran's method,[26] which gives the standard potential, E°′, and the ionic product of water 13.78, whereas in the case of the water/ACN mixture used this value was 14.6.[14] The computer program HYPERQUAD[13] was used to calculate the protonation and stability constants, and the HySS29[27] program was used to obtain the distribution diagrams. The pH range investigated was 2.0-12.0 and the concentration of the metal ions and of the ligands 0.1 mM with M^{2+}:L molar ratios as 1:1. The different titration curves for each system (at least two) were treated either as a single set or as separated curves without significant variations in the values of the stability constants. Finally, the sets of data were merged together and treated simultaneously to give the final stability constants.

^{1}H NMR experiments

The ^{1}H spectra were recorded on a Varian INOVA 500 spectrometer (500 and 125 MHz for ^{1}H and ^{13}C NMR, respectively). The solvent signal was used as a reference standard.

UV-Vis and CD measurements

UV-Vis absorption spectra were recorded using a Hewlett-Packard 8453 device. All measurements were performed at room temperature and spectra were recorded from 200 nm to 900 nm. For metal titration experiments, a 2.5 mM of M^{2+} solution in MeOH/H_2O 80/20 and 30 mM of compound **4** in MeOH/H_2O 80/20 were used and aliquots of the ligand solution were gradually added to the metal solution using a micropipette. After equilibration, the corresponding absorptions were measured. For job-plot measurements stock solutions of compound **4** (5 mM in MeOH/H_2O 80/20) and $Cu(OAc)_2$ (5 mM in MeOH/H_2O 80/20) were prepared and mixed in variable proportions so that the final concentration of the mixture was maintained constant at 5 mM. After equilibration, the absorbance at 490 nm of each solution was independently measured. A plot of absorbance against the mole fraction of Cu^{2+} was used to determine the ratio of metal–ligand.

CD experiments were performed using a JASCO J-810 spectrometer. All measurements were performed at room temperature and spectra were recorded from 200 nm to 900 nm with 1.0 nm step and 1.0 nm bandwidth and the scanning speed was 200 nm per minute.

LOD values were calculated using the relation[24]

$$\text{Detection limit} = 3\sigma/k$$

where σ is the standard deviation of the blank measurements, and k is the slope between the absorbance for UV and mdeg for CD versus [L]. For such experiments, the UV-Vis and CD spectra of the solvent (blank) were measured 10 times and the standard deviation of the measurements was determined. The slope was obtained from the plot of absorbance at 490 nm for UV-Vis and the mdeg for the 525 nm in CD measurements respectively versus concentration of ions.

Mass spectrometry

Mass spectra were recorded on a Q-TOF Premier mass spectrometer with an orthogonal Z-spray electrospray interface (Micromass, Manchester, UK) either by electrospray positive mode (ES^+) or by electrospray negative mode (ES^-). The desolvation gas, as well as nebulizing gas, was nitrogen at a flow of 700 L/h and 20 L/h, respectively. The temperature of the source block was set to 120 °C and the desolvation temperature to 150 °C. A capillary voltage of 3.5 and 3.3 kV was used in the positive and negative scan mode, respectively. The cone voltage was typically set to 20 V to control the extent of fragmentation of the identified ions. Sample solutions were infused via syringe pump directly connected to the ESI source at a flow rate of 10 mL/min. The observed isotopic pattern of each intermediate perfectly matched the theoretical isotope pattern calculated from their elemental composition using the MassLynx 4.0 program.[28]

IR spectroscopy

FT-IR spectra were acquired on a JASCO 6200 equipment with a MIRacle single reflection ATR diamond/ZnSe accessory. The raw IR spectral data were processed with the JASCO spectral manager software.

Crystallography

Single crystals of ligand **4** and complexes **5a** - **6b** were obtained. A suitable crystal was selected and measured on a single crystal X-Ray diffractometer. Using Olex2,[29] all the

structures were solved with the ShelXS 2014[30] structure solution program using Direct Methods and refined with the ShelXL 2014[30] refinement package using Least Squares minimization. The program MERCURY[31] was used to prepare artwork representations. Crystallographic data and refinement parameters are summarized in Table S1 in supporting information. Cambridge Crystallographic Data Centre CCDC 1481178 (**3**), 1481179 (**5a**), 1481180 (**5b**), 1481181 (**6a**), 1481182 **(6b)** contain the supplementary crystallographic data for this paper.

Acknowledgements

Financial support from Spanish MINECO (CTQ2015-68429-R), Generalitat Valenciana (PROMETEO/2012/020) and PPI-UJI (P1-1B-2013-38) is gratefully acknowledged. L.G. thanks, Generalitat Valenciana for a Grisolia fellowship (GRISOLIA 2012/015). The support of the SCIC for the different instrumental techniques at Universitat Jaume I is acknowledged.

Notes and references

1 (*a*) W. Wang, Q. Wen, Y. Zhang, X. Fei, Y. Li, Q. Yang and X. Xu, *Dalton Trans*., 2013, **42**, 1827-1833; (*b*) P. C. Dhar, A. Pal, P. Mohanty and B. Bag, *Sens. Actuators, B*, 2015, **219**, 308-314; (*c*) D. Singhal, N. Gupta and A. K. Singh, *RSC Adv*., 2015, **5**, 65731-65738; (*d*) A. P. de Silva, H. Q. N. Gunaratne, T. Gunnlaugsson, A. J. M. Huxley, C. P. McCoy, J. T. Rademacher and T. E. Rice, *Chem. Rev*., 1997, **97**, 1515-1566; (*e*) L. Pu, *Chem. Rev.*, 2004, **104**, 1687-1716; (*f*) G. W. Gokel, W. M. Leevy and M. E. Weber, *Chem. Rev.*, 2004, **104**, 2723-2750; (*g*) P. D. Beer and P. A. Gale, *Angew. Chem., Int. Ed.*, 2001, **40**, 486-516; (*h*) L. Prodi, F. Bolletta, M. Montalti and N. Zaccheroni, *Coord. Chem. Rev.*, 2000, **205**, 59-83; (*i*) V. Amendola, L. Fabbrizzi, F. Foti, M. Licchelli, C. Mangano, P. Pallavicini, A. Poggi, D. Sacchi and A. Taglietti, *Coord. Chem. Rev.*, 2006, **250**, 273-299.

2 (*a*) E. Gaggelli, H. Kozlowski, D. Valensin and G. Valensin, *Chem. Rev.*, 2006, **106**, 1995-2044; (*b*) A. Mathie, G. L. Sutton, C. E. Clarke and E. L. Veale, *Pharmacol. Ther.*, 2006, **111**, 567-583; (*c*) K. J. Barnham, C. L. Masters and A. I. Bush, *Nat. Rev. Drug Discovery*, 2004, **3**, 205-214; (*d*) D. J. Waggoner, T. B. Bartnikas and J. D. Gitlin, *Neurobiol. Dis.*, 1999, **6**, 221-230; (*e*) L. I. Bruijn, T. M. Miller and D. W. Cleveland, *Annu. Rev. Neurosci.*, 2004, **27**, 723-749. (*f*) C. Zhao, B. Liu, X. Bi, D. Liu, C. Pan, L. Wang and Y. Pang, *Sens. Actuators, B,* 2016, **229**, 131-137.

3 (*a*) Y. Xiang, Z. Li, X. Chen and A. Tong, *Talanta*, 2008, **74**, 1148-1153; (*b*) B. High, D. Bruce and M. M. Richter, *Anal. Chim. Acta*, 2001, **449**, 17-22; (*c*) L. Tapia, M. Suazo, C. Hödar, V. Cambiazo and M. González, *Biometals*, 2003, **16**, 169-174; (*d*) F. Chen, G. Liu, Y. Shi, P. Xi, J. Cheng, J. Hong, R. Shen, X. Yao, D. Bai and Z. Zeng, *Talanta*, 2014, **124**, 139-145.

4 (*a*) B. Valeur and I. Leray, *Coord. Chem. Rev.*, 2000, **205**, 3-40; (*b*) N. Kaur and S. Kumar, *Tetrahedron*, 2011, **67**, 9233-9264.

5 L. Fabbrizzi and A. Poggi, *Chem. Soc. Rev*., 2013, **42**, 1681-1699.

6 (*a*) B. Dangel, M. Clarke, J. Haley, D. Sames and R. Polt, *J. Am. Chem. Soc.*, 1997, **119**, 10865-10866; (*b*) B. D. Dangel and R. Polt, *Org. Lett.*, 2000, **2**, 3003-3006; (*c*) R. Polt, B. D. Kelly, B. D. Dangel, U. B. Tadikonda, R. E. Ross, A. M. Raitsimring and A. V. Astashkin, *Inorg. Chem.*, 2003, **42**, 566-574; (*d*) M. Merschky and C. Schmuck, *Org. Biomol. Chem*., 2009, **7**, 4895-4903; (*e*) Ł. Weseliński, E. Słyk and J. Jurczak, *Tetrahedron Lett.*, 2011, **52**, 381-384; (*f*) J. Paradowska, M. Pasternak, B. Gut, B. Gryzło and J. Mlynarski, *J. Org. Chem.*, 2012, **77**, 173-187; (*g*) F. Adrián, M. I. Burguete, J. M. Fraile, J. I. García, J. García, E. García-España, S. V. Luis, J. A. Mayoral, A. J. Royo and M. C. Sánchez, *Eur. J. Inorg. Chem.*, 1999, **1999,** 2347-2354.

7 (*a*) S. Blasco, M. I. Burguete, M. P. Clares, E. García-España, J. Escorihuela and S. V. Luis, *Inorg. Chem*., 2010, **49**, 7841-7852; (*b*) I. Martí, A. Ferrer, J. Escorihuela, M. I. Burguete and S. V. Luis, *Dalton Trans*., 2012, **41**, 6764-6776; (*c*) V. Martí-Centelles, D. K. Kumar, A. J. P. White, S. V. Luis and R. Vilar, *CrystEngComm*, *2011*, **13**, 6997-7008; (*d*) Lingaraju Gorla, Vicente Martí-Centelles, Belén Altava, M. Isabel Burguete and Santiago V. Luis, *Inorganic Chemistry* 2016.
8 E. Faggi, R. Gavara, M. Bolte, L. Fajari, L. Julia, L. Rodriguez and I. Alfonso, *Dalton Trans.,* 2015, **44**, 12700-12710.
9 J. Becerril, M. Bolte, M. I. Burguete, F. Galindo, E. García-España, S. V. Luis and J. F. Miravet, *J. Am. Chem. Soc.*, 2003, **125**, 6677-6686.
10 (*a*) I. Alfonso, M. Bolte, M. Bru, M. I. Burguete, S. V. Luis and J. Rubio, *J. Am. Chem. Soc.*, 2008, **130**, 6137-6144; (*b*) M. Bru, I. Alfonso, M. Bolte, M. I. Burguete and S. V. Luis, *Chem. Commun.*, 2011, **47**, 283-285.
11 A. E. Martell and R. J. Motekaitis, *Coord. Chem. Rev*., 1990, **100**, 323-361.
12 (*a*) E. García-España, P. Díaz, J. M. Llinares and A. Bianchi, *Coord. Chem. Rev*., 2006, **250**, 2952-2986; (*b*) A. Bianchi, B. Escuder, E. García-España, S. V. Luis, V. Marcelino, J. F. Miravet and J. A. Ramírez, *J. Chem. Soc., Perkin Trans. 2*, 1994, 1253-1259; (*c*) V. J. Arán, M. Kumar, J. Molina, L. Lamarque, P. Navarro, E. García-España, J. A. Ramírez, S. V. Luis and B. Escuder, *J. Org. Chem.*, 1999, **64**, 6135-6146; (*d*) J. A. Aguilar, E. García-España, J. Guerrero, S. V. Luis, J. Llinares, J. Ramírez and C. Soriano, *Inorg. Chim. Acta*, 1996, **246**, 287-294.
13 P. Gans, A. Sabatini and A. Vacca, *Talanta*, 1996, **43**, 1739-1753.
14 M. Á. Herrador and A. G. González, *Talanta*, 2002, **56**, 769-775.
15 The colourless H_2O/MeOH solution of **4** did not absorb in the visible-UV region from 350 to 800 nm.
16 (*a*) M. A. Pauly, E. M. Erwin, D. R. Powell, G. T. Rowe and L. Yang, *Polyhedron*, 2015, **102**, 722-734; (*b*) W. Wang, Y. A. Lee, G. Kim, S. K. Kim, G. Y. Lee, J. Kim, Y. Kim, G. J. Park and C. Kim, *J. Inorg. Biochem.*, 2015, **153**, 143-149; (*c*) P. D. Wadhavane, L. Gorla, A. Ferrer, B. Altava, M. I. Burguete, M. A. Izquierdo and S. V. Luis, *RSC Adv*., 2015, **5**, 72579-72589.
17 (*a*) F. A. Cotton, G. Wilkinson, C. A. Murillo, M. Bochmann, *Advanced Inorganic Chemistry*, Wiley, New York, 6th edn., 1999; (*b*) G. Bussière and C. Reber, *J. Am. Chem. Soc.*, 1998, **120**, 6306-6315; (c) W. Liu, A. Migdisov and A. Williams-Jones, *Geochim. Cosmochim. Acta*, 2012, **94**, 276-290.
18 (*a*) M. G. Basallote, M. J. Fernandez-Trujillo and M. A. Manez, *J. Chem. Soc., Dalton Trans.,* 2002, 3691-3695; (*b*) F. T. R. d. Almeida, B. C. S. Ferreira, A. L. d. S. L. Moreira, R. P. d. Freitas, L. F. Gil and L. V. A. Gurgel, *J. Colloid Interface Sci.*, 2016, **466**, 297-309.
19 (*a*) M. Rajasekar, S. Sreedaran, R. Prabu, V. Narayanan, R. Jegadeesh, N. Raaman and A. Kalilur Rahiman, *J. Coord. Chem.*, 2010, **63**, 136-146; (*b*) J. Manonmani, R. Thirumuruhan, M. Kandaswamy, V. Narayanan, S. Shanmuga Sundara Raj, M. N. Ponnuswamy, G. Shanmugam and H. K. Fun, *Polyhedron*, 2001, **20**, 3039-3048.
20 As has been recently highlighted, the use of the Job plot needs to be handled always with care: F. Ulatowski, K. Dąbrowa, T. Bałakier and J. Jurczak, *J. Org. Chem.*, 2016, **81**, 1746-1756.
21 P. Thordarson, *Chem. Soc. Rev.*, 2011, **40**, 1305-1323.
22 (*a*) S. K. Sharma, G. Hundal and R. Gupta, *Eur. J. Inorg. Chem.*, 2010, **2010**, 621-636; (*b*) S. Kumar and R. Gupta*, Indian J. Chem.*, 2011, **50A**, 1369-1379; (*c*) N. Tounsi, L. Dupont, A. Mohamadou, E. Guillon, M. Aplincourt and G. Rogez, *Polyhedron*, 2008, **27**, 3674-3682; (*d*) L.-M. Luis Miguel, S.-O. Hisila, R. E. Navarro, M. L. Lorena, R. Sugich-Miranda and O. L. Karen, *Polyhedron*, 2014, **79**, 338-346.
23 (*a*) S.-P. Wu, K.-J. Du and Y.-M. Sung, *Dalton Trans.*, 2010, **39**, 4363-4368.
24 (*a*) F. L. Capitán-Vallvey, E. Arroyo-Guerrero, D. M. Fernández-Ramos and F. Santoyo-González, *Microchim. Acta*, 2005, **151**, 93-100; (*b*) IUPAC. Compendium of Chemical Terminology, 2nd ed. (the "Gold Book"). Compiled by A. D. McNaught and A. Wilkinson. Blackwell Scientific Publications, Oxford (1997). XML on-line corrected version: http://goldbook.iupac.org (2006) created by M. Nic, J. Jirat, B. Kosata; updates compiled by A. Jenkins. ISBN 0-9678550-9-8.
25 X. Wu, L. Xu, L. Liu, W. Ma, H. Yin, H. Kuang, L. Wang, C. Xu and N. A. Kotov, *J. Am. Chem. Soc*., 2013, **135**, 18629-18636.
26 (*a*) G. Gran, *Analyst*, 1952, **77**, 661-671; (*b*) F. J. C. Rossotti and H. Rossotti, J. *Chem. Educ.*, 1965, **42**, 375.
27 L. Alderighi, P. Gans, A. Ienco, D. Peters, A. Sabatini and A. Vacca, *Coord. Chem. Rev.*, 1999, **184**, 311-318.
28 (*a*) MassLynx Software, version 4.0; (*b*) S. Moco, R. J. Bino, O. Vorst, H. A. Verhoeven, J. de Groot, T. A. van Beek, J. Vervoort and C. H. R. de Vos, *Plant Physiol.*, 2006, **141**, 1205-1218.

29 O. V. Dolomanov, L. J. Bourhis, R. J. Gildea, J. A. K. Howard and H. Puschmann, *J. Appl. Cryst.*, 2009, **42**, 339-341.
30 G. Sheldrick, *Acta Cryst.*, 2008, **64**, 112-122.
31 C. F. Macrae, I. J. Bruno, J. A. Chisholm, P. R. Edgington, P. McCabe, E. Pidcock, L. Rodriguez-Monge, R. Taylor, J. van de Streek and P. A. Wood, *J. Appl. Crystallogr.*, 2008, **41**, 466-470.

Chapter VI

Coordination behaviour of new open chain and macrocyclic peptidomimetic compounds with Cu^{2+}

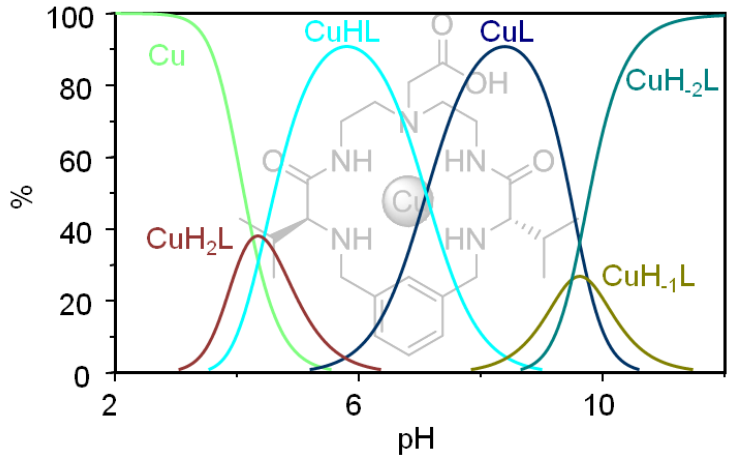

RSC Adv. **2015**, *5*, 72579–72589

RSC Advances

PAPER

Cite this: *RSC Adv.*, 2015, **5**, 72579

Coordination behaviour of new open chain and macrocyclic peptidomimetic compounds with copper(II)†

Prashant D. Wadhavane, Lingaraju Gorla, Armando Ferrer,‡ Belén Altava, M. Isabel Burguete, M. Ángeles Izquierdo and Santiago V. Luis*

Received 22nd June 2015
Accepted 12th August 2015

DOI: 10.1039/c5ra15852d

www.rsc.org/advances

Two valine-derived bis(amino amides) ligands have been prepared and fully characterized. Both compounds contain additional functionalities that implement their basicity and their water solubility. Besides, compound **1** is an open chain ligand, while **2** is a macrocycle. Their protonation constants as well as their stability constants for the formation of the corresponding Cu^{2+} complexes have been determined potentiometrically. Important differences are associated to the macrocyclic effect and to the additional functionalities in the spacer. The presence of an additional amine group and/or the inclusion of a carboxylic side chain in this spacer increase the stabilities of the Cu^{2+}complexes, suggesting its participation in the interaction with the metal. Thus, **2** is the first pseudopeptidic cyclophane of this family displaying the ability to form highly stable metal complexes in water. UV-Vis and ESI-MS were used for analyzing the complex species detected in the speciation diagram.

Introduction

Enzymes are essential for biological processes. In many cases their activity is associated to the presence of metalloenzymes in which metal cofactors mediate the corresponding biological transformations.[1] In particular, for enzymatic systems involving transport of electrons and dioxygen, as well as oxidation and oxygenation processes, the presence of copper is important.[2] The exact properties of those active centers are often related to the coordination geometry of copper. As a diverse family of proteins, copper proteins could be divided into several types.[1d] One classical example is that of azurins, which catalytic center harbors a type 1 copper site.[1d,3] In those systems a carboxylate group, derived from the side chains of aspartate and glutamate, is present. The involvement of a carboxyl group in the coordination environment of the metal center also takes place, moreover, in binuclear enzymes like the metalloenzyme Zn-phosphorotriesterase.[4]

The most common geometries reported for copper complexes include octahedral, tetrahedral,[5] distorted tetragonal,[6] distorted trigonal pyramidal or bipyramidal,[7] and square planar arrangements around the metal center.[8] Copper complexes with open-chain and macrocyclic polydentate amine ligands are frequently pentacoordinate.[9] With this coordination number the complexes can adopt structures that can be described as either square pyramidal (sp) or trigonal bipyramidal (tbp) depending mainly on the actual nature of the ligand. One illustrative example is that of tripodal tetradentate ligands that favour tbp coordination.[10] In this regard, the design and synthesis of ligands functionalized to achieve metal complexation in a biomimetic approach is a challenge of current interest.[11,12]

Although many model complexes use non amino acid ligands mimicking various aspects of the ligand environment in proteins, the development of new ligands based on the presence of amino acid subunits is a fundamental approach in this area.[12,13] In this context, amino acid derived open-chain and macrocyclic compounds have recently drawn much attention in very different fields like synthetic,[14] bioorganic,[15] medicinal,[16] supramolecular chemistry,[17] and catalysis,[18] and recent contributions from our group have shown how minimalistic pseudopeptides derived from simple natural amino acids can have important applications,[19] for instance in the selective recognition of carboxylic acids[20] and amino acid derivatives,[21] and for developing new self-assembled materials[22] or molecular rotors.[21a,23]

Previous studies have revealed the capacity of some C_2-symmetric open-chain pseudopeptides to form stable metal complexes in aqueous solution.[24] However, the same capacity is absent in most of the related pseudopeptidic cyclophanes studied because of their higher lipophilic character, decreasing their water solubility, and the structural strain developed for the coordination of several donor atoms in the macrocycle to the

Departament of Inorganic and Organic Chemistry, Universitat Jaume I, Campus del Riu Sec, Av. Sos Baynat, s/n, E-12071, Castellón, Spain. E-mail: luiss@uji.es

† Electronic supplementary information (ESI) available: Potential protonation equilibria for 2 (S1). ^{1}H NMR spectra of compound **1** at different pH values (S2), Mass Spectra (S3) and computational models (S4). See DOI: 10.1039/c5ra15852d

‡ Permanent address: Departamento de Química, Facultad de Ciencias Naturales, Universidad de Oriente, Avda. Patricio Lumumba s/n., 90 500 Santiago de Cuba, Cuba.

same metal center. Taking all this into account, the design and study of macrocyclic pseudopeptides incorporating carboxylate pendant groups coexisting with amino and amide groups is an important target. In such systems, besides the inclusion of additional donor groups, the presence of the carboxylic group can provide an important contribution to the water solubility of the resulting ligand, allowing its study under aqueous conditions of biological relevance.

Here we present our results on the acid–base and coordination properties of the macrocyclic pseudopeptide **2** containing a pendant carboxylic group. The structurally related open-chain pseudopeptide **1**, lacking the carboxylic functionality has also been studied for a better analysis of the effect of the carboxylic group and the macrocyclic nature present in **2**.

Results and discussion

The structure of the ligands (**1**–**3**) considered in this work is displayed in Chart 1. The synthesis of compounds **1** and **2** is presented in Scheme 1 and follows the general synthetic approaches previously developed by us.[25] The synthesis and study of the open-chain ligand **3**, containing a central spacer of the same length than **1** but lacking the additional amino group has been reported elsewhere.[24] The open-chain bis(amino amide) compound **1** can be easily prepared starting from *N*-Cbz protected valine through the initial formation of the corresponding activated *N*-hydroxysuccinimide ester, coupling with diethylenetriamine and final *N*-deprotection. The *N*-Cbz protected precursor of **1** (Cbz-protected compound **6**) was also a key intermediate for the synthesis of the macrocyclic compound **2**. Nevertheless this synthetic procedure is more complex as it requires a proper definition of the step at which the pendant group is introduced at the central nitrogen atom of the spacer. In this regard, we followed successfully the approach recently used for the preparation of related derivatives containing fluorescent subunits that can act as markers of acidic organelles within live cells.[26] Thus, the open-chain intermediate **6** was reacted with methyl-2-bromoacetate in DMF at 50 °C for 24 h, using K_2CO_3 as the base, to introduce the ester functionalized pendant arm. Then, deprotection of the Cbz group was carried out by hydrogenolysis to provide the intermediate **8**. Reaction of this compound with 1,3-bis(bromomethyl)benzene provided the macrocyclic structure **9** from which, after hydrolysis of the ester group using lithium hydroxide in a 2 : 1 THF–water mixture, the desired cyclic pseudopeptide **2** was obtained in 41% yield. The resulting pseudopeptide is a highly functional macrocycle with a relatively large and flexible cavity, which increases its potential for the interaction with metal cations and its water solubility.

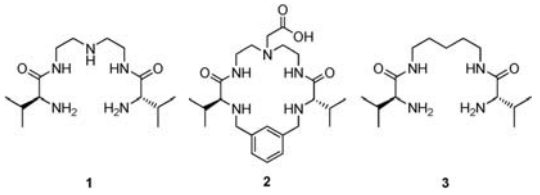

Chart 1 Bis(amino amide) ligands studied in this work.

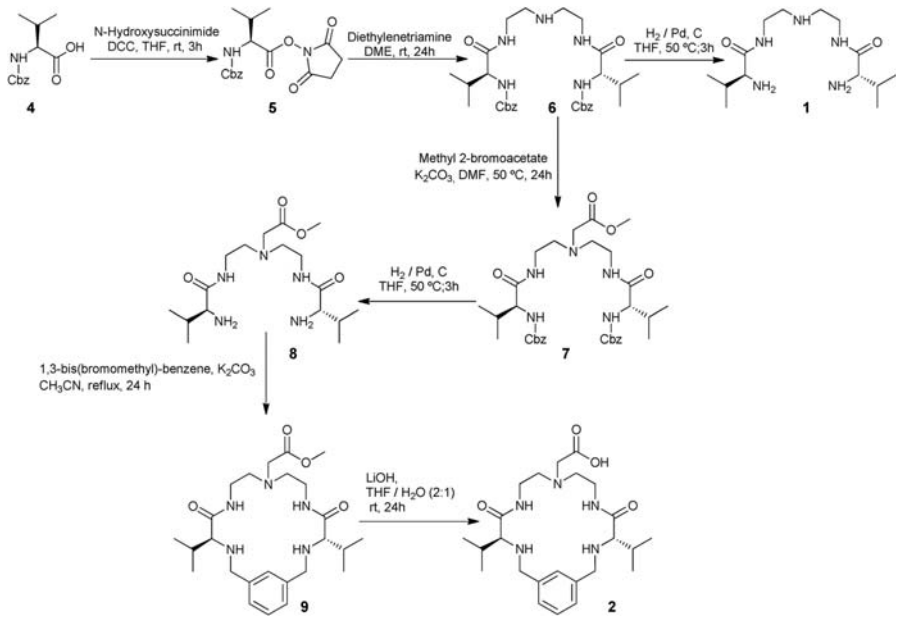

Scheme 1 Synthetic route for the preparation of the open chain (**1**) and macrocyclic (**2**) pseudopeptidic compounds.

Acid–base studies

The presence of the additional nitrogen atom in the central spacer, in particular the tertiary one in **2**, and the carboxylic group present in the pendant arm of the macrocyclic derivative **2** must significantly affect the acid–base properties of these compounds when compared to those of related systems (*i.e.* **3**). Thus, the acid–base properties of **1** and **2** were studied using potentiometric titrations. All the titrations were carried out as is fully described in the experimental section, at 298.1 ± 0.1 K using NaCl 0.1 M to maintain a constant ionic strength. The cumulative and stepwise stability constants for the protonation of these pseudopeptidic valine derivates obtained following this methodology are presented in Table 1, along with those for the related compound **3** previously determined.[24] According to their structure, three protonation constants are detected for **1** and four for **2**, while only two protonation constants are present in the related compound **3**. To facilitate the analysis of the data the monoanionic carboxylate derived from **2** has been considered as the L species (see Fig. 1). Charges have been omitted for clarity in the description of the different protonated and complex species.

Table 1 Logarithms of the stepwise protonation constants of pseudopeptidic compounds **1–3** determined in NaCl 0.1 M at 298.1 + 0.1 K

Reaction[a]	**1**	**2**	**3**[b]
$H + L \rightleftharpoons HL$	9.02(1)[c]	10.01(1)	8.11(4)
$H + HL \rightleftharpoons H_2L$	7.86(1)	7.95(1)	7.31(4)
$H + H_2L \rightleftharpoons H_3L$	6.93(1)	6.45(1)	
$H + H_3L \rightleftharpoons H_4L$	—	5.87(2)	

[a] Charges omitted for clarity. [b] Taken from ref. 24. [c] Values in parentheses are the standard deviations in the last significant figure. Values lower than 2 have not been considered. Charges omitted for clarity.

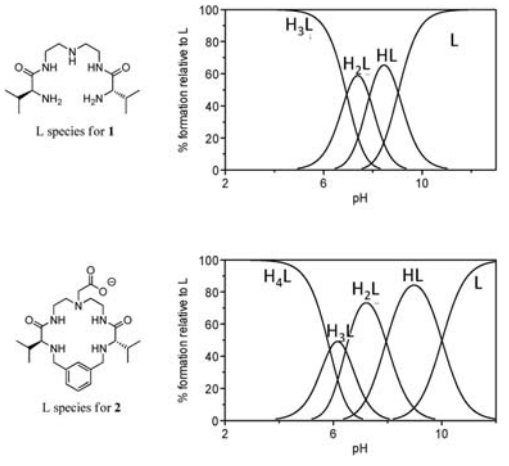

Fig. 1 Distribution diagrams for protonated species of **1** (top) and **2** (bottom) in 0.1 M NaCl at 298.1 K. Charges have been omitted for clarity.

Regarding the values of the stepwise protonation constants, data in Table 1 show that compound **2**, having three basic nitrogen atoms and one basic carboxylate, displays the higher constant ($\log K = 10.01$) for the formation of the [HL] species. This first protonation can be assigned to the carboxylate group or to one of the amine groups, leading to the formation of a neutral or a zwitterionic species. In this regard, computational calculations carried out at the PM3 level revealed a strong stabilization of the zwitterionic structures for **2** relative to the neutral species. In the same way, as could be expected, this first protonation is easier for the open-chain pseudopeptide **1** with three basic nitrogen atoms than for the reference dibasic compound **3** ($\log K = 9.02$ for **1** and 8.11 for **3**). However, the second and third protonation constants are relatively similar for **1** and **2** ($\log K = 7.86$ and 7.95 for $[H_2L]$, 6.93 and 6.45 for $[H_3L]$, respectively). Compound **3** presents a second protonation constant that is only slightly lower that the ones obtained for **1** and **2**. This seems to suggest that the $[H_2L]$ species for **1** and **2** involves the preferential protonation at the two more distant amine nitrogen atoms to reduce the electrostatic repulsion. The higher conformational freedom of the open chain compounds and the more favourable solvation of the primary ammonium groups could partly compensate the effect in **2** of the presence of the carboxylate group. For the macrocyclic ligand a fourth constant is identified, which can be associated with its full protonation, including the acid group in the pendant arm ($\log K = 5.87$).

The resulting distribution diagrams for the protonated species of **1** and **2** are shown in Fig. 1. For the open chain ligand the diagram shows the predominance of non-protonated species (L) at pH values slightly higher than 9. For compound **2**, the anionic species (L), corresponding to the presence of a carboxylate group and non-protonated amino groups, predominates in the very basic region (pH > 10), while the neutral species (HL), is prevalent at the pH range 8–10. In general, the different positively charged species of **2** appear at slightly more acidic regions that those with the same charge in **1**, in particular for the fully protonated species (H_4L for **2** and H_3L for **1**).

The location of the protons in the protonated species is not a simple matter, in particular for **2**, considering the presence of several basic fragments, which leads to the existence of a very complex set of potential protonation equilibria at most protonation steps (see ESI† for protonation equilibria). The ^1H NMR spectra obtained at different pH values in D_2O are in agreement with the distribution diagrams obtained and suggest that all the different nitrogen atoms are protonated, at some extent, in the different $[H_xL]$ species. Fig. 2 displays the ^1H NMR spectra, at different pH values, for the macrocyclic compound **2** (see ESI† for data regarding compound **1**). The coexistence of several structures for each protonated species is confirmed by the complexity of the spectra at intermediate pH values. Interestingly, the formation of the zwitterionic species seems to involve the protonation of one of the benzylic nitrogen atoms, as the corresponding signals (AB doublets at >3.6 ppm) are the ones experiencing a more significant shift when changing from pH 11.4 to pH 8.3, although the signal corresponding to proton b located in α relative to the tertiary amine group is also slightly

shifted. On the other hand, the last protonation also seems to affect significantly to this position as shown by the additional changes observed at very acidic pH values. This is also in good agreement with the observation in fluorescent systems related to **2** that full protonation of the benzylic amine groups, required for activating the fluorescence, takes place only at the acidic regions ($pK_a = 4.45–4.83$).

Determination of the Cu^{2+} complexes formation constants

The interaction of Cu^{2+} and ligands **1** and **2** was systematically studied by potentiometric titrations in aqueous solution over the 2–11 pH range. The stability constants for the formation of Cu^{2+} complexes were determined in water for a 1 : 1 metal–ligand ratio, using 0.1 M NaCl to maintain a constant ionic strength and a temperature of 298.1 K. The results obtained are presented in Table 2 and the corresponding distribution diagrams are displayed in Fig. 3.

The presence of an additional nitrogen donor atom in the central spacer linking the two amino acid subunits provides, as could be expected, the formation of significantly more stable complexes. This is clearly observed when comparing the values of the constants for open chain pseudopeptides **1** and **3**. As shown in the table, these values are at least two orders of magnitude higher for the ligand **1**. This is particularly relevant for the formation of the [CuL] species. The value of this constant for **1** is higher than that reported for ethylenediamine ($\log K = 10.60$)[27] in spite of the more favourable chelating ring that can be achieved in the case of ethylenediamine, suggesting that more than two nitrogen atoms are involved in the coordination to the metal. The existence of an additional carboxylate donor group in L for **2** provides [CuL] formation constants significantly higher for this ligand. However, if we compare the complex formation constants calculated for the neutral ligands (L for **1** and HL for **2**) the situation is different. Thus, the value of the constant for the formation of the [CuL] dicationic species for **1** ($\log K = 11.03$) can be compared to that for the dicharged [CuHL] species for **2** (HL + Cu ⇄ CuHL, $\log K = 9.28$). This seems to preclude a relevant contribution of the macrocyclic effect in this case, most likely for it is counterbalanced by the increase in structural stress associated to the presence of the rigid aromatic ring. As has been observed for other C_2 symmetric pseudopeptides like **3**, ligands **1** and **2** can form stable copper complex through mono- and bisdeprotonation of the N–H amide functional groups, which can be easily monitored through spectroscopic measurements.[24] Both

Table 2 Logarithms of the cumulative and stepwise formation constants for the Cu^{2+} complexes of ligands **1–3** determined in 0.1 M NaCl at 298.1 ± 0.1 K

Reaction[a]	**1**	**2**	**3**[b]
Cu + L ⇄ CuL	11.03(1)[c]	12.19(2)	6.76(1)
Cu + L + H ⇄ CuHL	16.46(1)	19.29(3)	12.51(4)
Cu + L + 2H ⇄ CuH_2L	—	23.73(3)	—
Cu + L ⇄ $CuH_{-1}L$ + H	3.052(2)	2.44(1)	−0.23(2)
Cu + L ⇄ $CuH_{-2}L$ + 2H	−6.457(2)	−7.05(1)	−9.89(3)
Cu + L ⇄ $CuH_{-3}L$ + 3H	−16.96(4)	—	—
CuL + H ⇄ CuHL	5.43(1)	7.10(2)	5.74(3)
CuHL + H ⇄ CuH_2L	—	4.44(3)	—
CuL ⇄ $CuH_{-1}L$ + H	−7.978(1)	−9.75(1)	−7.00(2)
$CuH_{-1}L$ ⇄ $CuH_{-2}L$ + H	−9.509(1)	−9.49(1)	−9.66(4)
$CuH_{-2}L$ ⇄ $CuH_{-3}L$ + H	−10.503(1)	—	—

[a] Charges omitted for clarity. [b] Taken from ref. 24. [c] Values in parentheses are the standard deviations in the last significant figure. Values lower than 2 have not been considered.

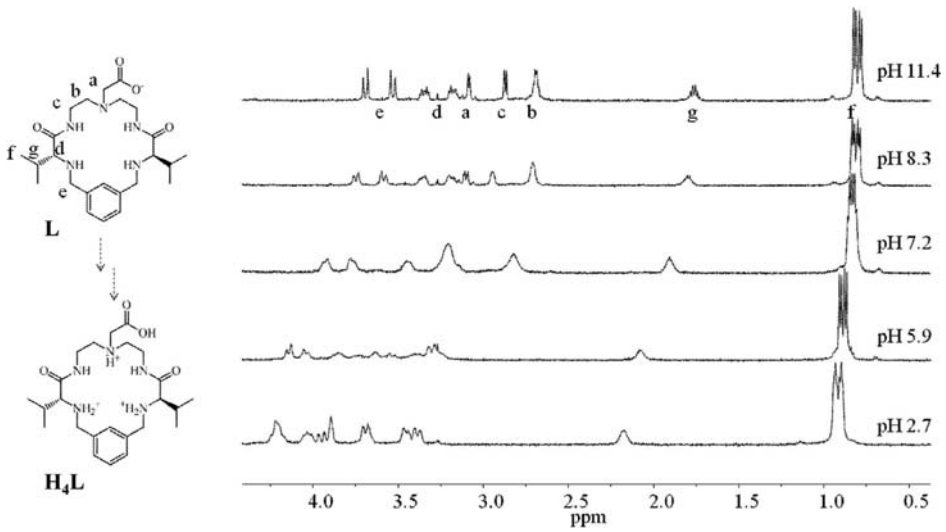

Fig. 2 ^1H NMR spectra in D_2O for the different protonated species derived from compound **2** at different pH values. Major species present according to the distribution diagrams: pH 11.4 (L); pH 8.3 (HL); pH 7.2 (H_2L); pH 5.9 (H_3L); pH 2.7 (H_4L).

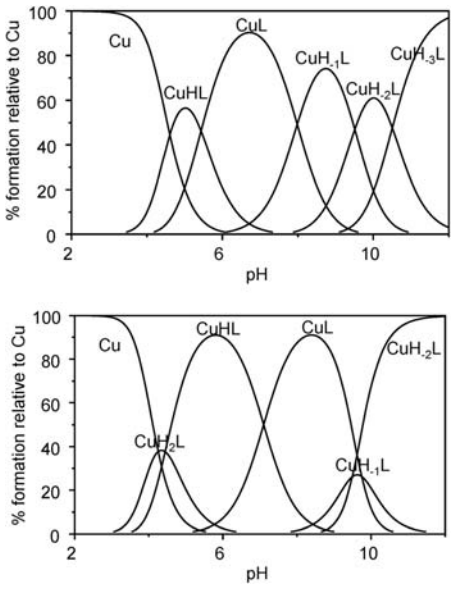

Fig. 3 Distribution diagrams for the systems Cu^{2+}-**1** (top) and Cu^{2+}-**2** (bottom) determined in 0.1 M NaCl. Charges omitted for clarity.

deprotonation steps are detected and should correspond to the formation of the monocationic [$CuH_{-1}L$] and neutral [$CuH_{-2}L$] species for **1** and the neutral [$CuH_{-1}L$] and monoanionic [CuH neutral [$CuH_{-2}L$] species$_2$L] species for **2**. Although, formally, in the case of **2** a species like [$CuH_{-1}L$] could also correspond to the complex formed by the ligand bisdeprotonated at both amide groups and protonated at the carboxyl group, the large difference between the pK_a values for both functionalities seems to preclude this possibility. The analysis of the distribution diagrams is also consistent with this situation, as this species is only present for **2** at pH values around 10 at which the carboxyl group should not be protonated.

It is worth mentioning that the presence of an additional nitrogen atom in the central spacer is not reflected in an increased basicity of the [CuL] complex for **1**, indicating a strong participation of all the amino groups in the coordination to the metal. Thus, the constants determined for the process CuL + H $\rightleftarrows$ CuHL are log $K = 5.43$ for **1** and log $K = 5.74$ for the reference compound **3**. A higher first protonation constant is detected for 2 (log $K = 7.10$), but this must correspond to the protonation of the carboxylate fragment in the monocationic [CuL] species. As a matter of fact, a second protonation for this complex, that should correspond to the protonation of a nitrogen atom, is also detected (log $K = 4.44$). Interestingly, in the case of **1**, the formation of a monoanionic complex species, [$CuH_{-3}L$] is detected, which should correspond to the deprotonation of a coordinated water molecule to form the corresponding hydroxide. Such a complex has not been detected for **3**, revealing the important structural differences associated to the presence of the third amino group in the spacer. As this species starts to be present at pH values above 8 (Fig. 3), this could be of interest in the development of catalytic applications and biomimetic models, for instance as simplified HCA mimics.[28] For the macrocyclic ligand **2**, this is not observed as the carboxylate group can coordinate to the copper center instead of the hydroxide anion.

The distribution diagrams for **1** and **2** displayed in Fig. 3 show that species with similar total charge are predominant at each pH region. In both cases, the monocationic and dicationic complexes ([$CuH_{-1}L$] and [CuL] for **1** and [CuL] and [CuHL] for **2**) are the major species identified around neutral pH values. Overall, the macrocyclic ligand **2** represents the first example of this family of pseudopeptidic cyclophanes being able to display a significant capacity to form stable copper complexes in aqueous solutions and for a broad range of pH values.

The use of ESI-MS has been revealed to be of great help for the identification of supramolecular species.[29] Nevertheless, it is important to realize that the nature of the species present in purely aqueous solutions can differ from those under the conditions required for ESI-MS analysis, in particular taking into account that ESI-MS experiments require the use of methanolic solutions or water–methanol mixtures. In spite of this, its potential to detect species even at very low concentrations is a unique feature of this technique.[30] On the other hand, many different studies have shown how ESI-MS allows properly detecting the complex species observed in solution. The identification of metal–ligand species is of particular relevance as the exact nature of the complex can be efficiently confirmed by the analysis of the corresponding isotopic patterns. This has been used previously to confirm the metal complex species formed by ligands related to **3**, revealing that similar results are obtained in methanol and in aqueous solutions containing some methanol.[24] Accordingly, the ESI technique in the positive mode of analysis was used to confirm the species observed at the different pH regions in the distribution diagrams for **1** and **2**. Thus, for instance (Fig. 4), at basic pH values (pH range 9–11) a peak at 403 was clearly detectable for ligand **1** (Fig. 4). This peak can be assigned to the solvated (H_2O) sodium ion adduct of the neutral species [$CuH_{-2}L$], [$CuH_{-2}L + H_2O + Na^+]^+$. The base peak, however, appears at 363 corresponding to the monocationic species [$CuH_{-2}L + H$] obtained from the neutral complex [$CuH_{-2}L$], or directly from the monocationic species [$CuH_{-1}L$]. In addition, a peak at 385 can be assigned to [$CuH_{-2}L + Na^+]^+$, whose +H_2O and +2H_2O species are [$CuH_{-2}L + H_2O + Na^+]^+$ (403) and [$CuH_{-2}L + H_2O + Na^+]^+$ (421), respectively. Complex species formed by the monodeprotonated or bisdeprotonated ligand predominate in solution in this pH region. The second most intense peak appears at 302, corresponding to the protonated free ligand [HL]. The monoanionic [$CuH_{-3}L]^-$ species could not be observed even with the use of the ESI in negative mode.

The ESI^+ MS spectra for the Cu^{+2} complexes with **2** at pH = 11.5 presents a base peak at 545. Taking into account that L has been defined for **2** as monoanionic (see Fig. 1), this peak can be assigned to the monocationic [$CuH_{-2}L + H^+ + Na^+]^+$ species, while the peak at 561 should correspond to the monocationic [$CuH_{-2}L + H^+ + K^+]^+$ species (see ESI†), again in good agreement with the distribution diagram.

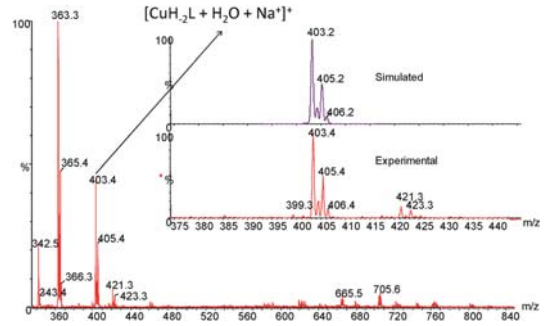

Fig. 4 ESI$^+$-MS spectra for Cu^{2+} complexes with **1** at pH = 11.0 in methanol.

Spectroscopic analyses also provided additional information on the exact nature of the complex species. As for other ligands related to **3**, FT-IR spectra of the Cu^{2+} complexes formed by **1** and **2** under basic condition revealed the participation of deprotonated amide groups, with the observation of the corresponding amide bands at *ca.* 1670 cm^{-1}.[31] Taking advantage of the distribution diagrams presented in Fig. 3, a UV-visible spectroscopic study was carried out, by selecting preferentially those pH regions at which one of the complex species is dominant. A selection of the UV-visible spectra, obtained for **1** and **2** at different pH values are gathered in Fig. 5. The spectral window selected is the region corresponding to the d–d transitions, which provides useful information on the coordination geometries of the respective copper complexes.[9h,32] The respective observed values of λ_{max} are presented in Table 3. Interestingly, the observed pH dependence patterns of the molecular spectra for **1** and **2** are very similar and clearly differ from those reported for tetradentate ligands related to **3** and having different central aliphatic spacers and amino acids side chains.[24] In the case of compounds related to **3**, significant differences are observed in the electronic spectra with changes in the pH that were associated to the presence/absence of deprotonated complexes $[CuH_{-x}L]^{(2-x)+}$. For regions involving the uncomplexed cation or complexes with the fully protonated ligands absorption maxima were observed in the 640–690 range, characteristic for octahedral copper complexes. On the contrary, for regions involving the predominant formation of complexes with deprotonated ligands, the maxima appear at the 490–560 range, corresponding to square planar to square-pyramidal geometries. In the case of ligands **1** and **2**, however, no significant shifts in the maxima are observed for most of the pH values studied, although the intensity of the bands is variable. Only at very acidic pH values, where the uncomplexed Cu^{2+} cation is the major species in solution, the appearance of a new diffuse band at much larger wavelengths and a strong decrease of the original band, accompanied by a shift in its maximum, are detected. In the case of **1**, the observed maxima range from 545 to 549 nm, except for the more acidic region, while for **2** the maxima of the spectra, for the same pH range, appear at 579–590 nm.

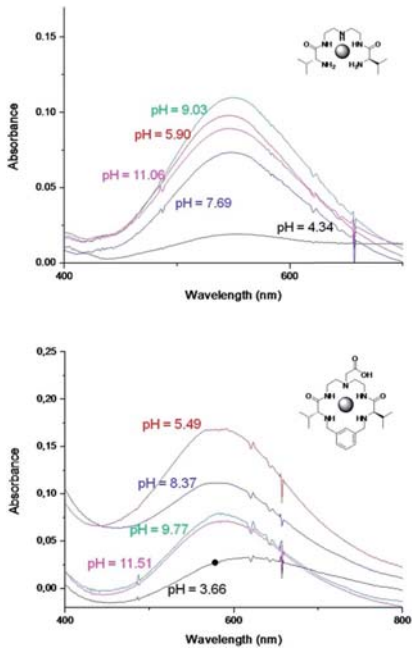

Fig. 5 UV-visible spectra obtained for 1 : 1 Cu : L mixtures for ligands **1** (top) and **2** (bottom) at different pH values.

Table 3 Observed values of λ_{max} for the UV-visible spectra of Cu complexes with **1** and **2** at different pH values

L	pH	λ_{max} (nm)	Major species from distribution diagrams (abundance in %)
1	4.3	555	Cu (45), CuHL (45), CuL (10)
	5.9	545	CuL (70), CuHL (30),
	7.7	546	CuL (60) $CuH_{-1}L$ (40)
	9.0	549	$CuH_{-1}L$ (70), $CuH_{-2}L$ (10), CuL (10)
	11.0	547	$CuH_{-3}L$ (90)
2	3.7	624	Cu (40), CuH_2L (40), CuHL (20)
	5.5	590	CuHL (90)
	8.4	579	CuL (90)
	9.8	583	$CuH_{-1}L$ (30), $CuH_{-2}L$ (30), CuL (30)
	11.5	585	$CuH_{-2}L$ (95)

This should be in good agreement with the maintenance, for the different complex species formed, of a predominant square planar to square-pyramidal geometry (500–600 nm).[9h] This last geometry is common to many complexes formed by pentadentate ligands,[33] and many five-coordinate copper(II) complexes adopt square pyramidal arrangements of the donor atoms around the metal center, in some cases with a clear distortion towards a trigonal pyramidal coordination.[34] For **1**, the square planar base can be easily formed by the two amides and two amine groups from the amino acid moieties, while the additional nitrogen atom or, in basic media, a hydroxide anion could occupy the apical position.

A similar situation can be expected for the complexes formed by ligand **2**, although in this case we need to take into account the steric constrains imposed by the macrocyclic structure and the presence of the carboxyl/carboxylate group that could act as an additional donor group in the coordination to copper(II). This can lead to distorted square pyramidal complexes or distorted square planar complexes. In some cases, the transition from square pyramidal to trigonal bipyramidal has been observed to be associated to a bathochromic shift from around 550 to *ca.* 600 nm, as is observed here.[33]

Computational models (MMFF) reveal, in good agreement with experimental data, that distorted square planar and square pyramidal geometries can be easily achieved, for instance, for complexes of both deprotonated ligands (see ESI†). They suggest, taking also into consideration former studies with related systems, that a square planar arrangement can be achieved involving the two deprotonated amide groups and two amine nitrogen atoms. The additional coordination to the third amino group, to the carboxylate in **2** or to a water molecule could transform this square planar arrangement into square pyramidal. However, the existence of different possible structural possibilities for those arrangements and the low energy differences calculated for many of them does not allow an unambiguous definition of the coordination geometries in the absence of additional data, in particular crystal structures. Thus, different complex structures could coexist, for instance, for the $[CuH_{-2}L]$ species predominant at the basic region. The same can apply for [CuL] and the related protonated complex species for which an efficient coordination to the metal seems to take place and can involve the amino groups and the carbonyl oxygen atoms of the amide groups. Similar results are obtained in the case of the ligand **1** (see ESI†).

Conclusions

The introduction of a nitrogen atom in the central spacer linking the two amino acid subunits in C_2 symmetric pseudopeptides provides important changes in the properties of the resulting derivatives (*i.e.* **1** and **2**) relative to those of the parent compounds like **3**. The presence of this additional nitrogen atom increases the basicity of the resulting system and the number of donor atoms for coordination to metal ions like Cu(II), but besides, facilitates the building of more elaborated structures as is illustrated in the case of **2**. Overall, this modification significantly increases their solubility in water and affords pentadentate ligands that are able to form more stable Cu(II) complexes than the parent ligand **3**. Copper complex species dominate the distribution diagram for pH values above 5. The geometry of these complexes, having different protonation states, seems to be very similar, most likely from square planar to square-pyramidal, a behaviour clearly divergent from the one found for ligand **3** and related compounds. The existence of a large enough flexible cavity in the case of the macrocyclic compound **2** and the presence of the six potential donor groups in the macrocyclic structure allows the formation of strong metal complexes for this ligand, in spite of the important steric constraints often found for structures of this class like polyaza[*n*]cyclophanes.[35] Thus, the macrocyclic ligand **2** represents the first example of this family of receptors with a significant capacity to form stable copper complexes in aqueous solutions and for a broad range of pH value.

Experimental section

Materials and reagents

All reagents were obtained from commercial sources and used as received unless otherwise stated. Dimethoxyethane (DME) was dried and distilled from molecular sieves (4 Å) and then stored over molecular sieves. Deionised water was used from a Milli-Q water system by Millipore.

Synthesis and characterization of organic compounds

Synthesis of 5. To a clear solution of *N*-Cbz-L-valine **4** (25 g, 99.49 mmol) and *N*-hydroxysuccinimide (11.45 g, 99.49 mmol) at 0 °C was added DCC (20.52 g, 99.49 mmol) in anhydrous THF in a dropwise manner, and the reaction mixture was stirred at 0–5 °C for 3 h. The dicyclohexylurea formed was filtered off and the filtrate was concentrated to dryness. The crude product was recrystallized from 2-propanol to obtain the pure product. Yield 87% (49 g); m.p. 119–120 °C; $[\alpha]_D^{25} = -20.1°$ ($c = 0.1$, $CHCl_3$); IR (KBr) 3360, 1741, 1526 cm^{-1}; ^1H NMR (300 MHz, $CDCl_3$) (δ, ppm): 1.02 (d, 6H, $J = 7.4$ Hz), 1.06 (d, 6H, $J = 7.7$ Hz), 2.31 (m, 1H), 2.77 (s, 4H), 4.66 (dd, 1H, $J = 4.7$ Hz), 5.13 (s, 2H), 5.43 (d, 1H, $J = 9.5$ Hz), 7.28–7.41 (m, 5H); ^{13}C NMR (75 MHz, $CDCl_3$): (δ, ppm): 17.2, 18.7, 25.5, 31.5, 57.4, 67.2, 128.0, 128.1, 128.3, 135.8, 155.6, 167.5, 168.6; anal. calcd (%) for $C_{17}H_{20}N_2O_6$: C, 58.6; H, 5.8; N, 7.7; found: C, 58.1; H, 5.9; N, 8.0.

Synthesis of 6. To a clear solution of the *N*-hydroxysuccinimide ester of *N*-Cbz-L-valine **5** (30.0 g, 86.12 mmol) in anhydrous dimethoxyethane (DME, 250 mL) at 0 °C, diethylenetriamine (4.46 g, 43.06 mmol) dissolved in dry DME (20 mL) was added in a dropwise manner. The reaction mixture was stirred at room temperature for 18 h and then was heated to 40–50 °C for 6 h. The white solid formed was filtered and washed with cold water and cold methanol. Yield 94% (23.27 g), m.p. = 175 °C; $[\alpha]_D^{25} = 11.39°$ ($c = 0.1$, $CHCl_3$); IR (ATR) 3285, 2957, 1685, 1649, 1535, 1236 cm^{-1}; ^1H NMR (500 MHz, DMSO-d_6) (δ, ppm): 7.83 (s, 2H), 7.38–7.23 (m, 8H), 7.19 (d, 2H, $J = 8.3$ Hz), 5.07–4.94 (m, 4H), 3.83–3.68 (m, 4H), 3.10 (dd, 4H, $J = 12.6$, 6.1 Hz), 1.98–1.84 (m, 2H), 0.82 (d, 12H, $J = 6.1$ Hz). ^{13}C NMR (75 MHz, DMSO-d_6) (δ, ppm): 174.7, 171.8, 156.8, 137.8, 129.0, 128.4, 128.3, 66.1, 61.1, 48.9, 30.9, 19.9, 18.9; HRMS (ESI-TOF)$^+$ Calcd for $C_{30}H_{43}N_5O_6$ (M + H^+) 570.3292. Found 570.3296 (M + H^+); anal. calcd for $C_{30}H_{43}N_5O_6$ H_2O: C, 61.3, H, 7.7, N, 11.9. Found. C, 61.4, H, 7.8, N, 11.9.

Synthesis of 7. A mixture of compound **6** (10 g, 17.55 mmol), anhydrous K_2CO_3 (24.25 g, 175.5 mmol) and methyl bromoacetate (2.68 g, 19.30 mmol) was placed in a flask containing dry dimethylformamide (DMF, 10 mL) and heated to 50 °C for 24 h under nitrogen atmosphere. The reaction was monitored by TLC. After complete consumption of the starting material, distilled water was added (30 mL). This solution was extracted by using ethyl acetate (EtOAc, 30 mL, ×3). The organic phase

was dried over anhydrous $MgSO_4$ and evaporated under vacuum. The product was purified by silica flash chromatography using $MeOH/CH_2Cl_2$ (1 : 50) to give the white solid **7** (8.19 g, 75% yield): m.p. 156–158 °C; $[\alpha]_D^{25} = -10.45°$ (*c* 0.1, 55 $CHCl_3$); IR (ATR) 3300, 3064, 3031, 2949, 2869, 2360, 1736, 1685, 1644, 1532 cm^{-1}; ^1H NMR (500 MHz, DMSO-d_6) (δ, ppm): 7.77 (s, 2H), 7.39–7.24 (m, 10H), 7.17 (d, 2H, $J = 8.8$ Hz), 5.00 (m, 4H), 3.78 (t, 2H, $J = 7.9$ Hz), 3.58 (s, 3H), 3.37 (d, 2H), 3.10 (m, 4H), 2.63 (m, 4H), 1.91 (m, 4H), 0.82 (m, 12H); ^{13}C NMR (126 MHz, DMSO-d_6) (δ, ppm): 173.7, 171.5, 139.8, 129.3, 128.6, 127.5, 67.5, 55.7, 55.0, 53.6, 51.5, 37.5, 31.2, 19.5, 18.0; HRMS (ESI-TOF)$^+$ (*m*/*z*) Calcd for $C_{33}H_{47}N_5O_8$ (M + H^+) 642.3503, found 642.3508. Anal. calcd (%) for $C_{33}H_{47}N_5O_8$: C, 61.8, H, 7.4, N, 10.9; found: C, 61.7, H, 7.5, N, 10.9.

Synthesis of 8. To a clear solution of compound **7** (2.00 g, 3.11 mmol) in dry tetrahydrofuran (THF), 10 mol% of the catalyst (5 wt% Pd on activated carbon) was added. The reaction mixture was stirred under an H_2 atmosphere (H_2 balloon) at 50 °C for 4 h. The reaction was monitored by TLC, and after complete consumption of the starting material the catalyst was filtered off through a Celite® bed and washed with THF. The crude product was purified by column chromatography using $MeOH/CH_2Cl_2/NH_3$ (1 : 15 : 0.01) as eluent. Evaporation of the solvent under vacuum yielded the green oil **8** (0.462 g, 80% yield): $[\alpha]_D^{25} = 6.26°$ (*c* 0.1, $CHCl_3$); IR (ATR) 3289, 3073, 2963, 2869, 1736, 1640, 1526 cm^{-1}; ^1H NMR (500 MHz, $CDCl_3$) (δ, ppm): 7.50 (s, 2H), 3.26 (m, 4H), 3.09 (m, 2H), 2.66 (m, 4H), 2.10 (m, 2H), 1.59 (m, 5H), 0.87 (d, 6H, $J = 6.8$ Hz), 0.74 (d, 6H, $J = 6.8$ Hz); ^{13}C NMR (75 MHz, $CDCl_3$) (δ, ppm): 174.3, 171.8, 68.2, 54.8, 54.1, 51.0, 43.4, 36.9, 31.2, 19.6, 17.9, 15.2; HRMS (ESI-TOF)$^+$ (*m*/*z*) Calcd for $C_{17}H_{35}N_5O_4$ (M + H^+) 374.2767, found 374.2762. Anal. calcd (%) for $C_{17}H_{35}N_5O_4$: C, 49.9, H, 9.6, N, 17.1; found: C, 49.9, H, 9.7, N, 17.0.

Synthesis of 9. A mixture of compound **8** (0.50 g, 1.33 mmol), anhydrous K_2CO_3 (1.85 g, 13.38 mmol) and 9,10-bis(bromomethyl)-benzene (0.39 g, 1.47 mmol) in dry CH_3CN (175 mL) was stirred to reflux for 24 h under a nitrogen atmosphere. The reaction was monitored by TLC. After complete consumption of the starting material, the reaction mixture was filtered and the solvent was evaporated under vacuum. The crude product was purified by silica flash chromatography using $MeOH/CH_2Cl_2$ (1 : 25) as the eluent to yield the yellowish solid compound **9**. Yield 72% (0.459 g), m.p. 106 °C, $[\alpha]_D^{25} = -24.36$ ($c = 0.1$, $CHCl_3$); IR (ATR) 3323, 2947, 2922, 2856, 1741, 1651, 1592, 1198 cm^{-1}, ^1H NMR (500 MHz, $CDCl_3$) (δ, ppm): 7.68 (s, 2H), 7.38 (s, 1H), 7.26–7.07 (m, 5H), 3.65 (dd, 4H, $J = 30.0, 12.1$ Hz), 3.53 (s, 3H), 3.42 (d, 2H, $J = 40.9$ Hz), 3.30 (s, 2H), 3.19 (s, 2H), 2.85 (d, 2H, $J = 3.4$ Hz), 2.73 (dd, 4H, $J = 41.5, 34.7$ Hz), 2.06 (d, 2H, $J = 5.3$ Hz), 0.82 (dt, 12H, $J = 62.3, 31.1$ Hz); ^{13}C NMR (126 MHz, $CDCl_3$) (δ, ppm): 174.2, 171.9, 140.1, 129.3, 128.5, 127.6, 67.8, 55.6, 53.6, 51.5, 37.4, 31.3, 19.5, 18.0. HRMS (ESI-TOF)$^+$ Calcd for $C_{25}H_{41}N_5O_4$ (M + H^+) 476.3237. Found 476.3235 (M + H^+). Anal. calcd (%) for $C_{25}H_{41}N_5O_4$: C, 63.7, H, 8.7, N, 14.7; found. C, 63.5, H, 8.8, N, 14.7.

Synthesis of 2. To a clear solution of **9** (0.2 g, 0.42 mmol) in 7 mL of THF/H_2O (2 : 1), was added LiOH (0.07 g, 2.94 mmol) and the reaction was stirred at room temperature for 24 h (2 : 1, 3 mL). The reaction was monitored by using TLC; after complete consumption of the starting material, the reaction mixture was acidified (pH 6) by addition of 1 : 1 HBr/H_2O. To this solution was added washed DOWEX® ion exchange resin (4 g), and the mixture was left for 18 h at room temperature. (The standard procedure to wash the DOWEX® ion exchange resin was as follows: 50 mL deionized H_2O, 50 mL MeOH, 50 mL H_20, 50 mL THF, 50 mL H_2O, 50 mL 10% NH_3 in H_2O, H_2O till neutral pH, 50 mL 2 M HCl, H_2O till neutral pH). The solvent of this mixture was evaporated under vacuum, and the resulting solid was put in a column containing 20 g washed DOWEX® ion exchange resin and deionized H_2O. The eluents used for the resin column purification were: 100 mL H_2O; 1 : 1 THF/H_2O 100 mL; 5% NH_3 in H_2O. From this resin column purification the compound was isolated by the elution with 5% NH_3 in H_2O. Then the water was evaporated under vacuum to yield the off-white solid **2**. Yield 41% (0.80 g), m.p. 83 °C, $[\alpha]_D^{25} = -31.84°$ ($c = 0.1$, $CHCl_3$), IR (ATR) 3285, 2957, 1685, 1649, 1535 cm^{-1}; ^1H NMR (500 MHz, D_2O) (δ, ppm): 7.46–7.27 (m, 3H), 7.14 (s, 1H), 3.83 (d, 2H, $J = 12.9$ Hz), 3.68 (d, 2H, $J = 13.0$ Hz), 3.44–3.31 (m, 2H), 3.19 (dd, 2H, $J = 18.6, 8.9$ Hz), 3.13 (d, 2H, $J = 19.2$ Hz), 3.07 (d, 2H, $J = 5.9$ Hz), 2.74 (d, 4H, $J = 4.8$ Hz), 1.85 (dt, 2H, $J = 11.2, 5.6$ Hz), 0.83 (dd, 12H, $J = 14.6, 6.8$ Hz). ^{13}C NMR (126 MHz, D_2O) (δ, ppm): 178.3, 173.7, 136.1, 131.1, 129.7, 128.8, 71.5, 65.8, 57.3, 53.9, 50.9, 37.1, 31.0, 18.4, 17.8. HRMS (ESI-TOF)$^+$ Calcd for $C_{24}H_{39}N_5O_4$ (M + H^+) 462.3080. Found 462.3082 (M + H^+). Anal. calcd (%) for $C_{24}H_{39}N_5O_4 \cdot H_2O$: C, 60.1, H, 8.6, N, 14.6; found. C, 60.0, H, 8.6, N, 14.9.

Synthesis of 1. To a clear solution of compound **6** (10.0 g, 17.55 mmol) in dry tetrahydrofuran (THF), 10 mol% of the catalyst (5 wt% Pd on activated carbon) was added. The reaction mixture was stirred under an atmosphere of H_2 (H_2 balloon) at 50 °C for 4 h. The reaction was monitored by TLC, and after complete consumption of the starting material the catalyst was filtered off through a Celite® bed and washed with THF. The crude product was purified by column chromatography using $MeOH/CH_2Cl_2$ (1 : 15 : 0.01) as eluent. Evaporation of the solvent under vacuum yielded the white solid **1**. Yield 88% (4.69 g). ^1H NMR (300 MHz, $CDCl_3$) (δ, ppm): 7.50 (s, 2H), 3.34 (d, 4H, $J = 5.7$ Hz), 3.20 (d, 2H, $J = 3.6$ Hz), 2.76 (t, 4H, $J = 5.7$ Hz), 2.30–2.19 (m, 2H), 1.52 (s, 3H), 0.96 (d, 6H, $J = 6.9$ Hz), 0.82 (d, 6H, $J = 6.8$ Hz). ^{13}C NMR (75 MHz, $CDCl_3$) (δ, ppm): 174.7, 77.5, 77.0, 76.6, 60.4, 48.7, 38.8, 31.0, 19.7, 16.2; ESI-MS $m/z = 302.2$ (M + H^+). Anal. calcd (%) for $C_{14}H_{31}N_5O_2$: C, 55.8, H, 10.4, N, 23.3; found. C, 56.0, H, 10.5, N, 23.5.

Electromotive force measurements. The potentiometric titrations were carried out at 298.1 ± 0.1 K using NaCl 0.1 M as supporting electrolyte. The experimental procedure (burette, potentiometer, cell, stirrer, microcomputer, *etc.*) has been fully described elsewhere.[36] The acquisition of the emf data was performed with the computer program Crison Capture. The reference electrode was an Ag/AgCl electrode in saturated KCl solution. The glass electrode was calibrated as a hydrogen-ion concentration probe by titration of previously standardized amounts of HCl with CO_2-free NaOH solutions and the equivalent point determined by the Gran's method, which gives the standard potential, $E^{o\prime}$, and the ionic product of water [$pK_w = 13.78(1)$]. The computer program HYPERQUAD was used to

calculate the protonation and stability constants,[37] and the HySS program was used to obtain the distribution diagrams.[38] The pH range investigated was 2.0–12.0 and the concentration of the metal ions and of the ligands ranged from 1×10^{-3} to 5×10^{-3} M with Cu^{2+} : L molar ratios as 1 : 1. The different titration curves for each system (at least two) were treated either as a single set or as separated curves without significant variations in the values of the stability constants. Finally, the sets of data were merged together and treated simultaneously to give the final stability constants.

NMR measurements. The ^{1}H spectra were recorded on a Varian INOVA 500 spectrometer (500 and 125 MHz for ^{1}H and ^{13}C NMR, respectively). The solvent signal was used as a reference standard. Adjustments to the desired pH were made using drops of DCl or NaOD solutions. The pD was calculated from the measured pH values using the correlation, pH = pD − 0.4.[39]

Mass spectrometry. Mass spectra were recorded on a hybrid QTOF I (quadrupole-hexapole-TOF) mass spectrometer with an orthogonal Z-spray-electrospray interface (Micromass, Manchester, UK) either by electrospray positive mode (ES+) or by electrospray negative mode (ES−). The desolvation gas as well as nebulizing gas was nitrogen at a flow of 700 L h^{-1} and 20 L h^{-1} respectively. The temperature of the source block was set to 120 °C and the desolvation temperature to 150 °C. A capillary voltage of 3.5 and 3.3 KV was used in the positive and negative scan mode, respectively. The cone voltage was typically set to 20 V to control the extent of fragmentation of the identified ions. Sample solutions were infused *via* syringe pump directly connected to the ESI source at a flow rate of 10 mL min^{-1}. The observed isotopic pattern of each intermediate perfectly matched the theoretical isotopic pattern calculated from their elemental composition using the MassLynx 4.0 program.[40]

UV spectroscopy. UV-Vis absorption spectra were recorded in MeOH, in a Hewlett-Packard 8453 apparatus, using solutions (1×10^{-3} M) at different pH values containing 1 : 1 ligand to metal molar ratios. Additional experiments were carried in NaCl 0.1 M solutions. Only minimal differences were observed in this case.

IR spectroscopy. FTIR spectra were acquired on a JASCO 6200 instrument with a MIRacle single-reflection ATR diamond/ZnSe accessory. The raw IR spectral data were processed with the JASCO spectral manager software. Solutions (2×10^{-3} M) at different pH values containing 1 : 1 ligand to metal molar ratios were used for those experiments.

Acknowledgements

Financial support from the Spanish MINECO (CTQ2012-38543-C03-01), Generalitat Valenciana (PROMETEO/2012/020) and PPI-UJI (P1-1B-2013-38) is gratefully acknowledged. P. D. W. and L. G. thank GV for a Santiago Grisolía fellowship. The authors are grateful to the SCIC of the Universitat Jaume I for the spectroscopic facilities.

Notes and references

1 (*a*) Y. Lu, N. Yeung, N. Sieracki and N. M. Marshall, *Nature*, 2009, **460**, 855; (*b*) N. Mitic, S. J. Smith, A. Neves, L. W. Guddat, L. R. Gahan and G. Shenk, *Chem. Rev.*, 2006, **106**, 3338; (*c*) M. L. Zastrow and V. L. Pecoraro, *Coord. Chem. Rev.*, 2013, **257**, 2565; (*d*) J. Liu, S. Chakraborty, P. Hosseinzadeh, Y. Yu, S. Tian, I. Petrik, A. Bhagi and Y. Lu, *Chem. Rev.*, 2014, **114**, 4366.

2 (*a*) R. H. Holm, P. Kennepohl and I. Solomon, *Chem. Rev.*, 1996, **96**, 2239; (*b*) N. Kitajima and Y. Morooka, *Chem. Rev.*, 1994, **94**, 737; (*c*) E. A. Lewis and W. B. Tolman, *Chem. Rev.*, 2004, **104**, 1047; (*d*) J. Reedijk and E. Bouwman, *Bioinorganic Catalysis*, MarcelDekker, New York, 2nd edn, 1999; (*e*) K. D. Karlin, D.-H. Lee, V. Obias and K. J. Humphreys, *Pure Appl. Chem.*, 1998, **70**, 855; (*f*) E. I. Solomon, F. Tuczek, D. E. Root and C. A. Brown, *Chem. Rev.*, 1994, **94**, 827; (*g*) L. M. Mirica, X. Ottenwaelder and T. D. P. Stack, *Chem. Rev.*, 2004, **104**, 1013; (*h*) L. Q. Hatcher and K. D. Karlin, *Adv. Inorg. Chem.*, 2006, **58**, 131; (*i*) W. Kaim and B. Schwederski, *Bioanorganische Chemie, 3 Aufl*, B. G. Teuber, Stuttgart, Germany, 2004; (*j*) P. Haack and C. Limberg, *Angew. Chem., Int. Ed.*, 2014, **53**, 4282.

3 (*a*) F. E. Dodd, J. van Beeumen, R. R. Eady and S. S. Hasnain, *J. Mol. Biol.*, 1998, **282**, 369; (*b*) K. Paraskevopoulos, M. Sundararajan, R. Surendran, M. A. Hough, R. R. Eady, I. H. Hillier and S. S. Hasnain, *Dalton Trans.*, 2006, 3067; (*c*) A. C. Merkle and N. Lehnert, *Dalton Trans.*, 2012, 3355.

4 (*a*) J. L. Vanhooke, M. M. Benning, F. M. Raushel and H. M. Holden, *Biochemistry*, 1996, **35**, 6020; (*b*) M. M. Benning, H. Shim, F. M. Raushel and H. M. Holden, *Biochemistry*, 2001, **40**, 2712.

5 (*a*) N. Kitajima, K. Fujisawa and Y. Morooka, *J. Am. Chem. Soc.*, 1990, **112**, 3210; (*b*) R. C. Elder and M. C. Hill, *Inorg. Chem.*, 1979, **18**, 729.

6 (*a*) P. Comba, T. W. Hambley, M. A. Hitchman and H. Stratemeier, *Inorg. Chem.*, 1995, **34**, 3903; (*b*) B. J. Hathaway, *J. Chem. Soc., Dalton Trans.*, 1972, 1196; (*c*) B. J. Hathaway and D. E. Billing, *Coord. Chem. Rev.*, 1970, **5**, 143; (*d*) M. Kalanithi, M. Rajarajan, P. Tharmaraj and S. Johnson Raja, *Med. Chem. Res.*, 2015, **24**, 1578.

7 (*a*) P. Comba, A. M. Sargeson, L. M. Engelhardt, J. M. Harrowfield, A. H. White, E. Horn and M. R. Snow, *Inorg. Chem.*, 1985, **24**, 2325; (*b*) P. V. Bernhardt, R. Bramley, L. M. Engelhardt, J. M. Harrowfield, D. C. R. Hockless, B. R. Korybut- Daszkiewicz, E. R. Krausz, T. Morgan and A. M. Sargeson, *Inorg. Chem.*, 1995, **34**, 3589; (*c*) P. Comba, C. Haaf and H. Wadepohl, *Inorg. Chem.*, 2009, **48**, 6604; (*d*) I. Castillo, A. C. Neira, E. Nordlander and E. Zeglio, *Inorg. Chim. Acta*, 2014, **422**, 152; (*e*) A. Kaur, T. G. Ribelli, K. Schröder, K. Matyjaszewski and T. Pintauer, *Inorg. Chem.*, 2015, **54**, 1474.

8 (*a*) E. V. Rybak-Akimova, A. Y. Nazarenko, L. Chen, P. W. Krieger, A. M. Herrera, V. V. Tarasov and P. D. Robinson, *Inorg. Chim. Acta*, 2001, **324**, 1; (*b*) J. P. Schneider and J. W. Kelly, *J. Am. Chem. Soc.*, 1995, **117**, 2533; (*c*) R. Kannappan, S. Tanase, I. Mutikainen, U. Turpeinen and J. Reedijk, *Inorg. Chim. Acta*, 2005, **358**, 383; (*d*) M. R. Bryant, A. D. Burrows, C. M. Fitchett,

C. S. Hawes, S. O. Hunter, L. L. Keenan, D. J. Kelly, P. E. Kruger, M. F. Mahonb and C. Richardson, *Dalton Trans.*, 2015, 9269.

9 (*a*) S. R. Batten, B. F. Hoskins, B. Moubaraki, K. S. Murray and R. Robson, *Chem. Commun.*, 2000, 1095; (*b*) T. Osako, K. D. Karlin and S. Itoh, *Inorg. Chem.*, 2005, **44**, 410; (*c*) M. Meyer, L. Fremond, E. Espinosa, R. Guilard, Z. P. Ou and K. M. Kadish, *Inorg. Chem.*, 2004, **43**, 5572; (*d*) K. Miyoshi, H. Tanaka, E. Kimura, S. Tsuboyama, S. Murata, H. Shimizu and K. Ishizu, *Inorg. Chim. Acta*, 1983, **78**, 23; (*e*) R. M. Nunes, R. Delgado, M. F. Cabral, J. Costa, P. Brandao, V. Felix and B. J. Goodfellow, *Dalton Trans.*, 2007, 4536; (*f*) H. Nagao, N. Komeda, M. Mukaida, M. Suzuki and K. Tanaka, *Inorg. Chem.*, 1996, **35**, 6809; (*g*) E. J. Laskowski, D. M. Duggan and D. N. Hendrickson, *Inorg. Chem.*, 1975, **14**, 2449; (*h*) A. Algarra, M. G. Basallote, C. E. Castillo, M. Paz, A. Ferrer, E. García-España, J. M. Llinares, M. A. Máñez and C. Soriano, *Inorg. Chem.*, 2009, **48**, 902; (*i*) C. E. Castillo, A. G. Algarra, M. Á. Máñez, C. Duboc and M. G. Basallote, *Eur. J. Inorg. Chem.*, 2012, 2514; (*j*) L. Acosta-Rueda, E. Delgado-Pinar, J. Pitarch-Jarque, A. Rodríguez, S. Blasco, J. González, M. G. Basallote and E. García-España, *Dalton Trans.*, 2015, 8255; (*k*) J. Pitarch-Jarque, R. Belda, F. Lloret, J. Ferrando-Soria, P. Navarro, A. Lopera and E. García-España, *Dalton Trans.*, 2015, 3378.

10 A. G. Blackman, *Polyhedron*, 2005, **24**, 1.

11 (*a*) J.-M. Lehn, *Angew. Chem., Int. Ed.*, 1988, **27**, 89; (*b*) K. D. Karlin, *Science*, 1993, **261**, 701; (*c*) R. M. Roat-Malone, *Bioinorganic Chemistry: A Short Course*, John Wiley & Sons, Inc., Hoboken, NJ, 2nd edn, 2007; (*d*) I. Bertini, I. H. B. Gray, E. I. Stiefel and J. S. Valentine, *Biological Inorganic Chemistry, Structure and Reactivity*, University Science Books, Sausalito, CA, 2007; (*e*) R. Gramage-Doria, D. Armspach and D. Matt, *Coord. Chem. Rev.*, 2013, **257**, 776; (*f*) O. Bistri and O. Reinaud, *Org. Biomol. Chem.*, 2015, **13**, 2849.

12 (*a*) H. Miyake and Y. Kojima, *Coord. Chem. Rev.*, 1996, **148**, 301; (*b*) C. Bazzicalupi, A. Bianchi, E. García-España and E. Delgado-Pinar, *Inorg. Chim. Acta*, 2014, **417**, 3.

13 (*a*) F. Fache, E. Schulz, M. L. Tommasino and M. Lemaire, *Chem. Rev.*, 2000, **100**, 2159; (*b*) M. Hechavarría-Fonseca and B. König, *Adv. Synth. Catal.*, 2003, **345**, 1173; (*c*) J.-C. Kizirian, *Chem. Rev.*, 2008, **108**, 140; (*d*) J. S. Prell, T. G. Flick, J. Oomens, G. Berden and E. R. Williams, *J. Phys. Chem. A*, 2010, **114**, 854; (*e*) S. K. Burke, Y. Xu and D. W. Margerum, *Inorg. Chem.*, 2003, **42**, 5807; (*f*) B. J. Green, T. M. Tesfai and D. W. Margerum, *Inorg. Chem.*, 2004, **43**, 1463; (*g*) B. J. Green, T. M. Tesfai and D. W. Margerum, *Dalton Trans.*, 2004, 3508; (*h*) T. M. Tesfai, B. J. Green and D. W. Margerum, *Inorg. Chem.*, 2004, **43**, 6726; (*i*) V. N. Dokorou, C. J. Milios, A. C. Tsipis, M. Haukka, P. G. Weidler, A. K. Powella and G. E. Kostakis, *Dalton Trans.*, 2012, 12501; (*j*) C. R. Dennis, J. C. Swarts and D. W. Margerum, *Reac. Kinet. Mech. Cat.*, 2012, **107**, 27; (*k*) J. Dong, Y. Wang, Q. Xiang, X. Lv, W. Weng and Q. Zeng, *Adv. Synth. Catal.*, 2013, **355**, 692.

14 (*a*) S. E. Gibson and C. Lecci, *Angew. Chem., Int. Ed.*, 2006, **45**, 1364; (*b*) J. F. Billing and U. J. Nilsson, *J. Org. Chem.*, 2005, **70**, 4847; (*c*) S. Punna, J. Kuzelka, Q. Wang and M. G. Finn, *Angew. Chem., Int. Ed.*, 2005, **44**, 2215; (*d*) P. P. Cristau, M.-T. Martin, M.-E. Tran Hu Dau, J.-P. Vors and J. Zhu, *Org. Lett.*, 2004, **6**, 3183; (*e*) J. E. Redman, K. M. Wilcoxen and M. R. Ghadiri, *J. Comb. Chem.*, 2003, **5**, 33; (*f*) E. Locardi, M. Stöckle, S. Garner and H. Kessler, *J. Am. Chem. Soc.*, 2001, **123**, 8189; (*g*) C. J. White and A. K. Yudin, *Nat. Chem.*, 2011, **3**, 509; (*h*) S. E. Gibson and C. Lecci, *Angew. Chem., Int. Ed.*, 2006, **45**, 1364; (*i*) B. Lewandowski, G. De Bo, J. W. Ward, M. Papmeyer, S. Kuschel, M. J. Aldegunde, P. M. E. Gramlich, D. Heckmann, S. M. Goldup, D. M. D'Souza, A. E. Fernandes and D. A. Leigh, *Science*, 2013, **339**, 189.

15 (*a*) S. Fernández-López, H.-S. Kim, E. C. Choi, M. Delgado, J. R. Granja, A. Khasanov, K. Kraehenbuehl, G. Long, D. A. Weinberger, K. M. Wilcoxen and M. R. Ghadiri, *Nature*, 2001, **412**, 452; (*b*) S. Kubik, *Chem. Soc. Rev.*, 2009, **38**, 585; (*c*) A. V. Gulevich, L. S. Koroleva, O. V. Morozova, V. N. Bakhvalova, V. N. Silnikov and V. G. Nenajdenko, *J. Org. Chem.*, 2011, **7**, 1135; (*d*) K. Klemm, M. R. Stojkovic, G. Horvat, V. Tomisic, I. Piantanida and C. Schmuck, *Chem.–Eur. J.*, 2012, **18**, 1352; (*e*) W.-C. Lin, Y.-P. Tseng, C.-Y. Lin and Y.-P. Ye, *Org. Biomol. Chem.*, 2011, **9**, 5547.

16 (*a*) W. A. Loughlin, J. D. A. Tyndall, M. P. Glenn and D. P. Fairlie, *Chem. Rev.*, 2004, **104**, 6085; (*b*) R. C. Reid, L. K. Pattenden, J. D. A. Tyndall, J. L. Martin, T. Walsh and D. P. Fairlie, *J. Med. Chem.*, 2004, **47**, 1641; (*c*) R. C. Reid, G. Abbenante, S. M. Taylor and D. P. Fairlie, *J. Org. Chem.*, 2003, **68**, 4464; (*d*) X. Hu, K. T. Nguyen, C. L. M. J. Verlinde, W. G. J. Hol and D. Pei, *J. Med. Chem.*, 2003, **46**, 3771; (*e*) P. T. Lansbury and H. A. Lashuel, *Nature*, 2006, **443**, 774; (*f*) G. A. Silva, C. Czeisler, K. L. Niece., E. Beniash, D. A. Harrington, J. A. Kessler and S. I. Stupp, *Science*, 2004, **303**, 1352.

17 (*a*) For some examples on related systems: K. Choi and A. D. Hamilton, *Coord. Chem. Rev.*, 2003, **240**, 101; (*b*) K. Choi and A. D. Hamilton, *J. Am. Chem. Soc.*, 2003, **125**, 10241; (*c*) K. Choi and A. D. Hamilton, *J. Am. Chem. Soc.*, 2001, **123**, 2456; (*d*) L. Somogyi, G. Haberhauer and J. Rebek, *Tetrahedron*, 2001, **57**, 1699; (*e*) M. M. Conn and J. Rebek, *Chem. Rev.*, 1997, **97**, 1647; (*f*) R. J. Brea, C. Reiriz and J. R. Granja, *Chem. Soc. Rev.*, 2010, **39**, 1448; (*g*) Y.-D. Wu and S. Gellman, *Acc. Chem. Res.*, 2008, **41**, 1231; (*h*) J. S. Nowick, *Acc. Chem. Res.*, 2008, **41**, 1319; (*i*) D. Ke, C. Zhan, A. D. Q Li and J. Yao, *Angew. Chem., Int. Ed.*, 2011, **50**, 3715; (*j*) M. Suzuki and K. Hanabusa, *Chem. Soc. Rev.*, 2009, **38**, 967; (*k*) D. Das, S. Maiti, S. Brahmachari and P. K. Das, *Soft Matter*, 2011, **7**, 7291.

18 (*a*) A. Arbaoui, C. Redshaw, N. M. Sanchez-Ballester, M. R. J. Elsegood and D. L. Hughes, *Inorg. Chim. Acta*, 2011, **365**, 96; (*b*) M. Merschky and C. Schmuck, *Org. Biomol. Chem.*, 2009, **7**, 4895; (*c*) L. Weselinki, E. Szyk and J. Jurczak, *Tetrahedron Lett.*, 2011, **52**, 381; (*d*) J. Paradowska, M. Pasternak, B. Gut, B. Gryzzo and J. Mlynarski, *J. Org. Chem.*, 2012, **77**, 173; (*e*) F. Adrian,

M. I. Burguete, J. M. Fraile, J. I. García, E. García-España, S. V. Luis, J. A. Mayoral and A. J. Royo, *Eur. J. Inorg. Chem.*, 1999, 2347.

19 S. V. Luis and I. Alfonso, *Acc. Chem. Res.*, 2014, **47**, 112.

20 (*a*) F. Galindo, J. Becerril, M. I. Burguete, S. V. Luis and L. Vigara, *Tetrahedron Lett.*, 2004, **45**, 1659; (*b*) B. Altava, M. I. Burguete, N. Carbó, J. Escorihuela and S. V. Luis, *Tetrahedron: Asymmetry*, 2010, **21**, 982.

21 (*a*) I. Alfonso, M. I. Burguete, F. Galindo, S. V. Luis and L. Vigara, *J. Org. Chem.*, 2009, **74**, 6130; (*b*) S. V. Luis, F. Galindo, M. I. Burguete and L. Vigara, *J. Photochem. Photobiol., A*, 2010, **209**, 61; (*c*) B. Altava, M. I. Burguete, N. Carbó, S. V. Luis, V. Martí and C. Vicent, *Tetrahedron Lett.*, 2013, **54**, 72; (*d*) V. Martí-Centelles, M. A. Izquierdo, M. I. Burguete, F. Galindo and S. V. Luis, *Chem.–Eur. J.*, 2014, **20**, 7465; (*e*) E. Faggi, A. Moure, M. Bolte, C. Vicent, S. V. Luis and I. Alfonso, *J. Org. Chem.*, 2014, **79**, 4590.

22 (*a*) J. Becerril, B. Escuder, R. Gavara, S. V. Luis and J. F. Miravet, *Eur. J. Org. Chem.*, 2005, 481; (*b*) I. Alfonso, M. Bru, M. I. Burguete, E. García-Verdugo and S. V. Luis, *Chem.–Eur. J.*, 2010, **16**, 1246; (*c*) J. Rubio, I. Alfonso, M. I. Burguete and S. V. Luis, *Soft Matter*, 2011, **7**, 10737; (*d*) J. Rubio, I. Alfonso, M. I. Burguete and S. V. Luis, *Chem. Commun.*, 2012, **48**, 2210; (*e*) J. Rubio, V. Martí-Centelles, M. I. Burguete and S. V. Luis, *Tetrahedron*, 2013, **69**, 2302.

23 (*a*) I. Alfonso, M. I. Burguete and S. V. Luis, *J. Org. Chem.*, 2006, **71**, 2242; (*b*) I. Alfonso, M. I. Burguete, F. Galindo, S. V. Luis and L. Vigara, *J. Org. Chem.*, 2007, **72**, 7947; (*c*) E. Faggi, S. V. Luis and I. Alfonso, *RSC Adv.*, 2013, **3**, 11556.

24 (*a*) S. Blasco, M. I. Burguete, M. P. Clares, E. García-España, J. Escorihuela and S. V. Luis, *Inorg. Chem.*, 2010, **490**, 7841; (*b*) I. Martí, A. Ferrer, J. Escorihuela, M. I. Burguete and S. V. Luis, *Dalton Trans.*, 2012, **41**, 6764.

25 (*a*) J. Becerril, M. Bolte, M. I. Burguete, F. Galindo, E. García-España, S. V. Luis and J. F. Miravet, *J. Am. Chem. Soc.*, 2003, **125**, 6677; (*b*) S. Blasco, M. I. Burguete, M. P. Clares, E. García-España, J. Escorihuela and S. V. Luis, *Inorg. Chem.*, 2010, **49**, 7841; (*c*) I. Martí, A. Ferrer, J. Escorihuela, M. I. Burguete and S. V. Luis, *Dalton Trans.*, 2012, 6764.

26 P. D. Wadhavane, M. A. Izquierdo, D. Lutters, M. I. Burguete, M. J. Marin, D. A. Russell, F. Galindo and S. V. Luis, *Org. Biomol. Chem.*, 2014, **12**, 823.

27 P. Paoletti, *Pure Appl. Chem.*, 1984, **56**, 491.

28 (*a*) B. Altava, M. I. Burguete, S. V. Luis, J. F. Miravet, E. García-España, V. Marcelino and C. Soriano, *Tetrahedron*, 1997, **53**, 4751; (*b*) S. Andrés, B. Escuder, A. Domènech, E. García-España, S. V. Luis, V. Marcelino, J. M. Llinares, J. A. Ramírez and C. Soriano, *J. Phys. Org. Chem.*, 2001, **14**, 495.

29 (*a*) F. Rosu, E. de Pauw and V. Gabelica, *Biochimie*, 2008, **90**, 1074; (*b*) E. B. Erba, K. Barylyuk, Y. Yang and R. Zenobi, *Anal. Chem.*, 2011, **83**, 9251; (*c*) L. Cera and C. A. Schalley, *Chem. Soc. Rev.*, 2014, **43**, 1800.

30 (*a*) K. Schug, P. Fryčák, N. M. Maier and W. Lindner, *Anal. Chem.*, 2005, **77**, 3660; (*b*) A. Di Tullio, S. Reale and F. J. De Angelis, *Mass Spectrom.*, 2005, **40**, 845; (*c*) T. Becherer, D. Meshcheryakov, A. Springer, V. Böhmerb and C. A. Schalley, *J. Mass Spectrom.*, 2009, **44**, 1338; (*d*) W. Jiang, A. Schäfer, P. C. Mohr and C. A. Schalley, *J. Am. Chem. Soc.*, 2010, **132**, 2309; (*e*) V. Lemaur, G. Carroy, F. Poussigue, F. Chirot, J. de Winter, L. Isaacs, P. Dugourd, J. Cornil and P. Gerbaux, *ChemPlusChem*, 2013, **78**, 959; (*f*) D. Cubrilovic, W. Haap, K. Barylyuk, A. Ruf, M. Badertscher, M. Gubler, T. Tetaz, C. Joseph, J. Benz and R. Zenobi, *ACS Chem. Biol.*, 2014, **9**, 218.

31 (*a*) T. R. Wagler, Y. Fang and C. J. Burrows, *J. Org. Chem.*, 1989, **54**, 1584; (*b*) B. Dangel, M. Clarke, J. Haley, D. Sames and R. Polt, *J. Am. Chem. Soc.*, 1997, **119**, 10865; (*c*) C. L. Weeks, P. Turner, R. R. Fenton and P. A. Lay, *J. Chem. Soc., Dalton Trans.*, 2002, 931; (*d*) M. I. Burguete, F. Galindo, S. V. Luis and L. Vigara, *Dalton Trans.*, 2007, 4027; (*e*) J. Singh, G. Hundal and R. Gupta, *Eur. J. Inorg. Chem.*, 2008, 2052; (*f*) R. Shakya, A. Jozwiuk, D. R. Powell and R. P. Houser, *Inorg. Chem.*, 2009, **48**, 4083.

32 (*a*) R. Polt, B. D. Kelly, B. D. Dangel, U. B. Tadikonda, R. E. Ross, A. M. Raitsimring and A. V. Astashkin, *Inorg. Chem.*, 2003, **42**, 566; (*b*) S. Autzen, H.-G. Korth, R. Boese, H. de Groot and R. Sustmann, *Eur. J. Inorg. Chem.*, 2003, 1401.

33 G. A. McLachlan, G. D. Fallon, R. L. Martin and L. Spiccia, *Inorg. Chem.*, 1995, **34**, 254.

34 E. C. Constable, C. E. Housecroft, J. R. Price and J. A. Zampese, *CrystEngComm*, 2010, **12**, 3163.

35 E. García-España and S. V. Luis, *Supramol. Chem.*, 1996, **6**, 257.

36 (*a*) E. García-España, M.-J. Ballester, F. Lloret, J. M. Moratal, J. Faus and A. Bianchi, *J. Chem. Soc., Dalton Trans.*, 1988, 101; (*b*) M. I. Burguete, E. García-España, L. López-Diago, S. V. Luis, J. F. Miravet and D. Sroczynski, *Org. Biomol. Chem.*, 2007, **5**, 1935.

37 P. Gans, A. Sabatini and A. Vacca, *Talanta*, 1996, **43**, 1739.

38 L. Alderighi, P. Gans, A. Ienco, D. Peters and A. Vacca, *Coord. Chem. Rev.*, 1999, **184**, 311.

39 (*a*) P. K. Glasoe and F. A. Long, *J. Phys. Chem.*, 1960, **64**, 188; (*b*) A. K. Covington, M. Paabo, R. A. Robinson and R. G. Bates, *Anal. Chem.*, 1968, **40**, 700.

40 (*a*) *MassLynx Software, version 4.0*; (*b*) S. Moco, R. J. Bino, O. Vorst, H. a. Verhoeven, J. de Groot, T. A. van Beek, J. Vervoot and R. C. H. de Vos, *Plant Physiolgy*, 2006, **41**, 1205.

Chapter VII

Self-Assembly of pseudopeptidic systems

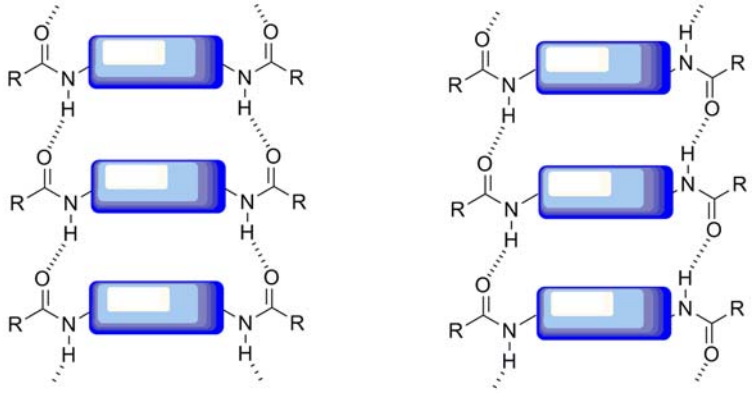

Manuscript to be submitted in CrystEngComm

Journal Name

ARTICLE

Self-Assembly of pseudopeptidic systems

Lingaraju Gorla, Vicente Martí-Centelles, Belén Altava,* M. Isabel Burguete and Santiago V. Luis*

Received 00th January 20xx,
Accepted 00th January 20xx

DOI: 10.1039/x0xx00000x

www.rsc.org/

Pseudopeptidic compounds have shown that in some instances can provide some interesting patterns in their self-assembling on solid and solution state. We have studied here in the crystalline state, the assembling pattern of these systems. We showed particular trends in their conformation and packing as a function of the spacer and the amino acid residue.

Introduction

Self-assembly is a common phenomenon mediated by intermolecular interactions through hydrogen bonding, electrostatic force, hydrophobic interaction and π-π stacking interaction.[1] The resulted superstructures could exhibit distinct physicochemical properties from their single molecular components and extend their applications in many fields, especially for the drug delivery and biomedical engineering.[2]

Nature uses a limited number of structural units for constructing complex systems being amino acids one such basic element. These systems spontaneously arrange into functional forms or morphologies. These forms are ubiquitous for different molecular processes which they control precisely over the time and length scales required.[3] The presence of hydrophilic and hydrophobic regions of a typical peptide molecule provides a local domain by which weak, non-covalent interactions[4,5,6] facilitate molecular self-assembly in such a delicate manner that the balance between these interactions can largely influence the morphology of the resulting nanostructures.[7] Thus, the generation of a precise functional structure usually requires large individual macromolecules, for which, however, the activity can be associated with a small specific peptidic fragment. Thus, the building of small model compounds has been used for the understanding of the structural parameters and factors determining the properties of interest in proteins and peptides.[8]

Ideally, however, the combination of natural and non-natural components, properly designed using the knowledge gathered from natural systems, could achieve the desired functionality with low molecular weight molecules. In this regard, our group has synthesized and study minimalist pseudopeptides containing the general structure I (Fig. 1).[9] These compounds can be prepared very efficiently in three steps (*ca.* 80% overall yields) starting from commercially available *N*-Cbz protected amino acids through the initial formation of their activated *N*-hydroxysuccinimide esters, coupling with a variety of diamines, *N*-deprotection, and final *N*-substitution.[10] C_2-open chain pseudopeptides I can be used as building blocks for the construction of macrocyclic structures II and III.[11]

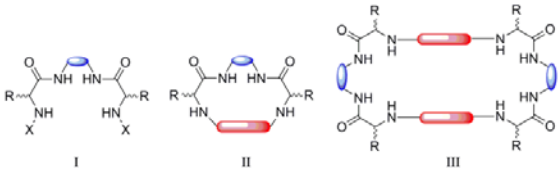

Fig. 1 General structure of pseudopeptides.

Despite the simplicity of C_2-pseudopeptides, changing the spacer, changing the amino acid (R), or functionalizing the amino terminal groups (X) provides a high level of molecular diversity and sites for supramolecular interactions. Amine and amide functionalities allow for electrostatic and H-bonding interactions, while the spacer, the side chains, and groups attached to the amino functions can be involved in hydrophobic and π-π interactions or in introducing additional functionalities.[12] We studied the self-assembly behaviour of some of these systems in solid a solution state,Some of these systems obtained, were able to display organogelating properties, [13] selective receptors for substrates of biological relevance,[14] as minimalistic molecular machines,[15] acting as '*in vivo*' fluorescent pH probes,[16] and as ligands for the preparation of chiral solvating agents or as enantioselective catalysts.[17,14b]

Departamento de Química Inorgánica y Orgánica, Universitat Jaume I, Av. de Vicent Sos Baynat, s/n 12071, Castellón, Spain, E-mail: luiss@uji.es; Tel: +34 964728239; Fax: +34 964728214

Electronic Supplementary Information (ESI) available: [details of any supplementary information available should be included here]. See DOI: 10.1039/x0xx00000x

Despite we studied previously the behavior of the architecture of some of these systems on solid and solution state,[18] in order to gain more information on the nature of the intermolecular interactions in the network formed, we attempted here to obtain crystals suitable for X-ray diffraction studies of open C_2-pseudopeptidic compounds derived from *L*-valine and *L*-phenyl alanine and study the role of the amino acid residue, the length and nature of the spacer and the *N*-substitution in the self-assembly of these systems. Preliminary results obtained have shown that in some instances this kind of pseudopeptidic compounds can provide some interesting patterns in their self-assembling in crystalline structure.[18]

Herein we have analysed in detail the assembling pattern in crystal structure for C_2-open chain pseudopeptidic compounds displayed in fig. 2.The crystal structures of compounds **1a, 1b, 2a**, **3a,** and **6a,** have been described previously.[18] Here, we got single crystals suitable for X-ray crystallography for compounds **3b, 4a, 4b, 5b** and **7a, 7b**, by slow vapor diffusion of the compounds in Toluene or DCM solution.

Results and discussion

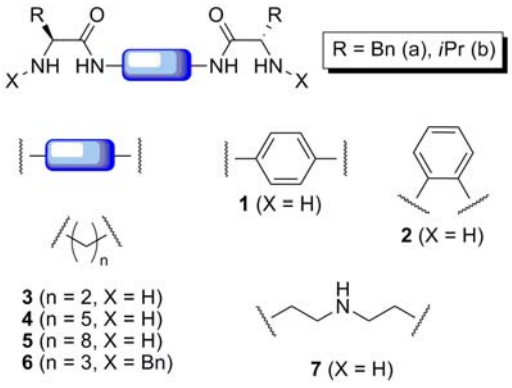

Fig. 2 Pseudopeptidic compounds used in this study (For the syntheses of these compounds see references 10, 13 and 18).

For C_2-pseudopeptidic compounds containing only two methylene groups in the aliphatic spacer **3a** and **3b** (n=2), fig. 3a show the molecular structure of compound **3b** derived from *L*-Val, the molecule presents an extended conformation with the two amide groups oriented in *anti* disposition in two planes displaying 5° and with {N(1)–C(4)–C(3)–O(1)} and {N(4)–C(9)–C(8)–O(2)} torsion angles of *ca.* 53° and 65°. Moreover, the unit cell is defined by two molecules of **3b** and four water molecules in which the two **3b** molecules are able to interact each other through hydrogen bonds involving two water molecules, thus, each water molecule acts as hydrogen bond donor with the nitrogen atom of the NH_2 group (N----H distances 1.994 and 2.115 Å) (Fig. S1, ESI). The three-dimensional structure is stabilized by intermolecular hydrogen bonds involving the NH amide and carbonyl groups (average NH---O distances 2.813 Å). On the contrary very different pattern was observed for compound **3a**, containing phenylalanine as side chain which solid state has been described previously.[18a] Compound **3a** presented a folding conformation with amide planes angle of 26° and aromatic rings pointed in opposite directions (Fig. 3b). The self-assembled structure is stabilized through hydrogen bond interactions between one hydrogen of the amino groups and the oxygen of the carbonyl groups (N---O 3.069 Å) and the aromatic side chains are able to form π-electronic channels (Fig. S2, ESI).[18a]

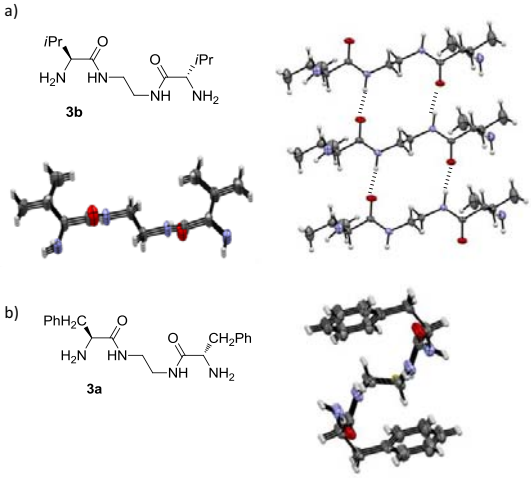

Fig. 3 (a) Molecular structure of **3b** and packing showing amide-amide hydrogen bonds. (b) Molecular structure of **3a**.

In the case of C_2-open chain, pseudopeptidic compounds with longer aliphatic spacer **4a** and **4b** (n=5), the molecular structure and crystal packing for these compounds are shown in fig. 4 and 5 respectively**.** For **4a,** the molecule shows an almost extended conformation with amide groups oriented in *anti* disposition with almost perpendicular planes (88°). Aromatic phenylalanine rings are oriented toward the cavity defined by the molecular folding, able to interact through the edge to face π-π intramolecular interactions (centroid—Har distance 3.061 Å). All the amide groups display the expected almost perfect *anti*-coplanar arrangement with O-C-N-H torsion angles between 179º and 178º. The crystal lattice is formed by four molecules with the amine groups oriented outside the folding able to interact with each other through hydrogen bonds displaying a distorted square arrangement (N---H distances 2.559 and 2.718 Å). The intermolecular polar amide-amide interactions through carbonyl and amide NH groups lead to the stabilization of the three-dimensional structure observed in the crystal packing with average N---O distances 2.917 Å.

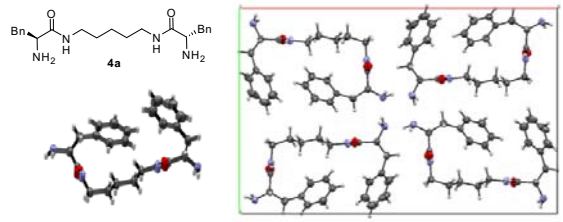

Fig. 4 Molecular structure of **4a** and crystal packing (c plane).

However, the analogous compound derived from *L*-Val **4b** (Fig. 5), shows an extended conformation with amide groups oriented in *syn* disposition with two planes of 78° and with {N(1)–C(7)–C(6)–O(1)}{N(4)–C(12)–C(11)–O(2)} torsion angles of *ca.* 53° and 65°. The crystal packing is stabilized by hydrogen bonds between the hydrogen atom of the amide and the oxygen of the carbonyl groups with average N---O distances of 2.841 Å and by hydrogen bonds between one hydrogen atom of the amine group and the oxygen of the carbonyl groups with average NH---O distances of 2.323 Å (Fig. S3, ESI). A detailed study of diffraction data showed the presence of some residual electron density that must be attributed to solvent molecules. Unfortunately, these solvent molecules are heavily disordered and, as a result of that, no valid model could be found. Therefore, the contribution of the solvent to the diffraction data was suppressed. Those solvent molecules could contribute to stabilizing the three-dimensional structure.

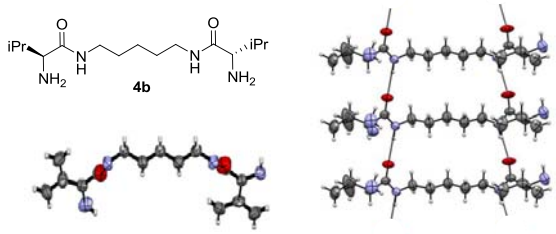

Fig. 5 (a) Molecular structure of **4b** and self-assembly showing amide-amide hydrogen bonds.

For pseudopeptidic compound **5b** derived from *L*-Val containing eight methylene groups in the aliphatic spacer, the extended molecular structure is shown in fig. 6. The amide groups are oriented in *anti* position with two planes of 26° and {N(1)–C(10)–C(9)–O(1)} {N(4)–C(15)–C(14)–O(2)} torsion angles of *ca.* 51° and 59°. The amide groups display the expected almost perfect *anti*-coplanar arrangement with O-C-N-H torsion angles between 180º and 177º leading the participation of the oxygen atoms of the carbonyl groups in the formation of an extensive network of intermolecular hydrogen bonding (average N---O distances of 2.847 Å). The water molecules play a key role in defining the intermolecular interactions leading to the stabilization of the three-dimensional structure observed in the crystal packing. Each water molecule acts as hydrogen bond donor with the nitrogen atom of the NH_2 group (Fig. S4, ESI).

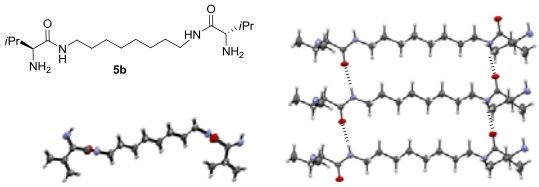

Fig. 6 (a) Molecular structure of **5b** and packing showing amide-amide hydrogen bonds.

In the case of C_2-pseudopeptidic compounds containing an amine group in the aliphatic spacer **7a** and **7b**, the molecular structure and packing obtained are displayed in fig. 7 and 8.

Compound **7a** presented an almost extended conformation with amide groups oriented in *anti* disposition with almost perpendicular planes (85°) and {N(1)–C(6)–C(5)–O(1)} {N(5)–C(15)–C(14)–O(2)} torsion angles of *ca.* 60° and 65° (Fig. 7). Aromatic Phe rings are oriented toward the cavity defined by the molecular folding able to interact through the edge to face π-π intramolecular interactions (aromatic centroid—Har distance of 2.972 Å), this folding conformation is analogous to the one observed for **4a**. The primary amine groups are oriented in opposite directions outside the folding able to interact through intermolecular hydrogen bonds while the central NH is oriented inside the cleft unable to participate in intermolecular hydrogen bonds. The three-dimensional structure is stabilized by the polar intermolecular hydrogen bonds between the hydrogen atom of amide groups and the oxygen of the carbonyl group (N---O average distances 2.902 Å) and the intermolecular hydrogen bonds involving four amine groups from four different molecules (N---H distances 2.583, 2.409, 2.657, and 2.660 Å) lead to stabilized the 3D structure. Finally, the self-assembled structure is also stabilized by π-π interactions involving aromatic side chains with Har---Har distances of 2.400 Å (Fig. S5, ESI).

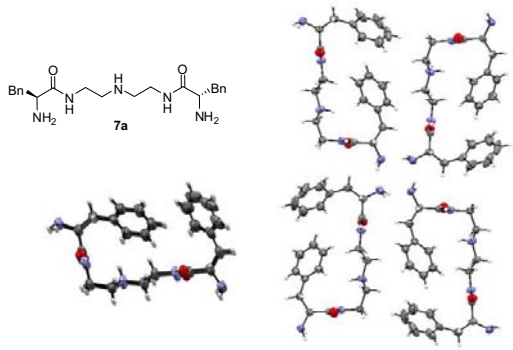

Fig. 7 (a) Molecular structure of **7a**. (b) Crystal packing stabilized by amine amine hydrogen bonds.

On the contrary different pattern again was observed for compound **7b**, containing valine as a side chain. Bis(amino amide) **7b** showed an extended conformation with amide groups oriented in *syn* disposition with plane angles of 79º and {N(5)–C(11)–C(10)–O(2)} and {N(1)–C(6)–C(5)–O(1)} torsion angles of *ca.* 53° and 52° (fig. 8). All the amide groups display the expected almost perfect *anti*-coplanar arrangement with O-C-N-H torsion angles between 177º and 178º. The crystal lattice is formed by four molecules of **7b** and six molecules of water. The network is stabilized by hydrogen bonds involving the oxygen atoms of the carbonyl groups and the hydrogen atom of the amide groups (average N---O distances of 2,827 Å). The water molecules play a key role in defining the intermolecular interactions leading to the stabilization of the three-dimensional structure observed in the crystal packing. Thus, each water molecule acts as hydrogen bond donor with the nitrogen atom of the NH_2 and the central NH atom (Fig. S6, ESI).

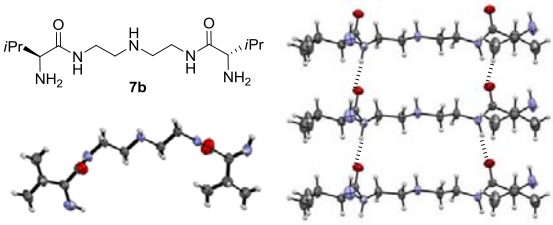

Fig. 8 (a) Molecular structure of **7b**. (b) Packing showing amide-amide hydrogen bonds.

In general, as has been observed in all the solid structures obtained, the H-bonds induce a global parallel disposition of the molecules with amide groups located in *anti* or *syn* disposition (Fig. 9).

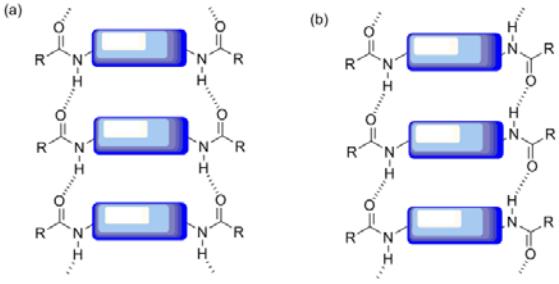

Fig. 9 Schematic representation of the packing observed in the solid state structures of the pseudopeptidic systems: (a) parallel, (b) antiparallel.

Thus, within this context, for pseudopeptidic compound with aliphatic spacers (**3**, **4**, **5**, and **7**) the results obtained suggest the formation of very different patterns as a function of the length of the spacer and the nature of the aminoacid residue. Thus, for *L*-Val derivatives containing an even number of atoms in the central spacer (**3b** and **5b**) the amide groups were oriented in *anti* disposition while the analogous compounds containing an odd number of atoms (**4b** and **7b**) the amide groups were oriented in *syn* disposition. However, the opposite behaviour was observed for *L*-Phe pseudopeptidic derivatives (**3a**, **4a**, and **7a**), for the compound with even number of atoms in the central spacer (**3a**) the amide groups were oriented in *syn* disposition (same behaviour was observed for *L*-Phe pseudopeptidic compound with 4 methylene groups n=4, not discussed here because of the disorder present for some atoms of the aliphatic spacer (Fig. S9, ESI)),[18a] while for compounds **4a** and **7a** (odd number of atoms in the central spacer) the amide groups were oriented in *anti* disposition (Fig. 10).

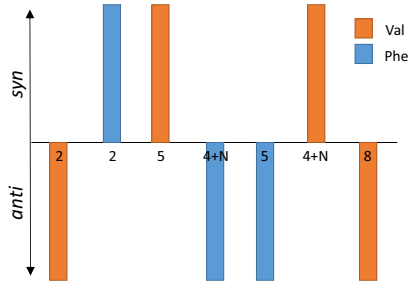

Fig. 10 Plot for parallel and antiparallel pseudopeptidic structures against the number of atoms of the central aliphatic spacer.

Regarding intermolecular amide-amide H-bond distances, the hydrogen bond distances for *L*-Phe derivatives are larger than for the *L*-Val analogous, this behaviour can be ascribed to the folding conformation observed for phenylalanine systems considered here **4a**, **7a**.[19] Moreover, for pseudopeptidic compound **3a** derived from *L*-phenylalanine and n=2, no intermolecular amide-

amide hydrogen bond is observed. By another side, as longer is the aliphatic spacer, larger is the amide-amide N---O distances following the order **3b < 7b < 4b < 5b** for valine derivatives.

As we mention above bis(amino amides) derived from phenylalanine **4a** and **7a** shown a folding conformation with π-π intramolecular interactions involving the two aromatic phenylalanine rings, although *L*-phenylalanine pseudopeptidic compound containing four methylene groups in the aliphatic spacer presented an extended conformation in solid state (Fig. S9, ESI),[18a] this can be ascribed to the length of spacer which in the last case is unable to adopt the folding conformation with favorable intramolecular π-π interactions. However, all the compounds derived from *L*-Val with aliphatic spacer presented an extended conformation that seems to assemble into a β–sheet-like structure.[20]

In the case of C_2-open chain pseudopeptidic compounds containing *p*-substituted aromatic spacer **1a** and **1b**, regarding the role of the nature of the amino acid residue, again different behaviour was observed related to the orientation of the amide groups when valine or phenylalanine was involved as has been discussed previously.[18b] Both compounds presented an extended conformation, although differences in the conformation of the two amide units were observed and associated with the different packing motif observed (i.e. differing intermolecular and intermolecular interactions involving NH_2 groups). (Fig. S7, ESI).

For pseudopeptidic compound **2a**, derived from *L*-Phe containing an *o*-substituted aromatic spacer, four independent molecules participate in the asymmetric unit and the presence of the aromatic central unit preorganizes the molecules in U-shape conformations, as has been described previously.[18d] In all independent molecules amide N-H fragments are oriented toward the cavity defined by the molecular cleft facilitating the formation of the extensive networks by intermolecular hydrogen bonding involving the oxygen atoms of the carbonyl groups (Fig. S8, ESI).[21]

Regarding the substitution on the aromatic central spacer for compound **2a,** the four independent molecules presented a U-shape conformation as was mention before while the two independent molecules of **1a** presented an extended conformation.

Finally, for *N,N'*-substituted C_2-open chain pseudopeptidic compound containing three methylene groups in the aliphatic spacer, compound **6a** displayed an almost extended conformation with one phenylalanine aromatic ring in a folding conformation. The intermolecular H-bonds induce a global parallel disposition of the molecules with carbonyl groups from amides located in *anti* position, pointing to the opposite direction.[18c] On the contrary, a different pattern was observed for the analogous compound with two methylene groups in the aliphatic spacer displaying carbonyl groups from amides located in *syn* position and both aromatic Phe rings in opposite directions.[22]

Finally, when plotting the occurrence of the observed N---O intermolecular distances considering compounds **1-7**, (Fig. 11), we obtained a distribution with a maximum at 2..85 Å, which is within the range of the natural peptides. Nevertheless as we mention above N---O distances are shorter for pseudopeptidic compounds derived from *L*-Val with aliphatic central spacer suggesting a stronger interaction in their supramolecular network, although for pseudopeptidic compounds with aromatic central spacer different behaviour is observed (Fig. 11 inset).

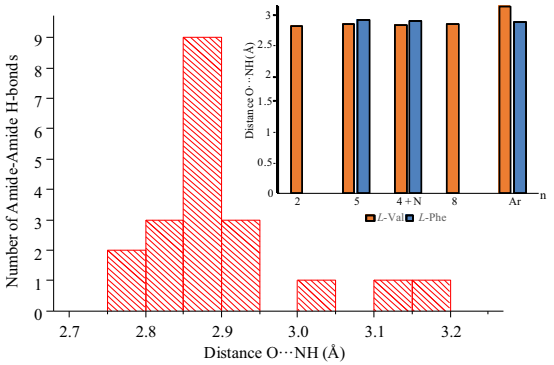

Fig. 11 Histogram of the amide bond distances found in the crystal packing of the pseudopeptidic compounds **1-7** (Fig. 11 inset, O—NH distances against the number of carbons (n) for **3, 5, 7** and (Ar) for **1**.

Conclusions

We have studied the role of the amino acid residue, the length, and nature of the spacer and the *N*-substitution in the self-assembly of open C_2-pseudopeptidic compounds derived from *L*-Val and *L*-Phe in the solid state. All systems preferred extended conformations and regarding aminoacid residue, different behaviour was observed related to the conformation when valine or phenylalanine was involved associated with the different packing motif observed. All *L*-Val pseudopeptidic compounds assembled into a β-sheet-like structure stabilized by polar intermolecular interactions while *L*-Phe pseudopeptidic compounds lead to display folding conformation of the side chain. For the pseudopeptidic compound with aliphatic spacers (**3**, **4**, **5**, and **7**) very different patterns as a function of the number of methylene groups of the spacer was observed associated with the different packing motif observed, thus, *L*-Phe compounds with enough length in the aliphatic spacer a folding conformation of the side chain was preferred stabilized by π–π intramolecular interactions. Overall, this study demonstrates that C_2-pseudopeptidic compounds showed

particular trends as a function of the spacer and amino acid residue.

Experimental

Crystallography

Single crystals suitable for X-ray crystallography were obtained by slow vapor diffusion of the compounds in Toluene or DCM solution. A suitable crystal was selected and mounted on a SuperNova, Dual, Cu at zero, Atlas diffractometer. Using Olex2,[23] the structure was solved with the ShelXS 2014[24] structure solution program using Direct Methods and refined with the ShelXL[24] refinement package using Least Squares minimization. The program MERCURY[25] was used to prepare artwork representations.

Acknowledgment

This research work was supported by the Spanish MINECO (CTQ2015-68429-R), Generalitat Valenciana (PROMETEO/2012/020) and PPI-UJI (P1-1B-2013-38). L.G thanks, Generalitat Valenciana for a Santiago Grisolia fellowship (GRISOLIA 2012/015). The support of the SCIC for the X-ray crystallographic measurements at Universitat Jaume I is acknowledged.

Notes and references

[1] (a) S. E. Paramonov, H.-W. Jun and J. D. Hartgerink, *J. Am. Chem. Soc.*, 2006, **128**, 7291-7298; (b) K. L. Niece, J. D. Hartgerink, J. J. J. M. Donners and S. I. Stupp, *J. Am. Chem. Soc.*, 2003, **125**, 7146-7147; c) C. J. Bowerman, W. Liyanage, A. J. Federation and B. L. Nilsson, *Biomacromolecules*, 2011, **12**, 2735-2745.

[2] (a) K. Pradeep, P. Viness, M. Girish, E. C. Yahya, C. d. T. Lisa and N. Dinesh, *Recent Pat. Drug Delivery Formulation*, 2011, **5**, 24-51; (b) S. Sundar, Y. Chen and Y. W. Tong, *Curr. Med. Chem.*, 2014, **21**, 2469-2479.

[3] L. Adler-Abramovich and E. Gazit, *Chem. Soc. Rev.*, 2014, **43**, 6881-6893.

[4] H. Cui, M. J. Webber and S. I. Stupp, *Pept. Sci.*, 2010, **94**, 1-18.

[5] S. Zhang, D. M. Marini, W. Hwang and S. Santoso, *Curr. Opin. Chem. Biol.*, 2002, **6**, 865-871.

[6] A. Trent, R. Marullo, B. Lin, M. Black and M. Tirrell, *Soft Matter*, 2011, **7**, 9572-9582.

[7] (a) Q. Meng, Y. Kou, X. Ma, Y. Liang, L. Guo, C. Ni and K. Liu, *Langmuir*, 2012, **28**, 5017-5022; (b) Y. S. Velichko, S. I. Stupp and M. O. de la Cruz, *J. Phys. Chem. B*, 2008, **112**, 2326-233; (c) S. Tsonchev, G. C. Schatz and M. A. Ratner, *J. Phys. Chem. B*, 2004, **108**, 8817-8822.

[8] Y.-D. Wu and S. Gellman, *Acc. Chem. Res.*, 2008, **41**, 1231-1232.

[9] (a) S. V. Luis and I. Alfonso, *Acc. Chem. Res.*, 2014, **47**, 112-124; (b) V. Marti, M. D. Pandey, M. I. Burguete and S.V. Luis and, *Chem. Rev.* 2015, 8736-8834

[10] (a) F. Adrián, M. I. Burguete, S. V. Luis, J. F. Miravet, M. Querol and E. García-España, *Tetrahedron Lett.*, 1999, **40**, 1039-1040; (b) J. Becerril, M. Bolte, M. I. Burguete, F. Galindo, E. García-España, S. V. Luis and J. F. Miravet, *J. Am. Chem. Soc.*, 2003, **125**, 6677-6686; (c) J. Rubio, I. Alfonso, M. I. Burguete and S.V. Luis, *Soft Matter* 2011, **7**, 10737-10748

[11] (a) M. Bru, I. Alfonso, M. I. Burguete and S. V. Luis, *Tetrahedron Lett.*, 2005, **46**, 7781-7785; (b) M. Bru, I. Alfonso, M. I. Burguete and S. V. Luis, *Angew. Chem., Int. Ed.*, 2006, **45**, 6155-6159; (c) I. Alfonso, M. Bolte, M. Bru, M. I. Burguete, S. V. Luis and J. Rubio, *J. Am. Chem. Soc.*, 2008, **130**, 6137-6144; (d) I. Alfonso, M. Bolte, M. Bru, M. I. Burguete and S. V. Luis, *Chem. - Eur. J.*, 2008, **14**, 8879-8891.

[12] (a) M. Ruben, J. Rojo, F. J. Romero-Salguero, L. H. Uppadine and J.-M. Lehn, *Angew. Chem., Int. Ed.*, 2004, **43**, 3644-3662; (b) M. W. Hosseini, *Acc. Chem. Res.*, 2005, **38**, 313-323; (c) B. H. Northrop, Y.-R. Zheng, K.-W. Chi and P. J. Stang, *Acc. Chem. Res.*, 2009, **42**, 1554-1563; (d) A. Mantion, L. Massüger, P. Rabu, C. Palivan, L. B. McCusker and A. Taubert, *J. Am. Chem. Soc.*, 2008, **130**, 2517-2526; (e) M. Llusar and C. Sanchez, *Chem. Mater.*, 2008, **20**, 782-820; (f) E. A. Meyer, R. K. Castellano and F. Diederich, *Angew. Chem., Int. Ed.*, 2003, **42**, 1210-1250; (g) S. Khademi, J. O'Connell, J. Remis, Y. Robles-Colmenares, L. J. W. Miercke and R. M. Stroud, *Science*, 2004, **305**, 1587-1594; h) A. Nakamura, M. Yao, S. Chimnaronk, N. Sakai and I. Tanaka, *Science*, 2006, **312**, 1954-1958.

[13] (a) J. Becerril, B. Escuder, J. F. Miravet, R. Gavara and S. V. Luis, *Eur. J. Inorg. Chem.*, 2005, **2005**, 481-485; (b) J. Becerril, M. I. Burguete, B. Escuder, S. V. Luis, J. F. Miravet and M. Querol, *Chem. Commun.*, 2002, 738-739; (c) J. Becerril, M. I. Burguete, B. Escuder, F. Galindo, R. Gavara, J. F. Miravet, S. V. Luis and G. Peris, *Chem. - Eur. J.*, 2004, **10**, 3879-3890; (d) M. I. Burguete, F. Galindo, R. Gavara, M. A. Izquierdo, J. C. Lima, S. V. Luis, A. J. Parola and F. Pina, *Langmuir*, 2008, **24**, 9795-9803; (e) M. I. Burguete, M. A. Izquierdo, F. Galindo and S. V. Luis, *Chem. Phys. Lett.*, 2008, **460**, 503-506; (f) I. Alfonso, M. Bru, M. I. Burguete, E. García-Verdugo and S. V. Luis, *Chem. - Eur. J.*, 2010, **16**, 1246-1255; (g) J. Rubio, I. Alfonso, M. I. Burguete and S. V. Luis, *Soft Matter*, 2011, **7**, 10737-10748; (h) J. Rubio, I. Alfonso, M. I. Burguete and S. V. Luis, *Chem. Commun.*, 2012, **48**, 2210-2212; (i) J. Rubio, V. Martí-Centelles, M. I. Burguete and S. V. Luis, *Tetrahedron*, 2013, **69**, 2302-2308.

[14] (a) F. Galindo, J. Becerril, M. Isabel Burguete, S. V. Luis and L. Vigara, *Tetrahedron Lett.*, 2004, **45**, 1659-1662; (b) B. Altava, M. I. Burguete, N. Carbó, J. Escorihuela and S. V. Luis, *Tetrahedron: Asymmetry*, 2010, **21**, 982-989; (c) I. Alfonso, M. I. Burguete, F. Galindo, S. V. Luis and L. Vigara, *J. Org. Chem.*, 2009, **74**, 6130-6142; (d) M. I. Burguete, F. Galindo, S. V. Luis and L. Vigara, *J. Photochem. Photobiol., A*, 2010, **209**, 61-67; (e) B. Altava, M. Isabel Burguete, N. Carbó, S. V. Luis, V. Martí-Centelles and C. Vicent, *Tetrahedron Lett.*, 2013, **54**, 72-79; (f) V. Martí-Centelles, M. A. Izquierdo, M. I. Burguete, F. Galindo and S. V. Luis, *Chem. - Eur. J.*, 2014, **20**, 7465-7478; (g) E. Faggi, R. Porcar, M. Bolte, S. V. Luis, E. García-Verdugo and I. Alfonso, *J. Org. Chem.*, 2014, **79**, 9141-9149.

[15] (a) I. Alfonso, M. I. Burguete and S. V. Luis, *J. Org. Chem.*, 2006, **71**, 2242-2250; (b) I. Alfonso, M. I. Burguete, F. Galindo, S. V. Luis and L. Vigara, *J. Org. Chem.*, 2007, **72**, 7947-7956; (c) E. Faggi, S. V. Luis and I. Alfonso, *RSC Adv.*, 2013, **3**, 11556-11565.

[16] F. Galindo, M. I. Burguete, L. Vigara, S. V. Luis, N. Kabir, J. Gavrilovic and D. A. Russell, *Angew. Chem., Int. Ed.*, 2005, **44**, 6504-6508.

[17] (a) F. Adrián, M. I. Burguete, J. M. Fraile, J. I. García, J. García, E. García-España, S. V. Luis, J. A. Mayoral, A. J. Royo and M. C. Sánchez, *Eur. J. Inorg. Chem.*, 1999, **1999**, 2347-2354.

[18] (a) J. Becerril, M. Bolte, M. I. Burguete, J. Escorihuela, F. Galindo and S. V. Luis, *CrystEngComm*, 2010, **12**, 1722-1725; (b) V. Martí-Centelles, D. K. Kumar, A. J. P. White, .S V. Luis and R. Vilar,

CrystEngComm, 2011, **13**, 6997-7008; (c) Inorg. Chem. 2016; (d) Dalton 2016
[19] (a) L. Marshall, K. Parris, J. Rebek, S. V. Luis and M. I. Burguete, *J. Am. Chem. Soc.*, 1988, **110**, 5192-5193; b) J. Rebek, *Acc. Chem. Res.*, 1990, **23**, 399-404; c) J. Rebek, *Science*, 1987, **235**, 1478-1484.
[20] (a) A. P. Bisson, F. J. Carver, D. S. Eggleston, R. C. Haltiwanger, C. A. Hunter, D. L. Livingstone, J. F. McCabe, C. Rotger and A. E. Rowan, *J. Am. Chem. Soc.*, 2000, **122**, 8856-8868; (b) V. Berl, I. Huc, R. G. Khoury, M. J. Krische and J.-M. Lehn, *Nature*, 2000, **407**, 720-723; (c) L. J. Prins, D. N. Reinhoudt and P. Timmerman, *Angew. Chem., Int. Ed.*, 2001, **40**, 2382-2426; (d) M. Amorín, L. Castedo and J. R. Granja, *Chem. - Eur. J.*, 2008, **14**, 2100-2111.
[21] (a) Marshall, L.; Parris, K.; Rebek, J.; Luis, S. V.; Burguete, M. I., *J. Am. Chem. Soc.* 1988, **110**, 5192-5193; (b) Rebek, J., *Acc. Chem. Res.* 1990, **23**, 399-40; (c) Rebek, J., *Science* 1987, **235**, 1478-1484.
[22] E. Faggi, R. Gavara, M. Bolte, L. Fajari, L. Julia, L. Rodriguez and I. Alfonso, *Dalton Trans.*, 2015, **44**, 12700-12710.
[23] O. V. Dolomanov, L. J. Bourhis, R. J. Gildea, J. A. K. Howard and H. Puschmann, *J. Appl. Crystallogr.*, 2009, **42**, 339-341.
[24] (a) G. Sheldrick, *Acta Crystallogr., Sect. A: Found. Adv.*, 2008, **64**, 112-122; (b) G. M. Sheldrick, *Acta Crystallogr., Sect. C: Struct. Chem.*, 2015, **71**, 3-8.
[25] C. F. Macrae, I. J. Bruno, J. A. Chisholm, P. R. Edgington, P. McCabe, E. Pidcock, L. Rodriguez Monge, R. Taylor, J. van de Streek and P. A. Wood, *J. Appl. Crystallogr.*, 2008, **41**, 466-470.

Chapter VIII

Conclusions

8.1 Conclusions

To conclude, the general conclusions of the work developed in this PhD are here presented.

In the field of cation molecular recognition and catalysis, in chapter IV, a family of bis(amino amide) ligands derived from *L*-valine and *L*-phenylalanine with an aromatic central spacer has been synthesized. A combination of different complementary techniques such as pH-metric titrations, spectroscopic studies, ESI-MS experiments and X-ray crystallographic techniques has been carried out in order to analyse the complex formation with the M^{2+} cations.

Potentiometric studies reveal that the substitution of the ethylenic spacer by the aromatic one seems not to have any effect on the observed basicity of the ligands.

The stability of the complexes formed with Cu^{2+} is several orders of magnitude higher when compared to those formed by the related ligand containing an ethylenic central spacer. It should be noted the formation of $[CuH_{-2}L]$ species even in relatively acidic regions, the increase in acidity of the amido groups can be responsible for this behaviour.

Zn^{2+} complexes were significantly less stable than those for Cu^{2+} and presented formation constants several orders of magnitude lower and no appreciable differences were obtained as a consequence of the change in the central spacer.

The central aromatic spacer also seems to facilitate the formation of crystals suitable for X-Ray diffraction. Crystal structures for the corresponding Cu^{2+} and Ni^{2+} have been obtained revealing the metal atom in an essentially square planar geometry, although in several instances, the oxygen atom of an amide carbonyl can act as a fifth coordination site. In the case of Zn^{2+} crystal structure obtained displays a square-pyramidal arrangement of the metal center.

Finally, preliminary experiments reveal the capacity of some of the former complexes to act as catalysts for the ring opening of the cyclohexene epoxide using aniline as the nucleophile in water. Interestingly, the results show that this is a ligand accelerated the catalytic process and Zn^{2+} complexes act as more efficient catalysts. Unfortunately, the catalytic reaction took place without any observer enantiomeric induction.

In chapter V, the studies of molecular recognition of cations have been carried out using *N,N'*-benzylated pseudopeptidic compounds.

It has been described herein the synthesis of *N,N'*-benzylated bis(amino amides) with C_2 symmetry containing an aliphatic central spacer and amino acid residues derived from *L*-valine and *L*-phenylalanine.

The binding with M^{2+} cations has been studied by potentiometric titrations, spectroscopic studies, ESI-MS experiments, and X-ray crystallographic techniques.

The *N,N'*-benzyl substitution decreases the basicity of the resulting bis(amino amides) and regarding the effect of the amino acid residue, the second protonation constant for phenylalanine pseudopeptide was more than one order of magnitude lower than for the analogous compound derived from valine.

The stability of the complexes formed with Cu^{2+} is several orders of magnitude higher when compared to those formed by the related ligand. It should be noted the formation of $[CuH_{-2}L]$ species even in relatively acidic regions, the increase in acidity of the amido groups can be responsible for this behaviour.

Regarding potentiometric studies for Cu^{2+} complexes, the presence of the additional benzyl groups in the terminal amino groups could significantly reduce the stability of the corresponding metal complexes. Thus, for the neutral $[CuH_{-2}L]$ species from **6a**, the formation constant was more than three orders of magnitude lower than the related formation constant for the

nonbenzylated ligand. In spite of this, these neutral complex species were predominant around pH 7 for both ligands.

Cu^{+2} bisdeprotonated complexes displayed 1:1 stoichiometries and square planar arrangements around the metal centre, as confirmed by the corresponding X-Ray crystal structures.

Strong selectivity in the interaction of **6a** with Cu^{2+}, in particular at short times was observed, in such a way that ligand **6a** could act as a chemosensor and detect Cu^{+2} with high selectivity against other metals and a good sensitivity.

Naked-eye detection was possible at concentrations in the submillimolar range (0.25 mM) and the LOD reached values of 85 μM from UV-Vis measurements and 28 μM from CD experiments.

The response time of **6a** to Cu^{2+} was less than 2 min, indicating that this chemosensor can be used for real-time tracing of Cu^{2+} in a test system.

On the other hand, in the chapter VI of the thesis, open-chain and macrocyclic pseudopeptides containing a diethylene triamine spacer derived from *L*-valine have been synthesised. A combination of different complementary techniques such as pH-metric titrations, spectroscopic studies, ESI-MS experiments has been carried out in order to analyse the complex formation with the Cu^{2+} cations.

The introduction of a nitrogen atom in the central spacer increased the basicity and water solubility of the resulting ligands. Overall, the presence of the additional nitrogen donor atom in the central spacer linking the two amino acid subunits provided the formation of significantly more stable complexes.

When the corresponding distribution diagrams were analysed, copper complex species dominated the distribution diagram for pH values above 5, and the monocationic and dicationic complexes were the major species identified around neutral pH values.

It is worth mentioning that the presence of an additional nitrogen atom in the central spacer is not reflected in an increased basicity of the $[CuL]^{2+}$ complexes for the open chain pseudopeptide, indicating a strong participation of all the amino groups in the coordination to the metal.

At basic pH values for the open chain ligand, the major detected species was the monoanionic $[CuH_{-3}L]^-$ which should correspond to the deprotonation of a coordinated water molecule to form the corresponding hydroxide. For the macrocyclic ligand, this species was not observed as the carboxylate group could coordinate to the copper center instead of the hydroxide anion.

The geometry of these complexes, having different protonation states, were very similar, most likely from square planar to square-pyramidal, a behaviour clearly divergent from related compounds. The existence of a large enough flexible cavity in the case of the macrocyclic compound and the presence of the six potential donor groups in the macrocyclic structure allowed the formation of strong metal complexes for this ligand, in spite of the important steric constraints often found for structures of this class like polyaza[n]cyclophanes.

Thus, these results have provided a better understanding of the behaviour of these ligands and the formation and stability of different metal complexes that could be potentially important for future catalytic, biomimetic and recognition studies.

Finally, in chapter VII, the self -assembling of C_2 symmetric open chain bis (amino amides) in the solid state has been studied.

It has been studied the role of the amino acid residue, the length, and nature of the spacer and the N-substitution in the self-assembly of open chain C_2-pesudopeptidic compounds derived from *L*-Val and *L*-Phe.

All pseudopeptidic systems preferred extended conformations and different behaviour was observed related to the conformation when valine or

phenylalanine was involved associated with the different packing motif observed.

Thus, *L*-Val pseudopeptidic compounds assembled into a β–sheet-like structure stabilized by polar intermolecular interactions while *L*-Phe pseudopeptidic compounds displayed a folding conformation of the side chain.

Overall, for the pseudopeptidic compound with aliphatic spacers very different patterns as a function of the number of methylene groups of the spacer was observed associated again with the different packing motif observed. In this regard, the H-bonds induce a global parallel disposition of the molecules with amide groups located in *anti* or *syn* disposition as a function of the length of the spacer.